

AD-A048 311

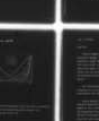
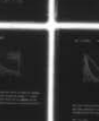
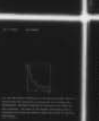
FOREIGN TECHNOLOGY DIV WRIGHT-PATTERSON AFB OHIO
INTERACTIONS OF HIGH-ENERGY PARTICLES AND ATOMIC NUCLEI WITH NU--ETC(U)
JUL 77 V S BARASHENKOV, V D TONEYEV
FTD-ID(RS)T-1069-77

F/6 20/8

UNCLASSIFIED

NL

1 OF 6
AD
A048 311



①

FOREIGN TECHNOLOGY DIVISION



INTERACTIONS OF HIGH-ENERGY PARTICLES AND
ATOMIC NUCLEI WITH NUCLEI
(CHAPTER 7 thru 11)

by

V. S. Barashenkov, V. D. Toneyev



DDC
RECEIVED
JAN 12 1978
F

Approved for public release;
distribution unlimited.

AD-A048311

UNEDITED MACHINE TRANSLATION

FTD-ID(RS)T-1069-77

13 July 1977

MICROFICHE NR: *FTD-77-C-000836 L*

INTERACTIONS OF HIGH-ENERGY PARTICLES AND ATOMIC
NUCLEI WITH NUCLEI (CHAPTER 7 thru 11)

By: V. S. Barashenkov, V. D. Toneyev

English pages: 504

Source: Vzaimodeystviya Vysokoenergeticheskikh
Chastits i Atomnykh Yader S Yadrami,
Moscow, 1972, pp 468-648

Country of origin: USSR

This document is a machine translation

Requester: FTD/ETDP

Approved for public release; distribution
unlimited

THIS TRANSLATION IS A RENDITION OF THE ORIGINAL FOREIGN TEXT WITHOUT ANY ANALYTICAL OR EDITORIAL COMMENT. STATEMENTS OR THEORIES ADVOCATED OR IMPLIED ARE THOSE OF THE SOURCE AND DO NOT NECESSARILY REFLECT THE POSITION OR OPINION OF THE FOREIGN TECHNOLOGY DIVISION.

PREPARED BY:

TRANSLATION DIVISION
FOREIGN TECHNOLOGY DIVISION
WP-AFB, OHIO.

Table of Contents

U.S. Board on Geographis Names Transliteration System.....	11
Russian and English Trigonometric Functions.....	111
Chapter 7. Intranuclear Cascades with Many-Body Interactions	1
Chapter 8. Emission of Complex Particles.....	100
Chapter 9. Fragmentation.....	175
Chapter 10. Nuclear Fission.....	259
Chapter 11. Inelastic Collisions of Nuclei.....	354

ACCESSION for	
NTIS	Write Section <input checked="" type="checkbox"/>
DDC	Buff Section <input type="checkbox"/>
UNANNOUNCED	<input type="checkbox"/>
JUSTIFICATION _____	
BY _____	
DISTRIBUTION/AVAILABILITY CODES	
Dist. AVAIL. and/or SPECIAL	
A	-

U. S. BOARD ON GEOGRAPHIC NAMES TRANSLITERATION SYSTEM

Block	Italic	Transliteration	Block	Italic	Transliteration
А а	<i>А а</i>	A, a	Р р	<i>Р р</i>	R, r
Б б	<i>Б б</i>	B, b	С с	<i>С с</i>	S, s
В в	<i>В в</i>	V, v	Т т	<i>Т т</i>	T, t
Г г	<i>Г г</i>	G, g	У у	<i>У у</i>	U, u
Д д	<i>Д д</i>	D, d	Ф ф	<i>Ф ф</i>	F, f
Е е	<i>Е е</i>	Ye, ye; E, e*	Х х	<i>Х х</i>	Kh, kh
Ж ж	<i>Ж ж</i>	Zh, zh	Ц ц	<i>Ц ц</i>	Ts, ts
З з	<i>З з</i>	Z, z	Ч ч	<i>Ч ч</i>	Ch, ch
И и	<i>И и</i>	I, i	Ш ш	<i>Ш ш</i>	Sh, sh
Й й	<i>Й й</i>	Y, y	Щ щ	<i>Щ щ</i>	Shch, shch
К к	<i>К к</i>	K, k	Ъ ъ	<i>Ъ ъ</i>	"
Л л	<i>Л л</i>	L, l	Ы ы	<i>Ы ы</i>	Y, y
М м	<i>М м</i>	M, m	Ь ь	<i>Ь ь</i>	'
Н н	<i>Н н</i>	N, n	Э э	<i>Э э</i>	E, e
О о	<i>О о</i>	O, o	Ю ю	<i>Ю ю</i>	Yu, yu
П п	<i>П п</i>	P, p	Я я	<i>Я я</i>	Ya, ya

*ye initially, after vowels, and after ъ, ы; e elsewhere.
 When written as ё in Russian, transliterate as yë or ë.
 The use of diacritical marks is preferred, but such marks may be omitted when expediency dictates.

GREEK ALPHABET

Alpha	A	α	α	Nu	N	ν
Beta	B	β		Xi	Ξ	ξ
Gamma	Γ	γ		Omicron	Ο	ο
Delta	Δ	δ		Pi	Π	π
Epsilon	E	ε	ε	Rho	Ρ	ρ ϑ
Zeta	Z	ζ		Sigma	Σ	σ ς
Eta	H	η		Tau	Τ	τ
Theta	Θ	θ	θ	Upsilon	Υ	υ
Iota	I	ι		Phi	Φ	φ φ
Kappa	K	κ	κ	Chi	Χ	χ
Lambda	Λ	λ		Psi	Ψ	ψ
Mu	M	μ		Omega	Ω	ω

RUSSIAN AND ENGLISH TRIGONOMETRIC FUNCTIONS

Russian	English
---------	---------

sin	sin
cos	cos
tg	tan
ctg	cot
sec	sec
cosec	csc
sh	sinh
ch	cosh
th	tanh
cth	coth
sch	sech
csch	csch
arc sin	\sin^{-1}
arc cos	\cos^{-1}
arc tg	\tan^{-1}
arc ctg	\cot^{-1}
arc sec	\sec^{-1}
arc cosec	\csc^{-1}
arc sh	\sinh^{-1}
arc ch	\cosh^{-1}
arc th	\tanh^{-1}
arc cth	\coth^{-1}
arc sch	sech^{-1}
arc csch	csch^{-1}

rot	curl
lg	log

GRAPHICS DISCLAIMER

All figures, graphics, tables, equations, etc. merged into this translation were extracted from the best quality copy available.

INTERACTIONS OF HIGH-ENERGY PARTICLES AND ATOMIC NUCLEI WITH NUCLEI.

V. S. Barashenkov, V. D. Toneyev.

Page 468.

Chapter 7.

INTRANUCLEAR CASCADES WITH MANY-BODY INTERACTIONS.

§80. Intranuclear cascades with superhigh energies.

Study of the interaction of particles with nuclei with the superhigh energies $T \gg 10$ GeV conjugate/combined with considerably great difficulties gives the less determined conclusions, than in the area of acceleration energies. This is caused, in the first place, by

an inaccuracy in the experimental data on the interactions of space particles with nuclei, which impedes comparison with the experiment of the results of the calculations (specifically, in many cases - especially, when matter concerns photoemulsion data, energy of initial particle is known only by order of value), in the second place, by the large laboriousness of the calculations, in the course of that also hundred of cascade particles. Furthermore, in the area of space energies we still comparatively little know about the properties of the interactions of elementary particles; therefore the information, embedded into the calculations of intranuclear cascades, is very assumed, and this, in turn, it cannot but pronounce on the results of the calculations.

Nevertheless the use of the contemporary high-speed calculators and the statistical analysis of known experimental data make it possible all the same to make a series sufficient reliable conclusions about the mechanism of the interactions of particles with nuclei with superhigh energies.

Among known at present experimental data especially important value for the calculation of intranuclear cascades has a conclusion about the fact that among secondary particles, which are formed with inelastic π - N- or N - N-collisions, is a particle, which on the basis of its properties substantially is isolated among all remaining

particles. This leading particle takes away on the average about 60-70% of total energy of colliding particles.

A similar effect occurs, also, in the area of accelerative energies; however, there it not so is noticeable, since kinetic energy of the leading particle still not is not very great in comparison with its rest mass; therefore its properties strongly do not differ from the properties of other being born particles. In the area of space energies the existence of such the slowly discarding its energy "rod" particle, kinetic energy of which considerably exceeds medium energy of other secondary particles, of course, significantly it manifests itself the development of intranuclear cascade.

In works [14-17] the calculations of intranuclear cascades were carried out on the assumption that at the fixed value of total energy of the characteristic of particles, which were being formed in elementary inelastic event/report in the system of their center of inertia, they do not depend neither on the type colliding nor on the type of the being born particles.

Page 469.

With the energies, greater than several dozen gigaelectron-volt, this

assumption equivalent to the exception/elimination of particles of the cascade/stage, generated by the leading particle, since this particle only insignificantly changes distant "tail" of the total energy spectrum, and energies of particles, determined by this spectrum with the aid of the Monte-Carlo method, virtually almost never are equal to energy of the leading particle. Although the average characteristics nucleon- of nuclear interactions in this case are obtained by sufficiently close to those observed in experiment, it is possible to compare them, of course, only with that part of the experimental data, which does not include the leading particle. (This especially is substantial for the medium energy of shower particles, which, it is completely understandable, proves to be considerably smaller than its experimental value).

In two following paragraphs we with the aid of the methods, developed in Chapter 4 and 6, will examine in detail the complete intranuclear cascade of two-body interactions, which includes contribution "rod", leading particle, the contributions of the subsequent generations of all other being born particles and evaporative cascade/stage [5, 6, 10]. This will allow us to explain, how conventional cascade a model will agree with the results of space experiments.

It should be noted that as a result of above difficulties

(inaccuracy in the experimental data and the large laboriousness of calculations) indicated the calculations in the area of space energies even for the low-energy component of intranuclear cascade are carried out within the framework of the simplified model. The basic simplifications are connected with failure of the continuous energy dependency of the characteristics of interaction and transition to the characteristics, averaged on the large energy range of incident particle T , and also with the statistical character of the execution of the law of conservation of energy - momentum/impulse/pulse in elementary inelastic collisions. It is understandable that in this case some parts of phenomenon can remain that which was not noticed.

The further generalization of cascade model is the account of many-body interactions within nucleus. Fundamental difficulty in the examination of many-body interactions consists in the fact that at present virtually completely nothing not is known about their properties, to say nothing of the numerical value of their characteristics, necessary for the calculation of cascade/stages. More reasonable now is represented the reverse/inverse formulation of the problem: to obtain the information about many-body interactions from the comparison of the results of cascade calculations with the known experimental data on the interactions of pions and nucleons with different atomic nuclei over a wide range of energies. The

calculation follows, is terminated, to begin with maximally simple and most common/general/total assumptions about the character of such interactions and to detail them only as this becomes completely necessary for the matching of the results of the calculations with experiment. It is possible to hope that this approach gives the determined guarantees against the inclusion into the theory of unjustified speculative cell/element [3, 6, 7, 9].

One should emphasize that the inelastic collisions of high-energy particles with nuclei represent now unique possibility to experimentally approach the study of the many-body interactions of elementary particles.

Besides the method of statistical simulation for the description of the inelastic interactions of particles with nuclei with high and superhigh energies some authors utilized the model, based on the assumption that the initial particle in its path within target nucleus forms the "tube" of the highly excited nuclear substance, which then statistically decomposes to nucleons and mesons. Still recently this approach was very popular, however, as shows more careful examination, the model of tube more or less correctly it reproduces only the those experimental data, which are determined in essence by the kinematics of process. As we will see below, with superhigh energies the intranuclear cascade to a considerable degree

also is realized in a comparatively narrow angular tunnel, in this case the kinematics turns out to be in general terms close to of the occurring in the model tube. This explains certain success of this model in the first works. To short discussion of these questions is dedicated the last/latter paragraph of this chapter.

Page 470.

§81. Model of high-energy cascade/stages with two-particle collisions.

Nuclear model and the experimental data, used for the calculation. For the description of target nucleus let us as before apply the model of fermi gas. Nuclear radius is placed equal by $R = 1.4 A^{1/3} \cdot 10^{-13}$ cm. The diffusivity of nuclear boundary for simplicity let us disregard ¹.

FOOTNOTE ¹. In the area of high energies the results of the calculations turn out to be very sensitive to the selection of the value of coefficient r_0 in formula for R ; specifically, because of a large multitude of particles, which are born in each event/report of

inelastic interaction, even a small increase in the mean free path of particles within nucleus ($\lambda \sim r^3_0$) leads to a noticeable decrease in the number of shower particles, which escape from nucleus.

ENDFOOTNOTE.

In accordance with the known now experimental data on the interactions of elementary particles (see surveys [11, 18, 19]) let us consider that with $T \gg 1$ GeV average number of particles, which are formed during inelastic collision, does not depend on the type of the colliding particles and wholly is determined by the value of the kinetic energy T :

$$\bar{n}(T) \simeq 3 \cdot T^{1/4}. \quad (7.1)$$

This dependence describes well the experimental data in the area of the accelerative energies $T \lesssim 30$ GeV. With large energies, generally speaking, it is difficult to select between the exponential (7.1) and logarithmic dependence $n \sim \ln T$; however dependence (7.1) to our view is more preferable, since it makes it possible to approximate experimental points in wider energy range ².

FOOTNOTE ². Another version of cascade calculations consists in the fact that the value of many being born particles $n(T)$ for each

$$\sum_{i=1}^{n-1} (\mathcal{E}_i + m_i) = k \mathcal{E}_c$$

event/report of inelastic interaction is determined from condition where \mathcal{E}_i is the developed on experimental histogram kinetic energy of i^{th} secondary particle; m_i - its mass; k is a coefficient of anelasticity; \mathcal{E}_c - total energy of the colliding particles in the center-of-gravity system (comp. with formula (7.3)). Drawing \mathcal{E}_i conducts taking into account the law of conservation of energy (see Chapter 4). However, as showed comparative calculations, the results weakly they depend on the method of the determination of number n .
ENDFOOTNOTE.

Let us also assume that in the inelastic collision of pi-meson with nucleon with $T > 200$ GeV the average number of being born heavy particles (k-mesons, baryons, antis-baryon) is 10o/o of total number of all secondary particles:

$$\bar{n}_T \simeq 0,1\bar{n}. \quad (7.2)$$

With $T < 200$ GeV the average number of heavy particles \bar{n}_T let us place equal to unity. The considerations, which lie at the basis of these assumptions, consist in the fact that for π - N-interactions in the area of accelerative energies the value of relation \bar{n}_T/\bar{n} approximately half than for N - N- interaction ; we consider that this relationship/ratio is retained with high energies. The selection of wall energy $T = 200$ GeV is very conditional and is determined only

themes that formula (7.2) is used only in the area, where $0.1n \gg 1$ (see [11, 18, 19]).

For the inelastic collisions of heavy particles with intranuclear nucleons let us assume $\bar{n}_T = 0,2\bar{n}$, if $T > 200$ GeV and $\bar{n}_T = 2$, if $T < 200$ GeV [11, 18, 19]. In accordance with such distributions of the mass of the being born particles we will fulfill relativistic transformations from the center-of-gravity system (more accurately - from C-system, see §47, 49) of the colliding particles, where are assigned all the characteristics, which describe elementary event/report, to the laboratory coordinate system.

Page 471.

P
Since in the area of energies T of the order several dozen gigaelectron-volt and above are sufficiently are reliably known only the total momentum distributions of the being born particles, averaged according to heavy and low-mass particles, with these energies for all types of the being born particles, with the exception of the leading nucleons ¹, in the center-of-gravity system let us utilize the identical energy distributions $W(\mathcal{T})$, taken, for example, from experimental works [29, 32, 34].

FOOTNOTE 1. As the leading particle for a concreteness further let us examine nucleon which, however, is unessential, so energy of this particle is very great in comparison with its rest mass. ENDFOOTNOTE.

It is assumed that these distributions do not depend also on the type of the colliding particles. (Unlike the energy distributions of the distribution of the secondary heavy and low-mass particles according to momentum/impulse/pulses considerably they are distinguished).

In the area of the accelerative energies $T \lesssim 30$ GeV for the being born pi-mesons and nucleons let us utilize those which are being distinguishing distribution.

The medium energy of leading nucleon $\bar{\mathcal{E}}_n = \bar{\mathcal{T}}_n + m_N$ it is possible to define in the center-of-gravity system of the colliding particles as

$$\bar{\mathcal{E}}_n = (1 - \bar{k}) \mathcal{E}_c, \quad (7.3)$$

where \mathcal{E}_c is total energy in the center-of-gravity system, k - the average coefficient of anelasticity, which in accordance with the experimental data let us place equal to 0.3-0.4 ².

FOOTNOTE 2. It is not difficult to fulfill the calculation in such a way that the values of coefficient of k will be developed in the experimental histogram $w(k)$. However, the results of this calculation do not differ from those which are obtained in the case, when for k is used its average value [6].

Another method of the determination of energy of the leading particle consists in the fact that for the assigned number of particles $\bar{n} = 3T^{1/4}$ on experimental histograms are developed the values of kinetic energy \mathcal{F} for $(n - 1)$ a particle and total energy of the leading particle is set/assumed equal to

$$\mathcal{E}_n = \mathcal{E}_C - \sum_{i=1}^{\bar{n}-1} (\mathcal{F}_i + m_i). \quad (7.3a)$$

The results of the calculations in all cases turn out to be close.
ENDFOOTNOTE.

The average kinetic energy of remaining particles, obviously, is equal to

$$\bar{\mathcal{F}} = \{k\mathcal{E}_C - \bar{n}_\pi m_\pi - (\bar{n}_\pi - 1) m_N\} / (\bar{n} - 1). \quad (7.4)$$

This value will agree well with the average kinetic energy, calculated directly from distribution $W(\mathcal{F})$ for the appropriate value of T . With the very high energies

$$\bar{\mathcal{F}}_n \sim T^{1/2}, \quad \bar{\mathcal{F}} \sim T^{1/4}. \quad (7.5)$$

After the isolation/liberation of the leading nucleon the angular distributions of all remaining secondary particles with $T \gg 10$ GeV, just as their energy distributions, let us consider not depending on the type of these particles (in the center-of-gravity system). It follows, however, to keep in mind that unlike energy distributions the angular distributions of secondary particles depend substantially on the type of the colliding particles: in $N - N$ -collisions secondary particles disperse on the average symmetrically relative to angle $\theta = \pi/2$, while in $\pi - N$ -collisions occurs considerable asymmetry [18, 19].

As concerns the angular distribution of the leading particle, about this at present known only that it escapes predominantly at small angle to the direction of initial particle. Respectively all other particles in the center-of-gravity system must escape predominantly to reverse side, in order to compensate for the high momentum/impulse/pulse of the leading particle.

Page 472.

For the rough estimate of the angular region of the escape of

the leading nucleon it is possible to use the relationship/ratio

$$\bar{p}_A \cos \theta_A = -(\bar{n}_T - 1) \bar{p}_T \cos \theta - \bar{n}_\pi \bar{p}_\pi \cos \theta, \quad (7.6)$$

by the being approximate consequence of the law of conservation of momentum/impulse/pulse in the center-of-gravity system. In this relationship/ratio $\bar{p}_A, \bar{p}_T, \bar{p}_\pi$ - the respectively mean momentum of the leading nucleon, all remaining being born heavy particles and pi-mesons, $\cos \theta_A$ and $\cos \theta$ - the average cosines of the angles of emission of the leading particle and all remaining particles. (Recall that angular distributions $w_T(\theta) = w_\pi(\theta)$).

By assigning values of $\cos \theta$, calculated according to the experimental angular distributions $w(\theta)$, it is possible to rate/estimate value $\cos \theta_A$ and to approximately construct distribution $w_\pi(\theta)$ with this value of the average cosine.

In the case of N - N-collisions on the strength of the symmetry of the initial system the leading nucleon in the half of the cases escapes at an angle θ_A , while in another half at an angle $\pi - \theta_A$, therefore the resulting angular distribution it is obtained by the addition of two distributions:

$$W_\pi(\theta) = w_\pi(\theta) + w_\pi(\pi - \theta).$$

Are symmetrical the angular distributions also of all other particles

$$W(\theta) = w(\theta) + w(\pi - \theta).$$

For the construction of these distributions it is possible to use, for example, the experimental data from works [20, 29, 32, 34].

Since for π - N-collisions with $T \gg 10$ GeV the experimental angular distributions of secondary particles are unknown, function $w(\theta)$ in this case let us select much the same as for particles, which are born in N - N-collisions with $\theta < \pi/2$ (or $\theta > \pi/2$):

$$W(\theta) \simeq w(\theta) = w(\pi - \theta).$$

However, immediately let us emphasize that in spite of the roughly qualitative character of constructed thus distributions, this does not introduce any essential errors into the results of cascade calculations, since as a result of the relativistic compression of angles with transition to the laboratory coordinate system the detailed form of angular distributions in the center-of-gravity system turns out to be not very important.

With energies $T \lesssim 30$ GeV of nucleons and pi-mesons, which are born in inelastic collisions, it is possible to utilize experimental histograms (see survey [18] and literature to the figures of Chapter 4) or to be based on the polynomial approximation, described into §48

and 50.

For the description of angular distributions elastic N - N- and π - N-interactions in the region of energies $T \gtrsim 30$ GeV, where there is no experimental data, let us apply the optical model, which, as this was shown in Chapter 2, it will agree sufficiently well with experiment in the area of accelerative energies. However, since at high energies the overwhelming majority of the elastic scattered particles is concentrated at very small angles, the concrete/specific/actual selection of angular distributions turns out to be not very essential.

Generally during the calculation of the intranuclear cascade/stages, initiated by the particles of very high energy, after is isolated the leading particle, the detailed information about angular and energy particle distributions in elementary collisions is considerably less important, than during calculations in the region of accelerative energies; determining in this case are the kinematic factors of relativistic transformations.

Let us further consider that all possible isotopic states in the process of developing intranuclear cascade are equiprobable, i.e., all the utilized in the course of calculations experimental characteristics of the elastic and inelastic interaction of

elementary particles will be averaged on isotopic back, and in final results the half of all heavy particles and two thirds of pi-mesons will be considered charged particles.

Page 473.

As concerns averaging on the isotopic spins of the initial states of the colliding particles, at high energies this it is represented by completely justified, since in cascade/stage participates the very large number of particles of the different signs of charge and, furthermore, with an increase of energy the isotopic dependence of strong interactions generally is attenuate/weakened; at the same time the average numbers of particles, which are distinguished by the projections of isospin, in the final states of inelastic interactions they can turn out to be somewhat different from each other (see §26). Unfortunately, if we utilize some very speculative assumptions, at present nothing cannot be assumed, besides complete isotopic symmetry. As we will see below, our basic conclusions actually do not depend on this assumption.

For simplification in the calculations entire region of energies we will divide into eleven intervals: <0.5 ; $0.5-1$; $1-3$; $3-7$; $7-10$; $10-30$; $30-175$; $175-375$; $375-625$; $625-875$; >875 GeV. In each of these intervals the angular and energy distributions of the being born

particles, obtained by the averaging of the experimental data, let us consider constants.

The interaction cross sections of nucleons and pi-mesons with intranuclear nucleons, the defining range/paths and the types of the interaction of particles within nucleus, let us consider as the continuous functions of energy. Scattering cross section with overcharging σ_{ex} will include in section σ_{el} , since the signs of electrical particle charge we now we do not distinguish. In region $T > 20$ GeV of interaction cross section let us select constant and equal to

$$\sigma_t(NN) = 39,5 \text{ mb}; \quad \sigma_{in}(NN) = 32,5 \text{ mb}; \quad \sigma_{el}(NN) = 7 \text{ mb};$$

$$\sigma_t(\pi N) = 24 \text{ mb}; \quad \sigma_{in}(\pi N) = 20 \text{ mb}; \quad \sigma_{el}(\pi N) = 4 \text{ mb}.$$

Calculation method. Let us follow, in essence, the procedure for of cascade and evaporative calculation, presented in the preceding/previous chapters. The basic difference is in the simpler calculation of the range/paths of particles (for this it is possible to directly utilize a formula (4.22), since the distribution of substance within nucleus is assumed to be uniform), also, in the statistical examination of the law of conservation of energy (see §49).

For each being born in inelastic intranuclear collision heavy or low-mass particle (with the exception of the leading nucleon) must be played the energy \mathcal{E} and angle of emission θ ; for the leading nucleon energy is defined by relationship/ratio (7.3), and angle of emission is developed as for all other particles.

For each event/report of inelastic interaction the average numbers \bar{n}, \bar{n}_1 must be calculated from the rules, indicated in the preceding/previous section. When one or both these numbers turned out to be fractional, in the value of the fractional part rose up, which nearest integers one should select (with deficiency/lack or with surplus). At each value of energy of primary nucleon was calculated not less than 400 cascade/stages.

In the case, when is calculated the interaction of particle with photoemulsion, we must preliminarily still play, by which nuclear component of photoemulsion occurred this interaction. However, the results of such calculations turn out to be very close to the fact that is obtained in the direct examination of the medium nucleus of photoemulsion ^{70}Ga (either, correspondingly, the neutral light/lung, or neutral heavy nucleus of photoemulsion).

Let us now move on to the discussion of the results of calculations [5, 6].

§82. Comparison with experiment.

As it was noted in Chapter 5, certain disagreement of usual cascade model with experiment is exhibited already with energies of initial particles several gigaelectron-volt. Nevertheless the propagation of such calculations for the region of space energies is of large interest, especially in connection with the explanation of that role, which they play the leading particles in the mechanism of the interaction of particles with nuclei ¹.

FOOTNOTE ¹. It must be noted that the cascade calculations in the region of cosmic energies were carried out still long before with the aid of more detailed calculations was reveal/detected a change in the mechanism of interaction already with energies $T \approx 5$ GeV.

Sections of nuclear interactions. The calculated by the Monte-Carlo method reaction cross-sections σ_{in} within the limits of statistical errors in the calculation turn out to be those which be independent of energy of incident particle and close to the results of the calculations according to optical model. This is evident, for example, from Table 107, where are given the results of the calculations for the medium nucleus of photoemulsion ^{70}Ga with three different energies, and from Fig. 361, where with experiment is compared the interaction cross section of π -meson with photoemulsion. The absence of the dependence of theoretical sections on energy of initial particle is a direct consequence of hypothesis about the constancy of sections $\pi - N$ - and $N - N$ -interactions in the region of high energies. All these results are determined by sections $\pi - N$ - and $N - N$ -collisions in nucleus and do not depend on detailed assumptions about the mechanism of intranuclear cascade.

Many being born particles. The comparison of the calculated and experimental values of the average set s - and g -particles is given in Table 108 and 109. A theoretical multitude of s -particles increases with an increase of energy of initial particle considerably faster than this is observed on experiment. The energy dependency of computed values with $T \gtrsim 100$ GeV remains, speaking in general terms, the same as for accelerative energies.

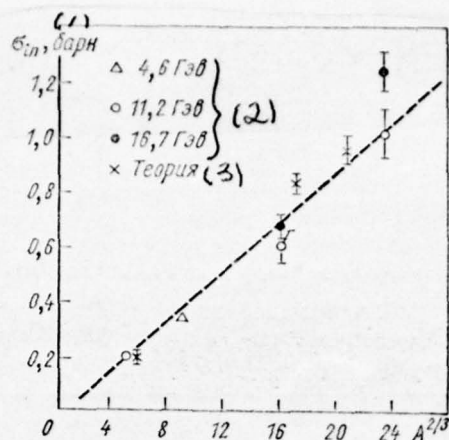


Fig. 361. The section pion- of nuclear interactions (crosses showed the results of cascade calculations ($r_0 = 1.4$), dotted line is the calculation according to optical model. Experimental points are taken from Table 6.).

Key: (1). barn. (2). GeV. (3). Theories.

Table 107. Interaction cross section of proton with nucleus ^{70}Ga , designed by the Monte-Carlo method.

(1) $T, \text{ ГэВ}$	$\sigma_{in}, \text{ мбарн (2)}$	
	$r_0 = 1,35$	$r_0 = 1,4$
100	810 ± 30	872 ± 32
500	817 ± 31	880 ± 33
1000	823 ± 32	884 ± 34

Note. Value σ_{in} , that which was calculated with the aid of optical model, composes with $T = 10^2 - 10^3$ GeV of approximately 820 mb.

Key: (1). GeV. (2). mb.

Table 108. Average number of particles, which are born during the inelastic interactions of protons with photoemulsion.

(1) T, GeV	(2) \bar{n}_s Теория	\bar{n}_s^{\pm}		(2) \bar{n}_g Теория	\bar{n}_g^{\pm}	
		(2) Теория	(3) Опыт		(2) Теория	(3) Опыт
75	$16,2 \pm 0,2$	$11,8 \pm 0,6$	9 *	$11 \pm 0,4$	$5,5 \pm 0,2$	5 *
100	$24,3 \pm 1,1$	$15,4 \pm 0,8$	9,5 *	$12,4 \pm 0,6$	$6,3 \pm 0,3$	—
250	$46,2 \pm 2,4$	$31,8 \pm 1,6$	$13,1 \pm 1$	$25 \pm 1,2$	$12,5 \pm 0,6$	$< 7,6 \pm 1,3$
500	$71,7 \pm 4,3$	$46,6 \pm 2,8$	$18,8 \pm 4,2$	$33,5 \pm 2,0$	$16,8 \pm 1,0$	$\leq 3,0 \pm 0,6$
1000	$95,1 \pm 9,5$	$61,3 \pm 6,1$	20 *	$42,6 \pm 4,2$	$21,3 \pm 2,1$	—
$5 \cdot 10^3$	—	—	$\leq 26,9 \pm 3,8$	—	—	$\leq 3,4 \pm 0,9$

Note. \bar{n} is the total number of being born particles; \bar{n}^{\pm} - the number of being born charged particles.

Key: (1). GeV. (2). Theories. (3). Experiment.

-----^{7P} FOOTNOTE *. Corrected value is obtained by interpolation of known experimental data (see Table 20). ENDFOOTNOTE.

Page 475.

Specifically, the number of being born shower particles $\bar{n}_s \sim T^m$, where $m \approx 0.6$; at the same time experimental dependence $\bar{n}_s(T)$ corresponds to index $m \approx 1/4$ and is close to the fact that is observed in the case of N - N-collisions.

Considerably faster than in experiment, grow/rises an average multitude of g-particles; any tendencies toward the retardation of this increase in interval of $T = 10^2 - 10^3$ GeV not noticeably, vice versa - experimental values \bar{n}_g^\pm they remain almost constants with $T \gg 10$ GeV (see Fig. 128).

With $T \gg 10$ GeV the difference between the calculated and experimental values \bar{n}_s^\pm and \bar{n}_g^\pm turns out to be so large that it cannot be removed by any reasonable variation of the used during calculations experimental data on high-energy π - N- and N - N-interactions. The reason for so powerful a disagreement consists in the fact that kinetic energy of the leading particle with the development of intranuclear cascade decreases sufficiently slowly;

therefore not only with the first, but also during each subsequent inelastic interaction of the leading particle with the nucleon of nucleus it is formed a large quantity of secondary particles. If we do not consider the contribution of the leading particle, then the average number of secondary particles proves to be sufficient to close to experimental, although in this case the theory gives somewhat high values [14-17].

In the region of accelerative energies of the property of the leading particle comparatively they differ little from the properties of other secondary particles and intranuclear cascade taking into account leading particle (within the margins of error in measurements and statistical errors in the calculation) in practice it does not differ from the cascade/stage, designed under the assumption of the complete mixing of the energy between all particles, which are formed after inelastic $N - N$ - and $\pi - N$ -collisions.

It should be noted that independently from assumptions about the role of the leading particle the cascade g-particles in accordance with experiment almost wholly consist of nucleons. As concerns evaporative particles, since average number of g-particles, and, therefore, and the number of chase/dislodged and the nuclei of nucleons, greatly exceeds experimental, the excitation energy of remanent/residual nuclei also it turns out to be exaggerated and the characteristic of evaporative particles considerably they differ from the experimental.

Table 109. Average number of particles, which are born during the inelastic interactions of protons with nucleus ^{12}C with $T = 100 \text{ GeV}$.

\bar{n}	(1) Теория
\bar{n}_s	$16,6 \pm 0,9$
\bar{n}_s^{\pm}	$10,5 \pm 0,3$ ($7,4 \pm 0,5$)
\bar{n}_g	$5,3 \pm 0,3$
\bar{n}_g^{\pm}	$2,7 \pm 0,2$

Note. All designations are the same as in Table 108. In brackets given average experimental value \bar{n}_s^{\pm} .

Key: (1). Theories.

Table 110. Average kinetic energy of particles, which are born during the inelastic interactions of protons with nuclei ^{12}C and ^{70}Ga .

T $\bar{\mathcal{E}}, \Gamma_{36}$	100 Γ_{36} (1)		(2)	(3)
	^{12}C	^{70}Ga	500 $\Gamma_{36}; ^{70}\text{Ga}$	100 $\Gamma_{36}; ^{70}\text{Ga}$
$\bar{\mathcal{E}}_s$	$5,7 \pm 0,3$	$3,8 \pm 0,2$	$6,5 \pm 0,4$	$10,1 \pm 0,9$
$\bar{\mathcal{E}}'_s$	$2,1 \pm 0,1$ ($2,9 \pm 0,3$)	$1,53 \pm 0,07$ ($2,4 \pm 0,9$)	$2,96 \pm 0,02$	$4,0 \pm 0,4$
$\bar{\mathcal{E}}_{-1}$	63 ± 3	$58 \pm 1,5$	260 ± 14	590 ± 60
$\bar{\mathcal{E}}_g$	160 ± 10	147 ± 7	140 ± 10	140 ± 10

Note. $\bar{\mathcal{E}}_s$ is the medium energy of all shower particles; $\bar{\mathcal{E}}'_s$ - the medium energy of shower particles minus leading particle. In brackets for a comparison are shown experimental values (see Table 49).

Key: (1) - GeV.

Page 476.

The energy spectra of the being born particles. From Table 110, where are compared the calculated and experimental values of the average kinetic energy of the being born particles, and from the histograms of Fig. 362 it is evident that calculated kinetic energy

of shower particles rapidly grow/rises with an increase in the energy of primary nucleon and considerably changes during passage from light nuclei to heavy. On the contrary, kinetic energy of the cascade g-particles practically is constant in the wide interval of $T \approx 10-10^3$ GeV and very weakly depends on the mass number of target nucleus. Since the leading particle, which escapes from nucleus, takes away about (54 ± 3) o/o energy of primary nucleon (if $k \approx 0.3$), the average values $\bar{\mathcal{E}}_s$ and $\bar{\mathcal{E}}'_s$ substantially are distinguished. Between experimental and theoretical energies of shower particles occurs considerable disagreement; however, this disagreement not as is impressive as for the average numbers \bar{n}_s . Theoretical value $\bar{\mathcal{E}}_g$ very close to experimental values $\bar{\mathcal{E}}_g = 130 \pm 12$ MeV and $\bar{\mathcal{E}}_g = 170$ by MeV, obtained in experiments with $T = 9$ and 16 GeV (see §32).

Distribution according to transverse impulse. Transverse impulses being born s- and g-particles in all energy range $T \gg 10$ in question GeV in practice do not depend on energy of primary nucleon and on the mass number of target nucleus. The average value \bar{p}_\perp for the shower particles, which are born in photoemulsion with $T = 100$, 500 and 1000 GeV, comprise with respect 410 ± 20 , 440 ± 20 , 490 ± 50 MeV/s; for the g-particles with these energies $\bar{p}_\perp = 350 \pm 20$, 300 ± 20 , 320 ± 30 MeV/s.

During interaction with the nucleus of carbon of protons 100 GeV

in energy $\bar{p}_{\perp s} = 430 \pm 30$

MeV/s,

 $\bar{p}_{\perp g} = 330 \pm 20$

MeV/s.

The results of the calculations will agree rather well with the experimental data (see Fig. 170 and 363).

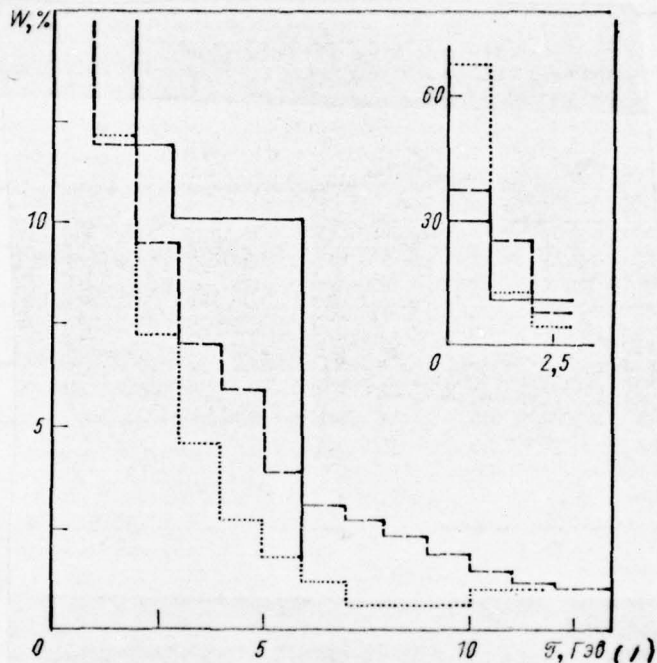


Fig. 362. Energy distribution of the shower particles, which are formed in the inelastic collisions of protons 100 GeV in energy with the nuclei of photoemulsion. Continuous histogram is experiment [37], broken and point histograms are a result of the calculation, made in accordance with account (see §83), also, without taking into account of many-body interactions within nucleus.

Key: (1) - GeV.

Page 477.

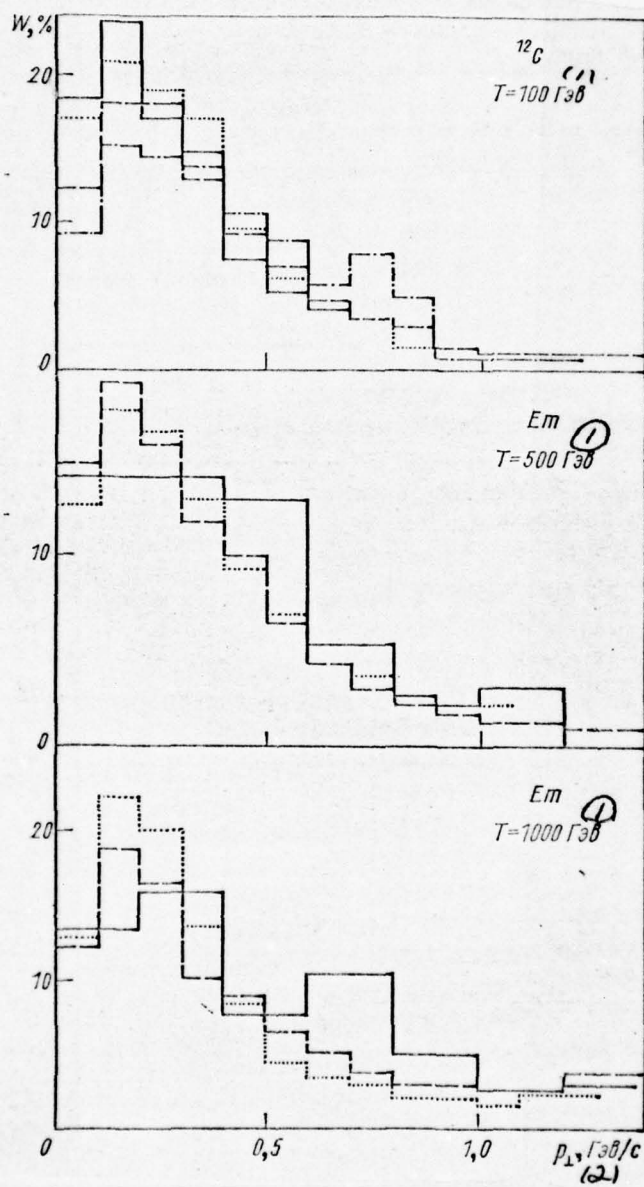


Fig. 363.

Fig. 363. Distributions according to transverse particle momentum from the inelastic interactions of protons with carbon and photoemulsion. Continuous and dot-dash histograms are experimental data from works [23, 27, 28]. Broken and point histograms are the calculation, made in accordance with account and without taking into account of many-body interactions in nucleus.

Key: (1) - GeV. (2) - GeV/s.

Page 478.

Angular distributions. Part of the obtained results is given in Table 111 and in Fig. 364. Theoretical distribution for shower particles in Fig. 364 is sufficiently close to experimental. The escape of cascade g-particles with considerable probability occurs to wide angles $\theta > 90^\circ$. Unfortunately, the experimental data for the g-particles with $T > 30$ GeV at present thus far is not.

In the case of N - N- collisions from the simple kinematic considerations, based on the transformations of Lorenz, it follows that the angle of emission of the half of all secondary particles in the laboratory system of the coordinates of $\theta_{1/2} \sim T^{-1/2}$. In nucleon-nuclear collisions the angle of $\theta_{1/2}$ with an increase of

energy decreases more slowly (see Table 111) due to the effect of the subsequent collisions within nucleus, which correspond to the smaller values of energy T . Therefore the use of a relationship/ratio $\gamma = \text{ctg } \theta_{1/2s}$ for determining energy of initial particle, as this sometimes is made in experimental works, can lead to essential errors.

If the angular distribution of shower particles for a separate star is presented as function by alternating/variable $x = \lg \text{tg } \theta$, then in many instances in this distribution sufficiently distinctly there are two maximums ("protuberance"). Certain irregularity, connected with these maximums, can be noted even in the distributions, averaged according to the large number of separate stars (Fig. 365). This character of the angular distributions of shower particles is the direct consequence of the double-humped character of the used during calculations angular particle distributions $N - N$ -collisions. The latter one can see well from Fig. 366, where is shown the evolution of the angular distribution of shower particles with an increase in the number of intranuclear collisions. With the development of intranuclear cascade the secondary interactions smooth angular distribution; therefore in the final angular distribution of shower particles double-peaked nature is considerably less noticeable, than for initial $N - N$ -interactions, especially, if distribution is obtained summation the large number of stars.

Table 111. Average angle of emission in the laboratory system of the coordinates of the half of all shower or cascade particles, which are formed during the interactions of proton with nuclei ^{12}C and ^{70}Ga .

$\theta_{1/2}$ <i>(1)</i> $\theta_{1/2}$, град	$100 \text{ } \theta_{36}$ θ_{36}		$500 \text{ } \theta_{36}$ θ_{36} ; ^{70}Ga	$103 \text{ } \theta_{36}$ θ_{36} ; ^{70}Ga
	^{12}C	^{70}Ga		
$\theta_{1/2}^s$	$9,3 \pm 0,5$	$11,5 \pm 0,6$ (12)	$5,1 \pm 0,3$ (7)	$4,0 \pm 0,3$ (5)
$\theta_{1/2}^g$	52 ± 3	$51,5 \pm 2,0$	$53 \pm 3,2$	53 ± 6

Note. In brackets are given values, obtained by interpolation of known experimental data.
 Key: (1) - deg. (a) - GeV.

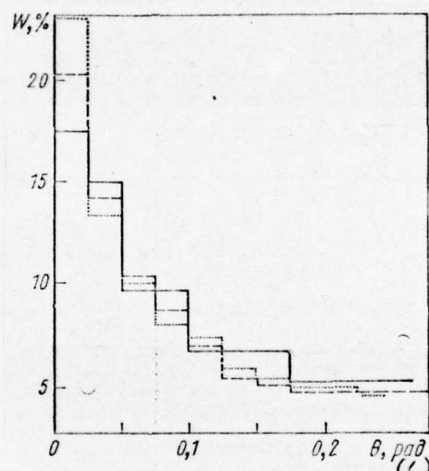


Fig. 364. The angular distribution of the shower particles, which are formed during the interactions of protons 500 GeV in energy with photoemulsion. Continuous histogram is experiment [35]; broken and point histogram - the result of the cascade calculations, made in accordance with account and without taking into account of many-body interactions.

Key: (1). rad.

Page 479.

At the same time one should emphasize that the angular particle distributions in N - N- collisions with $T > 30$ GeV are known badly/poorly and their variation very substantially manifests itself the form of curves Fig. 365 and 366. Specifically, if we for particles, which are born in N - N-collisions, select the distributions, which are more concentrated in regions $\theta \sim 0$ and $\theta \sim \pi$, then this will bring to considerably the more pronounced double-peaked nature in Fig. 365 and 366, but very weakly will pronounce on other design characteristics.

On the histograms of dependence on variables θ or $\cos\theta$ inaccuracies N - N- angular distributions manifest themselves considerably weaker than distributions $W(\lg \lg \theta)$.

Conclusions. We see that the model of the inelastic interactions of high-energy particles with nuclei on the basis of the cascade mechanism, considered as series of two-body interactions, sharply contradicts experiment.

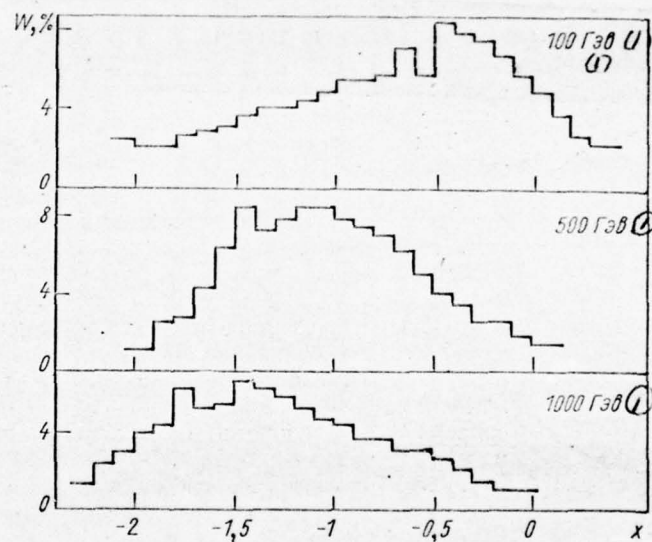


Fig. 365. Dependence of the angular distribution of shower particles depending on alternating/variable $x = \lg \operatorname{tg} \theta$.
Key: (1). GeV.

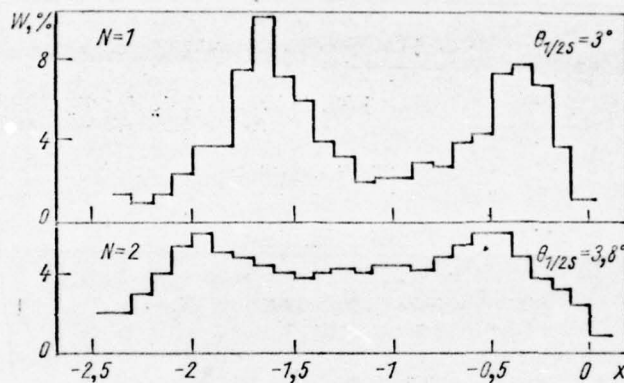


Fig. 366. The angular distribution of shower particles after N of intranuclear collisions, expressed; in alternating/variable $x = \lg \lg \theta$, during interaction $p + {}^{70}\text{Ga}$ with $T = 500 \text{ GeV}$.

Page 480.

The greatest disagreement occurs for many being born particles, which in experiments with $T \gtrsim 100 \text{ GeV}$ proves to be several times less than

this one follows from theory. Other experimental and theoretical characteristics s- and g-particles are distinguished not so strongly. In principle, it would be possible to hope to match these characteristics by the corresponding variation of the utilized during calculations experimental data on π - N- and N - N-interactions (within the limits of their experimental errors). However, in all cases the calculated and experimental values of many being born particles substantially are distinguished.

Since the overestimate of a calculated multitude is connected in essence with the leading particle, and the angular and energy distributions are determined predominantly by the interactions of secondary particles, the further improvement of cascade model must pass first of all in the direction of a reduction in the number of particles, which are formed during the intranuclear interactions of the leading particle. To this reduction, in particular, leads the account of simultaneous absorption by one intranuclear nucleon of the leading particle and even several accompanying particles, which are formed together with it in preceding/previous π - N- or N - N-collision (see Fig. 264). Such many-body interactions are represented by very probable, since particles at high energies escape into narrow solid angle. In the extreme limiting case, when all particles, which are formed during interaction with one nucleon, further are absorbed also by one nucleon, etc (Fig. 367), the

characteristics of nucleon-nuclear and nucleon-nucleon (or respectively pion-nuclear and pion-nucleon interactions are identical.

One should expect that the enlistment of multiple-particle interactions will lead also to an increase in the two-peaked nature of angular distributions $W(\lg \theta)$.

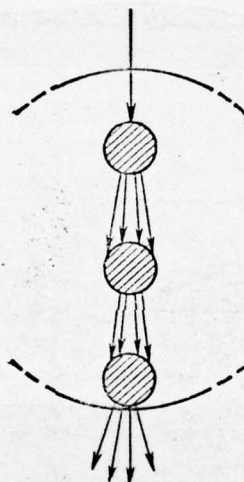


Fig. 367. Example nucleon- of nuclear interaction with very high energy. If energy of the primary nucleon T is so great that the angle of emission of all secondary particles in the laboratory coordinate system becomes very small, all the interaction can turn out to be that which was localized in narrow tunnel. In this case the properties of the shower particles, which escape from nucleus, will be the same as in the case inelastic $N - N$ -collision with energy T .

§83. Account of many-body interactions.

Model and the calculation procedure. The examination of intranuclear cascades with many-body interactions leads to a considerable increase in the labor expense of the calculations, since in this case for each collision of initial particle with nucleus it is required not only to statistically play and to memorize the coordinates of all intranuclear nucleons, but also to preserve in the memory, how many particles already absorbed one or another nucleon. Nevertheless the contemporary high-speed machines, in any case during some simplifications, make it possible to make such calculations with sufficiently good accuracy.

So as the preceding/previous paragraph, we will describe nucleus by the model of fermi gas with sharp boundary ($r_0 = 1.4$).

In usual cascade theory the nucleus is considered as certain continuous medium, each point of which can become the independent center of the emission of new particles. However, if with intranuclear nucleon collides the particle of very high energy, then the range/paths of formed in this case secondary particles frequently terminate at the points, distant from each other at the distances smaller than the diameter of nucleon. In this case it is already necessary to accept into consideration the size/dimensions of intranuclear nucleons and sufficient to accurately know the location of their centers within nucleus.

Page 481.

In the general case this problem is very complex; therefore we will be restricted somewhat simpler picture and will consider that the nucleons are approximately evenly distributed in spherical layers with thickness $\Delta R = \sqrt{3}l/2$, where $l \approx 2.26 \cdot 10^{-13}$ cm. are the average distance between nucleons in nucleus. If in certain layer nucleons cannot be arranged from each other accurately at a distance l , then some two of them let us arrange/locate at a distance, somewhat smaller or larger l . In order to ensure more even distribution, the positions of the centers of nucleons in two adjacent layers let us shift relative to each other (Fig. 368).

The position of each nucleon in nucleus is characterized by three numbers: by the number of the corresponding spherical layer n by angles ϕ^* and θ^* in certain rigidly connected with nucleus coordinate system. Used by us nucleon distribution makes it possible to find simple analytical expression for ϕ^* and θ^* - in this and consists its convenience. In the laboratory coordinate system respectively $\phi = \phi_0 + \phi^*$, $\theta = \theta_0 + \theta^*$, where the common for all nucleons angles ϕ_0 and θ_0 must be developed independently of each other with each new interaction of initial particle with nucleus.

The fundamental block diagram of the calculations is given in Fig. 369. In general terms (parts see in §81 and in chapter 4 and 6) calculations are reduced to the following.

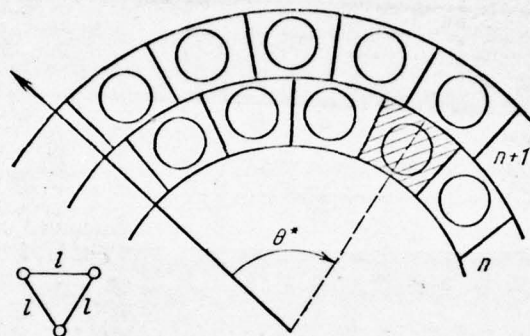


Fig. 368. Nucleon distribution in nucleus. Distance between centers of two any adjacent nucleons is equal l . It is considered that with nucleon interact all particles, caught into the shaded cell.

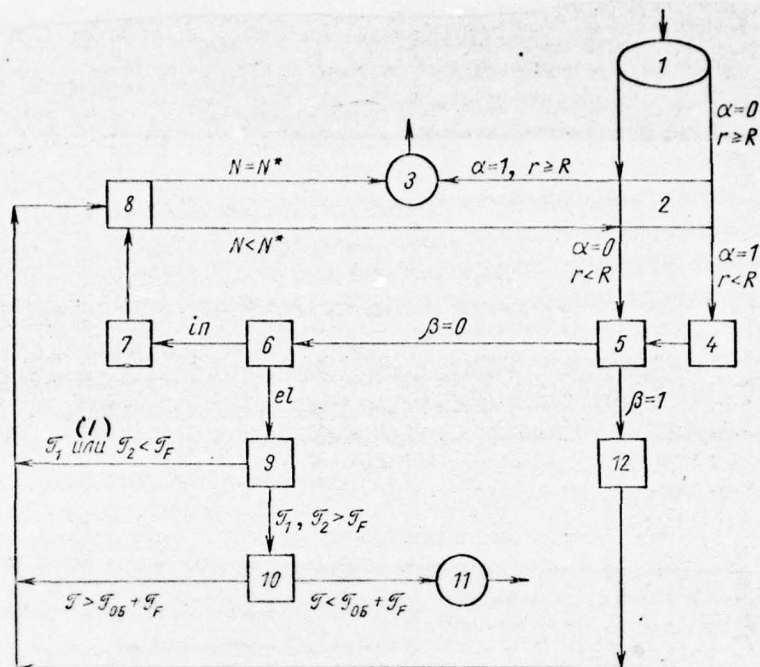


Fig. 369. Diagram of the calculation of intranuclear cascades with many-body interactions.

Key: (1). or.

Page 482.

Block/module/unit 1. Here are determined the coordinates of intranuclear nucleons in the laboratory coordinate system and the entrance point of initial particle into nucleus.

Block/module/unit 2. In terms of the assigned experimental values of total cross sections $\sigma - N - \text{or } N - N\text{-interactions } \sigma_t^{NN}(T)$ and $\sigma_t^{NN}(T)$ on the assumption that the nucleus on the average is the homogeneous medium, is determined the range/path of particle and is calculated the vector of the point of interaction r (for the center of nucleus $r=0$). If $r \gg R$, then depending on whether is examined initial particle either the particle, which was being formed in some preceding/previous intranuclear collision (these cases we will distinguish the values of the parameter $\alpha = 0$ and $\alpha = 1$), is made the passage respectively to block/module/unit 1 or to block/module/unit 3. The number of passages to block/module/unit 1 determines complete reaction cross-section σ_{in} , if the statistician of the played events it is considered sufficient and the calculation on this concludes. If $r < R$, then for $\alpha = 0$ is made the passage to block/module/unit 5, and for $\alpha = 1$ - to block/module/unit 4.

Block/module/unit 3. This is the output unit, where are constructed the total distribution of the different characteristics of the escaping from nucleus particles.

Unit 4. In this unit are calculated the coordinates (n, ϕ, θ) of the intranuclear nucleon, with which occurred the interaction. Let us consider that with nucleon interact all particles whose range/paths conclude in the cell, which corresponds to this nucleon; this answers the simplest assumption about the section of many-body interactions. The cases, in which the number of such particles $n = 1$, let us characterize the parameter $\beta = 0$, the cases with $n > 1$ (many-body interactions) - by the parameter $\beta = 1$. Is calculated the ordinate of the center of nucleon in the laboratory system of coordinates z ; for interaction with the minimum value of z (Fig. 370) one should pass to unit 5.

Unit 5. Is developed Fermi's three-dimensional momentum/impulse/pulse p_F . Taking into account p_F is made the passage to the center-of-gravity system of the colliding particles and to this system of coordinates L' , where $p'_F = 0$ (comp. §45). Further, depending on value β , it is necessary to pass to units 6 or 12.

Unit 6. Over experimental sections $\pi - N-$ and $N - N-$

interactions $\sigma_{el}(T')$ and $\sigma_{in}(T')$, where T' - kinetic energy of particle (pion or nucleon) in system L' , is developed interaction mode is elastic or inelastic - and depending on this is made passage to units 7 and 9.

Unit 7. In this unit is made the calculation of the inelastic collision of two particles. This part of the calculations completely coincides with the appropriate calculation in the preceding/previous paragraph. The angles and the momentum/impulse/pulses of the born particles one should transfer into the laboratory coordinate system, after which necessary to pass to unit 8.

Unit 8. Break of cascade/stage on the assigned number of intranuclear collisions N^* . If the number of preceded collisions $N < N^*$, then for each particle is made the passage to unit 2; but if $N = N^*$, then to unit 3. For the checking of calculations results it is expedient to issue sometimes consecutively for $N^* = 1, 2, 3$; however, for the calculation of complete cascade/stage value N^* is conveniently placed equal to one of the greatest machine numbers, in this case will be knowingly considered all the intranuclear collisions.

Unit 9. This is the unit of the calculation of the elastic collision of two particles. This part of the calculations also repeats the analogous calculations of the preceding/previous paragraph.

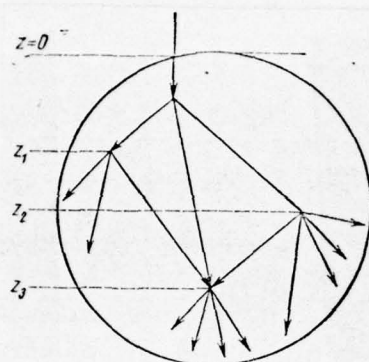


Fig. 370.

Fig. 370. The particles, which were being born in point z , can interact with all nucleons, arranged/located with $z > z_1$. Interactions are examined alternately from $(z_1)_{\text{MH}}$ to $(z_1)_{\text{MRC}}$ in this case automatically are considered all "entanglements" of particle.

Page 483.

If kinetic energies of particles after collision \mathcal{T}_1 and \mathcal{T}_2 turn out to be large energy \mathcal{T}_F , then one should pass to unit 10, but if \mathcal{T}_1 or \mathcal{T}_2 is less \mathcal{T}_F , then it is made passage to unit 8.

Unit 10. Determination of the capture of particles by nucleus. All particles with the energies smaller than energy of cutting $\mathcal{T}_{00} + \mathcal{T}_F$, enter unit 11, particles with energy $\mathcal{T} > \mathcal{T}_{00} + \mathcal{T}_F$ are transferred to unit 8.

Unit 11. In this unit is summarized the excitation energy of nucleus and with the method, described in chapter 6, is calculated the process of its evaporation.

Unit 12. Calculation of many-body interaction. This calculation can be fulfilled, on the whole, on the rules, as for usual two-particle collisions (see unit 7), with the only difference, that

for the characteristic of interaction one should utilize not the kinetic, but free energy

$$\mathcal{E} = [(\sum_i m_i)^2 + (\sum_i p_{iC})^2]^{1/2} - \sum_i m_i, \quad (7.7)$$

which it can be expended on the formation of new particles in the center-of-gravity system. Here m_i mass, p_{iC} the momentum/impulse/pulses of the interacting particles (for intranuclear nucleon-target $p_{iC} = p_{FC}$; see above point/item 5).

For simplification in the calculations entire region of energies is conveniently divided into the intervals: <2; 2-3; 3-7; 7-10; 10-30; >30 GeV. For each of these intervals in the center-of-gravity system must be assigned the angular and energy distributions of the being born particles $W(\theta)$ and $W(\mathcal{E})$, on which are developed the characteristics of these particles. (The separation of the region of energies indicated is utilized only for the calculation of the many-body interactions, about characteristics of which at present we nevertheless can speak only very tentatively; the calculation of two-particle collisions one should, of course, produce during the considerably smaller separation of the region of energies, for example, to eleven intervals, as this was made in the preceding/previous paragraph). As in §81, the laws of conservation of energy and momentum let us consider only on the average for the large number of interactions. This method of the calculation of many-body

interactions was used for the first time in works [3.7-9]. The calculations were made both taking into account the formation of the leading particle and without it. Energy of the leading particle was determined for the assigned value of the coefficient of anelasticity k in formula (7.3) or (7.3a); in this case were examined different values k in range from 0.5 to 0.7.

The fact that substantially isolated on energy are assumed to be a total of one, but not several secondary particles, is caused themes by consideration, that in usual $\pi - N$ - and $N - N$ - collisions is formed the only one leading particle; therefore in the subsequent many-body interactions with the nucleons of nucleus among the initial particles one particle proves to be exceeding on energy others. This particle to a considerable degree determines the kinematics of many-body interaction.

Again let us consider that in the center-of-gravity system the leading particle - nucleon, although in the region of high energies a difference of the masses of particles manifests itself very weakly and the results of the calculations remain virtually the same, if we as the leading particle select π -meson.

It is assumed that after the isolation/evolution of the leading particle, and also when it not at all is considered, the angular and

energy distributions of the being born particles on the average are identical for all types of many-body interactions regardless of the fact, they collide transaction, four or the larger number of particles (some from them can adhere into resonons, form two- or tri-nucleon systems or even compose "fireball" - fireball). Justification to this can be seen in that experimental fact that during annihilation, and also in inelastic π - N- and N - N-interactions in region $T \gg 1$ GeV these distributions very weakly depend on the type of the colliding particles and are determined, in essence, only by the value of energy ϵ [11, 18, 19].

Page 484.

Many-body interactions can, of course, occur and in such a way that the averaging indicated will occur only for part of particles, and remaining particles will have distributions as during elastic scattering. However, at high energies of the section of the elastic interactions of all strongly interacting particles they compose comparatively small portion of their total cross sections; therefore in contemporary stage this elaboration of inelastic many-body interactions is represented by still premature. At the same time we will separately consider the contribution of the elastic diffraction scattering, which corresponds to many-body interactions. In this case let us assume that the section $\sigma_{el} = \sigma_{\text{diff}} = \sigma_t/4$ and scattering occurs on

the average by angle $\theta \sim \lambda/r$, where λ is length of the de Broglie wave of being scattered particle, and $r \approx 10^{-13}$ cm. - the mean radius of multiparticle system, equal by order of value to a radius of strong interactions. In the region of high energies it will not large error consider that energies of particles after scattering remain virtually the same as before scattering; energy of recoil nucleon let us determine from that condition that in the center-of-gravity system this nucleon escapes to the side, opposite to the outgoing directions of the being scattered particles. After relativistic transformation to the laboratory coordinate system kinetic energy of recoil nucleon is approximately 100-150 MeV.

The number of secondary heavy particles \bar{n}_T , which are born in many-body interaction with not very high energies, let us set/assume equal to the total baryon number ($\bar{n}_T = B$), but for the region of very high energies to consider that \bar{n}_T is approximately 20% of total number of secondary particles: $\bar{n}_T = 0,2\bar{n}$. As boundary it is possible to utilize the same value of complete free energy in the center-of-gravity system \mathcal{E} , that one in the case of two-body interactions. If numbers \bar{n} and \bar{n}_T (one or both) turn out to be fractional, then according to the rules, indicated in §81, one should play nearest integer.

Finally angles and energies of all secondary particles,

calculated in unit 12, must be transferred into the laboratory coordinate system, after which it is made passage to unit 8.

Let us examine now the comparison of this model with experiment. In this case since the effect of many-body interactions, generally speaking, can be revealed even with energies of approximately ten gigaelectron-volt, we will not be limited to the region only of superhigh space energies, but let us examine also high accelerative energies, where there are disagreements with usual cascade model.

As already mentioned above, the cascade model in question with many-body interactions phenomenologically considers the contribution of resonances and adhering two-nucleon systems; therefore it is quite interesting to compare it with accelerative data in the region, where these data diverge from usual cascade model.

Photoemulsion data for energies $T = 40-80$ GeV are of now special interest in connection with the experiments, made with accelerator in Serpukhov on 76 GeV.

§84. Nucleon-nuclear collisions

The designed characteristics of shower and cascade g-particles are assembled in Table 112-115 and in Fig. 362-364, 371-373 [4, 8] (with $T \gg 1$ GeV of the property of the interactions of protons and neutrons with nuclei turn out to be identical). For a comparison are shown also the most characteristic experimental data. The calculations are made for the neutral, average-neutral and medium nuclei of photoemulsion. In tables, furthermore, are given the results of calculations for nuclei ^{27}Al and ^{56}Fe . Although for these nuclei now almost there are no experimental numbers, which it would be possible to compare with theory, as a whole Table 112-114 they make it possible with the aid of simple interpolation to obtain the appropriate estimations for compound nuclei, which is important for the calculation of targets in accelerative and space experiments.

Table 112. Average number of particles, which are born during the inelastic interaction of proton with atomic nucleus.

(i) $T_{\text{за}}$	(2) Ядро	\bar{n}_s	\bar{n}_s^{\pm}	\bar{n}_g^{\pm}	\bar{n}_b	\bar{n}_b^{\pm}	\bar{n}_h^{\pm}
6,2	Em	4,3±0,2	2,7±0,1 (2,84±0,05)	2,3±0,1 (3,58±0,11)	6,7±0,3	5,5±0,3	7,8±0,4 (7,7±0,2)
9	LEm	4,8±0,3	2,9±0,2 (3,0±0,2)	1,3±0,1 (1,4±0,1)	—	—	—
	Al	5,2±0,3	3,1±0,2	2,2±0,2	5,8±0,4	4,8±0,4	7,0±0,4
	Fe	5,5±0,3	3,2±0,2	2,4±0,2	6,5±0,4	5,4±0,2	7,8±0,4
	Em	5,7±0,3	3,4±0,2 (3,4±0,2)	2,9±0,1 (3,1±0,4)	6,8±0,3	5,6±0,3 (4,7±0,5)	8,5±0,4 (9,5±0,7)
	HEm	6,1±0,3	3,8±0,2 (4,5)†	3,5±0,2 (4,1±0,5)	8,8±0,5	7,2±0,4 (6,1±0,8)	10,7±0,6 (10,2±1,1)
17	Em	8,3±0,4	5,3±0,3 (5,89±0,06)	3,0±0,1	7,8±0,4	6,0±0,9	9,0±0,4 (8,5±0,1)
25	LEm	7,5±0,4	4,6±0,3 (4,8±0,15)	1,7±0,1 (1,7)†	—	—	—
	Al	7,8±0,5	5,0±0,3	2,1±0,1	6,1±0,4	5,1±0,2	7,2±0,3
	Fe	9,4±0,6	6,0±0,4	3,0±0,2	7,5±0,5	5,7±0,3	8,7±0,5
	Em	9,3±0,5	6,2±0,3 (6,1±0,05)	3,3±0,2 (3,9±0,4)	8,0±0,4	6,4±0,3 (4)†	9,7±0,5 (8)†
	HEm	12,6±0,6	7,9±0,4 (8±1)	4,7±0,3 (7±1)	12,9±0,6	10,5±0,5 (8±1)	15,2±0,8 (14±1)
50	LEm	9,9±0,5	5,6±0,3	1,8±0,1	—	—	—
	Em	12,9±0,5	8,2±0,4	3,4±0,2	10±0,6	7,4±0,3	10,8±0,6
	HEm	16,6±0,8	10,0±0,6	4,4±0,3	14,3±0,7	11,0±0,7	15,4±0,9
60	LEm	10,5±0,5	6,3±0,3	1,6±0,1	—	—	—
	Em	13,6±0,6	8,8±0,4	3,4±0,2	10,4±0,6	7,8±0,4	11,2±0,6
	HEm	17,5±0,8	10,9±0,5	4,5±0,2	14,6±0,7	11,3±0,5	15,8±0,7
80	LEm	11,4±0,6	7,0±0,4	1,7±0,1	—	—	—
	Em	14,6±0,7	9,7±0,5	3,5±0,2	11±0,7	8,2±0,4	11,7±0,6
	HEm	18,7±0,9	11,8±0,6	4,6±0,2	15,2±0,8	11,7±0,6	16,1±0,8
100	LEm	12,1±0,6	7,9±0,4 (7,5)†	1,7±0,1	—	—	—
	Al	13,5±0,9	8,7±0,6	2,7±0,2	7,2±0,5	5,8±0,3	8,5±0,5
	Fe	14,5±1,1	9,9±0,6	3,0±0,2	9,1±0,6	6,9±0,4	9,9±0,6
	Em	16,0±0,8	10,3±0,5 (9,5)†	3,6±0,2 (5)†	11,9±0,8	9,0±0,4 (4)†	12,6±0,6 (8)†
	HEm	19,5±1,0	12,4±0,6	4,5±0,2	15,6±0,8	11,8±0,6	16,3±0,8 (14,5)†
500	LEm	16,3±0,8	10,5±0,5 (10)†	1,9±0,1	—	—	—
	Al	19,4±1,0	12,4±1,0	2,5±0,2	7,1±0,5	5,9±0,3	8,4±0,5
	Fe	24,2±1,6	16,2±1,2	3,5±0,2	9,2±0,6	7,0±0,4	10,5±0,6
	Em	26,0±1,3	18,0±0,9 (18,8±4,2)	3,7±0,2 (≤3,6±0,6)	2,0±0,6	9,3±0,4 (≤6,1±0,9)	13,0±0,6 (≤9,7±1,5)
	HEm	30,2±1,5	19,2±0,9	4,6±0,2	19,2±0,9	14,5±0,7	19,1±0,9 (14,5)†
10 ³	LEm	18,7±0,9	12,1±0,6 (11,5)†	2,0±0,1	—	—	—
	Al	22,0±1,2	14,2±1,0	2,6±0,2	7,3±0,5	5,9±0,3	8,5±0,5
	Fe	29,0±2,0	18,6±1,3	3,3±0,2	9,5±0,6	7,5±0,5	10,8±0,7
	Em	32,5±1,6	20,5±1,1 (20)†	3,6±0,2 (≤35)†	13,1±0,6	10,5±0,5	14,1±0,7
	HEm	38,0±1,9	24,2±1,2	4,9±0,2	19,4±1,0	14,6±0,7	19,5±0,9 (15)†

BEST AVAILABLE COPY

DOC = 77106902

PAGE ~~45~~ 56

Key: (1). GeV. (2). Nucleus.

FOOTNOTE 1. It is obtained by interpolation of known experimental data. ENDFOOTNOTE.

Table 113. Average kinetic energy of particles from inelastic proton-nucleus collision.

(1) $T_{\text{пр}}$	(2) Ядро	$\bar{T}_{\text{п}}, \text{ГэВ}$	$\bar{T}'_{\text{с}}, \text{ГэВ}$	$\bar{T}_{\text{г}}, \text{МэВ}$	$\bar{T}_{\text{б}}, \text{МэВ}$
6,2	Em	—	$1,00 \pm 0,05$	148 ± 7	$10,6 \pm 0,5$
9	LEm	—	$1,6 \pm 0,1$	150 ± 10 (132 ± 20)	—
	Al	—	$1,5 \pm 0,1$	140 ± 10	$10,5 \pm 0,7$
	Fe	—	$1,4 \pm 0,1$	140 ± 10	$10,3 \pm 0,8$
	Em	—	$1,30 \pm 0,06$ ($1,6 \pm 0,3$)	142 ± 7 (120 ± 10)	$10,6 \pm 0,5$ (11 ± 1)
	HEm	—	$1,20 \pm 0,06$ (1) †	140 ± 7	$11,5 \pm 0,6$
17	Em	—	$1,8 \pm 0,1$	146 ± 7 (170 ± 10)	$12,5 \pm 0,6$
25	LEm	—	$3,2 \pm 0,2$ ($2,2 \pm 0,4$)	150 ± 10	—
	Al	—	$3,0 \pm 0,2$	140 ± 10	$11,3 \pm 0,8$
	Fe	—	$2,6 \pm 0,2$	140 ± 10	$11,1 \pm 0,8$
	Em	—	$2,4 \pm 0,1$ ($2,3 \pm 0,2$)	140 ± 7	$12,5 \pm 0,6$
	HEm	—	$1,8 \pm 0,1$ ($1,6 \pm 0,2$)	140 ± 7	$13,4 \pm 0,7$
50	LEm	20 ± 1	$3,1 \pm 0,2$	155 ± 8	—
	Em	18 ± 1	$2,6 \pm 0,2$	150 ± 8	$13,0 \pm 0,7$
	HEm	16 ± 1	$2,1 \pm 0,2$	140 ± 8	$13,5 \pm 0,8$
60	LEm	$25 \pm 1,2$	$3,1 \pm 0,2$	150 ± 8	—
	Em	$23 \pm 1,1$	$2,6 \pm 0,2$	145 ± 7	$13,2 \pm 0,7$
	HEm	$21 \pm 1,1$	$2,2 \pm 0,1$	150 ± 8	$13,6 \pm 0,7$
80	LEm	$45 \pm 2,2$	$3,1 \pm 0,2$	140 ± 7	—
	Em	38 ± 2	$2,6 \pm 0,2$	150 ± 8	$13,6 \pm 0,7$
	HEm	35 ± 2	$2,3 \pm 0,1$	145 ± 7	$13,7 \pm 0,7$
100	LEm	65 ± 3	$3,1 \pm 0,2$ ($2,9 \pm 0,3$)	160 ± 10	—
	Al	62 ± 4	$3,0 \pm 0,2$	145 ± 10	$13,5 \pm 0,9$
	Fe	$53 \pm 3,5$	$2,9 \pm 0,2$	140 ± 10	$13,0 \pm 0,9$
	Em	$50 \pm 2,5$	$2,8 \pm 0,2$ ($2,4 \pm 0,9$)	160 ± 8	$14,0 \pm 0,7$
	HEm	46 ± 2	$2,5 \pm 0,1$	150 ± 7	$14,0 \pm 0,7$
500	LEm	323 ± 15	$10,4 \pm 0,5$	160 ± 10	—
	Al	310 ± 21	$9,6 \pm 0,6$	140 ± 10	14 ± 1
	Fe	265 ± 18	$9,3 \pm 0,6$	145 ± 10	$13,5 \pm 0,9$
	Em	250 ± 13	$9,1 \pm 0,5$	150 ± 8	$14,0 \pm 0,7$
	HEm	230 ± 11	$8,7 \pm 0,4$	140 ± 7	$14,5 \pm 0,7$
10 ³	LEm	650 ± 30	$18,5 \pm 0,9$	160 ± 50	—
	Al	615 ± 40	$17,3 \pm 1,2$	145 ± 10	14 ± 1
	Fe	530 ± 35	$15,8 \pm 1,2$	145 ± 10	14 ± 1
	Em	500 ± 25	$15,3 \pm 0,9$	140 ± 7	$14,7 \pm 0,8$
	HEm	460 ± 23	$13,9 \pm 0,7$	150 ± 7	$15 \pm 0,8$

BEST AVAILABLE COPY

DOC = 77106902

PAGE ~~4~~ 58

Key: (1). GeV. (2). Nucleus. (3). MeV.

FOOTNOTE 1. It is obtained by interpolation of known experimental data. ENDFOOTNOTE.

Table 114. The mean angle, into which escapes the half of all particles, which are born in inelastic proton-nucleus collisions.

$T, \text{ Гэв}$ ⁽¹⁾	Ядро ⁽²⁾	$\theta_{1/2 s}, \text{ град}$ ⁽³⁾	$\theta_{1/2 g}, \text{ град}$ ⁽³⁾
6,2	Em	$29 \pm 1,5$ ($26,5 \pm 0,7$)	66 ± 3 (49 ± 2)
9	LEm	21 ± 1 ($22,5 \pm 1,0$)	58 ± 3 ($56,5 \pm 3,0$)
	Al	$23 \pm 1,5$	61 ± 4
	Fe	$24 \pm 1,6$	62 ± 4
	Em	$27 \pm 1,5$ ($25 \pm 1,5$)	64 ± 3 (65 ± 3)
	HEm	$28,7 \pm 1,5$ ($27,5 \pm 1,5$)	69 ± 3 (65 ± 3)
17	Em	22 ± 1	64 ± 3
25	LEm	$14 \pm 0,7$	61 ± 3
	Al	16 ± 1	63 ± 4
	Fe	$17 \pm 1,3$	63 ± 4
	Em	19 ± 1 ($20,0 \pm 1,8$)	64 ± 3
	HEm	21 ± 1	64 ± 3 (60 ± 6)
50	LEm	$11 \pm 0,6$	60 ± 3
	Em	$16 \pm 0,9$	$63 \pm 3,2$
	HEm	$17,4 \pm 1,1$	65 ± 4
60	LEm	$10,2 \pm 0,5$	$61 \pm 3,1$
	Em	$14,9 \pm 0,7$	$64 \pm 3,2$
	HEm	$16,5 \pm 0,8$	$64 \pm 3,2$
80	LEm	$8,9 \pm 0,4$	60 ± 3
	Em	$13,2 \pm 0,7$	$62 \pm 3,1$
	HEm	$14,9 \pm 0,7$	$61 \pm 3,1$
100	LEm	$8,0 \pm 0,4$	60 ± 3
	Al	$9 \pm 0,6$	64 ± 4
	Fe	$12 \pm 0,8$	61 ± 4
	Em	$12,4 \pm 0,8$ (12) #	$65 \pm 3,1$
	HEm	$14,6 \pm 0,9$	68 ± 3
500	LEm	$4,5 \pm 0,2$	61 ± 3
	Al	$5,1 \pm 0,3$	62 ± 4
	Fe	$6,0 \pm 0,3$	62 ± 11
	Em	$7,0 \pm 0,4$ (7) #	64 ± 3
	HEm	$9,0 \pm 0,5$	71 ± 3
10 ³	LEm	$4,0 \pm 0,2$	62 ± 3
	Al	$4,6 \pm 0,3$	63 ± 4
	Fe	$4,9 \pm 0,3$	60 ± 4
	Em	$6,0 \pm 0,3$ (5) #	$65 \pm 3,1$
	HEm	$7,0 \pm 0,3$	72 ± 3

BEST AVAILABLE COPY

Key: (1). GeV. (2). Nucleus. (3). deg. the -----

FOOTNOTE 1. It is obtained by interpolation of known experimental data. ENDFOOTNOTE.

Page 488.

A good agreement of calculated values in tables with known experimental values makes it possible to hope for the satisfactory agreement of theory with experiment and at other values of A and T . All errors in the calculated values indicated purely statistical. Since the number of designed cascade/stages somewhat changed from one case to the next, sometimes it proves to be that the equal values have the being distinguished errors.

Besides the results, which relate to the region of the superhigh energies $T > 100$ GeV, the given data include also the results of the calculations, which relate to the region of the accelerative energies $T \approx 5-80$ GeV.

The initial series of calculations was made on the assumption that all secondary particles, which were being formed during nucleon

multiparticle collision, fly away in the center-of-gravity system isotropically and have the identical energy distribution, close to the average distribution from inelastic π - N- and N - N-interactions (this version is close to statistical theories of Fermi's type).

With the space energies $T \gtrsim 100$ GeV the agreement with experiment in this case, generally speaking, is noticeably better than in the case of the cascade/stage, which does not consider many-body interactions; however, the value of the transverse impulse of shower particles considerably exceeds that observed in experiment. For example, taking into account interaction with the medium nucleus of photoemulsion with $T = 20-100$ GeV $\bar{p}_{\perp s} = 0,9 \pm 0,1$ GeV/s, while experimental value $\bar{p}_{\perp s} = 0,4$ GeV/s. Substantially overstated in comparison with experiment turns out to be the average kinetic energy of shower particles $\bar{\mathcal{E}}$. For example, with $T = 100$ GeV it is 7.5 ± 0.5 GeV, and experimental value 2.4 ± 0.9 GeV. The attempt to lower $\bar{p}_{\perp s}$ and $\bar{\mathcal{E}}$ with the appropriate change in the momentum distributions leads to the inadmissible increase in many shower particles \bar{n}_s . The noticeable disagreement of experimental and theoretical values occurs already in the region of the accelerative energies $T = 10-20$ GeV.

Table 115. Average transverse particle momentum q_{\perp} , MeV/s.

(1) $T, \text{ГэВ}$	(2) Ядро	$\bar{p}_{\perp g}$	(1) $T, \text{ГэВ}$	(2) Ядро	$\bar{p}_{\perp g}$
6,2	Em	340 ± 17	100	LEm	360 ± 20
9	Al	340 ± 20		Al	370 ± 25
	Fe	(344 ± 20)		Fe	365 ± 25
	Em	350 ± 20		Em	350 ± 18
		355 ± 25			(400 ± 100)
	HEm	340 ± 17	500	HEm	360 ± 18
25		(350 ± 20)		LEm	360 ± 20
		340 ± 25		Em	350 ± 18
		(354 ± 20)		HEm	370 ± 18
	LEm	350 ± 20			
	Al	370 ± 25	10 ³	LEm	360 ± 20
50	Fe	380 ± 25		Al	390 ± 26
	Em	350 ± 18		Fe	390 ± 26
		(265 ± 45)		Em	350 ± 18
	HEm	340 ± 17		HEm	360 ± 18
50	LEm	350 ± 18			
	Em	345 ± 21			
	HEm	460 ± 18			

Note. In brackets are given experimental values (see §35).

Key: (1) Gel; (2) nucleus.

Page 489.

The account of the anisotropy of the escape of the being born particles in the center-of-gravity system does not remove these disagreements, if we consider as before that the angular and energy distributions of the being born particles do not depend on their waste.

In the following series of the calculations of energy and the angles of emission of π -mesons and heavier particles were considered different. In this case it was assumed that as in elementary π - N- and N - N- interactions, the mesons and heavy particles try to preserve the direction of the motion primary meson and nucleon. This made it possible to considerably improve agreement with experiment. Specifically, with the accelerative energies $T = 6-25$ GeV was possible to obtain the agreement with all known photoemulsion data; however with high energies to obtain a good agreement with experiment and in this case very difficultly. Transverse impulse and energy of the being born particles remain as before more than experimental. For example, at the worst, when with $T \approx 500$ GeV all the being born π -mesons are assumed to be those which escape in the

center-of-gravity system strictly forward, and nucleons - back/ago, $\bar{p}_{1s} = 0,60 \pm 0,05$ GeV/s. Under more real assumptions $\bar{p}_{1s} \simeq 0,7$ GeV/s.

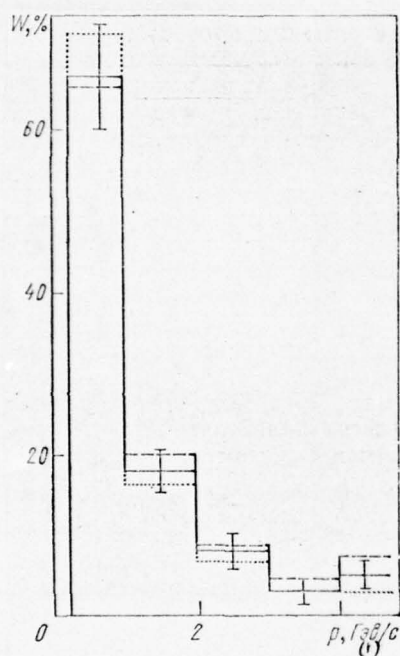


Fig. 371.

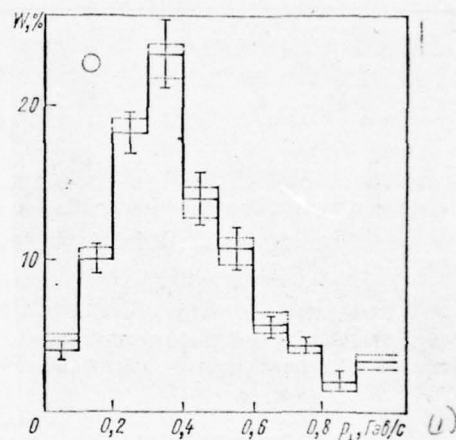


Fig. 372.

Fig. 371. The momentum distribution of the shower particles, which

are formed in the inelastic interactions of the protons of energy 25 GeV with the heavy nuclei of photoemulsion. Continuous histogram is experiment [24]; broken and point histogram - the calculation, made in accordance with account and without taking into account of many-body interactions within nucleus.

Key: (1). GeV/s.

Fig. 372. Distribution according to the transverse impulse of shower particles from the inelastic interactions of protons with the heavy nuclei of photoemulsion during $T = 25$ GeV. All designations are the same as in Fig. 371. Experimental histogram is taken from work [24].

Key: (1). GeV/s.

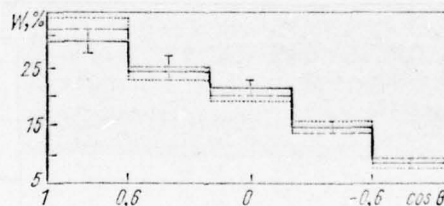


Fig. 373. The angular distributions of the cascade g-particles, which are formed during the interaction of the protons of energy 25 GeV

with the heavy nuclei of photoemulsion. All designations are the same as in Fig. 371. Experimental histogram is taken from work [24].

Page 490.

Agreement with space photoemulsion data succeeds in obtaining only in such a case, if one assumes that during many-body interactions, just as with high-energy inelastic π - N- and N - N- interactions, is formed the leading particle, which takes away 50-70% of entire initial energy.

In the region of space energies the variation of the coefficient of anelasticity in interval of 0.5-0.7 changes the average results of the calculations for 10-20%. These changes do not exceed the limits of the accuracy of known now experimental data; all the given in tables and in figures numerical results of the calculations are related to values of $k = 0.7$ for inelastic two-body interactions and $k = 0.5$ for many-body interactions (in the center-of-gravity system).

It should be noted that the assumption about the leading particle corresponds to the picture of the peripheral interactions of several colliding particles, for calculation of which it is possible to utilize usual diagram methods (see below). However, in this stage

of the calculations more interesting it is represented to determine the characteristics of many-body interactions from comparison with experiment.

The obtained thus angular and energy distributions of pi-mesons and heavy particles from many-body interactions for several energy ranges \mathcal{E} are given in Fig. 374 and 375. These distributions very close to the average particle distributions from inelastic π - N-interactions and comparatively slowly change with an increase of energy of the colliding particles ¹.

FOOTNOTE ¹. Nearness of distribution for many-body interactions precisely to π - N-, but not to N - N-interactions, it is possible to explain themes that at high energies the shower particles within nucleus consist in essence of π -mesons. ENDFOOTNOTE.

In the region of accelerative energies the special account of the leading particle little changes the results of the calculations, since its parameters still comparatively differ little from the parameters of remaining particles, although for the better/best agreement of the calculations with experiment the account of the contribution of the leading particle is very desirable in this case

(specifically, this somewhat it lowers theoretical values of set s- and g-particles).

Of course, to the parts of distributions in Fig. 374 and 375 now thus far still it cannot be been related too seriously: they noticeably change from one version of the calculation to another. Are more reliable the following two qualitative conclusions: the very fact of the existence of many-body interactions and that that the characteristics of particles, which are formed during such interactions, strongly do not differ from the case of usual two-body interactions at high energies, in particular, the presence of the leading particle and the asymmetric character of the angular distributions of remaining particles. For the more confident conclusions are necessary the detailed and precise experimental data on the interactions of particles with atomic nuclei with $T \gg 10 \text{ GeV}$.²

FOOTNOTE 2. In I. Z. Artykova's work [1] was undertaken the attempt to obtain the qualitative representations of the properties of many-body interactions on the basis of peripheral polar model (about this model see, for example, chapter XI in monograph [39]). As an example was examined the collision of three nucleons with one-pion exchange. The results of the calculations confirm above conclusions

indicated about the properties of many-body interactions.

ENDFOOTNOTE.

Theoretical data in Table 112-115 and in Fig. 362-364, 371-373 are acquired with the aid of the distributions, shown in Fig. 374 and 375.

As already mentioned, the section of the inelastic interaction of high-energy nucleon with nucleus wholly is determined by section $\sigma_t(NN)$ and therefore it turns out to be one and the same independent of assumptions about many-body interactions (see Table 107). As concerns many shower particles, from data Table 112 evidently that the account of many-body interactions substantially reduces the degree of increase $\bar{n}_s(T)$. The same can be said about many g-particles: in the model in question it in accordance with experiment with $T \gg 1$ GeV in practice does not depend on energy.

Page 491.

More badly is matter with the calculation of many low-energy b-particles. Agreement with experiment here occurs only in the region of accelerative energies, with $T \gg 10$ GeV theoretical values several times more experimental ¹.

FOOTNOTE ¹. For light nuclei evaporative model is knowingly inapplicable; therefore values \bar{n}_h and \bar{n}_b for LEm Table 112 shows. ENDFOOTNOTE.

The latter especially one can see well from the comparison of experimental and computed values \bar{n}_h (let us note that $\bar{n}_g^{\text{reop}} \simeq \bar{n}_g^{\text{stch}}$).

Disagreements are caused themes that the excitation of the nucleus, which remains after the passage of the intranuclear cascade, initiated by particle with an energy of $T \gg 10$ GeV, frequently turns out to be the so large that the usual theory of evaporation, used for the calculation of values \bar{n}_b in Table 112, becomes actually inapplicable and can give only roughly estimated results. For the description of the "luminescence" of residual-nucleus are more suitable the approaches of the type of the examined in the preceding/previous chapter nonequilibrium approach/approximation.

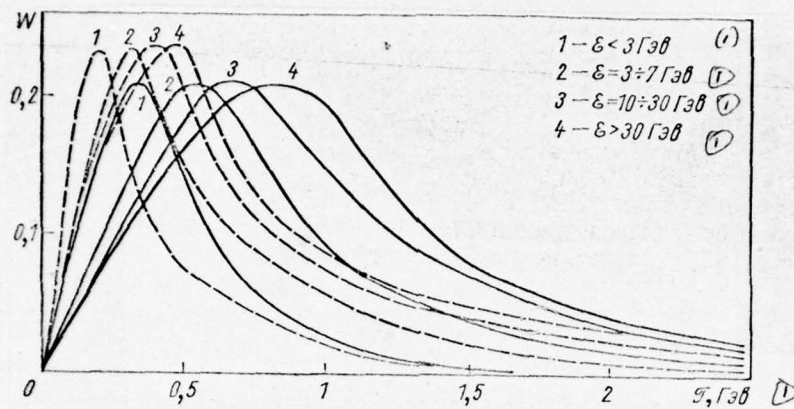


Fig. 374. Energy particle distributions, which are born in inelastic many-body interaction in the center-of-gravity system (ϵ - total energy of the multiparticle system, which can be expended on the formation of new particles; unbroken curves are the heavy particles, broken lines are π -mesons).

Key: (1) - GeV.

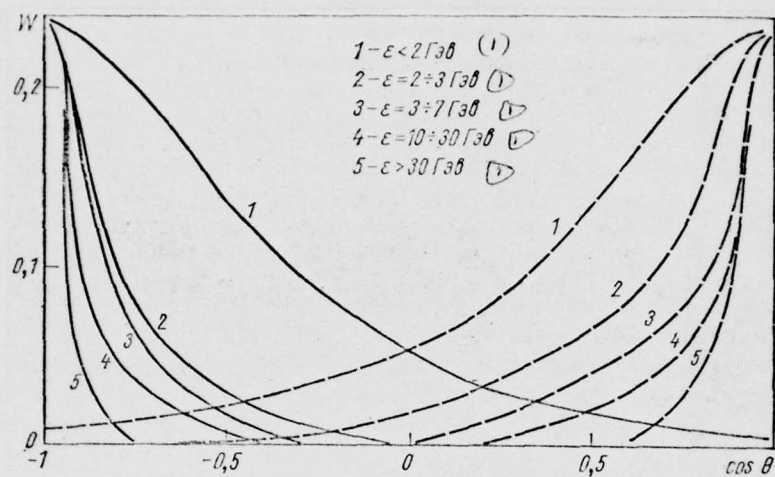


Fig. 375. Angular particle distributions, which are born in inelastic many-body interaction (in the center-of-gravity system). All designations are the same as in Fig. 374.

Key: (1). GeV.

Page 492.

Another reason for the disagreement of experimental and theoretical values \bar{n}_b is connected with the fact that at high energies is great the section of the formation of heavy fragments with large values of mass number $A > 4$; in works [4, 8], whence are taken data Tables 112, this effect was not considered. Supplementary errors into the determination of excitation energy were introduced by the inaccurate statistical account of the law of conservation of energy.

All these questions require also further refinement. (In this connection it is very interesting to compare the results of the calculations with experiment in the area $T \sim 50$ GeV).

During passage from light nuclei to heavy the number of shower particles grow/rises approximately proportionally A^α ($\alpha < 1$), but number g- and b- particles increases noticeably faster. Being born g- and b-particles they consist virtually by pillar of nucleons, the portion of pi-mesons in them is very small. This conclusion will agree well with experiment.

Table 113 gives the corrected values of the average kinetic energy of all being born shower particles minus leading particle ($\bar{\mathcal{E}}_s'$)

and separately the value of energy of this particle $\bar{\mathcal{E}}_n$. The corresponding average nuclear coefficient of anelasticity $\bar{k}_{nd} \simeq (T - T_n)/T$ does not depend on energy T and during passage from light/lungs to heavy photoemulsion nuclei grow/rises with an increase in mass number A . The portion of the primary energy, taken away by the leading particle $(=1 - \bar{k}_{nd})$ is approximately 650/c for a light/lung a total of about 450/o for the heavy nucleus of photoemulsion.

It is understandable that designed values $\bar{\mathcal{E}}_n$ and \bar{k}_{nd} are very sensitive to assumption about the value of the coefficient of anelasticity in the elementary event/report k .

In the region of the accelerative energies $T < 30$ GeV, where the characteristics of the leading particle strongly do not differ from the characteristics of remaining particles, the leading particle was not isolated and value $\bar{\mathcal{E}}_n$ in Table 113 for these energies were not shown.

The pulse and energy distributions of shower particles, calculated taking into account many-body interactions during $T \ll 100$ GeV, are sufficiently close to the distributions, obtained within the framework of usual cascade theory (see Fig. 362 and 371); at large values of T shower particles in theory with many-body interactions possess considerably greater energies. One should emphasize that

values $\bar{\mathcal{E}}_s$ strongly change depending on assumptions about the value of the coefficient of the anelasticity of many-body interaction.

Table 113 shows that the average kinetic energies g- and b-particles, $\bar{\mathcal{E}}_g$ and $\bar{\mathcal{E}}_b$, are virtually constant and depend neither on T nor on A.

From the fact that above was said about the calculation of the contribution of evaporative particles, it follows that values $\bar{\mathcal{E}}_b$ in Table 113 can be examined only as very estimated (specifically, certain increase in the energy of b-particles with an increase of T connected with inaccuracies in the calculation).

Table 114 gives the corrected values of the angles $\theta_{1/2s}$ and $\theta_{1/2g}$, into which escapes respectively the half shower and the half of cascade g-particles (evaporative b-particles fly away isotropically).

Experimental and theoretical angular distributions are compared in Fig. 364 and 373.

The half angle of emission of s-particles is approximately proportional to mass number A^{α} and rapidly decreases with an increase of energy of initial particle; the half angle of emission of g-particles very weakly depends on value A and is not sensitive to the value of energy T.

Both in the region of accelerative energies and during $T > 100$ GeV theoretical angular distributions will agree well with experiment and are sufficiently weakly sensitive to the contribution of many-body interactions, although the account of the latter somewhat improves agreement with experiment.

Page 493.

Above already repeatedly it was noted that a good agreement of theoretical and experimental angular distributions to a considerable degree is the consequence of the effect of the relativistic compression of angles during passage to the laboratory coordinate system.

Figure 362 and 372 shows the distributions of the transverse impulse of the being born particles. In an entire region of energies $T \gg 1$ GeV the experiment and theory completely satisfactorily agree, especially if we consider many-body interactions. At the same time average theoretical values of the transverse impulse of shower particles are somewhat overstated in comparison with experimental. In the case of interactions with photoemulsion, the latter in an entire region of energies $T \approx 10-10^3$ GeV are approximately 400 MeV/s, while computed values with $T = 10, 10^2$ and 10^3 GeV are equal to with respect $430 \pm 20, 480 \pm 25, 500 \pm 25$ MeV/s. The disagreement

between theory and experiment small can be removed, if we consider the correlations of the angular and momentum distributions of the being born particles (see §50).

Value \bar{p}_{\perp} somewhat increases with passage to more heavy nuclei; for example, with $T = 100$ GeV for interactions with the groups of the nuclei of photoemulsion LEm, Em, HEm value \bar{p}_{\perp} equally with respect 435 ± 30 , 480 ± 25 and 480 ± 20 MeV/s.

The average transverse particle momentum q_{\perp} , as is evident from Table 115, within the limits of statistical errors in the calculation remains constant in all energy range $T \approx 10-10^3$ GeV and does not depend on the type of target nucleus; the results of the calculations completely satisfactorily agree with known experimental values.

Figure 376 and 377 shows the relative contribution of many-body interactions in intranuclear cascade (with respect to the total number of elastic and inelastic intranuclear collisions). As is evident, already with energy $T = 10$ GeV this interaction mode is approximately 30% of all interactions; however, the characteristics of the being born in this case particles relatively differ little from the fact that occurs in the usual collision of two particles. Noticeable differences begin to be exhibited only with the energies, greater than several dozen gigaelectron-volt ¹.

FOOTNOTE ¹. It should be noted that the great contribution of many-body interactions with $T \sim 10$ GeV is caused partly themes that in the calculations was not considered a decrease in the nuclear density, the contribution of resonances etc., and all the deviations from usual cascade model were approximated by many-body interactions.

ENDFOOTNOTE.

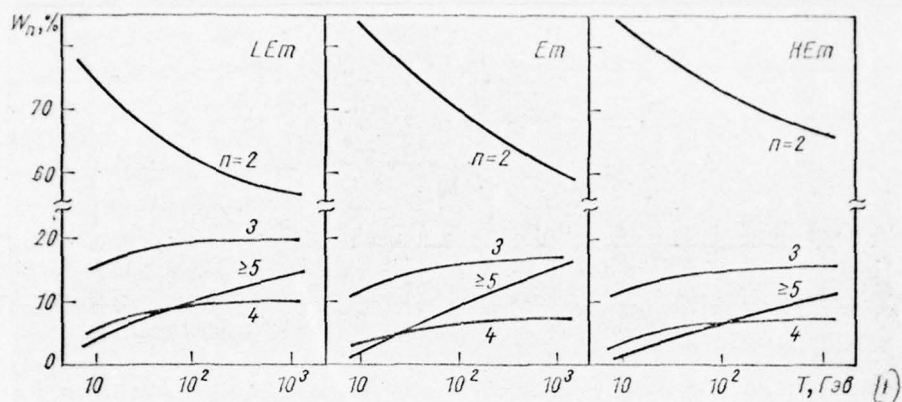


Fig. 376. The relative number of intranuclear collisions with n by particles in the initial state ("n-partial" collisions).

Key: (1). GeV.

The contribution of many-body interactions more distinct is exhibited in light nuclei; in heavy nuclei it somewhat is shaded by the effect of the two-body interactions whose probability it grow/rises in proportion to shower particles they spend its energy in consecutive intranuclear collisions.

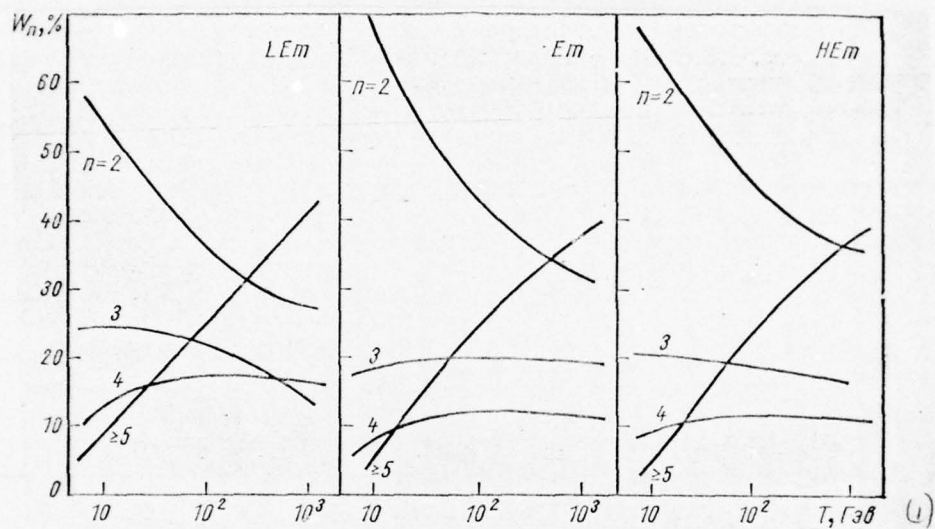


Fig. 377. The relative percentage of particles, which participate in n -partial intranuclear collisions (n of particles in the initial state).

Key: (1) - GeV.

§85. Interactions of π -mesons with nuclei.

The results of cascade calculations (see Table 116-119 and Fig. 378) are obtained by very close to the fact that occurs for nucleon-nuclear interactions. All these data are related in the accuracy to of themes to the approach/approximations themselves and assumptions about the properties of many-body interactions within nucleus, as in the examined above case of nucleon- nuclear collisions; no changes in the program of the calculations were made.

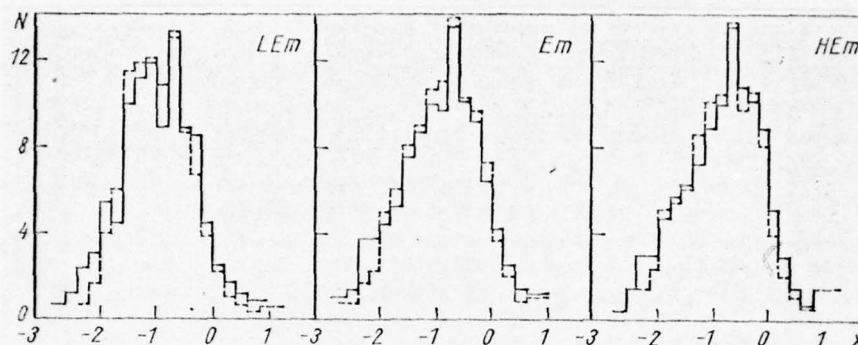


Fig. 378. Distribution according to value $x = \lg \tg \theta$ the charged shower particles, which are born in the inelastic interactions of pi-mesons with the nuclei of photoemulsions at $T \approx 200$ GeV.

Continuous histograms are an experiment of Giyerul, etc. [25], dotted line is the calculation with the drawing of energy of primary mesons according to the real distribution of their energies, which was being observed in work [25].

Table 116. Average number of particles, which are born during inelastic pion- nuclear interaction.

$T, \text{ГэВ}$	Ядро	\bar{n}_s	\bar{n}_s^{\pm}	\bar{n}_g^{\pm}	\bar{n}_b	\bar{n}_b^{\pm}	\bar{n}_h^{\pm}
9	LEm	3,5 \pm 0,2	2,1 \pm 0,2	1,1 \pm 6,1	—	—	—
	Al	4,4 \pm 0,2	2,6 \pm 0,1	1,4 \pm 0,1	5,2 \pm 0,3	4,3 \pm 0,2	5,7 \pm 0,3
	Fe	4,8 \pm 0,2	2,8 \pm 0,2	2,1 \pm 0,1	6,1 \pm 0,3	5,1 \pm 0,3	7,2 \pm 0,4
	Em	5,0 \pm 0,3	3,0 \pm 0,2	2,6 \pm 0,2	6,4 \pm 0,3	5,3 \pm 0,3	7,9 \pm 0,4
	HEm	6,0 \pm 0,3	3,7 \pm 0,2 (4,5) \uparrow	3,3 \pm 0,2 (3,5) \uparrow	8,6 \pm 0,4	7,0 \pm 0,4 (9,5) \uparrow	10,3 \pm 0,5 (13) \uparrow
25	LEm	5,8 \pm 0,3	3,6 \pm 0,2 (5) \uparrow	1,4 \pm 0,1	—	—	—
	Al	7,0 \pm 0,3	4,4 \pm 0,2	1,7 \pm 0,1	5,9 \pm 0,3	5,0 \pm 0,2	6,7 \pm 0,3
	Fe	8,5 \pm 0,4	5,4 \pm 0,3	2,6 \pm 0,2	7,3 \pm 0,3	5,5 \pm 0,3	8,1 \pm 0,4
	Em	8,8 \pm 0,4	5,7 \pm 0,3 (6) \uparrow	3,1 \pm 0,2 (3) \uparrow	7,8 \pm 0,4	5,9 \pm 0,3 (8) \uparrow	9,0 \pm 0,4 (11) \uparrow
	HEm	11,0 \pm 0,5	6,8 \pm 0,4 (7,5) \uparrow	3,8 \pm 0,2 (4) \uparrow	11,5 \pm 0,5	9,3 \pm 0,4	13,1 \pm 0,6
50	LEm	8 \pm 0,4	4,6 \pm 0,3	1,5 \pm 0,1	—	—	—
	Em	12 \pm 0,4	7,2 \pm 0,4 (8) \uparrow	3,2 \pm 0,2 (3) \uparrow	9,4 \pm 0,4	6,7 \pm 0,4	9,7 \pm 0,5
	HEm	14,9 \pm 0,6	8,8 \pm 0,5	3,9 \pm 0,2	12,6 \pm 0,6	9,7 \pm 0,7	13,6 \pm 0,8
60	LEm	8,4 \pm 0,4	5,1 \pm 0,3	1,6 \pm 0,1	—	—	—
	Em	12,9 \pm 0,5	7,8 \pm 0,4	3,3 \pm 0,2	9,8 \pm 0,4	7,0 \pm 0,4	10,3 \pm 0,5
	HEm	15,8 \pm 0,7	9,3 \pm 0,5	4,0 \pm 0,2	12,9 \pm 0,6	10,5 \pm 0,5	14,5 \pm 0,6
80	LEm	9,3 \pm 0,5	5,8 \pm 0,3	1,7 \pm 0,1	—	—	—
	Em	14,2 \pm 0,6	8,7 \pm 0,4	3,4 \pm 0,2	10,5 \pm 0,5	7,6 \pm 0,4	11 \pm 0,6
	HEm	17,3 \pm 0,8	10,4 \pm 0,5	4,1 \pm 0,2	13,4 \pm 0,7	11,0 \pm 0,6	15,1 \pm 0,7
100	LEm	10,0 \pm 0,5	6,5 \pm 0,3	1,6 \pm 0,1	—	—	—
	Al	11,7 \pm 0,5	7,3 \pm 0,4	1,9 \pm 0,2	6,7 \pm 0,3	5,4 \pm 0,3	7,3 \pm 0,3
	Fe	14,1 \pm 0,7	9,3 \pm 0,4	2,8 \pm 0,2	8,5 \pm 0,4	6,6 \pm 0,3	9,4 \pm 0,4
	Em	15,4 \pm 0,8	9,8 \pm 0,5	3,2 \pm 0,2	11,0 \pm 0,5	8,6 \pm 0,4	11,8 \pm 0,6
	HEm	18,5 \pm 0,9	11,3 \pm 0,5 (12,5) \uparrow	4,1 \pm 0,2	13,8 \pm 0,6	10,5 \pm 0,5	14,6 \pm 0,7 (11,5) \uparrow
200	LEm	15 \pm 0,6	9,7 \pm 0,4 (8,0 \pm 0,9)	1,7 \pm 0,1	—	—	—
	Em	17,5 \pm 1,1	11,2 \pm 0,6 (10,7 \pm 0,9)	3,9 \pm 0,3	12,1 \pm 0,6	9,4 \pm 0,5	13,3 \pm 0,4
	HEm	24 \pm 1,4	15,4 \pm 0,7 (14,7 \pm 2)	4,7 \pm 0,3	17,0 \pm 0,9	13,1 \pm 0,7	17,8 \pm 0,9
500	LEm	15,5 \pm 0,8	10,0 \pm 0,5	1,9 \pm 0,1	—	—	—
	Al	18,6 \pm 0,9	11,8 \pm 0,6	2,2 \pm 0,1	7,1 \pm 0,3	5,8 \pm 0,3	8,0 \pm 0,4
	Fe	22,6 \pm 1,1	15,2 \pm 0,7	3,1 \pm 0,2	9,3 \pm 0,4	7,1 \pm 0,3	10,2 \pm 0,5
	Em	23,8 \pm 1,2	15,9 \pm 0,8 (12,7 \pm 0,9)	3,6 \pm 0,2	11,8 \pm 0,5	9,1 \pm 0,4	12,7 \pm 0,6
	HEm	29,9 \pm 1,5	18,8 \pm 0,9	4,4 \pm 0,2	17,9 \pm 0,9	13,5 \pm 0,7	17,9 \pm 0,9
10 ³	LEm	17,3 \pm 0,8	11,2 \pm 0,5	2,0 \pm 0,1	—	—	—
	Al	19,4 \pm 1,0	12,5 \pm 0,6	2,4 \pm 0,2	7,2 \pm 0,4	5,8 \pm 0,3	8,0 \pm 0,4
	Fe	27,2 \pm 1,4	17,4 \pm 0,9	3,3 \pm 0,2	9,4 \pm 0,5	7,4 \pm 0,3	10,7 \pm 0,5
	Em	30,1 \pm 1,5	19,0 \pm 1,0	3,8 \pm 0,2	11,8 \pm 0,6	10,2 \pm 0,5	14,0 \pm 0,7
	HEm	35,4 \pm 1,8	22,7 \pm 1,1	4,7 \pm 0,2	18,7 \pm 0,9	14,1 \pm 0,7	18,8 \pm 0,9

DOC = 77106902

PAGE ~~57~~84

Key: (1). GeV. (2). Nucleus.

FOOTNOTE ¹. It is obtained by interpolation of known experimental data. ENDFOOTNOTE.

Page 496.

Table 117. Average kinetic energy of particles from inelastic pion-nuclear collision.

$T, \text{ Гэв}$ ⁽¹⁾	Ядро ⁽²⁾	$\bar{T}_d, \text{ Гэв}$ ⁽³⁾	$\bar{T}_s, \text{ Гэв}$ ⁽⁴⁾	$\bar{T}_g, \text{ Мэв}$ ⁽⁵⁾	$\bar{T}_b, \text{ Мэв}$ ⁽⁶⁾
9	LEm	—	$2,3 \pm 0,1$	155 ± 10	—
	Al	—	$1,8 \pm 0,1$	150 ± 7	$10,3 \pm 0,5$
	Fe	—	$1,6 \pm 0,1$	147 ± 7	$10,5 \pm 0,5$
	Em	—	$1,5 \pm 0,1$	143 ± 6	$10,4 \pm 0,5$
	HEm	—	$1,3 \pm 0,1$	140 ± 6	$11,2 \pm 0,5$
25	LEm	—	$3,9 \pm 0,2$	148 ± 7	—
	Al	—	$3,4 \pm 0,2$	140 ± 7	$11,0 \pm 0,5$
	Fe	—	$2,9 \pm 0,2$	145 ± 7	$11,3 \pm 0,5$
	Em	—	$2,7 \pm 0,2$	150 ± 7	$11,8 \pm 0,6$
	HEm	—	$2,2 \pm 0,1$	145 ± 7	$12,6 \pm 0,6$
50	LEm	$23 \pm 1,5$	$3,9 \pm 0,2$	150 ± 10	—
	Em	19 ± 1	$2,8 \pm 0,2$	146 ± 9	$12,4 \pm 0,6$
	HEm	15 ± 1	$2,5 \pm 0,2$	143 ± 7	$13,1 \pm 0,9$
60	LEm	$32 \pm 1,6$	$3,8 \pm 0,2$	145 ± 7	—
	Em	$27 \pm 1,3$	$2,8 \pm 0,2$	150 ± 8	$15,5 \pm 0,6$
	HEm	$24 \pm 1,2$	$2,4 \pm 0,2$	150 ± 8	$13,4 \pm 0,6$
80	LEm	$47 \pm 2,3$	$3,9 \pm 0,2$	145 ± 7	—
	Em	$41 \pm 2,3$	$2,9 \pm 0,2$	150 ± 8	$13,3 \pm 0,6$
	HEm	39 ± 2	$2,4 \pm 0,2$	145 ± 7	$13,6 \pm 0,6$
100	LEm	60 ± 3	$4,0 \pm 0,2$	155 ± 9	—
	Al	$58 \pm 2,9$	$3,6 \pm 0,2$	160 ± 9	$12,7 \pm 0,6$
	Fe	$55 \pm 2,8$	$3,2 \pm 0,2$	140 ± 7	$12,9 \pm 0,6$
	Em	$53 \pm 2,6$	$2,9 \pm 0,2$	145 ± 7	$13,2 \pm 0,6$
	HEm	$49 \pm 2,5$	$2,7 \pm 0,2$	140 ± 7	$13,8 \pm 0,7$
500	LEm	305 ± 16	$12,2 \pm 0,6$	140 ± 7	$13,6 \pm 0,6$
	Al	300 ± 15	$10,7 \pm 0,5$	150 ± 8	$13,5 \pm 0,7$
	Fe	280 ± 14	$9,7 \pm 0,4$	145 ± 7	$13,7 \pm 0,7$
	Em	270 ± 14	$9,6 \pm 0,4$	145 ± 8	$14,1 \pm 0,7$
	HEm	240 ± 12	$8,8 \pm 0,4$	150 ± 8	$14,0 \pm 0,7$
10^3	LEm	610 ± 30	$22,5 \pm 1,3$	155 ± 10	$14,2 \pm 0,7$
	Al	585 ± 29	$21,6 \pm 1,2$	150 ± 9	$14,1 \pm 0,7$
	Fe	560 ± 28	$16,0 \pm 0,8$	140 ± 7	$14,5 \pm 0,7$
	Em	535 ± 27	$15,5 \pm 0,7$	140 ± 7	$14,4 \pm 0,7$
	HEm	480 ± 24	$14,7 \pm 0,7$	145 ± 8	$14,8 \pm 0,7$

DOC = 77106902

PAGE ~~85~~ 86

Key: (1). GeV. (2). Nucleus. (3). MeV.

FOOTNOTE 1. It is obtained by interpolation of known experimental data. ENDFOOTNOTE.

Page 497.

Table 118. The mean angle, into which escapes the half of all particles, which are born in inelastic pion-nuclear collisions.

$T, \text{Гэв}$ ⁽¹⁾	Ядро ⁽²⁾	$\theta_{1/25}, \text{град}$ ⁽³⁾	$\theta_{1/25}, \text{град}$ ⁽³⁾
9	LEm	$19,5 \pm 0,9$	57 ± 3
	Al	$21,2 \pm 1,1$	60 ± 3
	Fe	$22,5 \pm 1,2$	61 ± 4
	Em	$24,8 \pm 1,3$	62 ± 4
	HEm	$27,6 \pm 1,4$ (29) *	64 ± 4
25	LEm	$12,9 \pm 0,6$	59 ± 3
	Al	$14,8 \pm 0,8$	59 ± 3
	Fe	$16,1 \pm 0,8$	62 ± 3
	Em	$17,2 \pm 0,9$ (13) *	61 ± 3
	HEm	$18,8 \pm 0,9$ (20) *	62 ± 3
50	LEm	$10,5 \pm 0,7$	60 ± 4
	Em	15 ± 1	62 ± 4
	HEm	$16,3 \pm 0,8$	63 ± 3
60	LEm	$9,6 \pm 0,5$	$62 \pm 3,1$
	Em	$14,1 \pm 0,7$	$61 \pm 3,1$
	HEm	$15,4 \pm 0,8$	$64 \pm 3,2$
80	LEm	$8,4 \pm 0,4$	$3 \pm 3,2$
	Em	$12,5 \pm 0,6$	$61 \pm 3,1$
	HEm	$13,7 \pm 0,6$	$62 \pm 3,1$
100	LEm	$7,1 \pm 0,4$	60 ± 3
	Al	$7,9 \pm 0,4$	61 ± 3
	Fe	$10,7 \pm 0,5$	60 ± 3
	Em	$11,2 \pm 0,5$	63 ± 3
	HEm	$12,3 \pm 0,6$	65 ± 4
200	LEm	$6,5 \pm 0,3$	61 ± 3
		$(6,2 \pm 0,4)$	
	Em	$9,0 \pm 0,5$	64 ± 4
	HEm	$(8,3 \pm 0,6)$ $12,0 \pm 0,6$ $(11,0 \pm 1,1)$	70 ± 4
500	LEm	$4,0 \pm 0,2$	59 ± 3
	Al	$4,5 \pm 0,2$	61 ± 3
	Fe	$5,3 \pm 0,3$	61 ± 3
	Em	$6,0 \pm 0,3$	62 ± 3
	HEm	$7,9 \pm 0,4$	66 ± 4
10^3	LEm	$3,2 \pm 0,2$	60 ± 3
	Al	$4,0 \pm 0,2$	62 ± 3
	Fe	$4,4 \pm 0,2$	61 ± 3
	Em	$5,1 \pm 0,3$	63 ± 3
	HEm	$6,2 \pm 0,3$	65 ± 4

Key: (1). GeV. (2). Nucleus. (3). deg.

FOOTNOTE 1. It is obtained by interpolation of the experimental data.
ENDFOOTNOTE.

Page 498.

With $T \gg 10$ GeV the results of calculations can be compared with the photoemulsion data, obtained recently by the group of Miyezovich and Giyerul [25]. These data are related to the medium energy of π -mesons $T \approx 200$ GeV. If energy of primary mesons to play is direct according to the experimental distribution $W(T)$, that was being observed in experiment [25], then the results of the calculations change very little: values \bar{n}_s and \bar{n}_s^+ grow/rise by 100/o, angle $\theta_{1/2}$ on the contrary, decreases by 100/o (see Fig. 378), remaining average values within margins of error they remain virtually constant/invariable.

From the preceding information it is evident that calculation and experimental data will agree sufficiently well.

If we do not consider many-body interactions within nucleus, then the difference between a calculated and experimental multitude of shower particles turns out to be not as impressive as in the case nucleon- of nuclear interactions, since with picn- nuclear interaction within nucleus it occurs, speaking in general terms, half collisions, than during interaction nucleon + nucleus; however, the account of many-body interactions turns out to be very essential for explaining the angular distributions of shower particles.

Table 120 shows that the portion of many-body interactions within nucleus is very considerable.

Table 119. Average transverse particle momentum \bar{p}_{\perp} , MeV/s.

$T, \Gamma_{90}^{(1)}$	$\text{Ядро}^{(2)}$	$\bar{p}_{\perp g}$	$T, \Gamma_{90}^{(1)}$	$\text{Ядро}^{(2)}$	$\bar{p}_{\perp g}$
9	LEm	370 \pm 19	100	Fe	350 \pm 17
	Al	340 \pm 17		Em	370 \pm 18
	Fe	360 \pm 18		HEm	350 \pm 17
	Em	330 \pm 16			
25	HEm	350 \pm 18	500	LEm	380 \pm 19
				Em	370 \pm 19
				HEm	375 \pm 19
			1000	LEm	350 \pm 17
100	LEm	360 \pm 17		Al	355 \pm 18
	Al	350 \pm 17		Fe	370 \pm 19
				Em	360 \pm 18
				HEm	390 \pm 20

(1). GeV. (2). Nucleus.

Table 120.

Contribution of multi-particle interactions in pion-nuclear collisions with $T = 200$ GeV, %.

n	LE		Em		HEm	
	$W_{B3}(n)$	$W_{qACT}(n)$	$W_{B3}(n)$	$W_{qACT}(n)$	$W_{B3}(n)$	$W_{qACT}(n)$
2	61	42	70	51	74	56
3	18	19	15	17	14	16
4	10	14	7	11	6	9
5	6	9	4	8	3	7
≥ 6	5	16	4	13	3	12

Note. $W_{B3}(n)$ - the relative number of n-partial interactions, when with intranuclear nucleon interacts (n - 1) particle (with respect to the total number elastic and inelastic, collisions s- and g-particles within nucleus); $W_{qACT}(n)$ - the relative percentage of particles, which participate in n-partial interactions (in the initial states) [5].

Page 499.

As in the case of nucleon-nuclear collisions, these interactions compose larger percentage in light nuclei. Attention is drawn to the considerable contribution of the collisions, when with nucleon interacts immediately more than four particles.

Thus, we see that the account of many-body interactions under completely reasonable assumptions about their properties makes it possible to match entire totality of known experimental data on the interactions of high-energy particles with atomic nuclei in the region of energies up to several thousand gigaelectron-volt. For more detailed conclusions is necessary the refinement of the experimental data, especially the value of energy of shower particles, and the more careful theoretical examination of the stage of process, connected with the luminescence of the nucleus, which was being formed after the passage of cascade avalanche.

For testing the model of many-body interactions are very interesting the experiments on the Serpukhov accelerator, where the energy is sufficiently high and at the same time can be obtained considerably better/best accuracy, than in cosmic rays.

Let us emphasize again, that even so during calculations we nowhere clearly considered that fact that during the collisions of particles within nucleus is possible the generation of resonances, but with very high energies perhaps and fireballs however the mechanism of many-body interactions indirectly effectively considers the possibility of such processes, since the characteristics of

AD-A048 311

FOREIGN TECHNOLOGY DIV WRIGHT-PATTERSON AFB OHIO
INTERACTIONS OF HIGH-ENERGY PARTICLES AND ATOMIC NUCLEI WITH NU--ETC(U)
JUL 77 V S BARASHENKOV, V D TONEYEV
FTD-ID(RS)T-1069-77

F/G 20/8

UNCLASSIFIED

NL

2 OF 6
ADI
A048 311



particles, which are born in many-body interactions, are determined, in essence, only by the value of free energy ϵ , independent of the initial state of multiparticle system. The type of particles in the initial state manifests itself, mainly, only on the value of the section of many-body interaction, about which we now nevertheless can speak only purely phenomenologically.

The theoretical and experimental studies of nuclear interactions with very high energies $T \gg 10$ GeV are located even in the initial stage. For judgments about the mechanism of such interactions it is very important to investigate the "transient" region of energies T from 2 to 30 GeV. In this case of interest is the study as many integral, average characteristics, as differential distributions and correlations between separate values. Special attention deserves low-energy the component of the being born particles.

§86. Model of tube.

Already from the purely kinematic considerations, connected with the effect of the relativistic compression of angles, it follows that basic part of the intranuclear cascade, initiated by particle with a high energy of T , must be localized in the comparatively narrow

tunnel region of nucleus, angular dimensions of which $\Delta\Omega$ the lesser, the greater energy T . The reaction of the collisions of high-energy particle with nucleus occur/flow/lasts so rapidly that the interaction within nucleus does not manage to be propagated to sides.

Above we saw that the process, which was being realized within this tunnel region, or as accepted to still speak, within the tube of nuclear substance, consists of the series of the consecutive collisions, each of which is independent event/report two- or of many-body interaction.

At the same time some authors (for example, see [26, 30, 33]) advanced another model, in a sense alternative the models of intranuclear cascades and based on the assumption that the initial particle ejects whole tube of nuclear substance, which is the single strongly excited system, which decomposes outside nucleus (Fig. 379). With energies T of the order several dozen gigaelectron-volt for the calculation of the decomposition/decay of this system is utilized the statistical theory of the multiple formation of fermions, with high energies - the statistical model, based on the solution to the equations of relativistic hydrodynamics.

In this case it is considered that the decomposition/decay of system, the crystallization of single particles it begins after this system will be expanded so, that the mean free path of particles stops the order of its size/dimensions. Thus far nuclear tube is considered as certain continuous medium, the number of particles in which because of the processes of strong interaction not defined.

Now it is not possible to give any any convincing considerations, which would explain, why time of the interaction of particles within nucleus is so great that the separate interactions run together and envelop with disturbance the range with geometric dimensions on the order of the dimensions of the nucleus itself ¹.

FOOTNOTE ¹. Sometimes they speak (for example, see Shane's work [31]), that because of the effect of the relativistic compression of the longitudinal size/dimensions the length of the tube, by which is transferred the very high momentum/impulse/pulse by initial particle, becomes comparable with the radius of action of the nuclear forces $r_0 \sim 10^{-13}$ cm., in consequence of which becomes meaningless to distinguish separate interactions within this system. However, in this case one ought not to forget that to equal compression ratio experience/tests all the longitudinal scales, including the radius of action of nuclear forces.

Another consideration, which sometimes is led in favor of the mechanism of tube, consists in the fact that as a result of relativistic effects the momentum/impulse/pulse, transferred to recoil nucleon lengthwise, can be very small, thanks to which the effective region of space, in which is realized the interaction in accordance with uncertainty principle $\Delta x \cdot \Delta p_{\parallel} \sim \hbar$, can stop the order of the size/dimensions of entire nucleus [22]. However, this is extremely rare case. K. D. Tolstov with the aid of uncertainty principle by the direct analysis of the dispersion of the longitudinal pulse component of particles $\sqrt{(\Delta p_{\parallel})^2}$ in inelastic $\pi - N$ - and $N - N$ -collisions showed that the effective region $\pi - N$ - and $N - N$ -interaction many times is less than nuclear sizes [36]. However, always remains the possibility to say that we still very little know about processes at high energies, and to consider the model of tube as certain assumption.

The model of tube was especially popular into 1955-1960, when with its aid they explained virtually all experimental data on the nuclear interactions of cosmic rays, even with energies T of the order of several GeV, and the only analysis of the experimental data, obtained on Dubna 10-GeV accelerator, showed the inadequacy of this model in any case with $T \sim 10$ GeV [13]. First of all turned out to be

END FOOTNOTE

those which are not agreeing with experiment the average half angles of shower particles both for light/lungs and for the heavy nuclei of the photoemulsion: the model of tube leads to considerably larger angles how this it was observed in experiment [13].

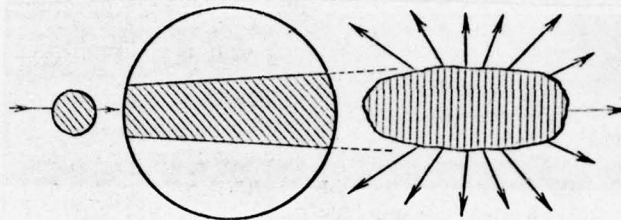


Fig. 379. Initial particle ejects the "tube" of nuclear substance with section by the approximately equal to the section of initial particle. After escape from nucleus the tube decomposes to single particles. Remanent/residual nucleus loses excitation energy by means of the process of evaporation or division (if this nucleus sufficiently heavy).

Page 501.

Further, if one assumes that the initial event of nucleon-nuclear collision is interaction nucleon - tube, then the speed of the center of inertia of this system in the case of collisions with heavy nuclei Ag and Br it must be considerably smaller than in the case of collisions with nuclei C, N, O, since the average length of tube in the first case almost is twice as more as;

consequently, and the number of s-particles in the case of heavy nucleus must be considerably greater. This conclusion also was not coordinated with the experiment: with $T = 9$ GeV in work [33] was obtained $\bar{n}_s = 3.5 \pm 0.3$ and 3.0 ± 0.2 respectively for the medium-weight and average- light nuclei of photcemulsion.

The mechanism of tube contradicted the fact that among particles with gray traces was observed only the very minor constituent of π -mesons; the suppressing number of g-particles were nucleons. As we saw above, this fact is explained well by cascade mechanism, while the calculation of the decomposition/decay of tube according to Fermi's theory showed that with $T = 9$ GeV the contribution of low-energy π -mesons must be considerable.

It is still more difficult within the framework of the mechanism of tube to explain the characteristics of nuclear disintegration with 28-30 gray and black traces, which with $T = 9$ GeV are observed into more than 20/o of all cases. In these splitting/fissions occurs the complete disintegration of nucleus, in essence to protons and neutrons with the light portion of α -particles, but value \bar{n}_s , $\theta_{1/2s}$ and the energy, transferred to nucleus, are close to their average values for all nuclear disintegration Ag and Br [13].

The analysis of nuclear interactions in region 10-30 GeV also

shows that known here experimental data cannot be matched with the model of tube. The agreement with this model, which is noted in various works, based on the examination only of some narrow groups of facts bears random character; in a number of cases this agreement was the consequence of serious systematic defects. (Detailed analysis/selection and the critic of part of such works are given in the article of K. D. Tchlstova [36]; see also [21]).

In the region of very high space energies the pipe model of the interactions of particles with nuclei most investigated in detail G. A. Milekhin [30]. He showed that agreement with experiment can be obtained only by order of value. At the same time, analysis shows that those point/items, in which the model of tube succeeds in agreeing with experiment, they have, as a rule, kinematic origin and actually barely connected with model itself.

Thus, it is possible to count that the known at present experimental data do not confirm assumption about the existence of the special mechanism, which leads to the rise of the single excited system - nuclear tube. In essence, all known now experimental data can be matched with the model of intranuclear cascades.

LITERATURE

1. Артыков И. З. Сообщение ОИЯИ Р2-4176. Дубна, 1968. Трехчастичные взаимодействия при высоких энергиях.
2. Артыков И. З. Диссертация. ОИЯИ, Дубна, 1968. Многочастичные взаимодействия во внутриядерных каскадах при высоких и сверхвысоких энергиях.
3. Artykov I. Z., Barashenkov V. S. Nucl. Phys., B6, 628 (1968).
4. Артыков И. З., Барашенков В. С. Сообщение ОИЯИ Р2-4510. Дубна, 1969. Каскадные взаимодействия мезонов и нуклонов с эмульсией в области энергий 50—80 Гэв.
5. Артыков И. З., Барашенков В. С., Елисеев С. М. «Ядерная физика», 3, 978 (1966).
6. Artykov I. Z., Barashenkov V. S., Eliseev S. M. Nucl. Phys., 87, 241 (1966).
7. Артыков И. З., Барашенков В. С., Елисеев С. М. «Изв. АН СССР. Сер. физ.», 31, 1448 (1967).
8. Artykov I. Z., Barashenkov V. S., Eliseev S. M. Nucl. Phys., B6, 11 (1968).
9. Артыков И. З., Барашенков В. С., Елисеев С. М. «Изв. АН СССР. Сер. физ.», 32, 350 (1968).
10. Артыков И. З. и др. «Изв. АН СССР. Сер. физ.», 30, 1581 (1966).
11. Барашенков В. С. «Изв. АН СССР. Сер. физ.», 29, 1634 (1965).
12. Барашенков В. С. Сечения взаимодействия элементарных частиц. М., «Наука», 1966.
13. Barashenkov V. S. et al. Nucl. Phys., 14, 522 (1959/60).
14. Барашенков В. С., Елисеев С. М. Сообщение ОИЯИ Р-1678. Дубна, 1964. Механизм взаимодействия космических частиц большой энергии с атомными ядрами.
15. Барашенков В. С., Елисеев С. М. «Изв. АН СССР. Сер. физ.», 29, 1631 (1965).
16. Барашенков В. С., Елисеев С. М. Сообщение ОИЯИ Р-1796. Дубна, 1964. Взаимодействие частиц с веществом при очень высоких энергиях.
17. Барашенков В. С., Елисеев С. М. «Изв. АН СССР. Сер. физ.», 29, 1631 (1965).
18. Barashenkov V. S., Maltsev V. M. Fortschr. Phys., 15, 435 (1967).
19. Barashenkov V. S. et al. Fortschr. Phys., 14, 357 (1966).
20. Dobrotin N. A. et al. Nucl. Phys., 35, 152 (1962).
21. Елисеев С. М. Диссертация. ОИЯИ, Дубна, 1967. Механизм взаимодействия элементарных частиц с атомными ядрами при высоких энергиях.
22. Фейнберг Е. Л. «Ж. эксперим. и теор. физ.», 28, 241 (1955).
23. Фреттер В. Б., Хансен Ф. В. В кн.: «Труды международной конференции по космическим лучам. Москва», М., Изд-во АН СССР, 1959, стр. 134.
24. Garbowska K. et al. Nucl. Phys., 60, 654 (1964).
25. Gierula J., Krzywdzinski S. Nuovo cimento, 55, 370 (1968).
26. Heitler W., Terreoux C. Proc. Phys. Soc., A66, 929 (1953).
27. Lal S., Pal Y., Ravahan R. Nucl. Phys., 31, 415 (1962).
28. Lohrmann E., Teucher M. W., Schein M. Phys. Rev., 122, 672 (1961).
29. Matsumoto S. J. Phys. Soc. Japan, 18, 1 (1963).
30. Милехин Г. А. «Тр. Физ. института АН СССР», 16, 50 (1961).
31. Ming-Hiang Shen. Lane College preprint (1968). Множественное образование частиц в высокоэнергетических ядерных столкновениях.
32. Perkins D. H. In: Proceedings of the International Conference on Theor. Aspects of Very High Energy Phenomena. CERN Geneva, 1961, p. 99.
33. Roestler F. E., McCusker C. B. A. Nuovo cimento, 10, 127 (1953).
34. Шайн М. и др. В кн.: «Труды международной конференции по космическим лучам. Москва». Т. 1, М., Изд-во АН СССР, 1959, стр. 7.
35. Такибаев Ж. С. и др. Там же, стр. 51.
36. Tolstov K. Nucl. Phys., 47, 11 (1963).
37. Веницкий А. Х. и др. В кн.: «Труды международной конференции по космическим лучам. Москва». Т. 1, М., Изд-во АН СССР, 1959, стр. 61.

Page 503.

Chapter 8

EMISSION OF COMPLEX PARTICLES.

§87. Emission of light nuclei and fragments.

During the inelastic collisions of high-energy particles the nuclei along with nucleons and mesons from nucleus of target escape also the complex particles d , t , ^3He , ^4He and the heavier fragments Li , Be , B and, etc with charges $Z \geq 3$.

Research on such reactions is of considerable interest in many respects: as is further study of the mechanism of evaporation and processes of more rapid decomposition/decay of strongly excited nuclei as investigation of the properties of clusters within target nucleus and the fluctuations of the density of intranuclear

substance, etc.

Special interest in reactions with the emission of complex particles began to be exhibited after it was established/installed that their significant part escapes with the momentum/impulse/pulses, close to the momentum/impulse/pulse of initial particles.

The formation of fragments with charges $Z \geq 3$ (the so-called fragments) has a series of the specific special feature/peculiarities (see Chapter 9). Here we will be restricted to the discussion of the experimental and theoretical data, which relate to one- and to doubly charged particles with the number of nucleons two and more.

The properties of low-energy particles partly were examined in chapter 3 and 6 in connection with discussion of properties of the isoenergetic components of cascade particles and by the theory of the evaporation of remanent/residual nuclei; therefore now we the primary attention will give to rapid particles with the energy, greater than several dozen million electron volts.

Immediately it should be noted that the overwhelming majority of the known at present experimental data on the generation of complex particles is related to proton-nucleus interactions. In addition to this, is only a small quantity of the partial data, which relate to

interactions with the nuclei of pi-mesons, antiprotons and α -particles (see, in particular, [39, 56, 104, 106]); almost nothing is known about the interactions of neutrons with nuclei. Are very great the errors of measurement, which reach sometimes several dozen percent.

§88. Sections of the formation of complex particles.

The basic known at present experimental data for energies $T \gtrsim 100$ MeV are assembled in Table 121; the representation of the behavior of sections with smaller energies they give Fig. 380-382. For a comparison on the first of these figures is shown also the section of the formation of deuterons in p - p-collisions ¹.

FOOTNOTE ¹ Sections for the interactions of protons with the nuclei of oxygen in Fig. 380-382 are obtained by interpolation known data for adjacent cell/elements [74]. The discussion of the sections of the formation of deuterons in p - p-collisions can be found in works [24, 89]. ENDFOOTNOTE.

Table 121. Sections of the formation of complex particles during the interactions of high-energy protons with nuclei.

(1) Ядро и многоза- рядная частица	(2) Энергия протона T , Гэв	(3) σ , мбарн	(4) Литера- тура	(5) Ядро и многоза- рядная частица	(6) Энергия протона T , Гэв	(7) σ , мбарн	(8) Литера- тура
^{12}C (d)	0,09 0,19	90 ± 10 50	[6, 59] * [6, 59]	^{27}Al (t)	0,12 0,13 0,15 0,153 0,2 0,3 0,3 0,34 0,45 0,45 0,45 0,48 0,5 0,55 0,55 0,6 0,6 0,66 0,66 0,66 2,05 2,05 2,2 3 5,7 6 10 25	8 $15,0 \pm 2,6$ $12 \pm 1,5$ 9 ± 1 18 ± 6 25 ± 7 19 ± 3 $16 \pm 1,6$ 24 ± 7 $24 \pm 3,3$ 23 ± 3 $17,5 \pm 1,8$ 37 ± 11 33 ± 10 30 ± 5 44 ± 13 32 ± 3 46 ± 14 30 ± 3 42 ± 6 44 37 ± 4 75 ~ 37 50 ~ 31 ~ 34 71	[27] [80] [20] [69] [64] [64] [80] [69] [64] [80] [28] [69] [64] [64] [80] [64] [42] [64] [69] [80] [27] [28] [42] [69] [27] [69] [69] [42]
^{27}Al	0,19	88	[6, 59]				
$^{58,7}\text{Ni}$	0,19	86	[6, 59]				
$^{107,9}\text{Ag}$	0,156 0,157	124 ± 16 $> 69 \pm 8$	[30] [79]				
^{197}Au	0,09 0,156 0,157	71 91 $> 32 \pm 5$	[30, 31] [30] [79]				
^{12}C (t)	0,15	$6,5 \pm 1$	[20]				
	0,23	7 ± 1	[48]				
	0,3	$7,0 \pm 0,8$	[48]				
	0,4	$8,6 \pm 1,0$	[48]				
	0,45	$7,3 \pm 0,5$	[28]				
	0,45	$7,4 \pm 1,0$	[80]				
	0,55	$10,1 \pm 1,5$	[80]				
	0,66	$10,6 \pm 1,6$	[80]				
	0,73	$7,6 \pm 1,2$	[48]				
	2,05	$17 \pm 1,2$	[27]				
	2,05	$14 \pm 1,2$	[28]				
	5,7	18	[27]				
	6,2	20	[27]				
				$^{28,1}\text{Si}$	0,6	48 ± 3	[42]
^{14}N	0,45	26 ± 4	[28]	^{51}V	0,6	52 ± 8	[42]
	2,05	$30 \pm 4,6$	[27]	^{52}Cr	0,6	49 ± 8	[42]
	2,05	25 ± 4	[28]	$^{54,6}\text{Mn}$	0,6	60 ± 9	[42]
	2,2	28 ± 4	[37]	$^{55,9}\text{Fe}$	0,05	4,2	[41]
	6,2	35	[27]		0,075	$4,3 \pm 0,8$	[41]
^{16}O	0,45	38 ± 5	[28]		0,093	5 ± 1	[41]
	2,05	36 ± 5	[27]		0,1	$4,8 \pm 0,9$	[41]
	2,2	33 ± 4	[28]		0,13	7,2	[23]
	2,2	33 ± 4	[37]		0,13	$6,4 \pm 1,5$	[80]
	6,2	38	[27]		0,135	$6,4 \pm 1,2$	[41]
$^{24,3}\text{Mg}$	0,3	19 ± 6	[64]		0,15	17 ± 2	[20]
	0,45	30 ± 9	[64]		0,15	$6,1 \pm 1,1$	[41]
	0,55	26 ± 8	[64]		0,16	7,2	[36]
	0,6	$15,4 \pm 4,0$	[42]		0,177	$6,6 \pm 1,2$	[41]
	0,66	43 ± 13	[64]		0,45	28 ± 5	[28]
	2,05	36	[27]		0,45	34 ± 8	[80]
	2,05	30 ± 2	[28]		0,6	48 ± 5	[42]
					1	65	[23]
^{27}Al	0,082	10 ± 2	[20]		2,05	53 ± 8	[28]
	0,12	16 ± 5	[64]		2,05	64	[27]
					2,2	66 ± 10	[42]
					2,2	62 ± 7	[36]
					3	88	[23]
					6,2	130	[23]
					6,2	110	[27]
					25	104 ± 10	[42]

Page 505 Table 121. (Cont'd)

① Ядро и многоза- рядная частица	② Энергия протона T, Гэв	③ σ , мбарн	④ Литера- тура	① Ядро и многоза- рядная частица	② Энергия протона T, Гэв	③ σ , мбарн	④ Литера- тура
$58,7\text{Ni}$ (t)	0,19	19	[6, 59]	209Bi (t)	0,66	167 ± 50	[64]
	0,45	22 ± 3	[28]		3	290 ± 30	[69]
	0,6	41 ± 15	[42]		6	492 ± 50	[69]
	2,05	75 ± 12	[28]		10	400 ± 70	[69]
	2,05	90	[27]	$232,1\text{Th}$	0,135	$19,5 \pm 0,05$	[70]
$63,5\text{Cu}$	2,2	135 ± 9	[42]		0,15	40 ± 5	[20]
	0,6	53 ± 3	[42]		0,157	≥ 44	[75]
	0,66	73 ± 22	[64]	$12\text{C}(^3\text{He})$	0,15	$6 \pm 1,6$	[72]
	2,2	132 ± 8	[42]		0,19	30	[6, 59]
$65,4\text{Zn}$	25	144 ± 20	[42]	27Al	0,15	$10 \pm 1,5$	[72]
	0,66	67 ± 20	[64]		0,19	20	[6, 59]
$87,6\text{Sr}$	0,66	88 ± 26	[64]		0,6	27	[42]
	0,66	88 ± 26	[64]		2,2	72	[42]
$92,9\text{Nb}$	0,15	20 ± 3	[20]	$28,1\text{Si}$	0,6	34	[42]
	0,15	20 ± 3	[20]		2,2	56	[42]
$107,9\text{Ag}$	0,157	$\geq 35,9$	[79]	$55,9\text{Fe}$	0,15	13 ± 2	[72]
	0,6	86 ± 10	[42]		0,16	11	[95]
	0,66	76 ± 23	[64]		0,43	45	[95]
	2,05	136 ± 18	[28]		0,6	34	[42]
$118,7\text{Sn}$	0,15	25 ± 3	[20]		2,2	63	[42]
	0,153	17 ± 2	[69]		3	240	[95]
	0,34	$15,2 \pm 3$	[69]		25	133	[42]
	0,48	48 ± 5	[69]	$58,7\text{Ni}$	0,19	18	[6, 59]
	0,66	61 ± 10	[69]		0,6	42	[42]
197Au	0,082	26 ± 3	[20]		2,2	58	[42]
	0,15	39 ± 4	[20]	$58,9\text{Co}$	0,6	36	[42]
	0,157	$\geq 41,5$	[79]	$63,5\text{Cu}$	0,6	52	[42]
$207,2\text{Pb}$	0,12	17 ± 5	[64]		2,2	80	[42]
	0,3	73 ± 22	[64]		25	129	[42]
	0,45	91 ± 27	[64]	$107,9\text{Ag}$	0,157	≥ 12	[79]
	0,45	71 ± 8	[28]		0,6	21	[42]
	0,55	87 ± 26	[64]	197Au	0,15	19 ± 2	[72]
	0,6	157 ± 47	[64]		0,157	$\geq 6,6$	[79]
	0,6	127 ± 10	[42]		0,16	7 ± 2	[31]
	0,66	186 ± 56	[64]		0,6	21	[42]
	0,66	133 ± 14	[69]	$207,2\text{Pb}$	0,157	6,5	[79]
	2,05	510 ± 72	[28]		0,6	22	[42]
	2,05	610	[27]		0,157	22	[42]
	2,2	405 ± 8	[42]	209Bi	0,157	6,5	[79]
	3	400 ± 80	[69]		0,6	22	[42]
	6	618 ± 100	[69]	$232,1\text{Th}$	0,15	20 ± 2	[72]
	6,2	480	[27]		0,15	20 ± 2	[72]
	10	276 ± 50	[69]				
209Bi	0,3	73 ± 22	[64]				
	0,55	75 ± 22	[64]				
	0,6	98 ± 15	[4]				

Table 121. (Cont'd)

① Ядро и многоза- рядная частица	② Энергия протона T , Гэв	③ σ , мбарн	④ Литера- тура	① Ядро и многоза- рядная частица	② Энергия протона T , Гэв	③ σ , мбарн	④ Литера- тура
$^{12}\text{C}(\alpha)$	0,09	121 ± 20	[6, 59] *	$\text{HEm}(\alpha)$	1	340 ± 60	[57]
	0,19	103	[6, 59]		2	960 ± 130	[57]
^{27}Al	0,19	192	[6, 59]		3	1160 ± 130	[57]
	0,6	268	[42]		3	960	[56]
	2,2	410	[42]	$^{107,9}\text{Ag}$	0,157	≥ 120	[79]
$^{28,1}\text{Si}$	0,6	302	[42]		0,16	231 ± 27	[30]
	2,2	330	[42]		0,6	350	[42]
$^{55,9}\text{Fe}$	0,6	120	[75]	^{197}Au	0,157	≥ 109	[79]
	0,43	450	[75]		0,16	109 ± 15	[31]
	0,6	336	[76]	$^{207,2}\text{Pb}$	0,6	340	[42]
	2,2	410	[57]		0,16	82 ± 10	[31]
	3	1300	[75]	^{209}Bi	0,24	110	[73]
$^{58,7}\text{Ni}$	25	750	[42]		0,42	220	[73]
	0,19	170	[6, 59]		0,55	320	[73]
	0,6	396	[42]		0,6	350	[42]
	2,2	470	[42]		0,085	35	[39]
$^{63,5}\text{Cu}$	0,6	575	[76]	^{232}Th	0,15	75	[39]
	2,2	620	[76]		0,157	≥ 81	[79]
	25	785	[42]		0,16	81 ± 10	[31]

* Приведенное сечение относится к взаимодействию $p + ^{12}\text{C}$.

Key: (1). Nucleus and multiply-charged particle. (2). Energy of proton t , GeV. (3). mb. (4). Literature.

FCCTNOTE * the given section is related to interaction $n + {}^{12}\text{C}$.

ENDFOOTNOTE.

Page 506.

As is evident, experimental information is very small, especially for the deuterons, experiments on which, as a rule, were made only for some values of angles of emission. It is possible to only say that with $T \gtrsim 100$ MeV of the section of the formation of deuterons on the average are approximately 50/o of baking of inelastic interactions; exception is interaction with the nuclei of helium, where the section of the formation of deuterons is approximately the fourth of section σ_{in} .

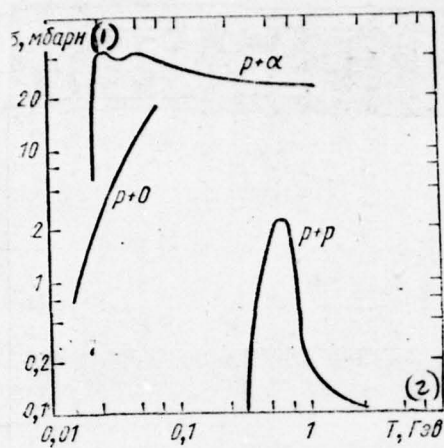


Fig. 380.

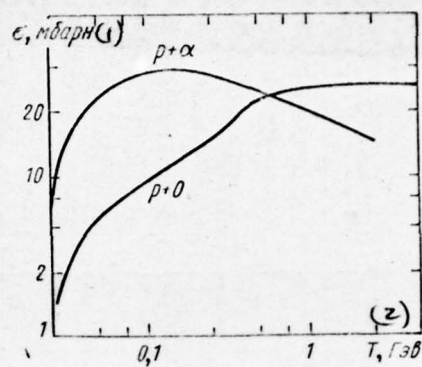


Fig. 381.

Fig. 380. Sections of the formation of deuterons in collisions $p + p$; $p + {}^4\text{He}$ and $p + {}^{16}\text{O}$ [74].

Key: (1) - mb. (2) - GeV.

Fig. 381. Sections of the formation of tritium in collisions $p + {}^4\text{He}$ and $p + {}^{16}\text{O}$ [74].

Key: (1). mb. (2). GeV.

Page 507.

Most are studied in detail the sections of the formation of tritium. With energies T , large several gigaelectron-volt, these sections they are approximately the third of the corresponding total cross sections of inelastic interactions (see Fig. 381 and 383). Approximately the same value the section of the escape of nuclei ${}^3\text{He}$. As concerns the sections of the formation of α -particles, they are already comparable in its value with cross sections σ_{in} (Fig. 384).

If we do not consider the sections of the escape ${}^3\text{He}$ in collisions $p + {}^4\text{He}$ (see Fig. 382), then with the energies, greater than several a gigaelectron-volt, all sections of the formation of doubly charged particles become the slowly changing functions of energy T and virtually emerge on plateau.

It is interesting to note that energy, at which is achieved "saturation", $T \simeq 3-5$ GeV, practically coincides with that, with which was noted a change in the mechanism of the interaction of

particles with nuclei (see §57).

In dependence from the mass number of target nucleus the production cross section of tritium grow/rises as $A^{2/3}$, i.e., it is proportional to section σ_{in} . This occurs as with energies $T \sim 100$ MeV (see [20]), after all with high energies (Fig. 385). The dependence of the sections of the nucleation of helium is more complex: these sections grow/rise during passage from light nuclei to the nuclei of the average atomic weight, and then slowly they decrease.

It is understandable that the course of the section of the formation of complex particles determines the behavior of many particles (see Table 121). An average multitude of deuterons and nuclei of tritium, arising in photoemulsion with $T \gg 1$ GeV, is shown also in Table 32 and 33; several values for smaller energies it is possible to find in Table 34 and 36.

As concerns many accompanying particles, as showed investigations of a number of the authors (see Table 122), many shower particles in stars with α -particles and without them within the margins of error in the measurements it turns out to be almost identical; at the same time many low-energy g - and b - particles in the stars, which contain the nuclei of helium, noticeably higher.

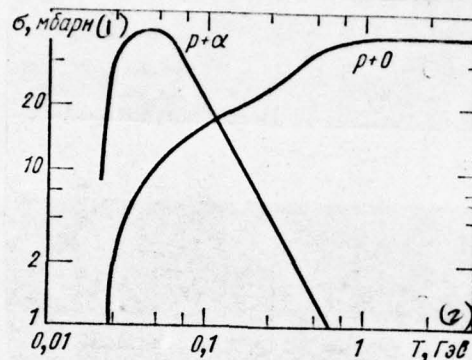


Fig. 382.

Fig. 382. Sections of nucleation ${}^3\text{He}$ in collisions $p + {}^4\text{He}$ and $p + {}^{16}\text{O}$ [74].

Key: (1). mb. (2). GeV.

Table 122. Average multitude of ray/beams in stars with the nuclei of helium and without them (interaction with the heavy component of photoemulsion; energy of the nuclei of helium $\{T > 100\}$ MeV).

BEST AVAILABLE COPY

(1) Пер- вич- ная час- тица	T, Гэв (2)	(3) Звезды с ядрами гелия				(4) Звезды без ядер гелия				(5) Лите- рату- ра
		\bar{n}_s	\bar{n}_h	\bar{n}_g	\bar{n}_b	\bar{n}_s	\bar{n}_h	\bar{n}_g	\bar{n}_b	
π^-	7,5	$4,3 \pm 0,3$	$15,4 \pm 0,5$	$5,5 \pm 0,3$	$9,9 \pm 0,4$	$3,2 \pm 0,2$	$11,6 \pm 0,5$	$4,6 \pm 0,3$	$7,0 \pm 0,3$	[106]
π^-	17,5	$7,7 \pm 0,3$	$19,8 \pm 0,4$	$7,2 \pm 0,3$	$12,6 \pm 0,1$	$6,3 \pm 0,3$	$13,7 \pm 0,5$	$5,3 \pm 0,3$	$8,4 \pm 0,3$	[106]
p	2,26	$0,8 \pm 0,1$	$14,0 \pm 0,6$	—	—	$1,06 \pm 0,08$	$11,2 \pm 0,3$	—	—	[104]
p	9	$5,4 \pm 0,2$	$18,8 \pm 0,3$	$6,2 \pm 0,2$	$12,6 \pm 0,2$	$4,5 \pm 0,2$	$10,4 \pm 0,3$	$3,2 \pm 0,1$	$7,2 \pm 0,2$	[103]
p	19,5	$8,4 \pm 0,2$	$20,9 \pm 0,4$	$6,7 \pm 0,2$	$14,2 \pm 0,3$	$7,1 \pm 0,2$	$12,8 \pm 0,3$	$4,3 \pm 0,1$	$8,5 \pm 0,2$	[103]
p	2,23	$2,7 \pm 0,4$	$16,4 \pm 1,1$	—	—	$2,9 \pm 0,2$	$11,2 \pm 0,3$	—	—	[104]

Key: (1). Initial particle. (2). T, GeV. (3). Stars with the nuclei of helium. (4). Stars without the nuclei of helium. (5). Literature.

Page 508.

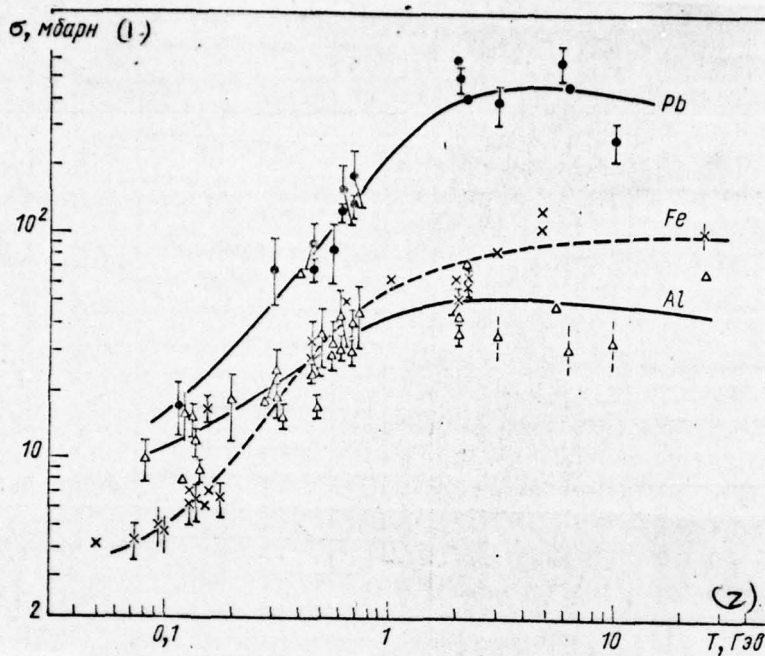


Fig 383.

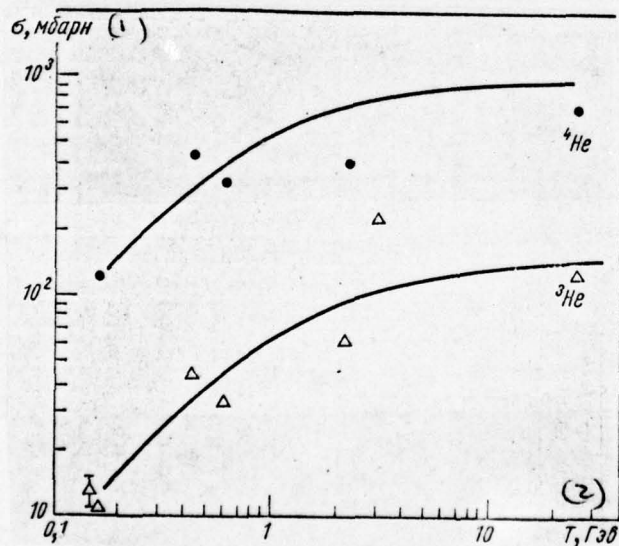


Fig 384.

Fig. 383. The energy dependency of the cross section of the formation of tritium during the collisions of protons with the nuclei of

aluminum, the gland also of lead.

Key: (1). mb. (2). GeV.

Fig. 384. The energy dependency of the sections of formation ^3He and ^4He in the case of the collisions of protons with the nuclei of iron.

Key: (1). mb. (2). T, GeV.

Page 509.

The latter indicates the high value of the total energy, transferred to nucleus during collision with initial particle when are born two-charge particles.

§89. Energy distributions.

These distributions were studied by many authors (for example, see [4, 10, 30, 44, 50, 57, 62, 63, 71, 75, 77, 81, 83, 84, 86, 91, 94, 97, 98, 112, 114, 118, 122], where it is possible to find further

bibliography). Their first distinctive features is the maximum in the area of coulomb barrier $\mathcal{T} \simeq V_R \simeq 10-20$ MeV whose position very weakly depends on type and energy of initial particle (Fig. 386 and 387). Their another distinctive features is the presence of the long high-energy "tail", which stretches up to the energies, close to energy of initial particle. For example, in experiments on 20-30-GeV by protons were observed the deuterons and the nuclei of tritium with energies of the order several a gigaelectron-volt (Fig. 388 and 389).

For the first time the investigation of doubly charged particles with the energies, close to energy of initial particle, were made by M. G. Meshcheryakov with the colleagues [4]. Studying with the aid of magnetic spectrometer the spectra of the charged particles, emitted by light nuclei Li, Be, C and O in beam 675-MeV of protons, these authors reveal/detected the distinct peak in the region of large pulses caused by the contribution of deuterons the position of this peak was approximately such as if primary proton elastic was scattered on deuteron (Fig. 390). Opened by them phenomenon the authors [4] interpreted as process of quasi-elastic scattering ¹ primary protons on the deuteron clusters, forming within target nucleus.

FOOTNOTE ¹. Above (see §22 and note on page 140) quasi-elastic we

called the nuclear reactions, in which as a result of interaction the target nucleus is retained as whole, but it remains not in essence, but in excited state. Examining process it is necessary to precisely call/name for quasi-free scattering particles on cluster or by elastic quasi-free interaction. However, for a brevity and into connection with the historically establishing terminology we will in this chapter call these processes quasi-elastic scattering. We hope that this will not cause misunderstandings. **ENDFOOTNOTE.**

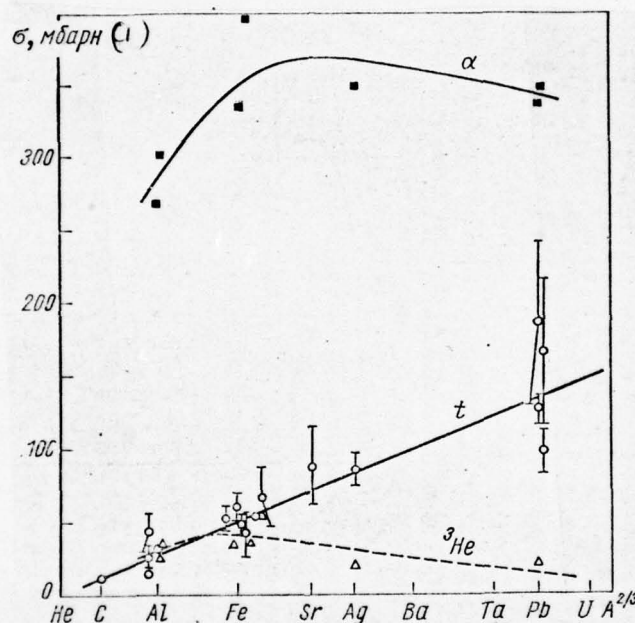


Fig. 385.

Fig. 385. Dependence of the sections of the formation of tritium and doubly charged particles in proton-nucleus collisions with $T = 600$ MeV on the mass number of target nucleus.

Key: (1) - mb.

Page 510.

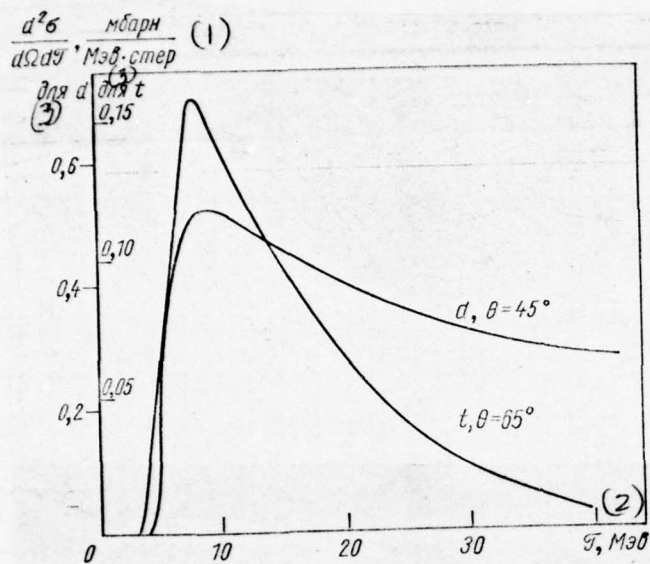


Fig. 386.

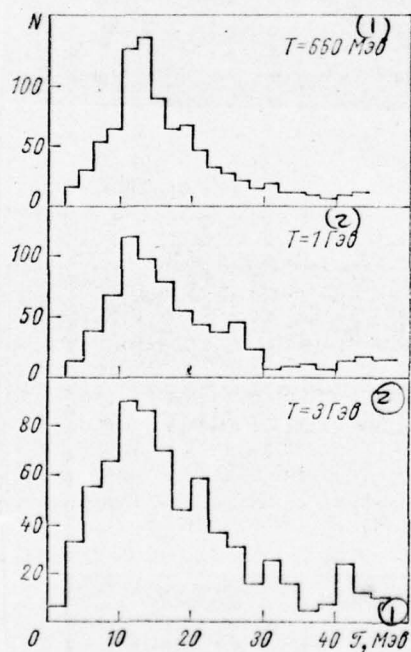


Fig. 387.

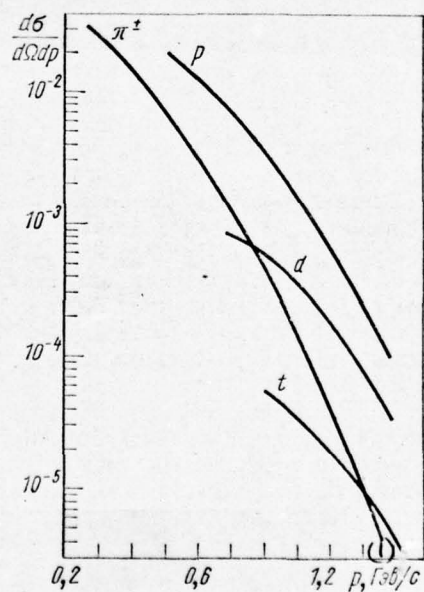


Fig. 388.

Fig. 386. The energy spectra of deuterons and nuclei of tritium, emitted by nuclei Ag under the action of protons 156 MeV in energy [30]. (θ - the angle of escape of particles in the laboratory coordinate system).

Key: (1). mb (MeV \cdot ster). (2). MeV. (3) For.

Fig. 387. Energy of the distribution of the α -particles, which are formed during the interaction of protons with photoemulsion [10, 44].

Key: (1). MeV. (2). GeV.

Fig. 388. Spectra of the rapid particles, formed during the inelastic collisions of protons 30 GeV in energy with nuclei Al and escaping at an angle $\theta = 90^\circ$ [91].

Key: (1). GeV/s.

page 511.

The ratio of the measured nuclear cross sections quasi-elastic p

- d-scattering $\sigma_d(0) = \int \frac{d^2\sigma}{d\Omega dp} dp$ to the elastic-scattering cross sections of protons on free deuterons $\sigma_{pd}(\theta)$ gives the rough estimate of the complete effective number of deuteron clusters in the appropriate target nucleus:

$$N_d = \sigma_d(0) / \sigma_{pd}(\theta). \quad (8.1)$$

Obtained thus values N_d are given in Table 123.

The results of the work of M. G. Meshcheryakova and his collaborators subsequently were detailed by Sutler, etc. [101]. Analogous results for reactions with the emission of the high-energy nuclei of helium recently were obtained by V. I. Komarov and co-authors [62, 63]. For these nuclei also are observed distinct peaks, in form and in position very close to corresponding distributions of nuclei ${}^3\text{He}$ and ${}^4\text{He}$ in the elastic processes $p + {}^3\text{He} \rightarrow p + {}^3\text{He}$ and $p + {}^4\text{He} \rightarrow p + {}^4\text{He}$ (Fig. 391-393). Corresponding values of effective number ${}^3\text{He}$ - and of ${}^4\text{He}$ -clusters $N_{{}^3\text{He}}$ and $N_{{}^4\text{He}}$ are shown in Table 123.

It focuses on itself attention the fact that values N_d , $N_{{}^3\text{He}}$ and $N_{{}^4\text{He}}$ determined for one and the same nucleus, with an accuracy to coefficient of 1.5-2 are equal to ratio A/n , where $n = 2, 3, 4$ are a number of nucleons in the appropriate cluster [63]. With the same accuracy the nuclear cross section of quasi-elastic scattering it is possible to calculate according to the formula

$$\sigma_x(0) = \sigma_{px}(0) A/n, \quad (8.2)$$

where $\sigma_{px}(0)$ is an elastic-scattering cross section of proton on nuclei:

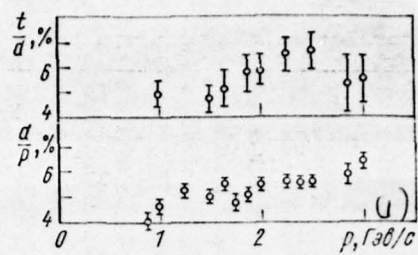


Fig 389.

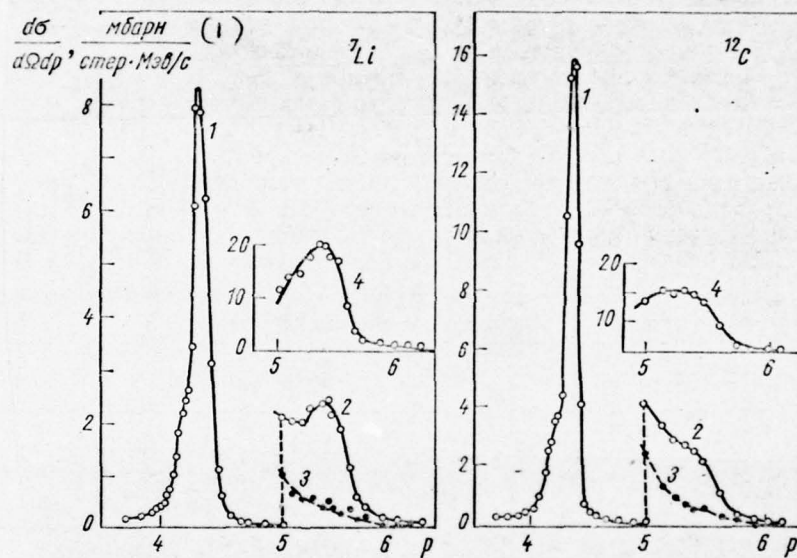


Fig 390.

Fig. 389. Relations of the numbers of particles, which are formed during the inelastic interactions of protons 30 GeV in energy with nuclei Al and escaping at an angle $\theta = 30^\circ$ with the different values of their momentum/impulse/pulse p [97].

Key: (1). GeV/s.

Fig. 390. Pulse spectrum of the charged particles, which are formed during the collisions of protons 675 MeV in energy with the nuclei of carbon and escaping at an angle $\theta = 7.6^\circ$ [4]: 1. , 2. sections of the total spectrum; 3, 4 - respectively the spectrum of protons and deuterons. (Curves 2-4 are shown on the 100-multiply increased scale. particle moment p - in relative units (reports of spectrometer)).

Key: (1). mb / (ster•MeV/s).

Page 512.

In recent years by the study of the processes of the emission of doubly charged particles for the purpose of obtaining the information about the properties of intranuclear clusters have been occupied many laboratories (see [4, 49, 53, 62, 63, 65, 92, 101, 119, 120, 122],

etc.). Errors of measurement and a difference in the experimental conditions still not make it possible at present to obtain sufficiently precise and matching with each other quantitative conclusions, nevertheless even the obtained estimated data are of enormous interest. As an example Table 124 gives the corrected values of the effective number of α -clusters in light nuclei, obtained by the different authors.

Table 123. The experimental data on quasi-elastic knocking out of rapid deuterons, nuclei ^3He and ^4He by protons with energy $T = 665-675$ MeV and data on elastic proton scattering on the free nuclei d , ^3He and ^4He under the same conditions.

(1) Частица; энергия T , Мэв	(2) Мишень	(3) θ , град	(4) $\sigma_x(\theta)$, $\frac{\text{мбарн}}{\text{стер}}$	$N_x = \frac{\sigma_x(\theta)}{\sigma_{px}(\theta)}$	(5) Литера- тура
d ; 675	p	7,6	$0,55 \pm 0,12$	1	[4]
	^7Li	7,6	$2,9 \pm 0,6$	$5,3 \pm 1,6$	[4]
	^9Be	7,6	$2,2 \pm 0,5$	$4,0 \pm 1,3$	[4]
	^{12}C	7,6	$3,7 \pm 0,8$	$6,7 \pm 2,1$	[4]
	^{16}O	7,6	$4,6 \pm 1,0$	$8,4 \pm 2,6$	[4]
^3He ; 665	p	5,4	$(4,3 \pm 1,0) \cdot 10^{-3}$	1	[63]
	^6Li	5,4	$(1,26 \pm 0,23) \cdot 10^{-2}$	$2,9 \pm 0,7$	[63]
	^9Be	5,4	$(1,75 \pm 0,38) \cdot 10^{-2}$	$4,1 \pm 1,1$	[63]
	^{12}C	5,4	$\leq (4,15 \pm 0,62) \cdot 10^{-2}$	$\leq 9,6 \pm 2,0$	[63]
	^{16}O	5,4	$\leq (6,6 \pm 1,0) \cdot 10^{-2}$	$\leq 15,3 \pm 3,2$	[63]
α ; 665	p	5,4	$(4,6 \pm 1,2) \cdot 10^{-4}$	1	[62]
	^6Li	5,4	$(3,6 \pm 0,7) \cdot 10^{-4}$	$0,8 \pm 0,2$	[62]
	^9Be	5,4	$(5,4 \pm 1,2) \cdot 10^{-4}$	$1,2 \pm 0,3$	[62]
	^{12}C	5,4	$(18,2 \pm 3,0) \cdot 10^{-4}$	$4,0 \pm 0,9$	[62]

Key: (1) - Particle; energy T , MeV. (2) - Target. (3) - deg. (4) - mbarn/ster. (5) - Literature.

Table 124. Data on the effective number of α -clusters in light nuclei.

N_α			(1) Реакция	(2) Энергия T , Мэв	(3) Литература
${}^6\text{Li}$	${}^9\text{Be}$	${}^{12}\text{C}$			
$0,8 \pm 0,2$	$1,1 \pm 0,3$	$\leq 1,9 \pm 0,4$	$(p, p\alpha)$	665	[62]
$0,2^*$	0,48	1,3	$(p, p\alpha)$	660	[65, 119, 120]
—	—	$0,30 \pm 0,23$	$(p, p\alpha)$	150	[49]
0,2	—	—	$(p, p\alpha)$	150	[92]
—	—	$3,9 \pm 3,1^{2*}$	$(\alpha, 2\alpha)$	915	[53]
—	$1,38^{3*}$	$2,37^{3*}$	$(p, p\alpha)$	(4) Теория	[8]
—	—	$7,22^{4*}$	$(p, p\alpha)$	(4) Теория	[15]
—	—	$7,25^*$	$(p, \dots \alpha)$	(4) Теория	[11]

Key: (1). Reactions. (2). Energy T , MeV. (3). Literature. (4). Theories.

FOOTNOTE 1. Was utilized the natural isotope mixture of lithium.

2. Given is the average value from work [53].

3. Designed on the assumption that clustering occurs in 1P-shell, i.e., actually on the surface of nucleus.

4. Given is the complete effective number, which considers the

possibility of the formation of cluster in 1S- and 1P-shells.

5. Corrected value to eat $w_\alpha A$ for $w_\alpha = 0.6$, at which is reached best fit with the experiment of the results of cascade calculations of the inelastic interaction of protons with the nuclei of carbon. However, to so good an agreement with the results of work [15], apparently, is not worth still giving serious value. ENDFOOTNOTE.

Page 513.

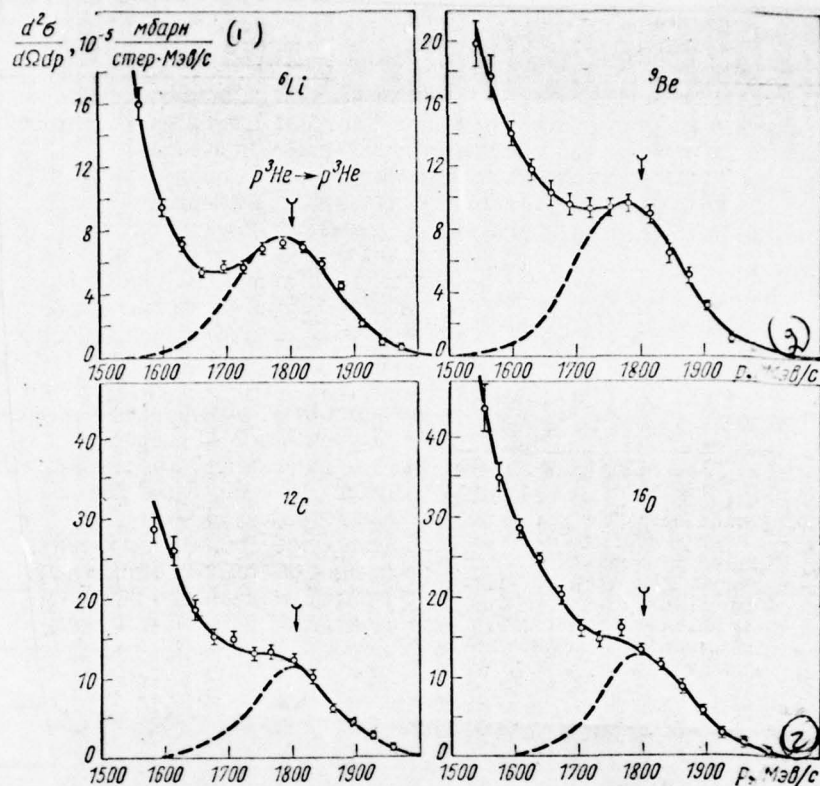


Fig 391.

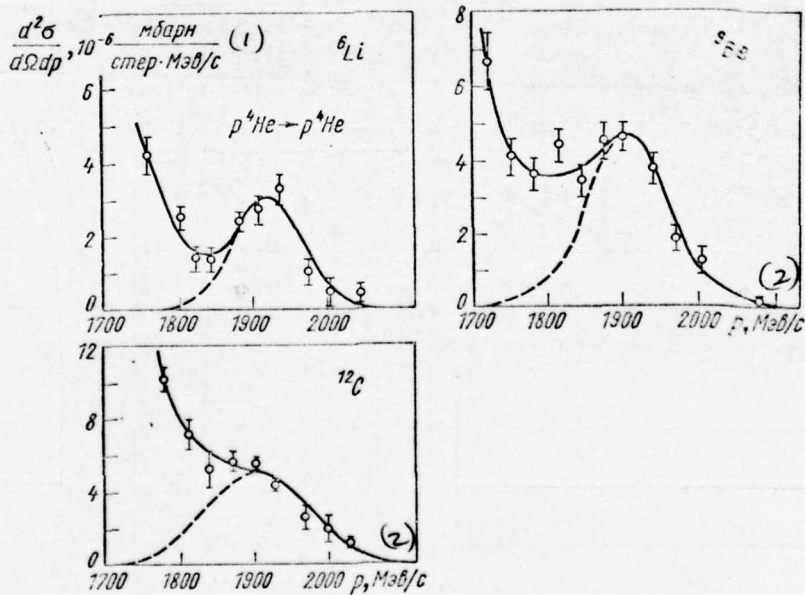


Fig 392.

Fig. 391. Output/yield of fast nuclei ^3He at an angle $\theta = 5.4^\circ$ to proton beam 665 MeV in energy, which interact with nuclei ^6Li , ^9Be , ^{12}C and ^{16}O [63]. By dotted line is shown the approximation of peaks by Gaussian distribution. Arrow/pointer showed the value of the momentum/impulse/pulse of nuclei ^3He elastic $p - ^3\text{He}$ -scattering under the same conditions; $p_{^3\text{He}} = 1803 \text{ MeV/s}$, $\mathcal{F}_{^3\text{He}} = 528 \text{ MeV}$.

Key: (1). mbarn/ (ster \cdot MeV/s). (2). MeV/s.

Fig. 392. Output/yield of rapid nuclei ^4He at an angle $\theta = 5.4^\circ$ to proton beam 665 MeV in energy, which interact with different nuclei [62]. Designations are the same as in Fig. 391.

Key: (1). mbarn/ (ster \cdot MeV/s). (2). MeV/s.

Page 514.

(This table is taken by us from work [62]; for a comparison are shown also theoretical estimations. In more detail about this see in §90).

Measured by V. I. Komarov et al. of value N_α is noticeably more values, obtained in works [49, 92] with $T = 150 \text{ MeV}$. It is possible

that this connected with the powerful absorption, which substantially lowers value N_α , measured with low energies (this was noted already and earlier: see, for example, [15])¹.

FOOTNOTE ¹. The noticeable effect of final-state interaction is observed also in the results of measurements [65, 119, 120], made with energy $T = 660$ MeV, but with the conditions of transmission to the α -clusters of momentum/impulse/pulse $\Delta q \sim 2$ fermi⁻¹. Analogous effect was observed in work yoke, etc. [53], where the effective number N_α in nucleus ¹²C, determined in reaction $(\alpha, 2\alpha)$ with $T = 915$ MeV, it had a tendency toward decrease during a decrease transferred to the α -cluster of momentum/impulse/pulse. ENDFOOTNOTE.

One should only emphasize that the comparison of experimental works regarding N_α , those which were made by the different authors, just as the comparison of theory with experiment, requires the most careful analysis of the conditions of experiment (see, in particular, work [65]). At the same time that fact that values N_α , measured with $T = 660$ -665 MeV in the range of energy of the driven out α -particles from 10 to 470 MeV, are distinguished not more than 2-3 times, although the absolute elastic-scattering cross sections are distinguished in this case to 4 orders, qualitatively confirms the correctness of the

basics idea of quasi-elastic scattering rapid protons during intranuclear associations over a wide range of energies [62]. It follows however to emphasize that the probability of quasi-elastic knocking out of doubly charged particles from nuclei is very low; so, the probability of knocking out 675-MeV by the proton of α -particle from the nucleus of carbon $(W \simeq \sigma_\alpha / \sigma_{in} \sim 10^{-4}\%)$ this is considerably less than the total section of the formation of rapid α -particles with energies $\mathcal{T} \gtrsim 50$ MeV in collisions $p + {}^{12}\text{C}$.

In other words, the doubly charged particles, which are formed in the processes of quasi-elastic proton scattering on intranuclear clusters, are only very small part of the high-energy "tail" in the total spectrum $W(\mathcal{T})$. Besides quasi-elastic scattering there are other processes, which lead to the emission of high-energy complex particles. Specifically, by these processes are caused the spectra of deuterons and nuclei of tritium in Fig. 389 and 390 and the spectrum of α -particles in Fig. 394.

As can be seen from Table 125, an average multitude of traces of different types in stars with α -particles does not depend on energy of these particles.

BEST AVAILABLE COPY

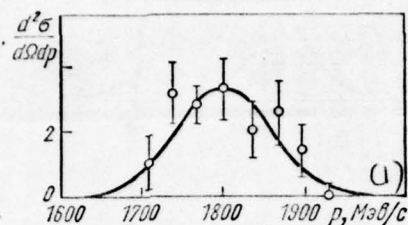


Fig. 393. Output/yield of nuclei ${}^3\text{He}$ at an angle $\theta = 5.4^\circ$ to proton beam 665 MeV in energy, elastic scattering on free nuclei ${}^3\text{He}$ [63]. Sections are given in relative units. The form of curve coincides well with curves, that describe the peaks of quasi-elastic scattering in Fig. 391 and 392.

Key: (†). MeV/s.

Table 125. Correlation of the average number of ray/beams and kinetic energy of α -particles in the stars, formed during the interaction of π -mesons with energy $T = 17.5$ GeV with the heavy nuclei of photoemulsion [106].

\bar{n} \ $T, \text{ } {}^3\text{He}$ (1)	$0,1 \div 0,2$	$0,2 \div 0,3$	$0,3 \div 0,4$	$0,4 \div 0,5$	$> 0,5$
\bar{n}_s	$6,9 \pm 0,3$	$7,7 \pm 0,4$	$7,8 \pm 0,8$	$5,2 \pm 0,7$	$9,1 \pm 0,7$
\bar{n}_g	$7,2 \pm 0,4$	$6,5 \pm 0,5$	$5,9 \pm 0,6$	$4,7 \pm 0,4$	$6,9 \pm 0,8$
\bar{n}_b	$12,3 \pm 0,5$	$15,3 \pm 0,8$	$13,6 \pm 1,0$	$10,1 \pm 0,6$	$12,7 \pm 1,0$
\bar{n}_h	$19,5 \pm 0,6$	$21,8 \pm 0,9$	$19,5 \pm 1,2$	$14,8 \pm 0,7$	$19 \pm 1,3$

Key: (1) GeV.

Page 515.

This fact it is difficult to understand, if we consider that the formation of the escaping from nucleus high-energy α -particles occurs evenly by entire volume of target nucleus ¹.

FOOTNOTE ¹. As a result of collisions with the intranuclear nucleons of the α -particles, which escape from the interior of nucleus, possesses noticeably smaller energy, than the α -particles, which were being formed on periphery. On the other hand, the formation of rapid α -particles within nucleus can occur only during the central collisions of the initial particles with nucleus-target which are characterized by the considerably large number of ray/beams, than the

peripheral collisions, when α -particles are formed in the surface layer of nucleus. ENDFOOTNOTE.

With this will agree the fact of an increase in the number of black and especially cascade gray ray/beams in stars with α -particles as compared with the stars, in which there are no traces of the nuclei of helium (see Table 124) ².

FOOTNOTE ². According to Ye. V. Shalaginoy's data the output/yield of rapid α -particles in collisions $p + E_n$ with $T > 1$ GeV exponentially depends on the number of h-ray/beams: $\sigma \sim \exp(\overline{an_h})$, where $a \approx 0.4-0.7$ [96]. As it was noted above, the probability of the generation of complex particles is determined by the value of the total energy, transferred to nucleus during collision with particle. ENDFCOTNOTE.

The mechanism of formation high-energy the components of complex particles in many respects remains still unclear.

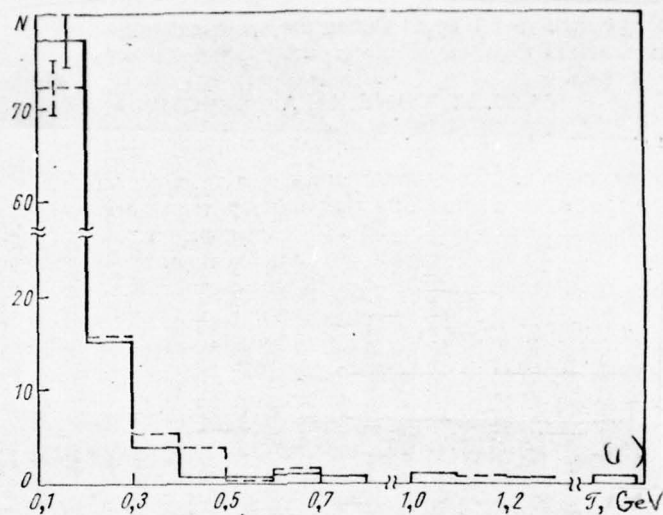


Fig. 394. Spectrum of rapid α -particles with energy $T > 0.1$ GeV, forming during interactions pi-mesons with energies $T = 7.5$ and 17.5 GeV in photoemulsion (respectively broken and continuous histogram) [106]. Histograms can be approximately approximated by exponential function $N(T) \sim T^{-3.0 \pm 0.4}$. By the same function are described the spectra of α -particles from interactions $p + E$ with $T = 2.3-20$ GeV [96].

Key: (1). GeV.

Table 126. Sections of the nucleation of helium with energy \mathcal{T} in photoemulsion, mb.

(1) Взаимо- действие	T Гэв	(3) $\mathcal{T} > 0,1$ Гэв	$> 0,2$	$> 0,3$	$> 0,4$	$> 0,5$	> 1 (2)	Лите- рату- ра
$\pi^+ + Em$	7,5	$15,75 \pm 1,89$	$3,76 \pm 0,8$	—	$0,98 \pm 0,48$	—	—	[106]
$\pi^- + Em$	17,5	$29,1 \pm 2,2$	$5,4 \pm 0,62$	—	$1,20 \pm 1,25$	$0,92 \pm 0,23$	—	[106]
$\rho^+ + Em$	2,26	$26,6 \pm 4,0$	$2,6 \pm 2,2$	$3,3 \pm 1,2$	$0,8 \pm 0,8$	—	—	[104]
$\rho^- + Em$	9,0	$51,2 \pm 6,1$	$19,3 \pm 3,5$	$6,5 \pm 1,8$	$4,3 \pm 1,6$	—	$0,46 \pm 0,3$	[103]
$\bar{\rho}^+ + Em$	19,5	$51,4 \pm 7,2$	$18,6 \pm 4,3$	$7,9 \pm 2,6$	$2,6 \pm 1,3$	—	$0,2 \pm 0,2$	[103]
$\rho^+ + Em$	2,23	53 ± 14	$8,4 \pm 6,3$	—	—	—	—	[104]

Key: (1). Interaction. (2). Literature. (3) GeV

Page 516.

In Table 126 are assembled the sections of the formation of the rapid nuclei of helium in photoemulsion with energies $T > 1$ GeV. All these data are related, mainly, to interactions with heavy nuclei,

since the relative number of interactions with the light/lung component of photoemulsion, which are accompanied by the emission of rapid α -particle, it comprises not more than 5c/o ¹.

FOOTNOTE ¹. Therefore with $T = 2.26$ and 19.5 GeV the section of the formation of α -particles with energy $\mathcal{E} > 100$ MeV as a result of collisions with group C, N, O composes respectively 1.7 ± 0.8 and 2.4 ± 1.6 mb [96]. ENDFCOTNOTE.

Data Tables 125 and 126 highly useful for a comparison with the experiment of the different theories, which describe the generation of rapid doubly charged particles.

§90. Angular characteristics.

Typical angular distribution of the α -particles, which are formed in photoemulsion, are shown in Fig. 395. The anisotropy of the escape of α -particles \vec{n}/\hat{n} comparatively is small; however, considerably grow/rises during passage to light nuclei (Fig. 396) and becomes the greater than the higher-energy part of the spectrum it is

examined. The latter one can see well from Fig. 397 and from the data of Table 127 (see also Fig. 185).

The analysis of the dependence of energy of particles of the helium on their angle of emission in the laboratory coordinate system, made in works [60, 96], shows that the experimental points do not lie down to curves, for designed for the case of the elastic collision of primary proton with motionless α -particle.

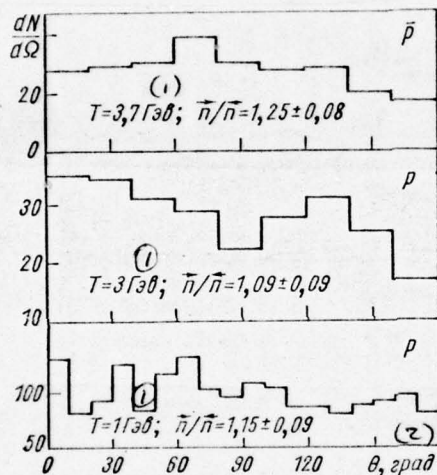


Fig. 395.

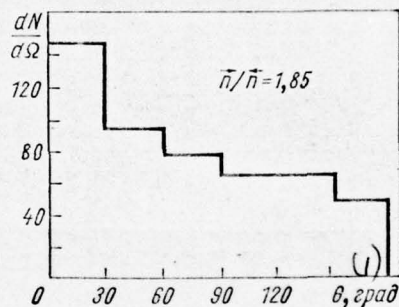


Fig. 396.

Fig. 395. The angular distributions of the α -particles, which are born during the interactions of protons and antiprotons in photoemulsion [10, 56].

Key: (1) - GeV. (2) - deg.

Fig. 396. The angular distributions of doubly charged particles with energy $\mathcal{E} < 30$ MeV (in essence of α -particles), formed during interaction protons of energy 660 MeV with the nuclei of carbon [121].

Key: (1). deg.

Table 127. Values of the average and half angles of emission of the nuclei of deuterium, tritium and helium, which are formed during high-energy interactions in photoemulsion (among the observed nuclei of helium basic part they compose α -particles).

(1) Первичная частица	(2) Быстрое ядро	(3) T, Гэв	(4) Угол	(5) $\mathcal{E} > 0,1$ Гэв	(6) $\mathcal{E} > 0,2$ Гэв	(7) $\mathcal{E} > 0,3$ Гэв	(8) Лите- рату- ра
π^-	d и t	7,5	$\theta_{1/2}$	$55 \pm 1,5$	$37,5 \pm 3,5$	—	[110]
π^-	t	7,5	$\theta_{1/2}$	$54 \pm 2,5$	$38,5 \pm 4$	—	[110]
π^-	He	7,5	$\theta_{1/2}$	$52 \pm 2,8$	$37,5 \pm 4,5$	—	[110]
π^-	He	17,5	$\theta_{1/2}$	$50 \pm 2,5$	34 ± 4	—	[106]
p	He	2,26	$\bar{\theta}$	44 ± 7	—	34 ± 12	[96]
p	He	9	$\bar{\theta}$	54 ± 5	—	35 ± 7	[96]
p	He	9	$\bar{\theta}_{1/2}$	$47,8 \pm 2,5$	$32,5 \pm 4$	—	[61, 102]
p	He	19,5	$\bar{\theta}$	54 ± 5	—	36 ± 7	[96]
p	He	2,23	$\bar{\theta}$	60 ± 15	—	—	[96]

Key: (1). Initial particle. (2). Rapid nucleus. (3). T, GeV. (4).

Angle. (5). Literature. (6). and.

Page 517.

The account of the internal motion of α -associations leads to the spreading of picture. During the calculation were made the assumptions that the α -substructures have energy ~ 10 MeV, and their momentum/impulse/pulses either coincide in the direction with the

momentum/impulse/pulse of the impinging nucleon or are opposite to it. The majority of experimental points does not fall into region between calculated curves; apparently, their spread it is not possible to explain by the presence of momentum/impulse/pulse of α -clusters. Only a small fraction of the low-power particles, which escape at angles of $60-100^\circ$, is located in the region between calculated curves. Since these particles are emitted from splitting/fissions with the large number of fine/thin and gray-black ray/beams, their escape is difficult to explain by direct/straight knocking out of α -complexes by primary protons.

One must not fail to note the weak dependence of the mean angles of $\theta_{1/2}$ and $\bar{\theta}$ from type and energy of initial particle in the case of interactions $\pi + E_m$ and $p + E_m$; for the interactions of antiprotons the angle of $\theta_{1/2}$ turns out to be noticeably greater (although statistical errors in this case are very great).

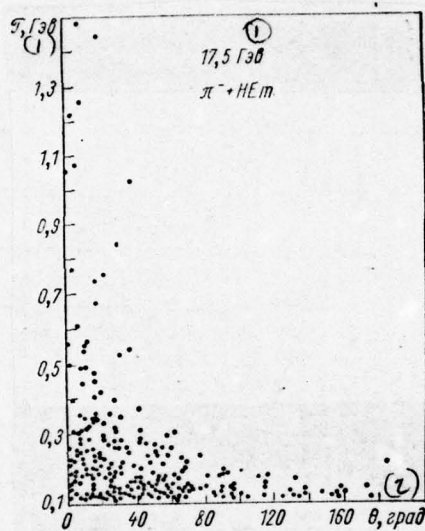


Fig. 397. Dependence of kinetic energy of α -particles on the angle of their escape [106].

Key: (1) - GeV. (2) - deg.

Table 128. The average angles of emission s- and of g-particles in photoemulsion stars with α -particles and in the stars, where there are no α -particles [96].

(1) Первичная частица	(2) T, Гэв	(3) Вторичная частица	(4) θ , град	
			(5) Звезды с α	(6) Звезды без α
p	2,26	s	64 \pm 10	53 \pm 7
		g	68 \pm 6	65 \pm 6
p	9	s	46 \pm 2	—
		g	73 \pm 4	—
p	19,5	s	40 \pm 1	33 \pm 1
		g	71 \pm 2	68 \pm 3
p	2,23	s	73 \pm 11	—
		g	74 \pm 10	—

Key: (1). Initial particle. (2). T, GeV. (3). Secondary particle. (4). deg. (5). Stars with α . (6). Stars without α .

Table 129. Sections of the processes of the formation of protons and complex particles, which are characterized isotropic ($\sigma_{из}$) and anisotropic ($\sigma_{аниз}$) by angular distributions in the center-of-gravity system [30, 31], of mb.

(1) Взаимодействие	T, Мэв (2)	p		d		t		^3He		α	
		$\sigma_{из}$	$\sigma_{аниз}$	$\sigma_{из}$	$\sigma_{аниз}$	$\sigma_{из}$	$\sigma_{аниз}$	$\sigma_{из}$	$\sigma_{аниз}$	$\sigma_{из}$	$\sigma_{аниз}$
p + Au	90	240 \pm 30	650 \pm 70	26 \pm 4	45	10 \pm 2	17	—	—	—	—
p + Ag	156	800 \pm 100	700 \pm 100	64 \pm 6	60 \pm 10	15 \pm 3	18 \pm 2	5,5	7,5 \pm 1	206 \pm 25	25 \pm 2
p + Ta	156	390 \pm 50	—	50 \pm 5	—	22 \pm 3	—	—	—	100 \pm 10	—
p + Au	156	320 \pm 50	800 \pm 100	41 \pm 4	50	17 \pm 3	22 \pm 2	3	4 \pm 1	75 \pm 6	37 \pm 5
p + Pb	156	320 \pm 50	—	42 \pm 4	—	18 \pm 3	—	—	—	60 \pm 6	—
p + Bi	156	350 \pm 50	—	47 \pm 5	—	24 \pm 3	25 \pm 3	3	3 \pm 1	45 \pm 7	37 \pm 7
p + Th	156	380 \pm 50	—	55 \pm 5	—	30 \pm 4	—	—	—	37 \pm 5	44 \pm 10

Key: (1). Interaction. (2). T, MeV.

END SECTION.

Page 518.

Angular distributions s^- and the g -ray/beams, which accompany the escape of α -particles, are less anisotropic, than the corresponding distributions for events without the emission of rapid α -particle. This fact can serve as indication of the large branching of intranuclear cascade with the formation of doubly charged particles (Table 128). As concerns the distributions of the angles of emission of deuterons, nuclei of tritium and ^3He , for bottom are characteristic the same features, as for α -particle distributions.

The anisotropy of the escape of complex particles with the energies, which do not exceed several dozen million electron volts, to a considerable degree is caused by the purely kinematic factors, connected with the emission/output nucleus-target, and almost completely it disappears during passage to the center-of-gravity system. At the same time the angular distributions of rapid two-charge particles remain substantially anisotropic, also, in the center-of-gravity system. This fact indicates that the mechanisms of the formation of slow and high-energy particles with charge $Z = 2$ completely different.

With energies $T \gtrsim 100$ MeV the processes with isotropic and anisotropic angular distribution give the contribution of one order of magnitude. This is evident, for example, from Table 129, that relates to the collisions of protons with silver and more heavy nuclei with $T = 90$ and 156 MeV.

Figures 398 and 399 separately shows energy particle distributions, which have respectively isotropic and anisotropic angular distributions in the center-of-gravity system.

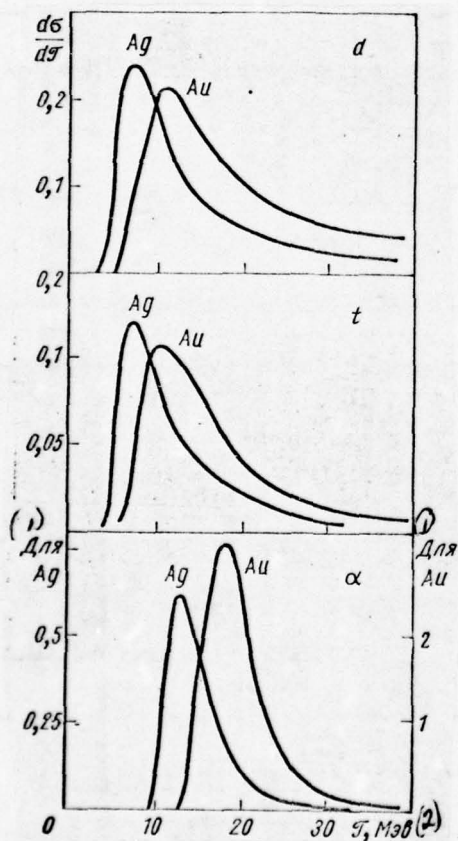


Fig. 398.

Fig. 398. Energy particle distributions with isotropic angular distributions in the center-of-gravity system. Of particle were formed during the collisions of the protons of energy 156 MeV with nuclei Ag and Au [30].

Key: (1). For. (2). MeV.

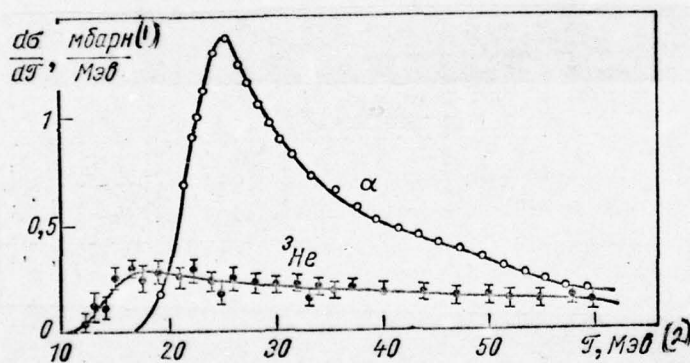


Fig. 399. The energy spectrum of nuclei He with anisotropic angular distribution in the center-of-gravity system, which were being formed in collisions $p + \text{Ag}$ during $T = 156$ MeV [30].

Key: (1). mbarn/MeV. (2). MeV.

Page 519.

Energy anisotropically of outgoing particles really/actually proves to be considerably larger than energy of particles with isotropic angular distribution; at the same time in both cases there is a sufficiently noticeable contribution of particles with very small and with high energies. Maximums in the spectra, which correspond to heavier targets, are shifted into high-energy region.

§91. Mechanisms of knocking out of complex particles.

Even the surface examination of the properties of the emitted complex particles suggests about the fact that their significant part is formed as a result of knocking out by initial particle or, that it is more probably by the high-velocity particles, which were being formed during intranuclear cascade, two-, the three- and four-nucleon nuclear clusters.

As showed theoretical studies of a number of the authors, within nucleus really/actually are realized the conditions, which facilitate

the "coagulation" of nucleons into the closely related associations; intranuclear nucleons the significant part of the time carry out in the form of such associations. Is especially probable the formation of α -clusters [8, 9, 15, 90, 100, 117]. Apparently, the most favorable conditions for the formation of clusters are on the periphery of nuclei [47, 113].

Are known at present several theoretical approaches, which make it possible to obtain the representation of the properties of clusters and the parameters of their motion within nuclei (see, in particular, [8, 9, 15], where as the basis of the calculations is placed shell model). However, these approaches are constructed on the mechanism of quasi-elastic knocking out of cluster by initial particle and, thus, they cannot be critical for basic part of the process of the formation of complex particles. On the other hand, since the experimental information about clusters is still very lean, and the corresponding theoretical estimations are insufficiently are reliable, is of interest the reverse/inverse setting of the problem, when the values, which characterize the formation of clusters in nucleus, are embedded into theory phenomenologically and subsequently are defined by means of the comparison of the results of the calculation with experiment under the condition that the calculation with the smallest number of parameters would explain a greatest quantity of the experimental data similarly, for example, as of the

experiments on scattering are determined the nucleon form factors and nuclei. The possibility of this approach is based on the Monte-Carlo simulation of the intranuclear cascades, which involve interactions with clusters [1, 3, 11, 34, 84, 85, 122].

Let us examine first the simplest model with the sharp boundary of nucleus and with the uniform the spatial distribution of α -clusters; besides the α -particles of no other clusters thus far consider let us [11]. This will allow us to explain, which experimental data can be reproduced within the framework of this model, which requires a comparatively small volume of computational work, and it can serve as basis for the further analysis of the effect of fine/thinner parts of nuclear structure.

The use of contemporary computers and a more precise experimental information about the interactions of nucleons and α -particles makes it possible to make more reliable conclusions, than in works [84, 85, 122]. Target nucleus let us consider as the degenerate Fermi gas in sphere with radius $R = 1.3 \cdot A^{1/3} \cdot 10^{-13}$ cm. The probability of the elastic collision of cascade nucleon with cluster let us place equal to

$$W_{el}^{\alpha}(T) = w_{\alpha} \sigma_{el}^{N\alpha}(T) / \sigma_t^{N\alpha}(T),$$

where value w_α let us consider as parameter, which is selected from the condition of the best fit of the results of the calculation with experiment. After the collision of nucleon with cluster is outlined the further motion of α -particle within nucleus and is considered its elastic scattering on intranuclear nucleons; in this case one should accept into consideration Pauli's principle. Let us consider also the possibility of the subsequent inelastic collisions of α -particle with the nucleons of nucleus, by characterizing their probability by value

$$W_{in}^\alpha(T) = \sigma_{in}^{N\alpha}(T) / \sigma_t^{N\alpha}(T);$$

since however energy of particles, which are formed in collisions $\alpha + N$, as a rule, is very small, these particles cannot overcome barrier and remain within nucleus. The processes of pion formation thus far consider we will not.

Page 520.

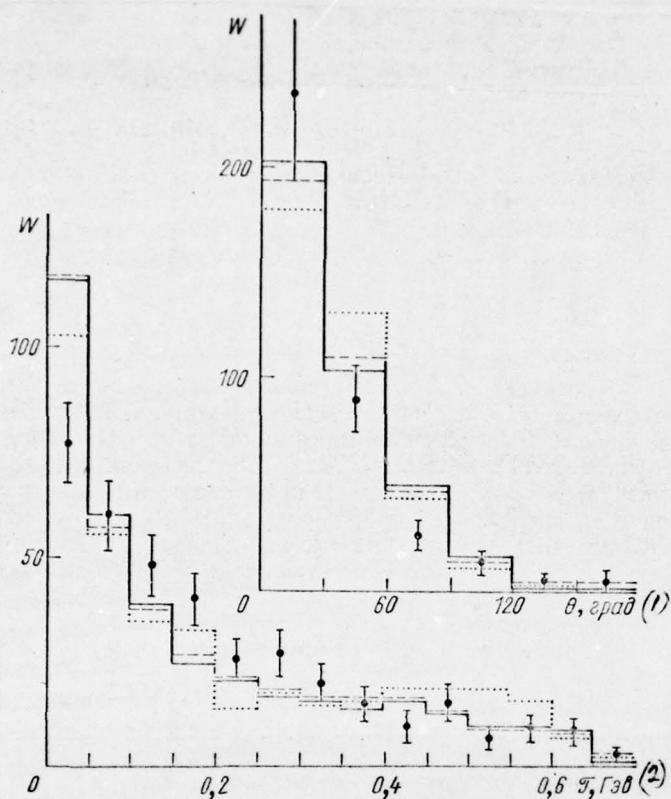


Fig. 400. Energy and angular distributions of the secondary protons, which are formed during the interactions of the protons of energy 660 MeV with the nuclei of carbon. Continuous histogram is the calculation with the parameters $w_\alpha = 0,2$, $a = 260$ MeV/s, $V = 10$ MeV; dotted line - for $V = 13$ MeV; point histogram is the calculation without α -clusters ($w_\alpha = 0$).

Key: (1). deg. (2). GeV.

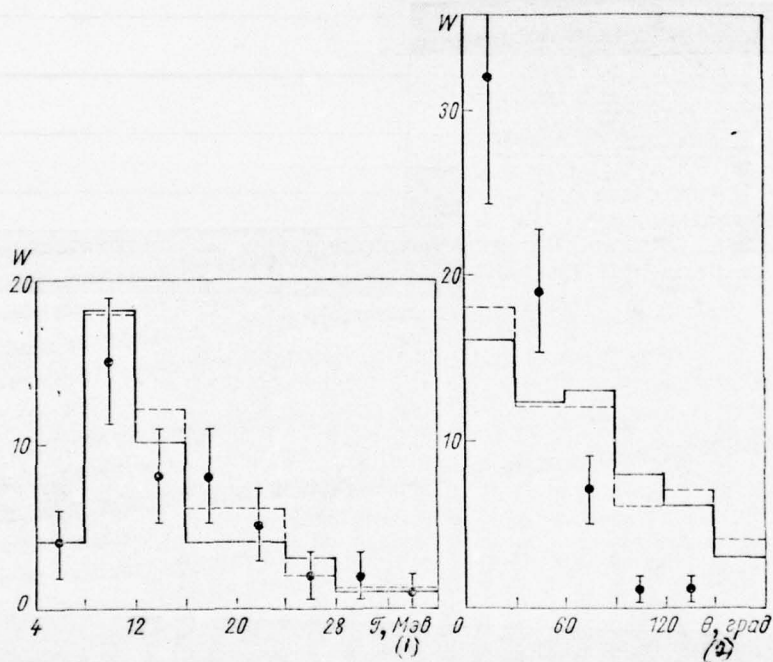


Fig. 401. Energy and angular distributions of the waiting α -particles. Designations are the same as in Fig. 400.

Key: (1). MeV. (2). deg.

Page 521.

α -particle distribution according to momentum/impulse/pulses in the nucleus of carbon let us select in the form $W(p) = \text{const} \cdot \exp(-p^2/a^2)$ $a \approx 260 \text{ MeV/s}$ (see [93]).

The angles of emission of the elastic scattered α -particles let us develop according to differential angular distribution in the center-of-gravity system $N + \alpha$, which, on the basis of known now experimental data, let us select in the form

$$W(\theta) d\Omega = \text{const} \cdot \exp \left\{ - \left(\sum_{i=0}^4 b_i T^i \right) \theta^2 \right\} d\Omega, \quad (8.3)$$

where $b_0 = 0.615$; $b_1 = 11.12$; $b_2 = 424.7$; $b_3 = 1461$; $b_4 = 1288$.

Let us consider α -particle flown out from nucleus, if this particle proves to be outside sphere with a radius $R'_\alpha = R - r_\alpha$, where r_α — a radius of α -particle itself, and its kinetic energy are not

less than the height/altitude of the coulomb barrier of the nucleus: $T \geq V_k$. In other words, we consider that if the α -particle is driven out from the center of nucleus up to distance $r > R'_\alpha$, then in exterior no longer it remains the nucleons, with which this particle could interact [11].

The results of cascade calculations together with the experimental data from the work of A. P. Zhdanov and P. I. Fedotov [121] are given in Table 130 and in Fig. 400-402. The calculations are made for three cases: without taking into account of α -clusters ($w_\alpha = 0$) and two versions with α -clusters, that are distinguished by the height/altitude coulomb barriers V_k .

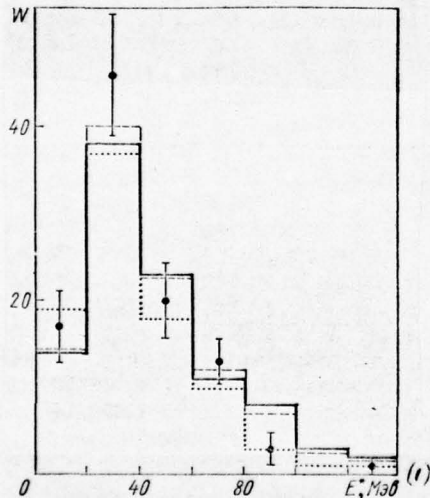


Fig. 402. Excitation energy of remanent/residual nuclei. Designations are the same as in Fig. 400.

Key: (1) - MeV.

Table 130. Comparison of experimental and theoretical data for interactions $p + {}^{12}\text{C}$ with $T = 660$ MeV depending on the parameters of the distribution of α -clusters within nucleus [11].

w_α	(1) $a, \text{Mev/c}$	(2) V_k, Mev	(3) Выход ядер, %				\bar{n}_α
			C	B	Be	Li	
0	—	—	25,6 \pm 2,4	34,6 \pm 2,8	31,1 \pm 2,7	8,5 \pm 1,4	0
0,2	260	10	27,2 \pm 2,1	28,4 \pm 2,2	31,6 \pm 2,3	12,9 \pm 1,5	0,17 \pm 0,02
0,2	260	13	28,2 \pm 2,1	33,7 \pm 2,1	29,3 \pm 2,2	12,1 \pm 1,4	0,11 \pm 0,01
(4) Эксперимент [121]			26,7 \pm 3,0	28,9 \pm 2,5	29,6 \pm 2,5	14,8 \pm 2,0	0,15 \pm 0,02

Key: (1). MeV/s. (2). MeV. (3). Output/yield of nuclei, o/o. (4). Experiment [121].

\bar{n}_α — the average number of cascade α -particles taking into account one splitting/fission.

Page 522.

Although in experiment are observed the total distribution of protons and α -particles, which include both particles, which escape

from nucleus as a result of knocking out by their cascade nucleons and the particle, which are formed upon decay of remanent/residual nuclei, in work [121] these two types of particles are divided and the experimental data in Fig. 400-402 and in Table 130 are related only to cascade particles ¹.

FOOTNOTE ¹. In work [121] was investigated the interaction of primary protons with diamond dust, introduced into photoemulsion, thanks to which it was possible to attempt to establish/install not only nature and the characteristics of decaying particles, but from decay products to identify also the type of the nucleus, remaining after the passage of the cascade stage of process, and its excitation energy E^* .

Cascade and decay particles were divided by means of the comparison of the angular and energy distributions of the being born particles in the center-of-gravity system and in the laboratory coordinate system. It was assumed that all the cascade particles escape in the center-of-gravity system into forward half sphere, whereas the dispersion/divergence of decay particles is isotropic in the system of the rest of residual-nucleus. ENDFOOTNOTE.

Since in experiment [121] of nucleus with the identical charge

2, but with the different mass numbers A they were not distinguished, the given in Table 130 data are related to the sum of all forming isotopes: $C \equiv 10, 11, 12C$; $B \equiv 8, 9, 10, 11B$; $Be \equiv 7, 8, 9, 10Be$; $Li \equiv 6, 7, 8, 9Li$.

If we do not consider some specific, also, up to end/lead to us thus far not clear phenomena on the periphery of nucleus (possibly, the pick-ups reaction of clusters 3He , or of the diffusivity of the boundary of nucleus, although according to the data [49] the latter, apparently, does not give large effect), then the portion of α -particles with energy $\mathcal{E} > 32$ MeV will comprise not more than 3-60/o. This will agree with 30/o- by value from experiment [82] (see also monograph [19]); however, considerably less than it was observed in work [121], where the portion of high-energy α -particles was 30 o/o and it was outlined up to energies $\mathcal{E} \simeq 70$ MeV.

Best fit with the experimental data [82, 121] in region $\mathcal{E} < 32$ MeV succeeds in obtaining, if the height/altitude of Coulomb barrier V_k is assumed equal to 10-13 MeV, and for other two parameters is selected values $w_\alpha = 0,2$ and $a = 260$ MeV/s².

FOOTNOTE 2. In order that it would be possible to draw a comparison with experiment, during calculations was utilized the same criterion

of selection one- and two-pronged stars as in work [121]. Particle was considered slow, if its energy $\mathcal{E} < 30$ MeV. ENDFOOTNOTE.

The variation of the value of the parameters w_α and a near these values weakly changes calculation data [2]. The values, which relate to protons, and the energy distribution of the excitation of the remanent/residual nuclei $W(E^*)$ generally sufficiently weakly depend on identification of parameters w_α , V_h and a .

It should be noted that the agreement of experiment and theory for the angular distributions of α -particles is worse than for their energy spectra. On experiment is observed noticeably the larger number of particles, which escape in the region of small angles (although errors of measurement are still sufficiently great). It is possible to think that partially this is connected with primary distribution of α -clusters on the periphery of nucleus - the fact, which we thus far did not consider.

Table 130 shows that the output/yield of remanent/residual nuclei in all cases turns out to be close to experimental; the account of α -clusters improves this agreement.

Thus, cascade model taking into account α -clusters explains

sufficiently well the properties of the significant part of the observed in experiment α -particles, which remain after the isolation/evolution of decay particles. For the elimination of disagreements with experiment in the high-energy part of the spectrum first of all is required the refinement of experiment, and also the more careful theoretical examination of phenomena on the periphery of nucleus.

It is possible to attempt to use cascade model for explaining this particular characteristic as, for example, recorded in the experiments of V. I. Komarov, G. Ye. Kcsareva and O. V. Savchenko [62] the escape of rapid α -particles in the direction, close to the direction of the motion of primary proton. For this is necessary the careful analysis of the parameters of model. However, for this separately taken characteristic can turn out to be that which determine and some other, special mechanism of interaction.

Page 523.

Almost all the made, until now, cascade calculations of the escape of α -particles are related to interactions with light nuclei. The analysis of processes in heavy nuclei is considerably more complex; in this case the important role plays the absorption of the driven out α -particles in the interior of nucleus, and that which

gives experiment, it is related, in essence, to the periphery of the nuclei, where the properties of clusters can be in no way such, as within nucleus.

The estimations of V. I. Ostroumova and R A. Filova [84] showed that knocking out of rapid α -particles from the heavy nuclei of photoemulsion by protons with energy $T \simeq 100 - 700$ MeV can be explained by cascade mechanism, if we assume, that in the surface layer of the nuclei of silver and bromine nucleons approximately the half of time they are in the form of α -clusters (analogous conclusion is obtained also for light nuclei C, N, O; this more than twice exceeds our estimation, see above). It is necessary, however, to keep in mind that from the viewpoint of present day the calculations, made in work [84], are represented by very approximately. The process of clustering in heavynuclei and the mechanism of the emission of rapid two-charge particles from these nuclei require more careful analysis.

In the same way as for α -particles, it is possible to examine knocking out deuteron clusters, clusters of tritium and ^3He . In the latter case is very important the account of the inelastic collisions of cascade particles with the α -clusters, with which the product nuclei ^3He ; other possible mechanisms of formation ^3He give relatively small contribution [15, 66, 69].

Unfortunately, the experimental information about the generation of the rapid particles d, t and ^3He considerably leaner than for α -particles; therefore the conclusions about the probabilities of formation and distributions within the nucleus of clusters d, t and ^3He are very uncertain. If we are based on these works [4, 63], then one should conclude that in any case in the peripheral regions of nuclei effective probability w_d, w_t and $w_{^3\text{He}}$ the same order of magnitude as the probability of the formation of α -clusters w_α , however, to this conclusion one should be related thus far even with large precaution.

In D. I. Blokhintseva's work [18] to evaluate the number of clusters are used the statistical considerations, based on the assumption that the clusters are the fluctuation of the density of intranuclear nucleons. According to this model the knocking out of the cluster, which consists of a of nucleons, by the rapid particle x occurs at that torque/moment, when these nucleons are located from each other on distances $R \simeq (2-3)\hbar/m_N c = (4-6) \cdot 10^{-13}$ cm. and strongly interact. In this case rapid particle has the capability to transmit its momentum/impulse/pulse to cluster as whole. The section of this interaction $\sigma = \sigma_{xa} W_a(R)$, where σ_{xa} — total cross section quasi-elastic $x - a$ - interaction, and value $W_a(R)$ is probability that a of intranuclear nucleons are located at the distances smaller than R .

If we $\psi_d(r)$ designate the wave function of deuteron, then by order of value

$$W_d(R) = 4\pi \int_0^R \psi_d^2(r) r^2 dr = (4\pi/3) \psi_d^2(0) R^3 = (2/3) \alpha \beta^2 E^3, \quad (8.4)$$

where the function $\psi_d(r)$ at $r \sim 0$ is approximated by the function of Hulthen

$$\psi_d(r) = \sqrt{\alpha/2\pi} [\exp(-\alpha r) - \exp(-\beta r)]/r. \quad (8.5)$$

Estimate of the magnitude $W_d(R)$ for other clusters is even more difficult. Entirely tentatively it is possible to count that, for example, for tritium probability $W_t(R)$ — the value of order $W_d^3(R)$ with correction for that fact that the parameter α for tritium $\frac{\sqrt{m_t Q_t/m_d Q_d}}{\lambda}$

times is higher the deuteron parameter α (here Q_t and Q_d — binding energy in tritium and deuteron, m_t and m_d — their reduced masses with respect to one driven out of nucleus nucleon [18]). This decrease in value α expresses the fact that tritium is the more closely related group of nucleons, than deuteron.

Similarly for a α -cluster one should select value $\alpha \sqrt{m_\alpha Q_\alpha/m_d Q_d}$

times larger than deuteron.

The total cross section of knocking out of cluster a from nucleus with Z by protons and N by the neutrons

$$\sigma_a = (ZN/2A) \sigma_{in} W_a(R) \quad (8.6)$$

(in this case is assumed, that knocking out of clusters with equal probability occurs on entire target nucleus; this is approximately correct for light nuclei).

Page 524.

The results of such simple estimations are sufficiently close to experiment in the case of knocking out of deuterons; however, give too low values of the sections of the formation of heavy doubly charged particles ¹.

FOOTNOTE ¹. One must not fail to note that with "fluctuating" estimations frequently are compared the total experimental sections of the formation of the rapid nuclei of tritium or ³He, significant part of which is caused by the cascade interactions, more complex than simple quasi-elastic scattering [108, 111]. It is understandable that in these cases are obtained the incorrect conclusions. As

already mentioned above (see page 514), probability of quasi-elastic knocking out of clusters is very small. ENDFOOTNOTE.

The very interesting mechanism of the emission of fast deuterons was proposed by Butler and Pearson [21, 22]. In their model the formation of deuterons occurs in the process of developing the intranuclear cascade, when cascade neutron and proton, the having approximately identical momentum/impulse/pulses, are united into the deuteron, which then escapes from nucleus. To this process correspond three diagrams (Fig. 403).

1. In the initial state there are a nuclear neutron with momentum/impulse/pulse k_1 and a cascade proton with momentum/impulse/pulse k_2 . Neutron is scattered by potential of $V(r)$ and transfer/converts to state k_1' . Further particles with momentum/impulse/pulses k_1' and k_2' under the action of nucleon-nucleon potential $V_{NN}(r)$ are united into deuteron. The formed deuteron with momentum/impulse/pulse k escapes from nucleus.

2. Process proceeds as in the case (1), but proton and neutron are changed by roles.

3. Neutron and proton interact with each other with the

formation of the deuteron, which is scattered by the nuclear potential of $V(r)$ and escapes from nucleus.

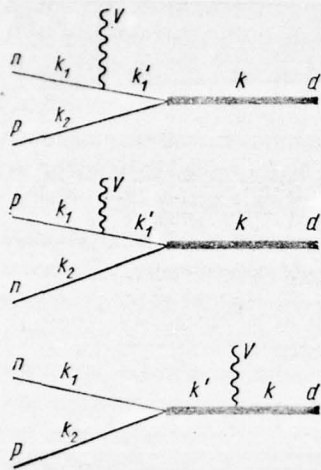


Fig. 403. Diagrams, which describe the formation of deuterons in the model of Butler and Pearson [21, 22].

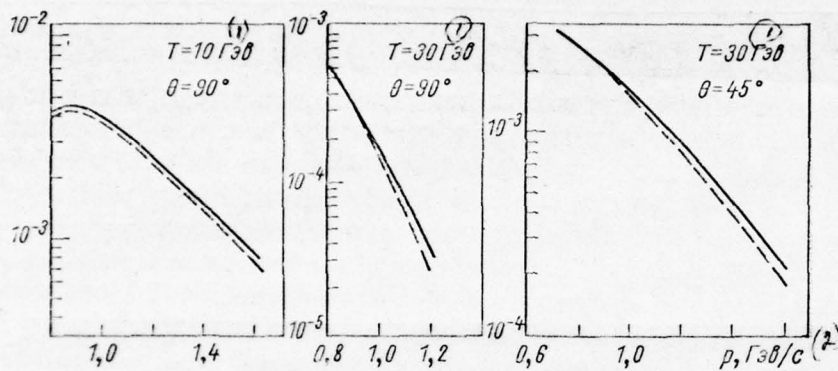


Fig. 404. The output/yield of high-energy deuterons during the collision of the protons of energy T with nuclei Be in units $\text{particle} \cdot \text{ster}^{-1} \cdot (\text{GeV/s})^{-1} \cdot (\text{first proton})^{-1}$ [22]; θ - the angle of emission of deuterons; unbroken curves are an experiment, dotted line is a result of the calculation according to formula (8.7).

Key: (1). GeV. (2). GeV/s.

Everything three diagrams can be designed with the aid of perturbation theory. Taking into account relativistic corrections the number of deuterons with momentum/impulse/pulse k , which are necessary on the average by one splitting/fission of target nucleus, is obtained equal to

$$n_d(k) = 3\pi (48)^2 \left(\frac{k_0}{k}\right)^4 \frac{\gamma}{\Lambda} \left[1 + \left(\frac{\hbar k}{2mc}\right)^2\right]^{3/2} \left(n_p\left(\frac{k}{2}\right)\right)^2 I_0(R), \quad (8.7)$$

where

$$I_0(R) = \int_0^\infty (d\eta/\eta^5) (\sin \eta - \eta \cos \eta)^2 \int_0^\infty \xi^2 d\xi \left\{ \frac{4}{(\xi^2 + \alpha^2 R^2)^2} + \frac{2}{(\xi^2 + \alpha^2 R^2 + \eta^2/4) - \xi^2 \eta^2} - \left(\frac{4}{\eta \xi (\xi^2 + \alpha^2 R^2)} - \frac{1}{\eta \xi (\xi^2 + \alpha^2 R^2 + \eta^2/4)} \right) \ln \left| \frac{\alpha^2 R^2 + (\xi + \eta/2)^2}{\alpha^2 R^2 + (\xi - \eta/2)^2} \right| \right\};$$

to R - a radius of target nucleus; α is the deuteron parameter in the function of Hulthen [see formula (8.5)]; $n_p(q)$ - the number of cascade protons with momentum/impulse/pulse q ; $k_0 = m_N V/\hbar^2$; V - the depth of the optical potential of target nucleus; Λ - the wave number of proton, which corresponds to momentum 1 GeV/s (value n_d are expressed taking into account the unit of solid angle, unit/single momentum/impulse/pulse 1 GeV/s and one primary proton).

As can be seen from Fig. 404, the designed by formula (8.7) spectra of the deuterons, which escape from nuclei under the action of protons with energy $T = 10-30$ GeV, they will agree well with experiment.

§92. Corpuscular emission d, t and He in the processes of the decay of remanent/residual nuclei.

The mechanism of knocking out knowingly cannot explain the emission of all complex particles, observed in experiment. This follows already from that fact that in the considerable number of cases from nuclei escape the "sub-barrier" particles whose energy is less than the height/altitude of the coulomb barrier of target nucleus (for example, see Fig. 201). On the existence of the different mechanisms of the formation of complex particles speaks also the fact that after the isolation/liberation of particles whose characteristics will agree with the calculations according to the cascade theories, which remained particles they have virtually isotropic angular distribution in the coordinate system, connected with target nucleus.

It is possible to think that the determined part of the complex particles with the energies, which do not exceed several dozen million electron volts, is formed in the processes of evaporation and the processes of more rapid decomposition/decay of the excited residual-nucleus. In this case qualitatively becomes clear the isotropy of the escape of particles, and the sub-barrier part of the spectrum can be interpreted as consequence of a reduction in the height/altitude of coulomb barrier, caused by the thermal expansion of remanent/residual nucleus.

The performance calculation of the complex particles, which are formed upon decay of remanent/residual nuclei, conducts by the same methods, as for the escaping nucleons (see Chapter 6). However, in order to obtain best fit with experiment, now very frequent necessary to select large values of parameter a , than for nucleons, whence it is possible to draw the conclusion that the doubly charged particles evaporate from nucleus at the earlier stage, when the temperature of nucleus is still great [50, 75, 77, 118] ¹.

FCOTNOTE ¹. Let us note that unlike the examined/considered in chapter 9 case of the emission of fragments with charges $Z > 4$ for

doubly charged particles the best fit with experiment is reached with values of the parameters, included within physically acceptable limits. ENDFOOTNOTE.

Figure 405 with experiment compares the obtained thus energy distributions $d\sigma/d\mathcal{T}$. The calculation correctly transfers the position of maximum and the absolute value of sections; differences become considerable only with $\mathcal{T} \gtrsim 20$ MeV, where the theory predicts the smaller probability of the emission of complex particles how this is observed on experiment. It is possible that partly this connected with insufficiently by correct isolation/evolution of "cascade" particles in work [38]. Will agree well with experiment also the results of the calculation of the probabilities of the separate channels of the decomposition/decay of the light/lung remanent/residual nuclei, which are formed after cascade/stage (see Table 106).

Work [81] compares calculated and experimental values of the angular asymmetry \vec{n}/\vec{n} for the α -particles of the different energies, which were being formed during interactions 140- MeV of protons in photoemulsion. First conducted the calculation of intranuclear cascade and it was determined the excitation energy of the remanent/residual nucleus E^* , then was calculated the evaporation of

α -particles.

Page 526.

For α -particles with energy less than several million electron volts, was obtained the agreement with experiment; however, with high energies computed values \vec{n}/\vec{n} considerably lower than observed in experiment. For example, with $\mathcal{E} > 8$ MeV $(\vec{n}/\vec{n})_{\text{эксп}} = 3,2 \pm 0,9$; $(\vec{n}/\vec{n})_{\text{теор}} = 1,4$. For the agreement of theory with experiment it is necessary to assume that on the average taking into account one star of 0.25 α -particles they are formed in the processes, different from evaporation. Analogous results are obtained for higher energies of initial particles.

In many other works, where were compared the results of the calculation with the total experimental data without the isolation/liberation of the contribution of cascade particles, also it is noted that vaporization theory explains only the part of the total cross section of the emission of complex particles. This is evident, in particular, from Table 131.

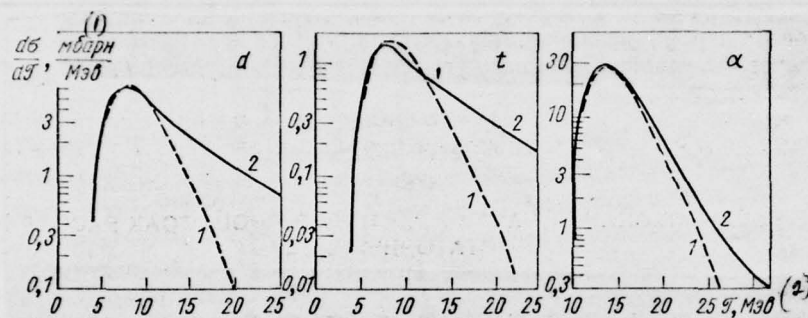


Fig. 405. Comparison of the calculated (1) and experimental (2) sections of the formation of complex particles with isotropic angular distribution in the system of target nucleus [38]. Particles were formed as a result of the interactions of the protons of energy 156 MeV with the nuclei of silver.

Key: (1). mbarn/MeV. (2). MeV.

Table 131. Comparison of the experimental and calculated cross-sections of the formation of tritium during the interactions of protons with the nuclei of iron and lead [87].

(1) Ядро	(2) T, Мэв	(3) Энергия возбуждения E*, Мэв	(4) Сечение образования трития, мб/арн		
			(5) Прямое испарение	(6) Прямое и косвенное испарение	(7) Опыт *
Fe	50	35	0,51	1,20	4,2
	75	41	0,86	2,00	4,3±0,8
	93	47	1,31	3,04	5±1
	100	48	1,34	3,16	4,8±0,9
	135	49	1,43	3,34	6,4±1,2
	150	50	1,54	3,58	6,1±1,1
	160	51	1,58	3,68	7,2
	177	53	1,74	4,05	6,6±1,2
	450	75	4,30	10,1	28±5
	1000	130	13,0	31,0	60
	2050	180	20,6	49,6	53±8
Pb	120	70	7,75	17,4	17±5
	300	100	17,0	38,2	73±22
	450	130	26,5	61,0	91±27
					71±8
	550	160	38,0	88,3	87±26
	600	170	41,7	97,0	157±47
	660	180	44,5	103,5	186±56
	2050	425	97,0	231,0	510±72

Key: (1). Nucleus. (2). MeV. (3). Excitation energy E*, MeV. (4). Section of the formation of tritium, mb. (5). Direct/straight

evaporation. (6). Direct/straight and indirect evaporation. (7).

Experiment 1.

FOOTNOTE 1. See Table 121. ENDFOOTNOTE.

Page 527.

At the same time that statistical theory of evaporation, which usually is utilized for the calculations of the emission of the deuterons and other complex particles (see Chapter 6), itself needs improvement, since it does not consider the processes of the so-called indirect evaporation, when complex particle is formed by the association of several less complex particles, which escape from nucleus as a result of the usual process of evaporation (this process conditionally let us call direct/straight evaporation) [87]. For example, the indirect evaporation of the nucleus of tritium can occur as a result of the direct/straight evaporation of neutron and two protons and their subsequent association or as a result of the association evaporative deuteron and neutron.

The theory of indirect evaporation is examined in detail by I. I. P'yanov and his co-authors [52, 54, 55, 87]. It was shown, that

the probability of the process of indirect evaporation can be represented in the form of the product of the probabilities, which correspond to the processes of the direct/straight evaporation of component parts, and to the probability of their subsequent association into the nucleus of tritium.

The results of the calculation of the sections, which consider the processes of indirect evaporation, are given in Table 131. We see that these processes give very considerable contribution. Unfortunately, the theory of indirect evaporation and its agreement with experiment are still very weakly investigated and any determined conclusions are represented thus far premature.

In conclusion let us mention even about the attempt of Hagedorn to explain the emission of rapid deuterons because of the purely statistical process of their formation during inelastic collisions within nucleus in the same way as this occurs, for example, for the strange particles whose generation is well described by Fermi's statistical theory [45, 46]. However, the sections of the formation of such deuterons, in the first place, are too small in order to explain experiment, and, in the second place, statistical theory predicts powerful increase with energy of the ratio of the number of emitted deuterons to the number of protons, what is not observed on experiment.

BEST AVAILABLE COPY

We see that the combined use of cascade and evaporative models, apparently, makes it possible to hope to explain the base properties of the processes of the emission of doubly charged particles. However, comparison with experiment made thus far still insufficiently thoroughly and thoroughly, here is required further experimental and theoretical work.

Bibliography.

1. Abate E. et al. Nuovo cimento, 22, 1206 (1961).
2. Абдинов О. Б. «Изв. АН АзССР» (в печати).
3. Абдинов О. Б., Барашенков В. С. Сообщение ОИЯИ Р2-4788 (1969). Сечения расщеплений легких ядер высокоэнергетическими протонами.
4. Ажгирей Л. С. и др. «Ж. эксперим. и теор. физ.», 33, 1185 (1957).
5. Ажгирей Л. С. и др. «Ж. эксперим. и теор. физ.», 34, 1397 (1958).
6. Bailey L. E. Report UCRL-3334 (1956). Угловые и энергетические распределения заряженных частиц, образующихся при высокоэнергетической бомбардировке различных элементов.
7. Balea E. et al. Nuovo cimento, 25, 214 (1962).
8. Balashov V. V., Bojarkina A. N., Rotter I. Nucl. Phys., 59, 417 (1964).
9. Балашов В. В. и др. «Ж. эксперим. и теор. физ.», 37, 1387 (1959).
10. Baker E. W., Katcuff S., Baker C. P. Phys. Rev., 117, 1352 (1960).
11. Барашенков В. С., Абдинов О. Б. Сообщение ОИЯИ Р2-4568 (1969). Внутриядерные каскады с учетом α -кластеров.
12. Barr D. W. Thesis, Univ. of California. UCRL-3793 (1957). Ядерные реакции в меди, индуцированные протонами при 5,7 Гэв.
13. Benioff P. A. Phys. Rev., 119, 316 (1960).
14. Bennett G. W. et al. Phys. Rev. Lett., 19, 387 (1967).
15. Beregi P. et al. Nucl. Phys., 66, 513 (1965).
16. Bhargadwaj P. D., Jain P. L. Nuovo cimento, 55, 765 (1968).
17. Bieri R. H., Rutsch W. Helv. phys. acta, 35, 553 (1962).
18. Блохинцев Д. И. «Ж. эксперим. и теор. физ.», 33, 1295 (1961).
19. Бриль О. Д. и др. Ядерные взаимодействия в защите космических кораблей. М., Атомиздат, 1968, стр. 121.
20. Brun C., Lefort J. M., Tarrago X. J. Phys. Radiation, 23, 167 (1962).

Pages 528 and 529.

21. Butler S. T., Pearson C. A. Phys. Rev. Lett., 7, 69 (1961).
22. Butler S. T., Pearson C. A. Phys. Rev., 129, 836 (1963).
23. Fierman E. L., Zahringer J. Phys. Rev., 107, 1695 (1957).
24. Chapman K. R. et al. Phys. Lett., 11, 253 (1964).
25. Cocconi G. In: Proc. Intern. Conf. on High-Energy Phys., Rochester, 1960.
26. Cocconi V. T. et al. Phys. Rev. Lett., 5, 19 (1960).
27. Currie A. Phys. Rev., 114, 878 (1959).
28. Currie A., Libby F., Wolfgang L. Phys. Rev., 101, 1557 (1956).
29. Dostrovsky I., Fraenkel Z., Friedlander C. Phys. Rev., 116, 683 (1959).
30. Dubost H. et al. J. Phys. Radiation, 28, 257 (1967).
31. Dubost H. et al. Phys. Rev., 136B, 1618 (1964).
32. Елисеев С. М. Диссертация. Дубна, 1967. Механизм взаимодействия элементарных частиц с атомными ядрами при высоких энергиях.
33. Елисеев С. М. Сообщение ОИЯИ Р2-4258 (1969). Образование ядер с массовыми числами $A = 2 - 4$ при столкновениях частиц высокой энергии со сложными ядрами.
34. Ephremer M., Gradstajn E. J. Phys. Radiation, 28, 745 (1967).
35. Evans D. et al. Nuovo cimento, 21, 740 (1961).
36. Fireman E. L. Phys. Rev., 97, 1303 (1955).
37. Fireman E. L., Rowland F. S. Ibid., p. 780.
38. Gatty B., Lefort M., Tarrago X. J. Phys. Radiation, 29, 705 (1968).
39. Gauvin H., Lefort M., Tarrago X. Nucl. Phys., 39, 447 (1962).
40. Gauvin H., Lefort M., Tarrago X. J. Phys. Radiation, 24, 669 (1963).
41. Goebel K. CERN report, 58-2 (1958). Образование трития в железе протонами при энергиях между 50 и 177 Мэв.
42. Goebel K., Schultes H., Zähringer J. CERN report 64-12 (1964). Сечения образования трития и редких газов в мишенях из различных элементов.
43. Gooding T. J., Igo C. Phys. Rev. Lett., 7, 28 (1961).
44. Григорьев Е. Л., Соловьева Л. Н. «Ж. эксперим. и теор. физ.», 31, 932 (1956).
45. Hagedorn R. Phys. Rev. Lett., 5, 276 (1960).
46. Hagedorn R. Nuovo cimento, 25, 1031 (1962).
47. Harada K. Progr. Theoret. Phys., 27, 430 (1962).
48. Honda M., Lal D. Phys. Rev., 118, 1618 (1960).
49. James A. N., Pugh H. G. Nucl. Phys., 42, 441 (1963).
50. Jaannet E., Russell J., Vaecher E. Helv. phys. acta, 30, 484 (1957).
51. Jones B. D. et al. Nuovo cimento, 19, 1077 (1961).
52. Иванов Н. С., Пьянов И. И. «Ж. эксперим. и теор. физ.», 31, 416 (1956).
53. Igo C., Hansen L. F., Gooding T. J. Phys. Rev., 131, 337 (1963).
54. Измайлов С. В., Пьянов И. И. «Ж. эксперим. и теор. физ.», 41, 118 (1961).
55. Измайлов С. В., Пьянов И. И. В сб. «Ядерная химия», М., «Наука», 1965.
56. Katkoff S. Phys. Rev., 157, 1126 (1967).
57. Katkoff S. Phys. Rev., 164, 1367 (1967).
58. Kamal A. A. et al. Nuovo cimento, 43, 91 (1966).
59. Kellogg D. A. Phys. Rev., 90, 224 (1953).
60. Кобзев В. А., Такибаев Ж. С., Шалагина Е. В. «Изв. АН КазССР. Сер. физ.», 2, 3 (1965).
61. Кобзев В. А. и др. «Тр. Ин-та ядерной физики АН КазССР», 6, 133 (1963).
62. Комаров В. И., Косарев Г. Е., Савченко О. В. Сообщение ОИЯИ Р1-4227 (1968). Квазиупругое рассеяние протонов с энергией 665 Мэв α -частичными ассоциациями в легких ядрах.
63. Комаров В. И., Косарев Г. Е., Савченко О. В. Сообщение ОИЯИ Р1-4373 (1969). Выбивание быстрых ^3He -фрагментов из легких ядер протонами с энергией 665 Мэв.
64. Кузнецов В. В., Мехедов В. Н. «Ж. эксперим. и теор. физ.», 35, 587 (1958).
65. Кузьмин В. Н., Яковлев Р. М. «Изв. АН СССР. Сер. физ.», 29, 1237 (1965).
66. Кузьмин В. Н., Яковлев Р. М. «Ядерная физика», 6, 1158 (1967).
67. Ле Кутер К. Дж. В кн. «Ядерные реакции». Под ред. П. М. Эндта и М. Демера. Перев. с англ. Под ред. И. С. Шапиро. М., Госатомиздат. 1962, стр. 309.
68. Lefort M., Tarrago X. Report de Lab. Joliot Curie. Faculte des Sciences de Paris (1960).

69. Lefort M., Cohen J. P., Tarrago X. Phys. Rev., 139B, 1500 (1965).
70. Lefort M. et al. J. Phys. Radiation, 20, 959 (1959).
71. Lefort M., Simonoff C., Tarrago X. Nucl. Phys., 19, 173 (1960).
72. Lefort M., Simonoff G. M., Tarrago X. Nucl. Phys., 25, 216 (1961).
73. Lefort M., Tarrago X. Nucl. Phys., 46, 161 (1963).
74. Lingenfelter R. E., Ramaty R. In: High Energy Nuclear Reactions in Astrophysics. W. A. Benjamin, Inc., N.Y. 1967.
75. Lock W. O., March P. V., McKeague R. Proc. Roy. Soc., 231, 368 (1955).
76. Ложкин О. В. и др. «Ж. эксперим. и теор. физ.», 38, 1388 (1960).
77. McKeague R. Proc. Roy. Soc., 236, 104 (1956).
78. Metropolis N. et al. Phys. Rev., 110, 185 (1958).
79. Мехедов Б. Н., Мехедов В. Н. «Ядерная физика», 11, 708 (1970).
80. Мехедов В. Н. «Ядерная физика», 5, 34 (1967).
81. Muirhead H., Rosser W. G. V. Philos. Mag., 46, 652 (1955).
82. Остроумов В. И., Филов Р. А. «Ж. эксперим. и теор. физ.», 31, 913 (1956).
83. Остроумов В. И., Перфилов Н. А., Филов Р. А. «Ж. эксперим. и теор. физ.», 36, 367 (1967).
84. Остроумов В. И., Филов Р. А. «Ж. эксперим. и теор. физ.», 37, 643 (1959).
85. Остроумов В. И., Перфилов Н. А., Филов Р. А. «Ж. эксперим. и теор. физ.», 39, 105 (1960).
86. Porile N. T. Phys. Rev., 135B, 371 (1963).
87. Пьянов И. И. Диссертация, Ленинград, 1963. Образование сложных частиц в ядерных реакциях высокой энергии.
88. Ранопорт Л. П., Крыловский А. Г. «Изв. АН СССР. Сер. физ.», 28, 388 (1964).
89. Rosenfeld A. H. Phys. Rev., 96, 139 (1954).
90. Rottenberg M., Wilets L. Phys. Rev., 110, 1126 (1958).
91. Rudstam G., Bruninx E., Pappas A. C. Phys. Rev., 126, 1850 (1962).
92. Ruhla C. et al. Phys. Lett., 6, 282 (1963).
93. Samman A., J. Phys. Radiation, 18, 77 (S) (1957).
94. Saniewska T., Skrzypozak E., Zielinski P. Nucl. Phys., 70, 567 (1955).
95. Schaeffer O. A., Zahringer J. Phys. Rev., 113, 674 (1959).
96. Шалагина Е. В. Диссертация. Алма-Ата, 1967. Испускание двухзарядных частиц большой энергии в ядерных расщеплениях.
97. Schwarzschild A., Zupančič C. Phys. Rev., 129, 854 (1963).
98. Silveira R. D. Phys. Lett., 9, 252 (1964).
99. Skjeggstad O., Sörensen S. O. Phys. Rev., 113, 1115 (1959).
100. Соловьев В. Г. «Докл. АН СССР», 131, 286 (1960).
101. Sutler S. T. et al. Phys. Rev. Lett., 19, 1189 (1967).
102. Такибаев Ж. С. и др. «Изв. АН СССР. Сер. физ.», 26, 592 (1962).
103. Такибаев Ж. С. и др. «Ядерная физика», 3, 849 (1966).
104. Такибаев Ж. С. и др. «Ядерная физика», 5, 703 (1967).
105. Такибаев Ж. С., Шалагина Е. В., Цадикова Г. Р. «Докл. АН СССР», 141, 1347 (1962).
106. Такибаев Ж. С. и др. «Изв. АН Каз.ССР», 2, 51 (1965).
107. Такибаев Ж. С., Тлеубергенова Г. А., Шалагина Е. В. «Докл. АН СССР», 156, 785 (1964).
108. Такибаев Ж. С., Токтаров К. А. «Ядерная физика», 6, 1015 (1967).
109. Tinland B., Bartolin F., Burdet A. J. Phys. Radiation, 24, 604 (1963).
110. Тлеубергенова Г. А., Лазарев Г. П., Морозов П. В. «Вестник АН Каз.ССР», 10, 35 (1964).
111. Токтаров К. «Ядерная физика», 8, 940 (1968).
112. Ваганов П. А., Остроумов В. И. «Ж. эксперим. и теор. физ.», 33, 1131 (1957).
113. Wilkinson D. H. In: Proceedings Rutherford International Conference. 1961, p. 339.
114. Vogt E. Advances Nucl. Phys., 1, 261 (1968).
115. Yasin M. Nuovo cimento, 28, 935 (1963).
116. Yasin M. Nuovo cimento, 34, 1145 (1964).
117. Яковлев Р. М. Диссертация. РИАН, Ленинград, 1968. Изучение α -подструктур легких ядер с помощью высокоэнергетических протонов.
118. Zanger C. L., Rosset J. Helv. phys. acta, 29, 507 (1956).
119. Жданов А. П., Кузьмин В. Н., Яковлев Р. М. «Ядерная физика», 1, 625 (1965).
120. Жданов А. П., Кузьмин В. Н., Яковлев Р. М. «Изв. АН СССР. Сер. физ.», 29, 239 (1965).
121. Жданов А. П., Федотов П. И. «Ж. эксперим. и теор. физ.», 37, 392 (1959).
122. Жданов А. П., Федотов П. И. «Ж. эксперим. и теор. физ.», 41, 1870 (1961); 43, 835 (1962); 45, 455 (1963).

Chapter 9.

FRAGMENTATION.

§93. Preliminary observations.

As for many other phenomena of nuclear high-energy physics, the first information about the formation of fragments - fragments with the masses, greater than for the nucleus of helium, and with charges $Z_{\phi} \geq 3$ - were obtained in experiments with cosmic radiation still during the prewar years) [62, 65, 115]; however, systematic research on the processes of fragmentation was begun only in 50-x years after inauguration of accelerator with the energy, greater than several hundreds of million electron volt. For investigation were utilized both radiochemical and photoemulsion methods and the precision electronic technology with proportional and scintillation counters.

At the present time is accumulated the enormous experimental material whose analysis showed that the fragmentation possesses a whole series of the very specific special feature/peculiarities,

which essentially differ this phenomenon from the cascade-evaporative process of nuclear disintegration and from fission reaction. However, since available now there is no consecutive theory, which describes the formation of fragments, fragmentation frequently is called the formation of heavy multiply-charged fragments with $Z_{\phi} \geq 3$ and mass number $A_{\phi} \simeq 5 - 40$ irrespectively of the type of the process, in which these fragments were formed (specifically, this process it can be the examined above evaporation of the excited nuclei). Thus, from the very beginning it is possible to expect that the phenomenon of fragmentation, since it now is understood, hardly be managed to explain by some mechanism; most likely this - the totality of several different in their nature processes.

Below we discuss the basic experimental laws governing the process of fragmentation and let us examine the models, which were being proposed by the different authors for their explanation. The detailed presentation of all these questions would take away far into the region of nuclear structure and would require, in essence, the writing of separate monograph; therefore for familiarization with parts we send away the reader to the original literature (see the copy of works on page 560) and to survey/coverages [39, 87, 105, 107], where also it is possible to find detailed bibliography.

§94. Sections of the process of fragmentation.

The experimental information about the sections of fragmentation for the basic target nuclei and most widely known fragments is assembled in Table 132. From the data of Table 133 it is possible to obtain the representation of the production cross sections of different fragments in photoemulsion. For a larger clarity the most characteristic experimental data are represented also in Figs. 406-408. Curves in these figures can be utilized for determining the value of sections σ_{ψ} at the intermediate values of energy T .

Pages 531-535.

Table 132. Sections of fragmentation under the action of protons with an energy of T.

(1) Ядро-мишень и фрагмент	(2) T, Гэв	(3) $\sigma_{\text{ф}}$, мбарн	(4) Литература	(1) Ядро-мишень и фрагмент	(2) T, Гэв	(3) $\sigma_{\text{ф}}$, мбарн	(4) Литература
$^{27}\text{Al} \rightarrow ^9\text{Li}$	1	0,133	[36]	$^{27}\text{Al} \rightarrow ^{18}\text{F}$	6	$6,52 \pm 0,33$	[29]
	2,8	0,238	[36]		10	$6,35 \pm 0,32$	[29]
$^{27}\text{Al} \rightarrow ^7\text{Be}$					17	$6,25 \pm 0,31$	[29]
					28	$6,03 \pm 0,11$	[27]
	0,0505	$0,31 \pm 0,03$	[44]	$^{27}\text{Al} \rightarrow ^{22}\text{Na}$	0,0505	37 ± 1	[44]
	0,0521	$0,31 \pm 0,1$	[44]		0,0513	36 ± 1	[44]
	0,0536	$0,35 \pm 0,1$	[44]		0,0521	35 ± 1	[44]
	0,0544	$0,32 \pm 0,1$	[44]		0,0528	34 ± 1	[44]
	0,0551	$0,35 \pm 0,2$	[44]		0,0536	32 ± 1	[44]
	0,07	$0,76 \pm 0,3$	[81]		0,0544	32 ± 1	[44]
	0,085	$1,06 \pm 0,01$	[81]		0,0551	31 ± 1	[44]
	0,155	$1,0 \pm 0,2$	[83]		0,335	12	[93]
	0,16	$1,4 \pm 0,3$	[58]		0,4	$15,5 \pm 1,6$	[78]
	0,2	$1,7 \pm 0,3$	[58]		0,42	$17 \pm 4,6$	[92]
	0,25	$2,2 \pm 0,4$	[58]		0,6	$19,6 \pm 2,0$	[42]
	0,3	$2,6 \pm 0,5$	[58]		1	$16 \pm 1,6$	[42]
	0,335	1,4	[93]		1,4	$17,7 \pm 1,8$	[42]
	0,36	$2,9 \pm 0,5$	[58]		1,6	$12 \pm 1,2$	[42]
	0,4	$3,1 \pm 0,6$	[58]		1,8	$15,6 \pm 1,6$	[42]
	0,66	$4,2 \pm 0,3$	[96]		2	$12,3 \pm 0,7$	[29]
	1	$7,6 \pm 1,9$	[4, 42]		2,2	$12 \pm 1,2$	[42]
	1,4	$8,3 \pm 2,1$	[4, 42]		2,9	$11,1 \pm 0,6$	[29]
	2,2	$10,8 \pm 2,7$	[4, 42]		3	$13,5 \pm 1,4$	[42]
	2,9	$7,5 \pm 0,4$	[29]		5,7	17 ± 3	[18]
	3	$11,7 \pm 2,9$	[4]		28	$9,85 \pm 0,31$	[27]
	5,7	$8,3 \pm 0,9$	[18]				
	28	$7,89 \pm 0,29$	[27]				
$^{27}\text{Al} \rightarrow ^{11}\text{C}$	0,335	1,9	[93]	$^{27}\text{Al} \rightarrow ^{24}\text{Na}$	0,202	$9,6 \pm 0,5$	[101]
	0,41	$2,9 \pm 1,0$	[42]		0,259	$9,8 \pm 0,5$	[101]
	0,42	$2,25 \pm 0,15$	[29]		0,294	$10 \pm 0,5$	[101]
	0,42	2,8	[92]		0,335	11	[93]
	0,6	$3,4 \pm 1,1$	[42]		0,342	$10,1 \pm 0,5$	[101]
	1	$5,05 \pm 1,6$	[42]		0,4	$10,5 \pm 0,7$	[78]
	1	$4,2 \pm 0,3$	[29]		0,42	10,8	[92]
	1,4	$4,9 \pm 1,8$	[42]		1	10,1	[42]
	2	$5,2 \pm 0,3$	[29]		1,6	8,7	[42]
	2,2	$5 \pm 1,7$	[42]		2,2	8,8	[42]
	2,9	$5,1 \pm 0,3$	[29]		3	8,1	[42]
	3	$4,9 \pm 1,6$	[42]		28	$8,34 \pm 0,23$	[27]
	6	$4,9 \pm 0,3$	[29]				
	10	$4,8 \pm 0,3$	[29]				
$^{27}\text{Al} \rightarrow ^{18}\text{F}$	17	$4,6 \pm 0,3$	[29]	$^{28}\text{Si} \rightarrow ^9\text{Li}$	1	0,077	[36]
	28	$4,73 \pm 0,10$	[27]				
	0,202	$5,7 \pm 0,6$	[101]	$^{28}\text{Si} \rightarrow ^7\text{Be}$	0,13	$1,07 \pm 0,27$	[111]
	0,294	$6,5 \pm 0,7$	[101]		0,208	$0,76 \pm 0,19$	[111]
	0,335	5,5	[93]		0,297	$1,69 \pm 0,34$	[111]
	0,342	$6,7 \pm 0,7$	[101]		0,396	$2,02 \pm 0,40$	[111]
	0,41	$7,1 \pm 0,7$	[42]		0,5	$2,4 \pm 0,5$	[112]
	0,42	$8,4 \pm 1,3$	[92]		0,8	$2,6 \pm 0,5$	[112]
	0,42	$7,6 \pm 0,4$	[29]		1,5	$2,8 \pm 0,6$	[112]
	0,6	$7,05 \pm 0,71$	[42]		2,2	$3,6 \pm 0,6$	[112]
	1	$7,1 \pm 0,7$	[42]		2,9	$4,1 \pm 0,8$	[112]
	1	$7,9 \pm 0,5$	[29]	$^{28}\text{Si} \rightarrow ^{22}\text{Na}$	0,13	$10,41 \pm 1,06$	[111]
	1,4	$5,9 \pm 0,6$	[42]		0,208	$10,28 \pm 1,03$	[111]
	2	$7,3 \pm 0,4$	[29]		0,297	$13,09 \pm 1,3$	[111]
	2,2	$5,8 \pm 0,6$	[42]		0,396	$12,46 \pm 1,3$	[111]
	2,9	$6,8 \pm 0,4$	[29]		0,4	$17,4 \pm 1,1$	[78]
	3	$5,3 \pm 0,5$	[42]		0,5	$8,6 \pm 1,7$	[112]
	5,7	$7,68 \pm 0,57$	[18]		0,8	$8,2 \pm 1,6$	[112]

Table 132. (cont'd).

① Ядро-мишень и фрагмент	② T, Гэв	③ σ _ф , мбарн	④ Лите- ратура	① Ядро-мишень и фрагмент	② T, Гэв	③ σ _ф , мбарн	④ Лите- ратура
$^{28}\text{Si} \rightarrow ^{22}\text{Na}$	1,5 2,2 2,9	$7,8 \pm 1,6$ $8,4 \pm 1,7$ $9,1 \pm 1,8$	[112] [112] [112]	$^{55,9}\text{Fe} \rightarrow ^{24}\text{Na}$	1,5 2,2 2,9 29	$3,2 \pm 0,6$ $3,8 \pm 0,8$ $3,9 \pm 0,8$ $3,8 \pm 0,1$	[112] [112] [112] [109]
$^{28}\text{Si} \rightarrow ^{24}\text{Na}$	0,13 0,208 0,297 0,396 0,4 0,5 0,8 1,5 2,2 2,9	$3,378 \pm 0,660$ $3,662 \pm 0,366$ $4,740 \pm 0,474$ $4,78 \pm 0,478$ $4,18 \pm 0,20$ $4,6 \pm 0,9$ $4,7 \pm 0,9$ $5,0 \pm 1,0$ $4,0 \pm 0,8$ $5,2 \pm 1,0$	[111] [111] [111] [111] [78] [112] [112] [112] [112] [112]	$^{55,9}\text{Fe} \rightarrow ^{32}\text{P}$	0,13 0,208 0,297 0,34 0,396 0,5 0,8 1,5 2,2 2,9	$0,020 \pm 0,008$ $0,086 \pm 0,013$ $0,320 \pm 0,050$ 0,044 $0,61 \pm 0,092$ $1,28 \pm 0,26$ $3,6 \pm 0,7$ $5,4 \pm 1,1$ $6,1 \pm 1,2$ $6,1 \pm 1,2$	[111] [111] [111] [114] [111] [112] [112] [112] [112] [112]
$^{47,9}\text{Ti} \rightarrow ^9\text{Li}$	1 2,8	0,125 0,409	[36] [36]	$^{58,7}\text{Ni} \rightarrow ^7\text{Be}$	0,085 0,13 0,208 0,297 0,396 0,5 0,8 1,5 2,2 2,9	$0,095 \pm 0,01$ $0,206 \pm 0,041$ $0,380 \pm 0,070$ $0,590 \pm 0,090$ $0,810 \pm 0,122$ $1,62 \pm 0,32$ $2,4 \pm 0,48$ $4,9 \pm 1,0$ $6,5 \pm 1,3$ $7,2 \pm 1,4$	[111] [111] [111] [111] [111] [112] [112] [112] [112] [112]
$^{47,9}\text{Ti} \rightarrow ^7\text{Be}$	0,065 0,085	0,074 $0,25 \pm 0,01$	[81] [81]	$^{58,7}\text{Ni} \rightarrow ^{22}\text{Na}$	0,4	$(9,58 \pm 0,45) \cdot 10^{-2}$	[78]
$^{47,9}\text{Ti} \rightarrow ^{22}\text{Na}$	0,4 29	$0,344 \pm 0,014$ $3,7 \pm 0,2$	[78] [109]	$^{58,7}\text{Ni} \rightarrow ^{24}\text{Na}$	0,4 0,5 0,8 1,5 2,2 2,9	$(7,18 \pm 0,27) \cdot 10^{-2}$ $0,185 \pm 0,037$ $0,65 \pm 0,13$ $1,82 \pm 0,36$ $3,4 \pm 0,7$ $3,9 \pm 0,8$	[78] [112] [112] [112] [112] [112]
$^{47,9}\text{Ti} \rightarrow ^{24}\text{Na}$	0,4 29	$0,538 \pm 0,016$ $4,2 \pm 0,3$	[78] [109]	$^{58,7}\text{Ni} \rightarrow ^{32}\text{P}$	0,13 0,208 0,297 0,396 0,5 0,8 1,5 2,2 2,9	$(7,0 \pm 1,4) \cdot 10^{-3}$ $(2,5 \pm 0,4) \cdot 10^{-2}$ $0,133 \pm 0,020$ $0,272 \pm 0,041$ $0,89 \pm 0,18$ $2,1 \pm 0,42$ $3,4 \pm 0,7$ $4,5 \pm 0,9$ $4,6 \pm 0,9$	[111] [111] [111] [112] [112] [112] [112] [112] [112]
$^{51}\text{V} \rightarrow ^7\text{Be}$	0,065 0,085 0,155	0,074 $0,147 \pm 0,007$ $0,23 \pm 0,04$	[81] [81] [83]	$^{63,5}\text{Cu} \rightarrow ^9\text{Li}$	1 2,8	0,120 0,44	[36] [36]
$^{51}\text{V} \rightarrow ^{22}\text{Na}$	0,4	$0,166 \pm 0,007$	[78]	$^{63,5}\text{Cu} \rightarrow ^7\text{Be}$	0,065 0,085 0,335 0,48	0,023 $0,065 \pm 0,01$ 0,5 $1,6 \pm 0,8$	[81] [81] [93] [96]
$^{51}\text{V} \rightarrow ^{24}\text{Na}$	0,4	$0,307 \pm 0,014$	[78]				
$^{55,9}\text{Fe} \rightarrow ^7\text{Be}$	0,085 0,13 0,208 0,297 0,396 0,5 0,8 1,5 2,2 2,9	$0,089 \pm 0,008$ $0,175 \pm 0,035$ $0,313 \pm 0,047$ $0,47 \pm 0,071$ $0,57 \pm 0,086$ $1,21 \pm 0,24$ $2,1 \pm 0,4$ $3,2 \pm 0,6$ $5,7 \pm 1,1$ $4,7 \pm 0,9$	[81] [111] [111] [111] [111] [112] [112] [112] [112] [112]				
$^{55,9}\text{Fe} \rightarrow ^{22}\text{Na}$	0,34 0,4 29	0,02 $0,108 \pm 0,004$ $3,4 \pm 0,3$	[114] [78] [109]				
$^{55,9}\text{Fe} \rightarrow ^{24}\text{Na}$	0,34 0,4 0,5 0,8	0,026 $0,133 \pm 0,008$ $0,29 \pm 0,06$ $1,07 \pm 0,21$	[114] [78] [112] [112]				

Table 132. (cont'd).

① Ядро-мишень и фрагмент	② $T_{\text{эв}}$	③ $\sigma_{\text{ф}}$, мбарн	④ Литература	① Ядро-мишень и фрагмент	② $T_{\text{эв}}$	③ $\sigma_{\text{ф}}$, мбарн	④ Литература
$^{63,5}\text{Cu} \rightarrow ^7\text{Be}$	1	4.4 ± 1.1	[4]	$^{63,5}\text{Cu} \rightarrow ^{31}\text{P}$	0,34	0,12	[8]
	2,2	10 ± 2	[125]		0,34	$0,018 \pm 0,006$	[80]
	3	$11,9 \pm 3,0$	[4]		0,48	0,05	[125]
	5,7	13,7	[66]		0,48	$0,024 \pm 0,01$	[80]
	10	11,9	[66]		0,66	$0,31 \pm 0,10$	[80]
	20	10,6	[66]	$^{63,5}\text{Cu} \rightarrow ^{32}\text{P}$	0,12	$(7 \pm 2) \cdot 10^{-4}$	[80]
	24	$7,0 \pm 0,8$	[66]		0,22	$(2,2 \pm 1) \cdot 10^{-3}$	[80]
$^{63,5}\text{Cu} \rightarrow ^{11}\text{C}$	0,37	$\sim 0,03$	[125]		2,2	$6,4 \pm 1,6$	[41]
	0,48	0,057	[125]		24	$3,1 \pm 0,4$	[113]
	2,2	$> 0,65$	[41]	$^{63,5}\text{Cu} \rightarrow ^{28}\text{Mg}$	0,7	0,049	[59]
$^{63,5}\text{Cu} \rightarrow ^{10}\text{F}$	0,37	$\sim 0,03$	[125]		24	$0,25 \pm 0,03$	[113]
	0,4	$0,08 \pm 0,04$	[92]	$^{107,9}\text{Ag} \rightarrow ^9\text{Li}$	1	0,220	[36]
	0,66	$0,10 \pm 0,03$	[96]		2,8	1,05	[36]
	1	0,51	[25]	$^{107,9}\text{Ag} \rightarrow ^7\text{Be}$	0,065	$\sim 0,024$	[81]
	2	0,55	[4]		0,085	$\sim 0,028$	[81]
	2,2	$1,0 \pm 0,2$	[41]		0,335	0,1	[93]
	3	$1,7 \pm 0,4$	[25]		1	$2,6 \pm 0,7$	[4]
	4,5	$2,5 \pm 0,6$	[25]		2,2	$11,3 \pm 2,8$	[4]
	5,9	$3,4 \pm 0,9$	[25]		3	$12,1 \pm 3,0$	[4]
	24	$1,5 \pm 0,1$	[113]		3	8	[76]
$^{63,5}\text{Cu} \rightarrow ^{22}\text{Na}$	0,34	0,037	[8]		29	$7,4 \pm 0,7$	[68]
	0,4	$(3,81 \pm \pm 0,09) \cdot 10^{-2}$	[78]		30	18,2	[76]
	0,66	0,043	[125]		30	$18,2 \pm 1,8$	[68]
	2,2	$1,8 \pm 0,4$	[41]	$^{107,9}\text{Ag} \rightarrow ^{18}\text{F}$	0,42	$0,016 \pm 0,008$	[92]
	3	1,85	[66]		1	0,2	[25]
	5,7	2,4	[66]		2	0,55	[4]
	10	2,9	[66]		3	$1,7 \pm 1,0$	[25]
	20	2,56	[66]		3	1,43	[76]
	24	$1,4 \pm 0,02$	[113]		4,5	1,9	[25]
	29	$3,0 \pm 0,2$	[109]		5,9	$1,5 \pm 0,4$	[25]
	30	2,75	[66]	$^{107,9}\text{Ag} \rightarrow ^{22}\text{Na}$	0,4	$(1,04 \pm \pm 0,03) \cdot 10^{-2}$	[78]
$^{63,5}\text{Cu} \rightarrow ^{24}\text{Na}$	0,12	$(9 \pm 3) \cdot 10^{-4}$	[80]		2,8	1,14	[76]
	0,22	$(2,2 \pm 1) \cdot 10^{-3}$	[80]		3	$1,1 \pm 0,1$	[68]
	0,34	0,03	[8]		29	2,35	[76]
	0,34	$0,013 \pm 0,005$	[80]		30	$2,2 \pm 0,2$	[68]
	0,37	0,03	[25]	$^{107,9}\text{Ag} \rightarrow ^{24}\text{Na}$	0,4	$(1,65 \pm \pm 0,08) \cdot 10^{-2}$	[78]
	0,4	$(4,81 \pm \pm 0,22) \cdot 10^{-2}$	[78]		0,7	0,1	[59]
	0,48	$0,036 \pm 0,021$	[80]		1	0,3	[25]
	0,66	$0,25 \pm 0,08$	[80]		2	1,4	[4]
	0,66	0,32	[25]		2,8	$2,7 \pm 0,4$	[25]
	0,7	0,368	[59]		2,8	2,24	[76]
	0,7	0,94	[125]		3	$2,1 \pm 0,2$	[68]
	1	1,0	[25]		4,5	4,1	[25]
	2	1,4	[4]		5,9	$3,3 \pm 0,8$	[25]
	2,2	$3,2 \pm 0,8$	[41]		29	4,1	[76]
	3	$4,0 \pm 1,0$	[25]		30	$4,7 \pm 0,5$	[68]
	3	2,96	[66]	$^{107,9}\text{Ag} \rightarrow ^{28}\text{Mg}$	0,7	0,012	[59]
	4,5	$4,6 \pm 1,2$	[25]				
	5,7	4,0	[66]				
	5,9	$4,8 \pm 1,2$	[25]				
	10	3,4	[66]				
	20	3,91	[66]				
	24	$1,8 \pm 0,2$	[113]				
	24	$3,5 \pm 0,3$	[109]				
	30	3,48	[66]				

Table 132. (cont'd).

① Ядро-мишень и фрагмент	② Т. Гэв	③ $\sigma_{\text{ф.}}$ мбарн	④ Лите- ратура	① Ядро-мишень и фрагмент	② Т. Гэв	③ $\sigma_{\text{ф.}}$ мбарн	④ Лите- ратура
$^{138}\text{La} \rightarrow ^9\text{Li}$	1 2,8	0,65 2,63	[36] [36]	$^{197}\text{Au} \rightarrow ^{18}\text{F}$	0,42 1 2 3 4,5 5,9	$(4,4 \pm \pm 2,2) \cdot 10^{-3}$ 0,07 0,25 0,73 1,7 2,5	[92] [25] [4] [25] [25] [25]
$^{138}\text{La} \rightarrow ^{24}\text{Na}$	0,12 0,12 0,22 0,22 0,34 0,48 0,66 0,66	$9,9 \cdot 10^{-4}$ $(1,0 \pm \pm 0,3) \cdot 10^{-3}$ $2,2 \cdot 10^{-3}$ $(3 \pm 1) \cdot 10^{-3}$ $5 \cdot 10^{-3}$ $0,02 \pm 0,008$ $0,21 \pm 0,07$ $0,19 \pm 0,07$	[80] [96] [80] [96] [80, 96] [80, 96] [80, 96] [80, 96]	$^{197}\text{Au} \rightarrow ^{22}\text{Na}$	0,4 30	$(3,61 \pm \pm 0,34) \cdot 10^{-3}$ $2,1 \pm 0,2$	[78] [68]
$^{138}\text{La} \rightarrow ^{31}\text{P}$	0,34 0,48	$(7,3 \pm \pm 1,2) \cdot 10^{-3}$ $0,014 \pm 0,005$	[80, 96] [80, 96]	$^{197}\text{Au} \rightarrow ^{24}\text{Na}$	0,335 0,4 0,48 0,66 0,7 1 2 3 4,5 5,9 30	$(5,9 \pm \pm 0,2) \cdot 10^{-3}$ $(2,15 \pm \pm 0,03) \cdot 10^{-2}$ $0,037 \pm 0,01$ $0,081 \pm 0,002$ 0,135 0,44 2,2 5,0 7,4 9,4 $10,4 \pm 1,0$	[80, 96] [78] [80, 96] [80, 96] [59] [25] [4] [25] [25] [25] [68]
$^{181}\text{Ta} \rightarrow ^9\text{Li}$	2	0,59	[36]	$^{197}\text{Au} \rightarrow ^{31}\text{P}$	0,34 0,34 0,48 0,66	0,056 $(3 \pm 1) \cdot 10^{-3}$ $0,011 \pm 0,003$ $0,022 \pm 0,008$	[80] [96] [80, 96] [80, 96]
$^{181}\text{Ta} \rightarrow ^7\text{Be}$	0,155 3 5,7 9 10 30	$0,042 \pm 0,008$ $7,2 \pm 0,7$ 26 ± 3 ~ 48 $19,6 \pm 2,0$ $19,9 \pm 2,0$	[83] [68] [61] [56] [68] [68]	$^{197}\text{Au} \rightarrow ^{28}\text{Mg}$	0,7	0,054	[59]
$^{181}\text{Ta} \rightarrow ^{22}\text{Na}$	0,4 3 5,7 10 30	$(6,18 \pm \pm 0,57) \cdot 10^{-3}$ $0,3 \pm 0,03$ $< 1,1$ $1,6 \pm 0,2$ $1,6 \pm 0,2$	[78] [68] [61] [68] [68]	$^{207,2}\text{Pb} \rightarrow ^9\text{Li}$	2,8	6,0	[36]
$^{181}\text{Ta} \rightarrow ^{24}\text{Na}$	0,4 1 2 3 3 5,7 5,9 10 30	$(1,87 \pm \pm 0,12) \cdot 10^{-2}$ 0,20 0,85 $2,3 \pm 0,6$ $4,7 \pm 0,5$ $8,7 \pm 0,5$ 8,7 $6,8 \pm 0,7$ $7,0 \pm 0,7$	[78] [25] [4] [25] [68] [61] [25] [68] [68]	$^{207,7}\text{Pb} \rightarrow ^7\text{Be}$	3 10 30	$6,2 \pm 0,6$ $21,4 \pm 2,1$ $22,1 \pm 2,2$	[68] [68] [68]
$^{182}\text{Ta} \rightarrow ^{32}\text{P}$	5,7	$4,4 \pm 0,5$	[61]	$^{207,2}\text{Pb} \rightarrow ^{18}\text{F}$	0,6 1 1 1,6 2 2,2 3 3 4,5 5,9	$0,005 \pm 0,001$ $0,039 \pm 0,008$ 0,05 $0,18 \pm 0,003$ 0,49 $0,39 \pm 0,08$ $0,40 \pm 0,08$ 0,83 1,1 1,4	[121] [121] [25] [121] [25] [121] [121] [121] [25] [25] [25]
$^{197}\text{Au} \rightarrow ^7\text{Be}$	0,065 0,085 0,155 0,335 0,55 1 1 2,2 3 30	$\sim 3 \cdot 10^{-3}$ $\sim 3,5 \cdot 10^{-3}$ 0,033 0,01 $0,35 \pm 0,05$ $1,7 \pm 0,4$ $1,0 \pm 0,2$ $5,9 \pm 1,5$ $8,7 \pm 2,2$ $21,6 \pm 2,2$	[81] [81] [83] [93] [83] [4] [4] [4] [4] [4] [68]	$^{207,7}\text{Pb} \rightarrow ^{22}\text{Na}$	0,4 1,6 2,2 3 3 10 30	$(5,10 \pm \pm 0,37) \cdot 10^{-3}$ $< 2,2$ $< 1,5$ $2,7 \pm 0,5$ $0,5 \pm 0,05$ $2,0 \pm 0,2$ $2,0 \pm 0,2$	[78] [121] [121] [121] [68] [68] [68]

Table 132. (cont'd).

(1) Ядро-мишень и фрагмент	(2) $T, \text{Гэв}$	(3) $\sigma_{\text{ф}}, \text{мбарн}$	(4) Литература	(1) Ядро-мишень и фрагмент	(2) $T, \text{Гэв}$	(3) $\sigma_{\text{ф}}, \text{мбарн}$	(4) Литература
$^{207}\text{Pb} \rightarrow ^{24}\text{Na}$	0,39	$0,030 \pm 0,006$	[121]	$^{238}\text{U} \rightarrow ^{18}\text{F}$	0,085	$(5,8 \pm \pm 0,3) \cdot 10^{-3}$	[96]
	0,4	$(1,75 \pm \pm 0,04) \cdot 10^{-2}$	[78]		0,66	$0,032 \pm 0,10$	[96]
	0,6	$< 0,02$	[121]		1	0,13	[25]
	1	$0,036 \pm 0,007$	[121]		2	0,55	[25]
	1	0,36	[25]		3	1,4	[25]
	1,6	$1,4 \pm 0,3$	[121]		4,5	2,0	[25]
	2	2,3	[25]		5,9	3,2	[25]
	2,2	$2,3 \pm 0,6$	[121]	$^{238}\text{U} \rightarrow ^{22}\text{Na}$	0,12	$(9,55 \pm \pm 0,67) \cdot 10^{-3}$	[78]
	3	$3,6 \pm 0,7$	[121]		3	$0,8 \pm 0,1$	[68]
	3	4,4	[25]		10	$2,0 \pm 0,2$	[68]
	3	$3,4 \pm 0,3$	[68]		30	$2,3 \pm 0,2$	[68]
	4,5	7,2	[25]	$^{238}\text{U} \rightarrow ^{24}\text{Na}$	0,085	$0,012 \pm 0,005$	[96]
	5,9	9,2	[25]		0,4	$(4,52 \pm \pm 0,12) \cdot 10^{-2}$	[78]
$^{207}\text{Pb} \rightarrow ^{32}\text{P}$	0,39	$< 0,01$	[121]		—	$0,09 \pm 0,02$	[96]
	0,6	$\sim 0,02$	[121]		0,66	0,230	[59]
	1	$0,09 \pm 0,02$	[121]		0,66	0,63	[25]
	1,6	$0,31 \pm 0,06$	[121]		1	2,9	[25]
	2,2	$0,89 \pm 0,16$	[121]		3	5,6	[125]
	3	$0,66 \pm 0,13$	[121]		3	$6,0 \pm 0,6$	[68]
$^{238}\text{U} \rightarrow ^9\text{Li}$	1	1,7	[36]		4,5	11,3	[25]
	2,8	7,5	[36]		5,9	12,0	[25]
$^{238}\text{U} \rightarrow ^7\text{Be}$	0,065	$\sim 0,02$	[12]		10	$16,5 \pm 1,6$	[68]
	0,085	$\sim 0,02$	[12]		11,6	$12,5 \pm 2,5$	[69]
	0,12	6 ± 1	[96]		30	$16,1 \pm 1,6$	[68]
	0,66	19 ± 3	[96]	$^{238}\text{U} \rightarrow ^{28}\text{Mg}$	0,66	0,115	[59]
	3	$7,0 \pm 0,7$	[68]		0,085	$(2 \pm 1) \cdot 10^{-3}$	[96]
	10	$20,2 \pm 2,0$	[68]	$^{238}\text{U} \rightarrow ^{31}\text{P}$	0,4	$0,03 \pm 0,01$	[96]
	30	$20,2 \pm 2,0$	[68]				

Key: (1). Target nucleus and fragment. (2). GeV. (3). mb. (4).

Literature.

Page 536.

Table 133. Cross sections of formation of fragments with interactions of High-Energy Protons with nuclei photoemulsion.

(1) Мишень	(2) Тип фрагмента	(3) $T, \text{ Гэв}$	(4) $\sigma_{\phi}, \text{ мбарн}$	(5) Литература
LEm	$Z_{\phi} \geq 3$	0,1	$1,16 \pm 0,36$	[2]
	$Z_{\phi} \geq 4$	0,1 0,3 0,35 0,46 0,56 0,66 0,93	$0,44 \pm 0,16$ $1,4 \pm 0,5$ $1,6 \pm 0,6$ $2,1 \pm 0,8$ $2,5 \pm 0,8$ $2,7 \pm 1,1$ 18 ± 5	[2]' [84]' [84]' [84]' [84]' [84]' [88]'
	Li	0,93	20 ± 8	[88]
HEm	$Z_{\phi} \geq 3$	0,1	$1,93 \pm 0,64$	[2]
	$Z_{\phi} \geq 4$	0,075 0,1 0,1 0,2 0,3 0,35 0,35 0,46 0,56 0,66 0,93 2 3 6 9 9	$0,3 \pm 0,1$ $1,0 \pm 0,3$ $0,81 \pm 0,29$ $2,5 \pm 0,5$ $2,6 \pm 0,5$ $3,3 \pm 0,7$ $2,9 \pm 0,8$ $4,7 \pm 1,2$ $7,8 \pm 1,4$ $10,7 \pm 2,1$ 62 ± 11 66 ± 7 65 ± 8 90 ± 17 88 ± 17 100 ± 30	[90] [90] [2]' [90] [84] [90] [84]' [84]' [84]' [84]' [88] [87] ² [87] ² [87] ² [87] ² [104] ²
	$3 \leq Z_{\phi} \leq 6$	1 2 3	52 ± 8 240 ± 40 270 ± 40	[73] [73] [73]
	Li	0,93	135 ± 31	[88]
	^8Li	0,93 0,95 2 2 3 3 6 9	~ 2 $1,1 \pm 0,3$ $3,0 \pm 0,7$ 6 ± 1 4 ± 1 $3,4 \pm 0,6$ $5,1 \pm 1,2$ $5,0 \pm 1,1$	[88] [97] [56] ² [73] [73] [56] ² [56] ² [56] ²
	$^8, ^9\text{Li}$	25	$2,0 \pm 0,5$	[9]

Table 133 (cont'd).

① Мишень	② Тип фрагмента	③ T, Гэв	④ $\sigma_{\text{ф}}$, мбарн	⑤ Литература
	Be	2	$31,5 \pm 10,8$	[56] ²
		3	$27,3 \pm 5,9$	[56] ²
		6	$37,8 \pm 11,6$	[56] ²
		9	$36,5 \pm 5,8$	[56] ²
	⁸ Be	2	$8,2 \pm 1,7$	[56] ²
		3	$7,7 \pm 1,3$	[56] ²
		6	$8,0 \pm 1,8$	[56] ²
		9	$10,4 \pm 2,2$	[56] ²
	B	2	$5,5 \pm 1,9$	[56] ²
		3	$8,3 \pm 2,7$	[56] ²
		6	$8,5 \pm 3,4$	[56] ²
		9	$9,0 \pm 1,5$	[56] ²
	⁸ B	2	$< 0,1$	[56] ²
		3	$0,05 \pm 0,03$	[56] ²
		6	$< 0,1$	[56] ²
		9	$0,07 \pm 0,04$	[56] ²
	C	2	$2,0 \pm 0,9$	[56] ²
		3	$2,2 \pm 1,3$	[56] ²
		6	$2,7 \pm 1,8$	[56] ²
		9	$2,6 \pm 0,8$	[56] ²

Key: (1). Target. (2). Type of fragment. (3). GeV. (4). mb. (5). Literature.

FOOTNOTE 1. When kinetic energy of fragment $T > 2$ MeV/nucleon. 2.

For stars with the number of gray and black ray/beams $n_h > 2$.

ENDFOOTNOTE.

Page 537.

Energy dependency. The examination of the experimental data shows that with $T < 1-2$ GeV the output/yield of fragments is very sensitive to energy of colliding protons. So, if in the region $Z_{\phi} \geq 4$ several hundreds of million electron volt fission yield with charges from nuclei Ag and Br is a total of 1-2 mb, then with an increase in the energy up to $T \approx 1-2$ GeV the section σ_{ϕ} grow/rises almost by two orders.

During a further increase in the energy of protons the section σ_{ϕ} remains virtually constant. As can be seen from Fig. 408, the value of the section of fragmentation on "plateau" comprises already about 100/o of the total cross section of inelastic processes.

Analogous energy dependency, independent of the type of nucleus-target, it is observed for separate fragments, although the degree of an increase in the section $\sigma_{\phi}(T)$ in region $T \sim 1$ GeV and the difference between values σ_{ϕ} at the "plateau" and in the region of several hundred megaelectron volts can differ noticeably from case to case.

Connection with cascade-evaporative interaction mechanism. We cannot fail to note that the power relation $\sigma_{\phi}(T)$ is very similar to function $\bar{n}_h(T)$ (comp. Fig. 408 and 126). Already this purely internal resemblance it suggests about communication/connection of the process of fragmentation with the value of total energy, which is transferred to nucleus during inelastic collision with high-energy particle.

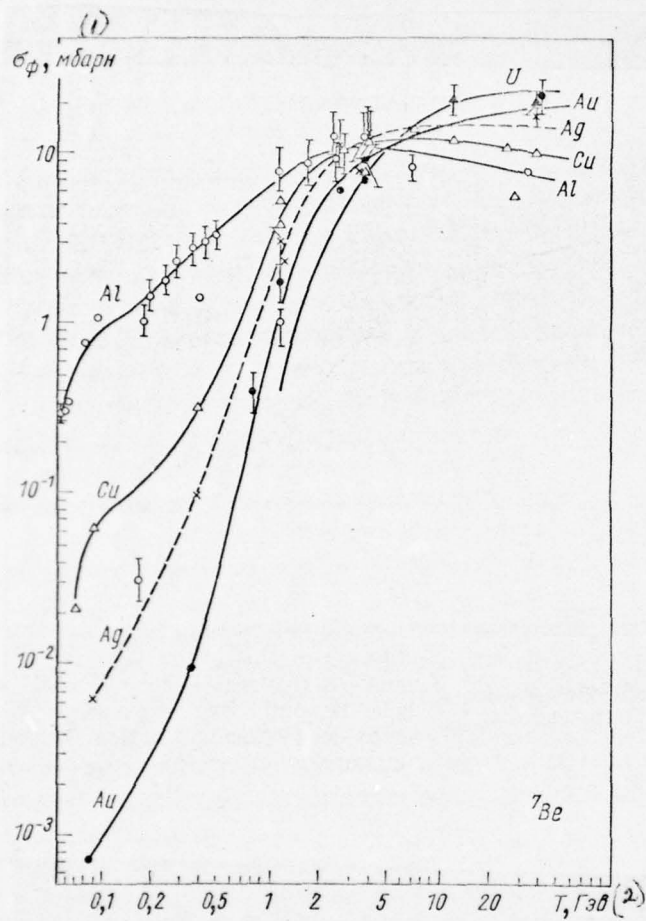


Fig. 406. Output/yield of fragments ${}^9\text{Be}$ from the nuclei, irradiated by the protons of the different energy T .

Key: (1) . mb. (2) . GeV.

AD-A048 311

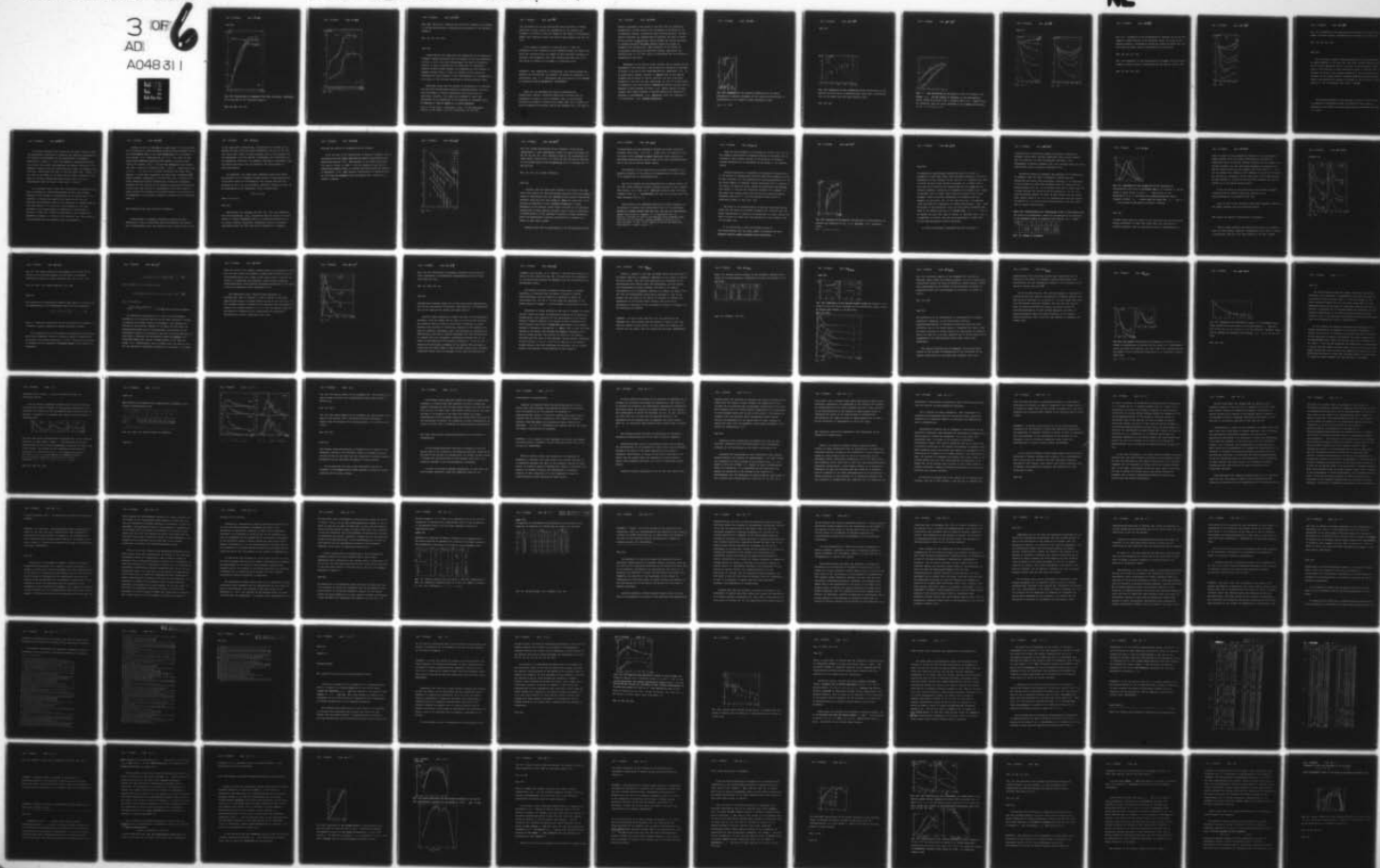
FOREIGN TECHNOLOGY DIV WRIGHT-PATTERSON AFB OHIO
INTERACTIONS OF HIGH-ENERGY PARTICLES AND ATOMIC NUCLEI WITH NU--ETC(U)
JUL 77 V S BARASHENKOV, V D TONEYEV
FTD-ID(RS)T-1069-77

F/6 20/8

UNCLASSIFIED

NL

3 OF 6
AD
A048 311



Page 538.

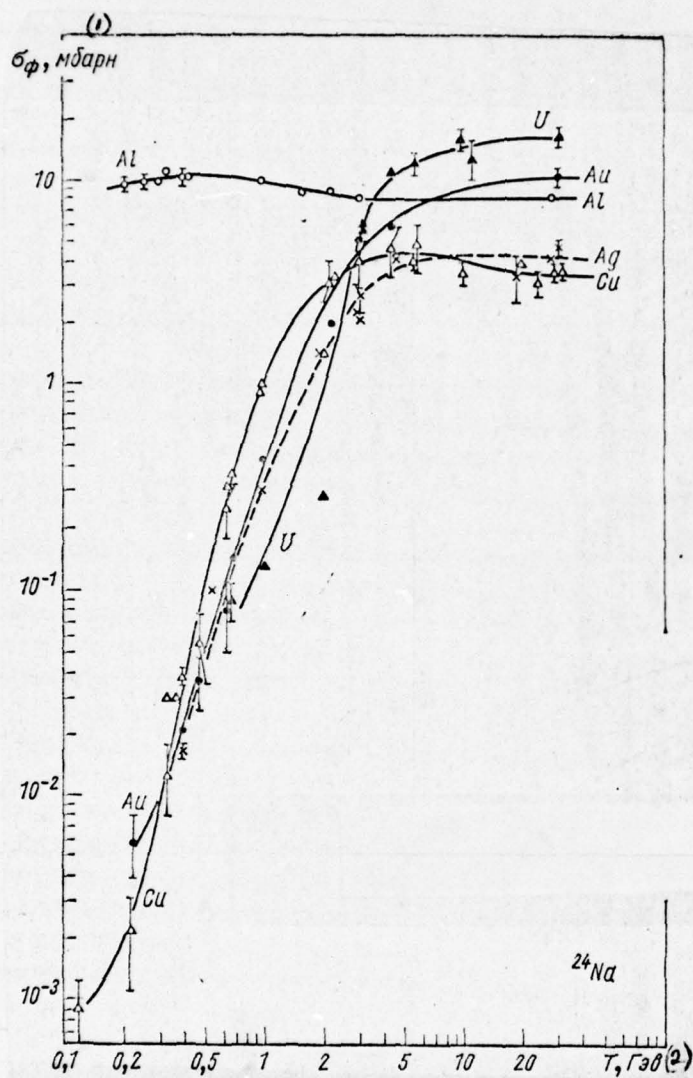


Fig. 407. Output/yield of fragments ^{24}Na from the nuclei, irradiated by the protons of the different energy T .

Key: (1). mb. (2). GeV.

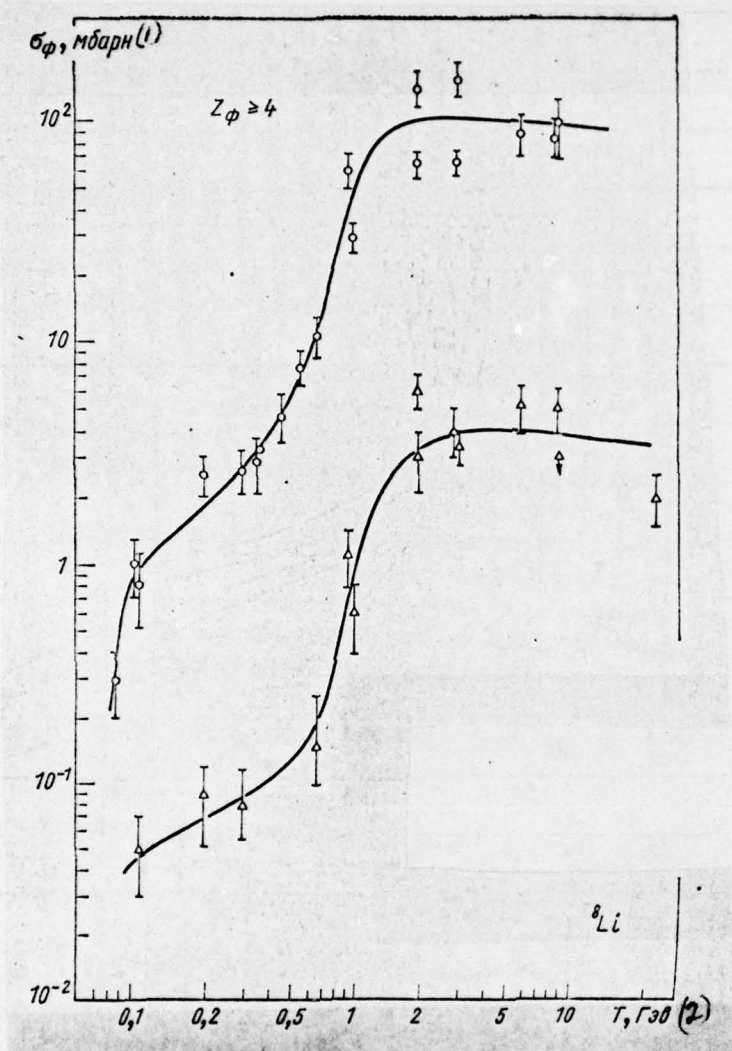


Fig. 408.

Fig. 408. Sections of formation ${}^6\text{Li}$ and of all fragments with charges $Z_{\phi} \geq 4$ in the photoemulsion, irradiated by the protons of the different energy T .

Key: (1). mb. (2). GeV.

Page 539.

Figures 409 and 410 shows that the probability of the emission of fragments rapidly grow/rises with an increase in the size/dimensions of star. If we in this case rate/estimate the value of excitation energy E^* , then it appears that in cases when E^* approaches complete nuclear binding energy, the probability of the emission of fragment becomes close to unity. An increase in the section of fragmentation during passage to the high energies T is accompanied by an increase in the relative percentage of multiple-pronged stars.

Experiment shows that the section of fragmentation is connected not only with the excitation energy of residual-nucleus, but also with the number of cascade g -particles. This can be seen, in particular, from Fig. 411, where as an example is shown the dependence of the probability of the formation of fragments $W_{\phi}(n)$ in reaction $p + \text{HE}$ on number s -, g - and b -particles

with $T = 9 \text{ GeV}$ [104]. Probability $W_{\phi}(n)$ in the same manner depends on the number of g - and b -particles, at the same

time noticeably not of any correlations with the number of shower particles; in other words, the probability of the formation of fragment in practice it does not depend on the number of accompanying mesons. This important result was noted by many authors [88, 99, 102, 117].

If we separate fragments to rapid and slow ¹, then the probability of the formation of slow fragments remains as before that which was correlated with the number of gray and black ray/beams; as concerns rapid fragments, then their output/yield turns out to be that which not depend on the number of b-particles [99].

FOOTNOTE ¹. This separation, is terminated, very conditionally. As boundary can be selected, for example, the energy of fragments $\mathcal{E} = 10$ MeV/nucleon; with $\mathcal{E} > 10$ MeV/nucleon the contribution of the process of evaporation can be disregarded. ENDFOOTNOTE.

Until now, we discussed only data on proton-nucleus interactions; however, analogous results were obtained also in experiments on rapid π^- and by K-mesons, also, on antinucleons (although the number of relating here works small and in majority of them is examined the emission only of one fragment ^6Li). All known at

present experimental data attest to the fact that the process of fragmentation closely related with the degree of branching of the intranuclear cascade, initiated by rapid initial particle. The more powerful branches the cascade/stage in nucleus, the more is formed recoil nucleons (g-particles), larger becomes the excitation energy of residual-nucleus ^{and} the more probable occurs the escape of fragments with charge $Z_{\phi} \geq 3$. The saturation of the number of intranuclear collisions and excitation energy, apparently, the occurring with $T \approx 3-5$ GeV, leads to "saturation" and the section of fragmentation (see §57).

Dependence on the type of target nucleus. Let us examine now the dependence of the sections of the formation of fragments on the mass of target A. As can be seen from Figs. 412-414, dependence $\sigma_{\phi}(A)$ is sufficiently complex: section σ_{ϕ} depends both on the type of fragment and on energy of initial particle. For more light/lung fragments of the type ${}^7\text{Be}$ and, apparently, ${}^8\text{Li}$ and ${}^{11}\text{C}$ in the region of energies of the order several hundreds of million electron volt is observed a sharp decrease in value $\sigma_{\phi}(A)$ during passage to heavy targets. With higher energies of initial particle the degree of a decrease in the function $\sigma_{\phi}(A)$ decreases, while with energies $T > 3-5$ GeV section $\sigma_{\phi}(A)$ becomes increasing.

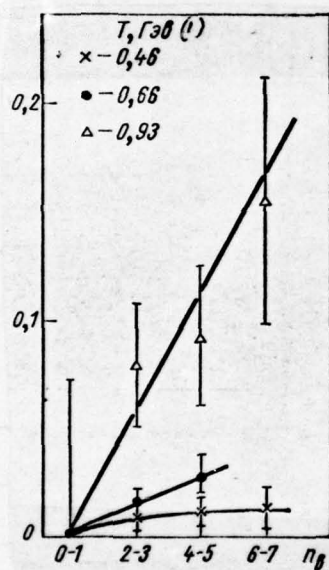


Fig. 409. Dependence of the relative probability of the being accompanied by emission fragments of the nuclear disintegration of photoemulsion on the number of black ray/beams in star.

Key: (1). GeV.

Page 540.

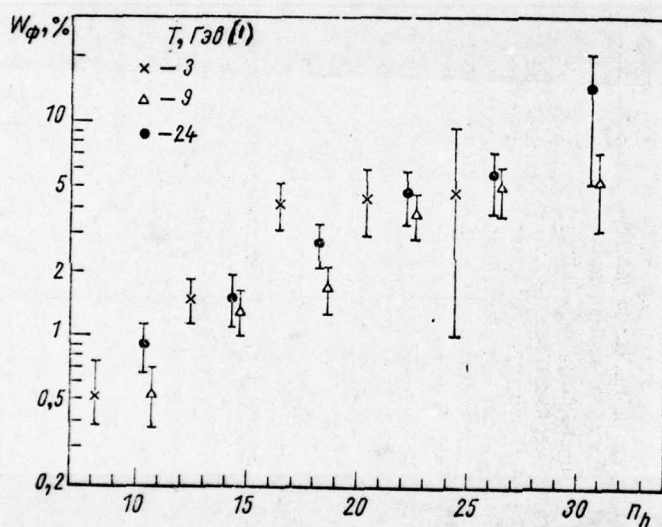


Fig. 410. Dependence of the probability of the interactions of the protons with the nuclei of photoemulsion, which lead to nucleation ^6Li , on the number gray and black beams in star.

Key: (1) - GeV.

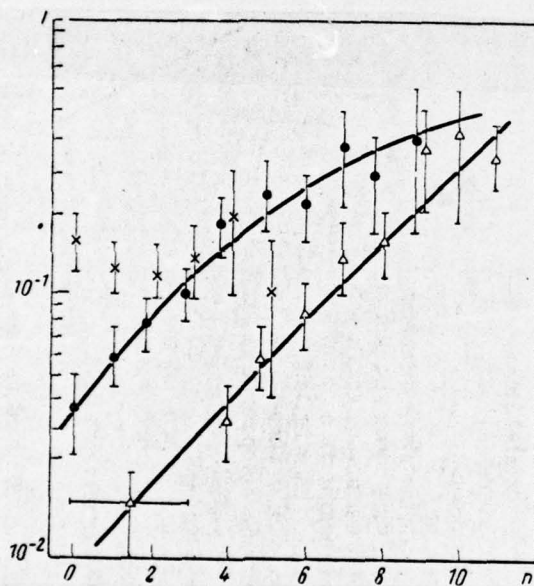


Fig. 411 . The correlation of the relative yield of fragments with charge $Z_{\phi} \geq 4$ and the number of ray/beams in the photoemulsion stars, formed by protons 9 GeV in energy [104]: x, e, Δ - respectively for fine/thin, gray and black ray/beams; n is a number of ray/beams of the determined type.

Page 541.

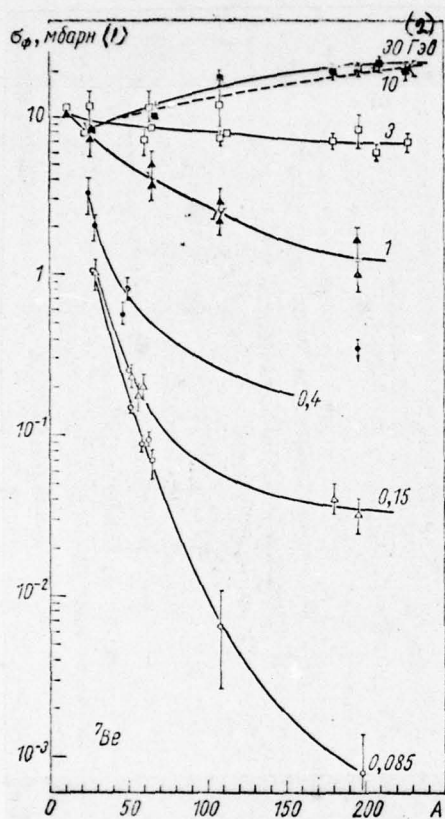


Fig. 4/2.

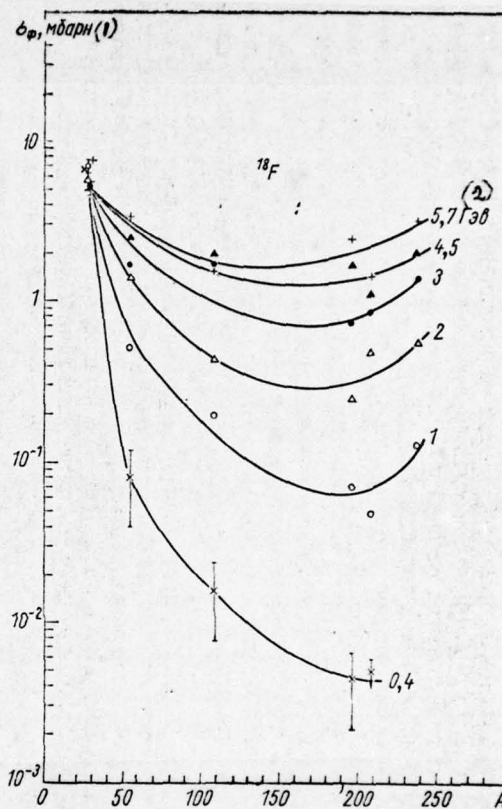


Fig. 4/3.

Fig. 412 Dependence of the output/yield of fragment ${}^7\text{Be}$ on the mass number of target nucleus at the different values of energy of the primary protons T. Experimental points are taken from Table 132, and also from the works, cited in connection with this table.

Key: (1). mb. (2). GeV.

Fig. 413. Dependence of the output/yield of fragment ${}^{16}\text{F}$ on the mass number of target nucleus. Designations are the same as in Fig. 412.

Key: (1). mb. (2). GeV.

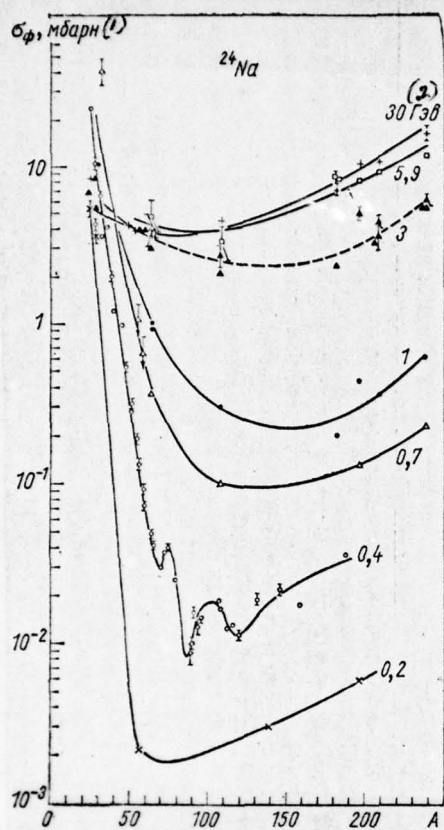


Fig. 414.

Fig. 414. Dependence of the output/yield of fragment ^{24}Na on the mass number of target nucleus. Designations are the same as in Fig. 412.

Key: (1). mb. (2). GeV.

Page 542.

The distinctive special feature/peculiarity of the output/yield of heavy fragments of the type ^{24}Na (and also, probably ^{28}Mg and ^{31}P) is the clearly expressed lift in the range of large values A , which leads to the formation of broad minimum in region $A \approx 70-150$. With an increase of energy T this minimum gradually is filled because of an increase in the output/yield of fragments from the neutral and heavy nuclei. Nevertheless the minimum of section σ_ϕ in the region of mass numbers $A \sim 70$ is noticeable even with $T \approx 30$ GeV.

The energy dependency of the section of nucleation ^{18}F in Fig. 413 appears as intermediate among two described above cases: an increase in the section in heavy nuclei region is observed only with $T \gtrsim 1$ GeV.

One should emphasize that in spite of the large volume of known now experimental information is required the essential improvement of the accuracy of measurement of the output/yield of fragments, especially in region $T < 1$ GeV. The scatter of experimental points now is still very great, and sometimes the results, obtained by the different authors, even they contradict each other. For example, work [96] for a output/yield ${}^7\text{Be}$ with $T = 660$ MeV gives value $\sigma({}^7\text{Be}) = 19$ mb, that by two orders it is higher than the value, expected on the basis of the data authors (see curve in Fig. 407), and it is approximately equal to value $\sigma({}^7\text{Be})$ with $T = 30$ GeV.

It is possible also to hope that the precision measurements will make it possible to reveal/detect/expose the new, also unknown features of the process of fragmentation. As an example here it is possible to indicate the results [78]. Made in this work the precision and systematic study of the generation of isotopes ${}^{22}\text{Na}$ and ${}^{24}\text{Na}$ with energy $T = 0.4$ GeV led to the detection of the fine structure of the output/yield of fragments: the dependences of sections $\sigma({}^{22}\text{Na})$ and $\sigma({}^{24}\text{Na})$ on mass number A are observed the maximums in regions $A \sim 65$ and $A \sim 100$ (see Fig. 414). The origin of these maximums thus far obtained still no explanation.

Besides the data on dependence on mass number A of the sections of the formation of concrete/specific/actual nucleus-fragment now are also experimental data on the total output/yield of all fragments with charges $Z_{\phi} \geq 4$ (actually for $Z_{\phi} = 4-9$). The value of this output/yield smoothly grow/rises with passage to heavier target nuclei. For example, with $T = 660$ MeV for interaction with targets LEm , HEm , Bi and U are obtained values $\sigma_{\phi}(Z_{\phi} \geq 4)$, respectively equal to 2.7 ± 1.1 ; 10.7 ± 2.1 ; ~ 22 and ~ 25 mb [30, 84, 103]. These results, it would seem, contradict the noted above dependence $\sigma_{\phi}(A)$. Matter consists, apparently, in the fact that with a change in the target changes and isotopic composition of being born fragments; therefore for the solution to the question concerning the dependence of the total cross section of fragmentation on the mass number of target nucleus are necessary the detailed studies of the sections of the formation of all possible isotopes of fragment with the assigned value Z_{ϕ} .

§95. Composition and many being born fragments.

Distributions of fragments according to charge and mass. Immediately it must be noted that these distributions are studied still insufficiently good. The reason for this consists first of all

in the experimental difficulties, connected with the study of any physical process, which has small probability, and also in the fact that among light nuclei is small isotopes with by the convenient for the measurement half-life periods. Furthermore, are difficulties of the fundamental character: the products, recorded in experiment, they can differ from those, that are formed at the torque/moment of splitting/fission.

In comparison with others most completely studied the charge distributions of the fragments, formed during the splitting/fissions of the heavy nuclei of photoemulsion. The relating here data are assembled in Fig. 415. As is evident, entire/all totality of data can be approximated by the dependence, close to exponential:

$$W(Z_{\phi}) \sim \exp(-Z_{\phi}^n),$$

where $n \approx 0.6-1.0$.

Page 543.

Some authors (for example, see [45, 105, 107]) they emphasized that the distribution $W(Z_{\phi})$ in practice does not depend not only on energy of incident particle T , but to a considerable degree and on its nature. However, experiment, apparently, does not contradict confirmation about the fact that with an increase of T somewhat

increases the portion of fragments with low charges.

If we now turn to the output/yield of separate isotopes, then is reveal/detected that their distribution differs significantly from charge distribution $W(Z_\phi)$. For example, as is evident from Table 132, ratio $\sigma(^{24}\text{Na}) / \sigma(^{18}\text{F}) > 1$ for all values of T and for all investigated target nuclei. As already mentioned during the analysis of dependence $\sigma_\phi(A)$, this apparent contradiction is connected with the fact that the fragments were distributed both on mass and on charge to numbers.

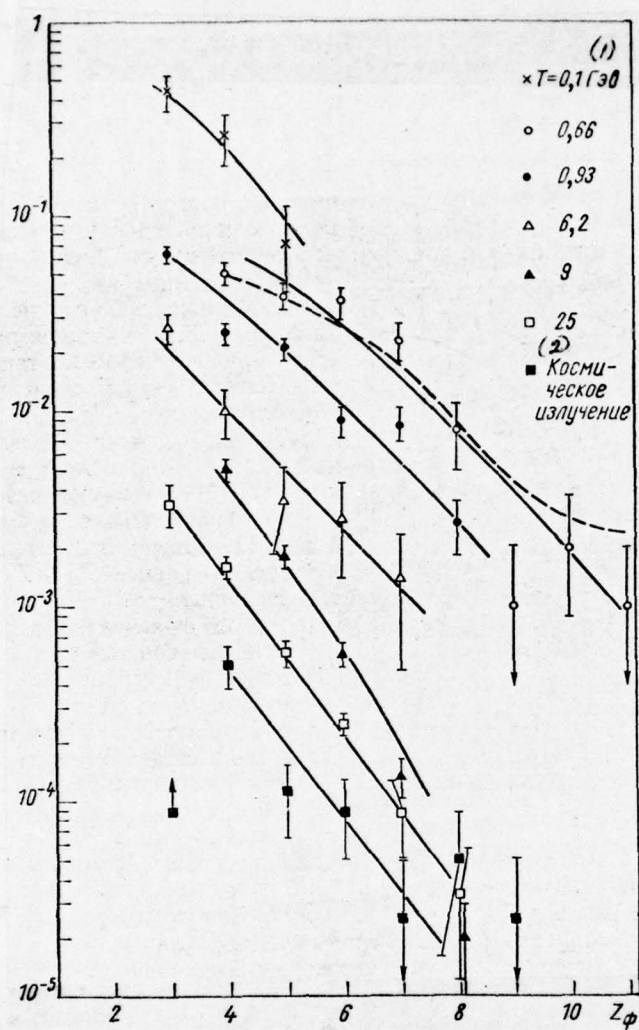


Fig. 415.

Fig. 415. Charge distribution of the fragments, formed during interactions $p + \text{HEm}$. Experimental points are taken from works [54, 84, 86, 88, 98, 102, 119]. Unbroken curves are an approximation of these points. Dotted curve is a result of the calculation according to the cascade model of the fragmentation of P. P. Denisova for $T = 660 \text{ MeV}$ [33].

Key: (1). GeV. (2). Cosmic radiation.

Page 544.

Actually, from the given above results it is evident that the total cross section for multiply-charged particles with this value Z_ϕ always is considerably more the sections of the separate radioactive isotopes, which have the same charge Z_ϕ . Thus, the large part of the isotopes in experiment is not recorded. Furthermore, a large difference in the sections (10-50 times) testifies to the preferred output/yield of some separate isotopes, since so large a difference in output/yield it is not possible to explain by simple assumption about the approximately identical output/yield of isotopes as a result of their small number.

Analysis shows that in experiments on the radiochemical methods

of measurements are not recorded in essence the stable light/lung isotopes, which have $Z_{\phi}/A_{\phi} \simeq 0,5$ [105, 107]. The portion of the lost short-lived isotopes is small, whereupon these isotopes are distributed approximately equally both to the side neutron-deficient and to the side of neutron excess nuclei.

The stability of the majority of the emitted fragments is the important property of the process of fragmentation; by some authors it is examined even as determining [85].

Now we can explain the relationship/ratio of fission yields ^{18}F and ^{24}Na : these fragments compose different portions of all fragments with charges $Z_{\phi} = 9$ and $Z_{\phi} = 11$, whereupon relative yield ^{18}F among fragments with $Z_{\phi} = 9$ considerably less than the relative yield ^{24}Na among fragments with $Z_{\phi} = 11$.

Being based on the preferred formation of stable fragments, it is possible to explain such experimental facts as the approximate equality of fission yields ^{22}Na and ^{24}Na , and also the considerably larger output/yield of fragment ^{32}P in comparison with ^{33}P . Actually, isotopes ^{22}Na and ^{24}Na are arranged along different sides from the line of stability, passing through the nucleus ^{23}Na , while isotopes ^{32}P and ^{33}P are located on one and the same side with respect to stable nucleus ^{31}P .

From the given examples it is distinctly evident, that even so the complete output/yield of fragments sharply it decreases with an increase in their charge, section of the formation of separate isotopes substantially is determined by the nature of the fragment itself.

Multiple generation of fragments. The important characteristic of the process of fragmentation are many being born fragments. As can be seen from Fig. 416, the probability of splitting/fissions with two and large numbers of fragments rapidly grow/rises with an increase in the energy. If among all stars, formed in photoemulsion by protons with energy $T = 660$ MeV and containing fragments with charge $Z_{\phi} \geq 4$, only about 50/o compose stars with two and more multiply-charged fragments, then with $T = 9$ GeV the portion of such events it grow/rises already to 160/o [86, 104].

The study of the characteristics of nuclear splitting/fissions shows that the events with several fragments are connected with even higher expenditures of energy on the excitation of target nucleus how this it occurs for events with the generation of one fragment (Fig. 417 and Table 134) .

It is interesting to note that during passage to splitting/fissions with the large number of fragments the most powerful relative change undergoes many g-particles.

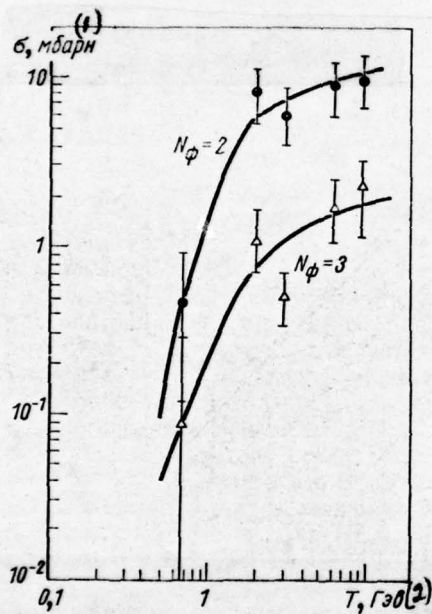


Fig. 416. Sections of the nuclear disintegration of photoemulsion by protons with formation of two ($N_\phi=2$) and more ($N_\phi=3$) fragments [104].

Key: (1) mb.; (2) GeV.

Page 545.

As concerns the experimental information about the nature of fragments in cases when occurs their multiple production, then this information is very limited. In the work of O. V. Lozhkina [85], made on nuclei Ag and Br with 660-MeV by protons, it is shown, that in this case can be observed any combinations of the charges of two forming fragments; a majority of fragments have charges $Z_\phi \leq 8$ also, as compared with the cases, when occurs the emission only of one fragment, there is certain predominance of fragments with low charges, in particular, ^8Li . At the same time with $T = 9 \text{ GeV}$ was noted virtually the independence of charge distribution $W(Z_\phi)$ from the number of born fragments; true, the last/latter conclusion was based on the observation only of fragments with $Z_\phi = 4 - 8$ [53]. If we examine the only this range of values Z_ϕ (see Fig. 415), then it is possible, of course, with the large basis/base to count $W(Z_\phi)$ the not energy-dependent initial particles.

It would be extremely interesting the more thorough to

investigate the correlations between the angles of emission of fragments during their multiple generation. Many authors consider that the character of these correlations testifies to the independence of emitted fragments [87, 107], although there are works whose authors send to opposite conclusion [10].

Excitation energy of fragments. The analysis of the composition of fragments they will make it possible to obtain also the information also about their excitation. Actually, it is represented by very unlikely in order that fragments would be formed with the neutron-proton ratio $(A - Z) / Z$, greater than this it would occur for a target nucleus. For nuclei Ag and Br relation $(A - Z) / Z \approx 1.3$, which noticeably exceeds the value of this relation for the stable light nuclei, where it is 1-1.2. If fragments were born with themes by relation $(A - Z) / Z$ as of the initial nucleus, then this would lead to neutron excess nuclei.

Table 134. Characteristics of interactions 25-GeV of the protons with the nuclei of photoemulsion, which are accompanied by the formation of the different number of fragments with charges $Z_{\phi} \geq 3$ [118].

(1) Число фрагментов N_{ϕ}	\bar{n}_s	\bar{n}_h	\bar{n}_g	\bar{n}_b
0	$2,6 \pm 0,2$	$13,6 \pm 0,3$	$5,0 \pm 0,1$	$8,6 \pm 0,1$
1	$2,9 \pm 0,1$	$17,2 \pm 0,2$	$7,8 \pm 0,1$	$9,4 \pm 0,1$
2	$3,5 \pm 0,2$	$18,4 \pm 0,5$	$9,0 \pm 0,3$	$9,4 \pm 0,3$
> 2	$3,3 \pm 0,3$	$19,0 \pm 0,8$	$8,7 \pm 0,6$	$10,3 \pm 0,6$

Key: (1). Number of fragments.

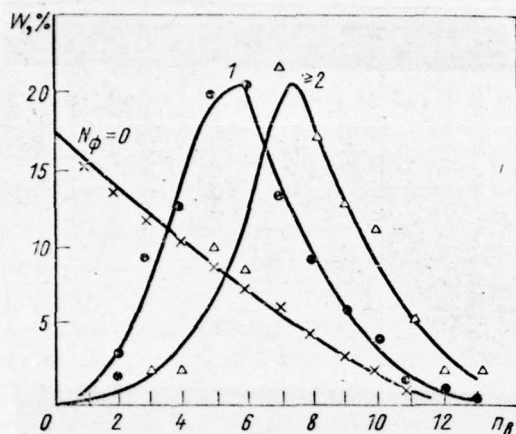


Fig. 417. Dependence of the probability of the formation of photoemulsion stars with the different number of fragments N_ϕ on the number of black traces in star n_b : \times — the results of the measurements of V. I. Ostroumova for splitting/fissions without fragments [1000]; \bullet, Δ — respectively for stars with $N_\phi = 1$ and $N_\phi = 2$ [85]; energy of the primary protons $T = 660$ MeV.

Page 546.

If these nuclei would be formed in this case even with the excitation energy, sufficient in order that could occur the evaporation of "excess" neutrons, then the appropriate events in photoemulsion it

would be cannot be distinguished of events with the generation of stable isotope, since for time, during which is realized the evaporative stage of process, nucleus virtually does not manage to be shifted. However, the fact that among fragments are observed such neutron excess nuclei as, for example, ${}^8\text{Li}$, whose level $E^* = 2.28$ MeV is unstable with respect to the emission of neutron and therefore any excitation, exceeding 2.28 MeV, must lead to the disintegration of this nucleus, it attests to the fact that fragments are born in essence or in the weakly excited states.

On the low value of the excitation of the emitted fragments testifies also the presence among the products of the splitting/fissions of isotopes ${}^8\text{B}$ and ${}^{13}\text{N}$.

Thus, we come to the conclusion that among fragments predominate the stable isotopes with low excitation energy.

§96. Energy and angular distributions of fragments.

Form of energy spectra. The energy distributions of fragments have, at first glance, typically "evaporative" form. This is evident, in particular, from Fig. 418, that relates to the most studied

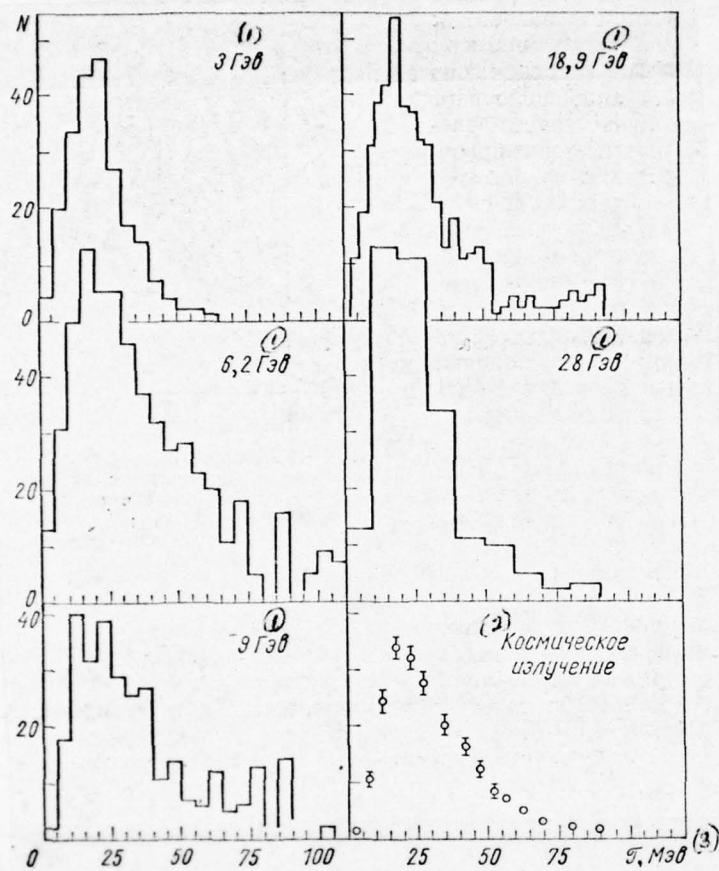
fragment ^8Li .

Fig. 418.

Fig. 418. The energy spectra of the fragments ${}^8\text{Li}$, formed by the protons of the different energy T on the nuclei of emulsion. Experimental points are taken from works [22, 26, 56, 99, 116].

Key: (1). GeV. (2). Cosmic radiation. (3). MeV.

Page 547.

This character of distributions impelled many authors to utilize for the approximation of the experimental data the known expression

$$W(\mathcal{F}) = \frac{\mathcal{F} - V}{r^2} \exp\left(-\frac{\mathcal{F} - V}{r}\right), \quad (9.1)$$

where V - effective coulomb barrier for the emission of fragment, a r - effective nuclear temperature (center-of-gravity system).

If we consider the an even velocity of following of the nucleus, which emits fragments, which, as a rule, is small as compared with the speed of the emitted particles ($v \ll v_\phi$), then for the spectrum of fragments in the laboratory coordinate system we will obtain the expressions

$$W(\mathcal{F}) = \frac{1}{2\tau b} \{1 - \exp[-(a+b)](1+a+b)\}, \quad (9.2a)$$

if $[V - (2mV)^{1/2}v] < \mathcal{F} < [V + (2mV)^{1/2}v]$, and

$$W(\mathcal{F}) = \frac{1}{2\tau b} \{\exp[-(a-b)](1+a-b) \exp[-(a+b)](1+a+b)\}, \quad (9.2b)$$

if $\mathcal{F} > [V + (2mV)^{1/2}v]$.

$$\text{Here } \underbrace{a = (\mathcal{F} - V)/\tau; b = (2m\mathcal{F})^{1/2}v/\tau}_{\text{}} \quad m - \text{the mass of the emitted fragment.}$$

By considering now values of V , τ and v as the adjustable parameters, it is possible with the aid of these formulas to attempt to describe the observed spectra of fragments. This approach was utilized by many authors. However, if we speak not only about the common/general/total form of distributions, then nearness of the experimental spectra to evaporative turns out to be very relative; on experiment is observed the considerable number of fragments with energy both lower than nominal coulomb barrier ($\mathcal{F} < V$), and with energy $\mathcal{F} \gg V$. Specifically, this is evident also from data in Fig. 418: the spectrum of fragments stretches up to energies $\mathcal{F} \simeq 100$ MeV,

while the value of the nominal coulomb barrier is approximately 20-25 MeV. For this reason the analysis of energy spectra with the aid of relationship/ratios (9.2) leads to such large values r and such low values of V (sometimes even negative), that actually completely become meaningless those physical prerequisite/premises, on the basis of which was obtained initial expression (9.1).

The experimental data, obtained from experiments on photoemulsion, make it possible to trace a change in the energy spectrum with energy of primary proton. As can be seen from Fig. 418, most probable energy of fragment ${}^6\text{Li}$ in practice does not depend on energy of the primary proton T , if $T \gtrsim 3$ GeV. At smaller values of T the spectra of fragments can be judged from the differential distributions of their range/paths (Fig. 419).

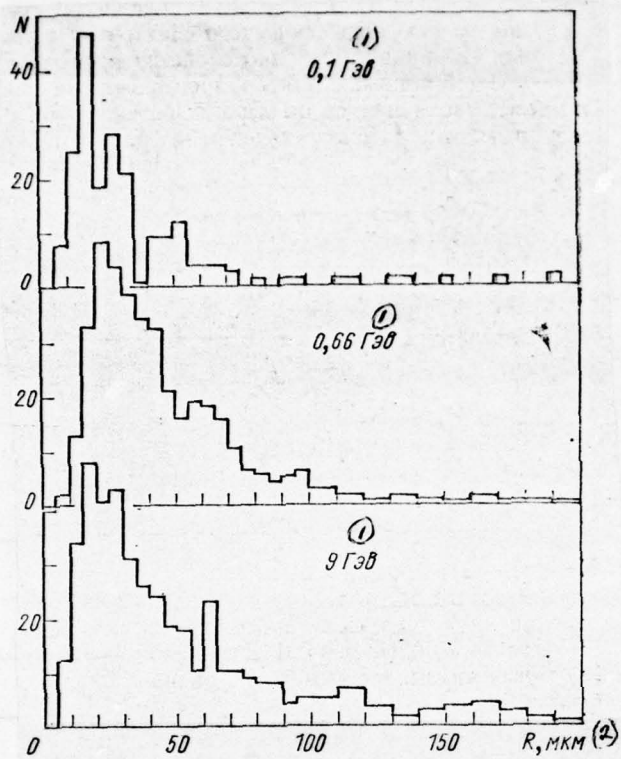


Fig. 419.

Fig. 419. The distribution of fragments according to the value of their range/paths in photoemulsion (experimental points are taken from works [2, 104]).

Key: (1). GeV. (2). μm .

Page 548.

Although most probable energy and in this case remains approximately one and the same however the relative contribution of the high-energy part of the spectrum the lesser, the lower energy T.

Spectral change depending on number and type of the accompanying particles. Since the number and the type of the being born particles are connected with the value of the energy, transferred to target nucleus in the process of interaction, research on this question can give the important information about the mechanisms of fragmentation. Unfortunately, existing at present knowledges are very contradictory. So, Gaevski with the colleagues, investigating emission ^8Li by the nuclei of photoemulsion with energies of protons $T = 9$ and 24 GeV, it observed the noticeable broadening of the spectra during passage to events with the large number of gray and black traces [49]. Analogous conclusion follows from the analysis of the range distributions of

fragments with charges $Z_{\phi} \geq 4$ during $T = 660$ MeV [85]. However, in a series of other works [21, 26, 116, 117] was noted the independence of the energy distributions of fragments from the size/dimensions of photoemulsion stars.

The analysis of entire totality of these makes it possible apparently, to conclude that the effect of energy of nuclear splitting/fission into the spectra of fragments is small. As illustration Fig. 420 for $T = 24$ GeV shows the dependence of the medium energy of fragment \mathcal{E} on the number of h-particles in star.

Dependence of energy spectrum on the type of fragment and target nucleus. Figure 420 shows one additional property of the process of fragmentation, very essential for the understanding of its nature: energy of fragment depends on its charge of mass, increasing with their increase. This effect becomes more noticeable, if we examine energies of fragments, averaged on n_h (Table 135). In Fig. 421 shown changes in the energy distributions of fragments depending on the type of target nucleus. The position of maximum in the spectra coincides with the value of the effective coulomb barrier, determined in work [74] as $V = V_0 / (1 + 0.001 E^*)$, where V_0 is the nominal coulomb barrier. This fact indicates the important role of coulomb forces in the process of the formation of the fragments.

Weakly it depends on the type of target nucleus and the form of the energy spectrum of fragments, especially in the region of neutral and heavy nuclei. This fact will agree with the conclusion of the preceding/previous section about the independence of these spectra from disintegration energy. However, the width of the energy distributions of the fragments, emitted, for example, by nuclei ^{27}Al and ^{238}U , is distinguished sufficiently noticeably ¹, and if one assumes that the width of the spectra is defined, in essence, the temperature of the excited target nucleus, then this can be considered as indication of the dependence of energy of fragments on the excitation of nucleus.

FOOTNOTE ¹. As can be seen from Fig. 421, the spectrum of the fragments ^6Li , which escape from the nucleus of copper, more rigid than for adjacent target nuclei. In later works (for example, see article [3]) was shown, that this result was erroneous. ENDFOOTNOTE.

Table 135. Average kinetic energies of the fragments, emitted by the nuclei of the photoemulsion, irradiated by protons with energy $T = 28$ GeV [119].

(1) Фрагмент	$\bar{T}, \text{Мэв}$ (2)	(1) Фрагмент	$\bar{T}, \text{Мэв}$ (2)
${}^6\text{Li}$	30 ± 1	${}^{10}\text{B}$	54 ± 1
${}^7\text{Li}$	32 ± 1	${}^{10}\text{C}$	53 ± 2
${}^8\text{Li}$	$23 \pm 0,5$	${}^{12}\text{C}$	57 ± 2
${}^7\text{Be}$	43 ± 1	${}^{12}\text{N}$	73 ± 4
${}^8\text{Be}$	33 ± 1	${}^{14}\text{N}$	73 ± 4
${}^9\text{Be}$	47 ± 1	${}^{14}\text{O}$	~ 87
${}^8\text{B}$	48 ± 4	${}^{16}\text{O}$	~ 90

Key: (1). Fragment. (2). MeV.

Page 549.

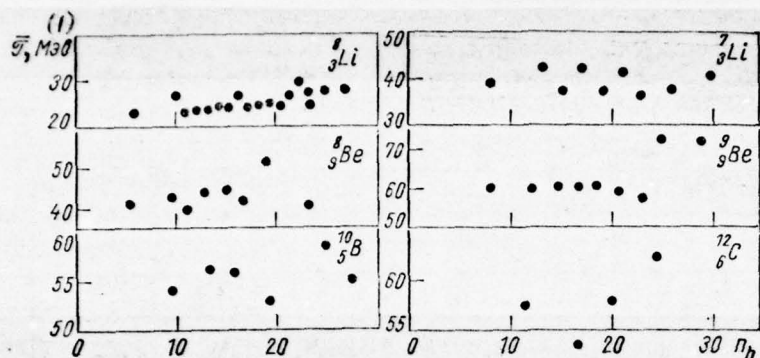


Fig. 420. Dependence of the average kinetic energy of fragment on the number of gray and black ray/beams in the photoemulsion stars, formed by protons with energy $T = 24$ GeV [117].

Key: (1). MeV.

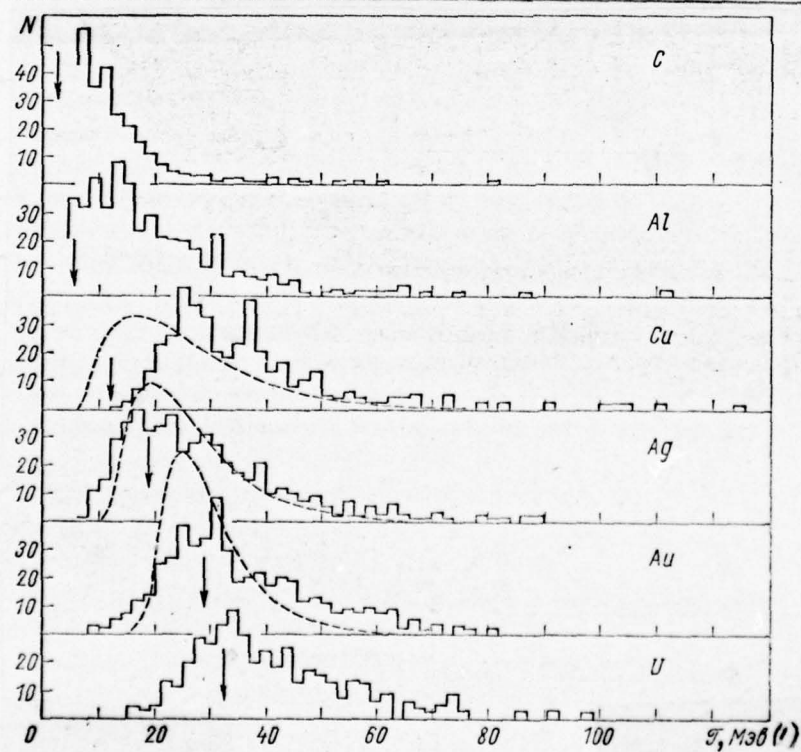


Fig. 421.

Fig. 421. The energy spectra of the fragments ${}^8\text{Li}$, emitted by different nuclei under the action of protons 2.2 GeV in energy [74]. Arrow/pointer showed the value of effective coulomb barrier. Dotted line plotted/applied the results of the calculation according to evaporative model with the parameter of the density of levels $a = A/12.4$.

Key: (1) . MeV.

Page 550.

The possibility of so contradictory an interpretation of results, apparently, indicates, in the first place, which the approach/approximation of evaporative model one should use very carefully, and, in the second place, it indicates that even at just one value of energy of initial particle in application to different nuclei can turn out to be more important one or another mechanism of fragmentation (if really/actually there exist several such mechanisms).

The angular distributions of fragments. The characteristic feature of the process of fragmentation is the anisotropy of the angular distributions of the being born fragments (Fig. 422).

Quantitatively this anisotropy usually they characterize by the relation of the number of fragments, emitted respectively into front/leading and rear hemispheres relative to the direction of the motion of initial particle \vec{n}/\vec{n} .

As can be seen from Fig. 423, with an increase in the energy of initial particle the angular distribution of fragments becomes ever more and more isotropic, up to energy $T = 3-5$ GeV, higher than which ratio \vec{n}/\vec{n} becomes virtually constant. The fact that the critical value of energy coincides with energy, with which occurs the disturbance/breakdown of usual cascade mechanism (see §57), it prompts assumption about the single mechanism of the nuclear splitting/fissions, which occur with the emission of fragments and without them.

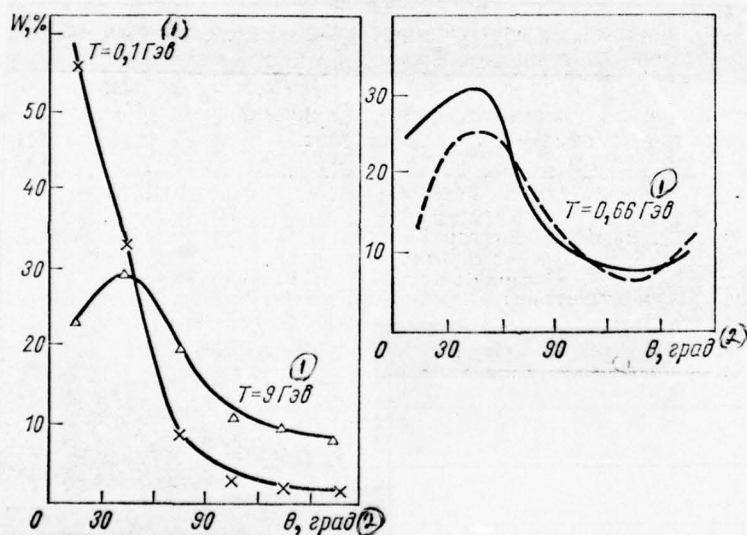


Fig. 422. The angular distribution of fragments with charges $Z_{\Phi} \geq 4$, formed in photoemulsion by protons with an energy of T . Experimental values are taken from works [2, 84, 104]. Dotted line plotted/applied the results of the calculation according to F. P. Denisova's cascade model [33].

Key: (1) GeV; (2) deg.

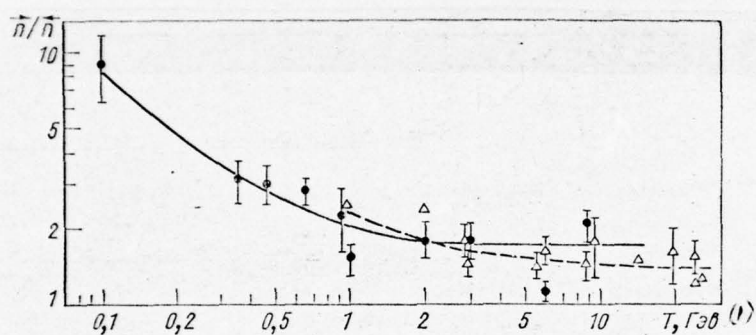


Fig. 423. Dependence of ratio \bar{n}/\bar{n} on energy T of the primary proton, which interacts with the nuclei of the photoemulsion: Δ - the data [13, 21-23, 26, 31, 49, 52, 56, 57, 75, 97, 119] for a fragment ${}^8\text{Li}$; \bullet - for the emission of fragments with charges $z_\phi \geq 4$ [2, 5, 85, 88, 98, 104].

Key: (1) . GeV.

Page 551.

One should emphasize that the angular anisotropy is inherent precisely in the mechanism of fragmentation and cannot be caused by the motion of recoil nucleus. With $T < 1$ GeV the account of this motion knowingly cannot give such the large values \vec{n}/\bar{n} . For high anisotropy energy of the escape of light/lung fragments (of type "Li" and Be) in principle can be explained under the assumption of their isotropic distribution in the center-of-gravity system; however, attempt to use to this isotropic distribution evaporative model again leads to the nonphysical values of temperatures.

Is less studied the question concerning the dependence of the angular distributions of fragments on the energy, transferred to nucleus in the course of collision. By Perkins was noted a decrease in the anisotropy of angular distribution ^8Li during transition to multiple-pronged stars [102], at the same time by N. P. Bogachev et al. with $T = 9$ GeV she was indicated the independence of distribution $W(\cos \theta)$ from the number of black tracks [21], but the authors [26] whose results were given in Table 136, observed an increase in ratio \vec{n}/\bar{n} during transition to stars with the large number of h-particles. It should be noted, however, that the observed in experiment

dependence \bar{n}/\tilde{n} on number n_h does not exceed the limits of statistical errors.

From the results, presented in Table 136 and Fig. 424, follows one additional essential feature of the angular distribution of the fragments: the presence of the correlations among energy and angle of emission of fragment; for fragments with higher energy the degree of anisotropy more.

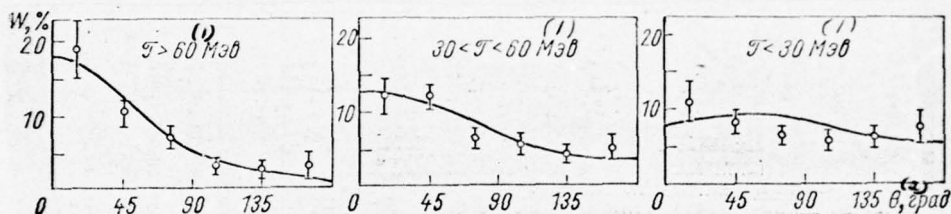


Fig. 424. The angular distributions of fragments ^8Li in the different intervals of their kinetic energy T . The experimental data are obtained with the aid of the photoemulsion, irradiated in cosmic rays [116]. Curves - the results of the calculation, made under the assumption of isotropic emission ^8Li in a system which moves with speed β of the nucleus-remnant; the energy spectrum ^8Li in this system is described by formula (9.1) with the parameters $\tau = 11.5 \text{ MeV}$, $V = 6 \text{ MeV}$, $\beta = v/c = 0.016$.

Key: (1). MeV. (2). deg.

Table 136

Ratio \bar{n}/n for the fragments ${}^6\text{Li}$, formed 28-GeV by protons on the nuclei of photoemulsion [26].

\mathcal{T}, MeV n_h	> 0	< 20	20 ÷ 40	40 ÷ 60
$7 \leq n_h \leq 17$	$0,744 \pm 0,182$	$0,500 \pm 0,194$	$0,750 \pm 0,286$	$3,000 \pm 1,414$
$n_h \geq 7$	$0,925 \pm 0,138$	$0,744 \pm 0,174$	$1,024 \pm 0,222$	$1,500 \pm 0,791$
$n_h > 18$	$1,056 \pm 0,201$	$0,957 \pm 0,285$	$1,192 \pm 0,317$	$1,000 \pm 0,816$

$\mathcal{T}^{(2)}$ — кинетическая энергия фрагментов.

Key: (1). MeV. (2). kinetic energy of fragments.

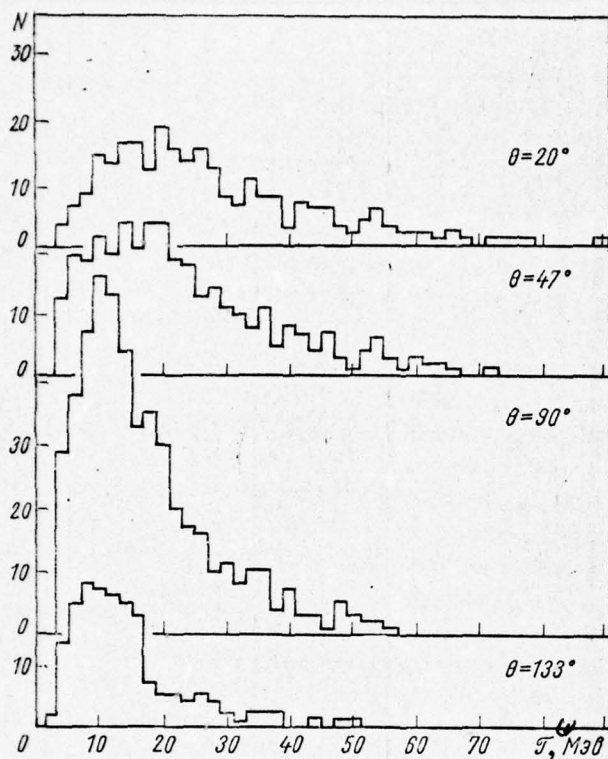


Fig. 425. Caption next page.

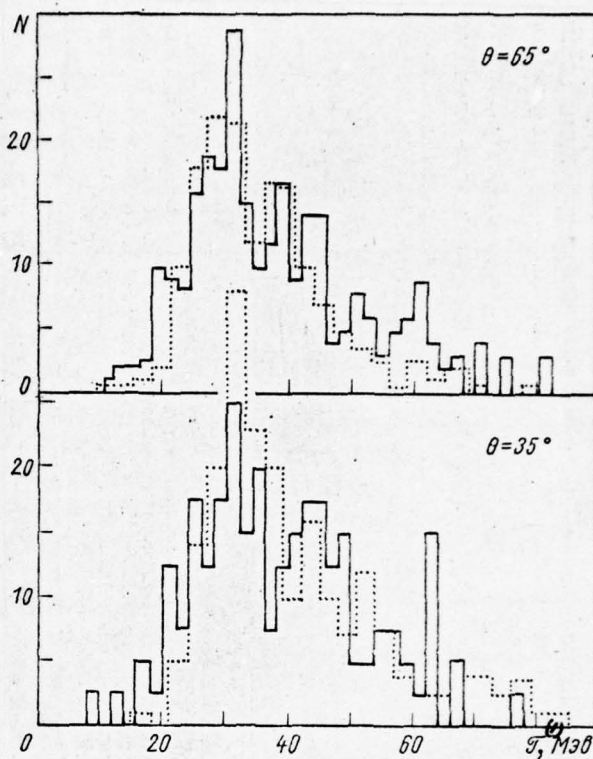


Fig. 426. Caption next page.

Fig. 425. The energy spectra of the fragments ^8Li , which escape at an angle θ from the nuclei ^{51}V , irradiated by protons with energy $T = 660$ MeV [3].

Key: (1). MeV.

Fig. 426. The energy spectra of the fragments ^8Li , which escape at an angle θ from nucleus ^{197}Au . Continuous and point histograms - respectively for energies of the primary proton $T = 2.2$ and 0.66 GeV [3.74].

Key: (1). MeV.

Page 553.

This special feature/peculiarity is exhibited in the spectra of the fragments, emitted at the determined angle; for example, from Fig. 425 and 426 one can see well that the transition to smaller angles is accompanied by the noticeable broadening of energy spectra.

Let us note that the form of the differential spectra of fragments $d^2\sigma/d\mathcal{T}d\Omega$ comparatively weakly depends on energy of initial particles and on target nucleus.

The examined above data were related in essence to light/lung fragments. In recent years were obtained the data on energy and angular distributions also for such heavy fragments as ^{24}Na and ^{28}Mg [59, 96]. All the basic laws, noted above, remain also in this case. The same it is possible to say about the angular and energy distributions of the fragments, which are formed under the action of the high-energy pi-mesons: the properties of these distributions are close to the fact that is observed for nucleon-nuclear interactions.

§97. Some other special feature/peculiarities of the process of fragmentation.

In the preceding/previous sections we attempted to give the general idea of the totality of the physical phenomena, known now by the name of the process of fragmentation. The attempt in more detail to discuss the characteristics of this process would lead to an essential increase in the size/dimensions of monograph.

In order to partially complete gap/spacing, we will point out still several questions, which have important value for the

investigation of fragmentation.

Emission of fragments during the splitting/fission of light nuclei. This case possesses some specific peculiarities associated with the possibility of the formation of fragments as remanent/residual nuclei. If we do not isolate these nuclei (but in practice this not always is possible), then completely different, different from that which was discussing is above, proves to be dependence $\sigma_{\phi} = \sigma_{\phi}(T)$ ¹; differences are observed also in the energy and angular distributions of fragments.

FOOTNOTE ¹. As an example of this dependence can serve, for example, the output/yield of fragments ^{18}F and ^{24}Na from nucleus ^{27}Al to Fig. 413 and 414. ENDFOOTNOTE.

There is another reason, why research on the formation of fragments in reactions with light nuclei is of special interest. It is completely possible that part of the fragments, emitted by heavy nuclei, is formed by means of knocking out, elastic or inelastic (for example, by cascade nucleons), the corresponding intranuclear clusters. In this connection it is very important to know, as occur/flow/last nuclear reactions on light nuclei.

In recent years the interest in the reactions of knocking out of clusters was initiated also themes by consideration, that hence can be obtained the important and sufficiently unambiguously interpretive information about the structure of target nucleus. For this purpose were investigated in detail the reactions (p, pd) , $(p, p\alpha)$, and also $(p, p^3\text{He})$ and, etc. In this case the greatest success in the explanation of the observed laws is connected with shell nuclear model [6, 7]. (Partially these questions were touched upon in chapter 8).

The obtained results can serve as basis/base for conducting analogous investigations also in the case of heavier fragments.

Remanent/residual nuclei in splitting/fissions with fragments. The representation of the properties of these nuclei can be obtained, already on the basis of the known properties of the emitted fragments. Specifically, if energy of the initial particles is not great, then one should expect the formation of neutron excess nuclei, since fragments are born, as a rule, in their basic stable states.

Secondary nuclear reactions [17, 79, 91, 95, 122, 123]. We are

speaking about the formation of isotopes with charge on several unity higher than the charge of target nucleus. The appearance of such isotopes can be explained only by secondary interactions of the being born fragments with the initial nuclei. Observation in the experiment of such isotopes serves also as one of the proofs of the emission of fragments with the energies, which considerably exceed coulomb barrier; the dependence of the output/yield of these isotopes on energy will agree with the discussed in §94 energy dependency of the section of fragmentation $\sigma_{\Phi}(T)$.

Page 554.

Research on the interactions of fragments can give the very important information about the badly/poorly still investigated processes of the interactions of two nuclei (see Chapter 11).

Generation of hyperfragments. With sufficiently high energies becomes possible the formation of hyperfragments - the light nuclei, into composition of which instead of the nucleon enters Λ - the hyperon. Since the lifetime Λ - hyperon is small, hyperfragments easily are identified. It is represented by very interesting to compare the properties of the process of the formation of hyperfragments with the generation of usual fragments. some spaces in this direction are already made [by 14-16, 50, 63, 82, 87]. If we

clear parts, then in general terms these distributions detect great similarity. Apparently, the mechanisms of the formation of fragments and hyperfragments do not differ strongly from each other. Research on the characteristics of the forming of hyperfragments helps to understand the nature of the usual process of fragmentation. Unfortunately, the number of works on hyperfragmentation is small, and the statistics of measurements is still very small.

§98. Different theoretical approaches to the explanation of the mechanism of fragmentation.

There is at present no unified theory, explaining entire totality of known experimental data on fragmentation, although were undertaken separate attempts at the construction of this theory. The reason for this consists first of all in the complexity of the phenomenon itself. Furthermore, apparently, not at all there exists some mechanism, which gives rise to this very polyhedral/multifaceted phenomenon; specifically, it does remain unclear, is it possible to understand all parts of reactions with the formation of fragments from the viewpoint of our usual representations of the mechanism of nuclear reactions at high energies. It is completely possible that some processes of fragmentation are connected with the completely new

mechanisms of intranuclear interactions, which differ significantly from the examined cascade-evaporative mechanism.

Let us discuss the basic approaches - both traditional and connected with hypotheses about new interaction modes, which were proposed by the different authors for explaining the experimental data on fragmentation.

Mechanisms of knocking out of fragments. A whole series of the observed in experiment laws governing the phenomenon of fragmentation gives grounds to assume that fragments - or, in any case, their significant part - is formed in the process of developing intranuclear cascade. Here mention should be made of, in particular, the powerful anisotropy of the angular distribution of fragments with their preferred escape the forward half sphere, the dependence of the output/yield of fragments on the number cascade g- and b-particles in star, the presence of fragments with energy, much larger value of the Coulomb barrier and, etc. All these parts can be explained, if we assume that within nucleus there are more or less stable groups of nucleons (clusters), capable of escaping from nucleus as a result of collision with cascade particles.

We will not be stopped now on the reasons for the formation of clusters, they can be very diverse ¹, and only let us consider that

since the mean free path in the nuclear substance of such complex formations as clusters, is small in comparison with nuclear sizes, it is logical to expect that for the process of fragmentation are most essential the collisions with clusters in the bounding area of target nucleus.

FOOTNOTE 1. At present large interest is of the reverse/inverse formulation of the problem: to obtain the information about number and properties of different clusters in nuclei by means of comparison with the experiment of the calculations of the formation of the fragments, made for different assumptions about number and distributions of clusters within nucleus. ENDFOOTNOTE.

In the initial versions of model were examined only the elastic collisions of cascade nucleons with clusters. It is understandable that in this case are effective only the high-energy nucleons, scattered to wide angles. Since elastic high energy scattering has, in essence, the diffraction character, the probability of such collisions is small.

In order to increase the probability of nucleon-cluster collisions, O. V. Lozhkin and Yu. P. Yakovlev assumed that as a result of the interaction of nucleon with cluster is formed the single excited system with the intense energy exchange between its components [87]. The decomposition/decay of this system is regulated purely by statistical laws in the same way as this is assumed in Fermi's statistical theory (see §77); in this case the emitted fragment is the peculiar remanent/residual nucleus, which was being formed as a result of the interaction of rapid nucleon with cluster. In favor of the model of O. V. Lozhkin and S. P. Yakovlev speaks also the surprising resemblance of the energy spectra ${}^8\text{Li}$, which escape from nuclei ${}^{27}\text{Al}$ and ${}^{12}\text{C}$, although in the latter case fragment ${}^8\text{Li}$ really/actually can be considered as remanent/residual nucleus [19, 20].

In the area of energies of the order several hundreds of million electron volt this model allowed its authors to qualitatively explain not only the anisotropy of the angular distribution of the escaping fragments and its dependence on energy, which was obtained already, also, in the model, considering little more than elastic collisions, but also to obtain the correct form of the energy spectrum of fragments and to explain communication/connection between this spectrum and the angular distribution.

Further development the cascade model of knocking out of fragments received in the work of O. V. Lozhkin et al. [89], where were examined already the elastic and inelastic interactions of cascade nucleons with clusters in the surface layer of nucleus. On the strength of Pauli's principle those which predominate in this case must be low-nucleon reactions of the type $(N, 2N)$.

Unfortunately, in spite of some successes, all works, which were made, until now, on the basis of cascade approach, have, in essence, only qualitative, descriptive character. For more precise quantitative conclusions it is necessary to fulfill the calculations of intranuclear cascades, in the same way as this was described in chapter 4 and 6. However, such calculations are connected with a whole series of the assumptions: are unknown the probabilities of the formation of different multinucleon groupings in nuclei and their distributions according to coordinates and momentum/impulse/pulses, little the information about the characteristics of the interaction of rapid nucleons with light nuclei, etc. Sufficiently precise calculations were made only for the case of knocking out of α -particles (see §91).

Most developed* with respect to calculations is F. P. Denisov's model [33, 34]. This model is based on the assumption that the clusters are connected with the remaining part of the nucleus only by

the means of the small number of nucleons. In the process of developing intranuclear cascade the nucleons, which perform the role of communication/connections, can be chase/dislodged, and since all this occurs in the field of the coulomb forces, which attempt to detach cluster away from remanent/residual nucleus, this cluster it can be emitted as fragment or to remain within nucleus, which was considered as capture by the nucleus by that moving of particle-cluster. The probability of knocking out of nucleon-communication/connections was determined by F. P. Denisov with the aid of several simplified model of intranuclear cascades, the probability of the absorption of the driving cluster by nucleus was estimated according to liquid drop model. However, even in this setting problem remains still very complex; therefore during calculations nucleus was divide/marked off on several areas whose part was considered clusters, and others were associated with nucleon- communication/connections. Further by the calculation of intranuclear cascade was estimated the probability of knocking out of nucleon- communication/connections; in this case kinetic energy of cluster was set/assumed equal to the sum energy of coulomb repulsion, which plays dominant role, and kinetic energy, which it had a cluster at the torque/moment of isolation/evolution. The last/latter value is equal to the kinetic energy, acquired by cluster because of the collisions of its composite nucleons with the nucleons of cascade avalanche. The account of absorption was reduced to the introduction

of certain minimum value T_0 at which still possibly the emission of fragment ¹.

FOOTNOTE ¹. In actuality, concrete/specific/actual calculations in works [33, 34] were even more simplified and they contained the cell/elements of arbitrariness. Furthermore, the calculations of usual nucleon-nuclear cascade/stages, made by F. P. Denisov, as we saw in chapter 5, strongly they overstate the number of intranuclear collisions. ENDFOOTNOTE.

Page 556.

Utilizing as the parameters a number of driven out nucleon-communication/connections and a number of emitted fragments, F. P. Denises it could obtain correct dependences for many characteristics of the process of fragmentation (for example, see Fig. 415 and 422, where is shown the comparison of the experimental data with the results of the calculation of F. P. Denisova); specifically, it was possible to match with experiment even the dependence of the probability of the formation of fragments on the number of ray/beams in star. However, all the calculations are made only at one value of energy $T = 660$ MeV and only for the interactions of protons with the

heavy component of photoemulsion; therefore it remains unclear, how the results of the calculations reflect physics of matter and how they are consequence successful sediment to experiment. In spite of adjustment, the high-energy "tail" of the spectrum of fragments and the connected with this angular distribution in the area of small angles (see Fig. 422) they remained as before those which were not explained. This could be expected; hardly the high-energy part of the fragments can be explained, being based only on the coulomb interaction of fragment with remanent/residual nucleus.

Thus, if we do not utilize as the adjustable parameters of the basic values, which must automatically be obtained in any sufficient satisfactory theory of fragmentation, then, remaining within the framework only of cascade mechanism of knocking out of fragments, for some characteristics it is impossible to obtain even the qualitative explanation. Specifically, remains incomprehensible one of the basic experimental facts: the large value of the section of fragmentation is not clear also the reason for comparatively small anisotropy of angular scatterings of fragments in the area of high energies; it is impossible to explain the sub-barrier range of energy spectrum, especially for fragments with large charges. At the same time, the fact that many calculated values all the same are created with experiment, by itself hardly is random and, apparently, it indicates that in any case part of the fragments is formed as a result of

knocking out of clusters.

Mechanism of evaporation. In §96 has already been noted that in its form the energy spectrum of fragments was close to the Maxwellian, or evaporative spectrum. In favor of the evaporative mechanism of the formation at least of part of the fragments tell also the dependence of the probability of the emission of fragments on the excitation energy of target nucleus and some data on their angular distribution. It is not amazing therefore that the model of the evaporation of multiply-charged particles from strongly excited nuclei was one of the first models of the process of fragmentation.

In many works (see articles [1, 11-13, 21-24, 32, 49, 71, 116] the form of energy spectra and the angular distributions of fragments was investigated on the basis of three-parameter approach (see formulas (9.2)), the majority of the authors examining the formation of fragment ^6Li in connection with the fact that this fragment sufficiently reliably identified on experiment.

The calculations showed, which, even if it is possible to obtain sufficiently good agreement with the experimental data on energy and angular distributions, the obtained in this case values of the parameters r , V and v are deprived of any physical sense. So, Table 137 shows that the temperature r is usually equal approximately to 10

MeV and above, which corresponds to the excitation energy of nucleus E^* about 1 GeV, if we use the relationship/ratio between E^* and r , which is given by the model of Fermi gas; in this case the complete nuclear binding energy is equal to ~ 800 to MeV. Hence it is possible to draw the conclusion that three-parameter formulation of the model of evaporation one should, apparently, examine only as the convenient method of the systematization of the experimental data. It does not save position and the supplementary account of the transverse component of the speed of evaporating nucleus [3].

Is more consecutively the examination of the evaporation of fragments directly from those excited nuclei, which remain immediately after completion of the cascade stage of interaction [37, 38, 60, 67, 74]. The characteristics of such nuclei can be calculated by the Monte-Carlo method in the same way as this was, for example, described in chapter 6.

Page 557.

The results of the calculations, given in Table 138, show that thus it is possible to attain fair agreement with the experimental yield cross sections of light/lung fragments. However, for the energy spectra of these fragments, as a rule, does not succeed in obtaining a good agreement with experiment (for example, see Fig. 421). For

heavier fragments ($Z_{\phi} \geq 5$) there is no agreement even in the relative probability of emission [28]. Experimental value of that probability is considerably greater than the value, designed according to vaporization theory.

Table 137.

Parameters of vaporization theory, utilized for the description of the energy spectrum of fragments ${}^6\text{Li}$, emitted by the heavy component of photoemulsion (according to the data of survey/coverage [87]).

(1) Первичная частица и ее энергия T , Гэв	(2) Температура τ , Мэв	(3) Эффективный кулоновский барьер V , Мэв	(4) Скорость ядра $\beta = v/c$	(5) Литература
π^- ; 4,3	10,3	8	0	[71]
4,5	11	6	0,018	[24]
4,6	14	9	0,02	[32]
16,9	8	8	0,0015	[11]
(6) Космические лучи	9,5 11,5	5 6	— 0,016	[1] [116]
p , 9	10	5	0,015	[21]
9	15	-2 ± 1	0,012	[49]
14	7	8	0,01	[13]
19	10	5	0,015	[22]
23,9	8	5	0,012	[23]
24	15	-2 ± 1	0,015	[49]
25	8	7	0,0015	[12]

Key: (1). Initial particle and its energy T , GeV. (2). Temperature τ , MeV. (3). Effective coulomb barrier of V , MeV. (4). Speed of nucleus $\beta = v/c$. (5). Literature. (6) Cosmic rays.

Table 138.

A comparison of experimental and calculated cross-sections of the formation of fragments by protons with an energy of T, mb [38].

(1) Ядро- мишень	(2) Фрагмент	$T = 0,94 \text{ ТэВ}$			$T = 1,84 \text{ ТэВ}$		
		$\sigma_{\text{эксп}}$	$\sigma_{\text{расчет}}$		$\sigma_{\text{эксп}}$	$\sigma_{\text{расчет}}$	
			I	II		I	II
Cu	^6He	2 ± 1	1,83	3,56	4 ± 2	4,10	9,01
	^8Li	—	—	—	3	2,26	4,72
	^7Be	$4,4 \pm 1,1$	2,80	3,66	$11,7 \pm 2,9$	7,56	6,45
Zn	^{13}N	0,13	0,028	0,029	0,33	0,079	0,056
Ag	^6He	4 ± 2	3,68	6,51	7 ± 4	7,65	13,8
	^8Li	—	—	—	4	3,61	5,75
	^7Be	$2,5 \pm 0,6$	3,02	4,11	$11,3 \pm 2,8$	7,38	8,75
In	^{13}N	0,020	0,025	0,025	0,19	0,041	0,044
Au	^8Li	—	—	—	9	8,45	10,75
	^7Be	$1,3 \pm 0,3$	1,31	2,07	$5,9 \pm 1,5$	6,12	6,50
	^6He	10 ± 5	6,11	9,55	21 ± 11	18,95	29,60
Pb	^{13}N	0,011	0,008	0,007	0,11	0,035	0,028
U	^{13}N	0,025	0,030	0,023	0,075	0,111	0,094

Key: (1). Nucleus-target. (2). fragment. (3). TeV. (4). experiment.
(5). the calculation.

FOOTNOTE 1. Columns I and II are related to two versions of the calculation, which are distinguished by the selection of the value of a radius of coulomb interaction or, in other words, the selection of the value of the effective coulomb interaction of fragment and residual-nucleus [38]. ENDFCOTNOTE.

Page 558.

The agreement of evaporative model with experiment for the individual characteristics of fragments cannot, of course, serve as the proof of the evaporative mechanism of the formation of basic part of the fragments. Furthermore, are experimental data, which it is generally very difficult to match with this model: many being born fragments, the character of the dependence of the section of fragmentation on the mass number of target nucleus, the presence of the high-energy part of the spectra and finally the high value of angular anisotropy.

Generally speaking, certain surprise causes already the very fact of the agreement of a series of the calculated and experimental

characteristics. The fact is that the statistical model of nuclear reactions assumes the presence of thermodynamic equilibrium. However, during the high excitations of the nuclei, when only can with noticeable probability evaporate fragments, the lifetime of the excited system little; therefore in the interval/gaps among the consecutive emissions of single particles is establish/installed only very relative equilibrium, especially because the delay time of the highly excited system comparable in the course of time of the development of intranuclear cascade and the separation of process at cascade and evaporative stage becomes very conditional [40]. Furthermore, during high excitations change many properties of nuclei; specifically, as a result of thermal expansion is reduced the coulomb barrier of nucleus, a decrease in the surface tension in nucleus leads to a considerable increase in the competition of the process of nuclear fission, are changed conditions for the coagulation of nucleons into the evaporating group-fragments. All this leads to the fact that from the existing theory of evaporation at best it is possible to require only the rough qualitative agreement with experiments in fragmentation.

Recently were made the attempts to develop the theory of the evaporation of complex particles, taking into account the possibility of so-called indirect evaporation [72, 120], when in the same way as this occurs in reaction (p, d), the evaporating from nucleus particle

can be combined with another evaporating particle, if these particles approaching quantum numbers [77]. The calculations in an example of the emission of the nuclei of tritium showed that for strongly excited nuclei the probability of indirect evaporation is really/actually greater than the probability of direct/straight evaporation.

The application/use of a theory of indirect evaporation to heavier fragments, apparently, will make it possible somewhat to improve agreement with experiment; however, the large part of the disagreements, of course, will remain.

One should mention even about the attempts to consider the mechanism of the evaporation of fragments as special case of the process of strongly asymmetric nuclear fission [35, 80, 125]. At the early stage of the investigation of the phenomena of fragmentation this approach seemed completely natural. For this there were some theoretical prerequisite/premises: Fudzhimoto and Yamaguchi they showed that at the temperatures of the nuclei of the order of the binding energy of nucleon the fission probability of these nuclei becomes comparable with the probability of neutron emission [43]. However, the subsequent analysis of experimental experimental data on nuclear fission at high energies of excitation showed that the process of division cannot be that critical for the formation of any

significant part of fragments [87, 107]. At present virtually it is not possible even to indicate the characteristic, which would be in sufficiently good agreement with the model of strongly asymmetric fission. The resemblance of the process of division and process of the decomposition/decay of the excited nucleus into fragment and residual-nucleus turned out to be purely external.

Other attempts at the explanation of the phenomenon of fragmentation. As we already saw above, all attempts to explain the basic laws governing fragmentation, remaining within the framework of any one of the known mechanisms - knocking out, evaporation or divisions - did not lead to success. In this connection by the different authors was proposed a whole series of the hypotheses, in which was made the departure/withdrawal from the usual representations of nuclear reactions at high energies. All these hypotheses can be divided into two groups. The first group includes the hypotheses, according to which the formation of fragments is caused by the already known mechanisms, which occur, however, under some specific conditions. Here it is possible to call/name: 1) the hypothesis of Telegdi (usual evaporation, but with the large angular momentum of the excited nucleus) [102]; 2) hypothesis about asymmetric nuclear fission with large angular momentum [106, 108]; 3) Heisenberg's turbulent effect [64]; 4) the hypothesis of the repeated exchange of mesons [124].

Page 559.

Immediately let us note that two last/latter hypotheses did not obtain the confirmation on experiment (are not observed predict by them to the correlation of the formation of fragments with the generation of mesons). As concerns of the first two hypotheses, then the calculations showed that the angular momentum, by product nucleus, really/actually affects the course of the process of the emission of fragments, increasing the relative probability of the emission of heavy fragments and shift/shearing the most probable value of energy of the emitted fragments to the side of smaller values [70]. However, the further development of hypothesis 1 and 2 were not obtained, and the question concerning the role of angular momentum remains thus far that which was opened.

To the second group can be attributed the hypotheses, which consider fragmentation as completely special process of nuclear disintegration, different from knocking out, evaporation and division [85, 121]. Specifically, in the works of Kruger, Wolfgang, etc. [85, 121] critical for the generation of fragments is considered the special meson mechanism of the transfer; it is assumed that the absorption of pi-mesons is accompanied by such powerful local

disturbance/perturbations in nucleus, that occurs the breaking of nucleon communication/connections and, as the final result, the rapid destruction of part of the nucleus.

Perkins for explaining fragmentation advanced idea about the existence of the long-range nuclear forces, critical for the interaction of rapid particles with the correlated group of nucleons.

In works [51, 110] was presented the hypothesis about the fact that the heavy fragments are driven out by the shock wave of Mach, which is formed in nuclear substance in transit through it of particle at "supersonic" speed.

Unfortunately, all these ideas appear by sufficiently artificial and not one of them it can explain the sufficiently wide circle of experimental facts. Nevertheless, by itself assumption about the existence of the special mechanism, critical for splitting/fissions with the formation of multiply-charged fragments, deserves attention. As we already emphasized above, the specific character of the formation of remanent/residual nuclei with high excitation energy was such, that here is rubbed the clear division between two stages of interaction. Actually in this case is realized the single rapid process, by which approximately equilibrium energy distribution between intranuclear nucleons, even if it begins, then only at the

very end/lead of the interaction. The development of this process is accompanied by the volumetric and surface vibrations of nucleus, which leads to the distortion of its form and to loss of stability with respect to decomposition/decay. In this case as it was noted in work [59], power engineering of deformations can play very important role.

Thus, we see that not one of the proposed, until now, approaches to the theoretical explanation of the processes of fragmentation cannot be considered completely satisfactory.

A greatest quantity of experimental facts can be explained with the aid of the single cascade-evaporative mechanism of the formation of fragments, although the detailed and sufficiently precise calculations actually still not is made ¹.

FOOTNOTE ¹. The made, until now, calculations were based on the cascade calculations of Metropolis, etc. [94]. However, used by these authors model now is represented by very rough. The given in chapter 5 results, which were obtained within the framework of the more advanced model, noticeably differ from the results of Metropolis. This difference will pronounce during the evaluations of the diverse characteristics of the process of fragmentation. Specifically, that

fact that the number of cascade g-particles in the calculations of Metropolis, etc. with $T < 1$ GeV turned out to be that which be independent of the mass number of target nucleus, of it served as basis/base for a conclusion about the fact that the cascade mechanism of knocking out of fragments cannot explain experimental dependence $\sigma_{\Phi}(A)$. In actuality, (for example, see Fig. 265), in region $T < 1$ GeV the number of driven out cascade nucleons increases with passage to more heavy nuclei. ENDFOOTNOTE.

Page 560.

Nevertheless the cascade-evaporative model is at present the unique model, within the framework of which is a possibility to rate/estimate the contributions, apparently, of the most important processes of the fragmentation: the process of knocking out and the process of evaporation.

It is possible to think that the further progress of theory first of all is connected with the perfection/improvement of this model.

It should also be noted that in cascade-evaporative model more or less naturally are considered also some other hypotheses about the

mechanism of fragmentation, for example, the mentioned above meson mechanism of the transfer to nucleus and the hypothesis of Telegdi.

The greatest difficulties are connected, apparently, with the explanation of the sections of the multiple emission of fragments.

BIBLIOGRAPHY

1. Alumkal A. et al. *Nuovo cimento*, 17, 316 (1960).
2. Арифханов У. Р. и др. «Ж. эксперим. и теор. физ.», 38, 1115 (1960).
3. Авдейчиков В. В. и др. Сообщение ОИЯИ Р-2092 (1965). Образование ^8Li из ядер ^{51}V и ^{197}Au под действием протонов с энергией 660 Мэв.
4. Baker E., Friedlander G., Hudis J. *Phys. Rev.*, 112, 1319 (1958).
5. Baker E. W., Katcoff S. *Phys. Rev.*, 123, 641 (1961).
6. Балашов В. В., Бояркина А. Н., Роттер И. Сообщение ОИЯИ Р-1357, Дубна (1963). Теория фрагментации в процессах квазиупругого рассеяния быстрых частиц на легких ядрах.
7. Балашов В. В., Бояркина А. Н. «Изв. АН СССР. Сер. физ.», 28, 359 (1964).
8. Batzel R. E., Miller D. R., Seaborg C. T. *Phys. Rev.*, 84, 671 (1951).
9. Baumann G. *Ann. Phys. (France)* 9, 471 (1964).
10. Baumann G. et al. *Nucl. Phys.*, 78, 650 (1966).
11. Baumann G., Broun H., Cüer P. J. *Phys. Radiation*, 23, 335 (1962).
12. Baumann G., Braun H., Cüer P. *Compt. rend.*, 254, 1966 (1962).
13. Baumann G., Braun H., Cüer P. *Phys. Lett.*, 8, 146 (1964).
14. Baumann G. et al. *Compt. rend.*, 259, 2821 (1964).
15. Baumann G. et al. *Nucl. Phys.*, 74, 557 (1965).
16. Baumann G. et al. *Phys. Rev.*, 138B, 350 (1965).
17. Беляев Б. Н. и др. «Ж. эксперим. и теор. физ.», 43, 1129 (1962).
18. Benioff P. A. *Phys. Rev.*, 119, 316 (1960).
19. Богатин В. И. и др. «Ж. эксперим. и теор. физ.», 46, 431 (1964).
20. Богатин В. И., Ложкин О. В., Яковлев Ю. П. «Ж. эксперим. и теор. физ.», 45, 2072 (1963).
21. Богачев Н. П. и др. «Ж. эксперим. и теор. физ.», 44, 493 (1963).
22. Богачев Н. П. Там же, стр. 1869.
23. Braun H., Baumann G., Cüer P. *Compt. rend.*, 253, 1559 (1961).
24. Breivik F. O., Jacobson T., Sorensen S. O. *Phys. Rev.*, 130, 1119 (1963).
25. Caretto A. A., Hudis J., Friedlander C. *Phys. Rev.*, 110, 1130 (1958).
26. Chakkalakal D. A., Barkow A. G. *Nuovo cimento*, 41A, 249 (1966).
27. Cumming J. B., et al. *Phys. Rev.*, 127, 950 (1962).
28. Cumming J. B. et al. *Phys. Rev.*, 134B, 164 (1964).
29. Cumming J. B. et al. *Phys. Rev.*, 128, 2392 (1962).
30. Даровских В. Ф., Кочеров Н. П., Перфилов Н. А. «Ж. эксперим. и теор. физ.», 37, 1292 (1959).
31. DeKa G. G., DeKa K. C. *Canad. J. Phys.*, 47, 226 (1969).
32. DeKa G. G. et al. *Nucl. Phys.*, 23, 657 (1961).
33. Денисов Ф. П. Труды ФИАН, 22, 129 (1964).
34. Денисов Ф. П., Косарев К. В., Черенков П. А. Труды Всесоюзной конференции по мирному использованию атомной энергии. Изд. АН УзССР, т. 1, стр. 117, Ташкент, 1961.
35. Deutsch R. *Phys. Rev.*, 97, 1110 (1953).
36. Dostrovsky I. et al. *Phys. Rev.*, 139B, 1513 (1965).
37. Dostrovsky I., Fraenkel Z., Rabinowitz P. *Phys. Rev.*, 118, 791 (1960).
38. Dostrovsky I., Fraenkel Z., Hudis J. *Phys. Rev.*, 123, 1452 (1961).
39. Елисеев С. М. Сообщение ОИЯИ Р-24160, Дубна, 1968. Образование многозарядных фрагментов при взаимодействии частиц высоких энергий с ядрами.
40. Ericson T. *Advances Phys.*, 9, 425 (1960).
41. Friedlander G. et al. *Phys. Rev.*, 94, 727 (1954).
42. Friedlander C., Hudis J., Wolfgang R. *Phys. Rev.*, 99, 263 (1956).
43. Fujimoto Y., Yamaguchi Y. *Progr. Theoret. Phys.*, 5, 76 (1950).
44. Furukawa M., Kume S., Ogawa M. *Nucl. Phys.*, 69, 362 (1965).
45. Гагарин Ю. Г., Иванова Н. С. «Ж. эксперим. и теор. физ.», 48, 1793 (1963).

46. Gajewski W., Gorichev P. A., Perfilov N. A. Nucl. Phys., 69, 445 (1965).
47. Gajewski W. et al. Nucl. Phys., 37, 226 (1962).
48. Gajewski W. et al. Nucl. Phys., 45, 27 (1963).
49. Gajewski W. et al. Nucl. Phys., 58, 17 (1964).
50. Gajewski W., Suchorzewska J., Votruba M. F. Phys. Lett., 11, 177 (1965).
51. Glassgold A. E., Hockrotte W., Watson K. M. Ann. Phys., 6, 1 (1959).
52. Goldsack S. J., Lock W. O., Munir B. A. Philos. Mag., 2, 149 (1957).
53. Горичев П. А., Ложкин О. В., Перфилов Н. А. «Ж. эксперим. и теор. физ.», 41, 35 (1961).
54. Горичев П. А. и др. Там же, стр. 327.
55. Горичев П. А., Ложкин О. В., Перфилов Н. А. «Ж. эксперим. и теор. физ.», 46, 1896 (1964).
56. Горичев П. А., Ложкин О. В., Перфилов Н. А. «Ядерная физика», 5, 26 (1967).
57. Горичев П. А., Пьянов И. И. «Ядерная физика», 2, 97 (1965).
58. Gray J., Progress Report. Carnegie Institute of Technology, 1962 (Цит. по работе [81]).
59. Gresro V. P., Alexander J. M., Hude E. K. Phys. Rev., 131, 1765 (1963).
60. Григорьев Е. Л. и др. «Ядерная физика», 6, 696 (1967).
61. Grover J. R. Phys. Rev., 126, 1540 (1962).
62. Гуревич И. И., Жданов А. П., Филиппов А. И. «Докл. АН СССР», 18, 169 (1938).
63. Harmsen D. M. et al. Phys. Lett., 9, 274 (1964).
64. Heisenberg W. J. Phys., 126, 569 (1949).
65. Heitler W., Powell C. F., Fertel G. E. F. Nature, 144, 283 (1939).
66. Hudis J. et al. Phys. Rev., 129, 434 (1963).
67. Hudis J., Miller J. M. Phys. Rev., 112, 1322 (1958).
68. Hudis J., Tanaka S. Phys. Rev., 171, 1297 (1968).
69. Juliano A., Porile N. T. J. Inorg. and Nucl. Chem., 29, 2859 (1967).
70. Ильинов А. С., Тонеев В. Д. «Ядерная физика», 9, 48 (1969).
71. Imaeda I. et al. J. Phys. Soc. Japan, 15, 1753 (1960).
72. Измайлов С. В., Пьянов И. И. «Ж. эксперим. и теор. физ.», 41, 118 (1961).
73. Katcoff S. Phys. Rev., 114, 905 (1959).
74. Katcoff S. Phys. Rev., 164, 1367 (1967).
75. Katcoff S., Baker E. W., Porile N. T. Phys. Rev., 140B, 1549 (1965).
76. Katcoff S., Fickel H. R., Wytttenbach A. Phys. Rev., 166, 1147 (1968).
77. Kikuchi K. Progr. Theoret. Phys., 18, 503 (1957).
78. Korteling R. G., Caretto Jr. A. A. J. Inorg. and Nucl. Chem., 29, 2863 (1967).
79. Курчатов Б. В. и др. «Ж. эксперим. и теор. физ.», 39, 56 (1958).
80. Лаврухина А. К. и др. «Атомная энергия», 3, 285 (1957).
81. Lafleur M. S., Porile N. T., Yaffe L. Canad. J. Chem., 44, 2749 (1966).
82. Lemonpe J. et al. Nuovo cimento, 41A, 235 (1966).
83. Ligonniere M., Vassent B., Bergas R. Compt. rend., 259, 1406 (1964).
84. Ложкин О. В. «Ж. эксперим. и теор. физ.», 33, 354 (1957).
85. Ложкин О. В. Диссертация, ИАН, Ленинград, 1957. Многозарядные частицы в ядерных расщеплениях, вызываемых протонами с энергией 300—600 Мэв.
86. Ложкин О. В., Перфилов Н. А. «Ж. эксперим. и теор. физ.», 31, 913 (1956).
87. Ложкин О. В., Перфилов Н. А. В сб. «Ядерная химия», «Наука», М., 1965.
88. Ложкин О. В. и др. «Ж. эксперим. и теор. физ.», 38, 1388 (1960).
89. Ложкин О. В., Перфилов Н. А., Яковлев Ю. П. «Докл. АН СССР», 151, 826 (1963).
90. Макаров М. М. «Ж. эксперим. и теор. физ.», 46, 809 (1964).
91. Мальцева Н. С., Мехедов В. Н., Рыбаков В. Н. «Ж. эксперим. и теор. физ.», 45, 852 (1963).
92. Marguez L. Phys. Rev., 86, 405 (1952).
93. Marguez L., Perlman I. Phys. Rev., 81, 957 (1950).
94. Metropolis N. et al. Phys. Rev., 110, 185; 204 (1958).
95. Mekhedov V. N. Nucl. Phys. 53, 225 (1964).
96. Москалева А. П. Диссертация, МГУ, Москва, 1964. Образование тяжелых фрагментов под действием протонов высоких энергий.
97. Munir B. A. Philos. Mag., 1, 355 (1955).
98. Nakagawa S. et al. J. Phys. Soc. Japan, 12, 747 (1957).
99. Nakagawa S., Tamai E., Namoto S. Nuovo cimento, 9, 780 (1958).
100. Остроумов В. И. «Ж. эксперим. и теор. физ.», 32, 3 (1967).
101. Parikh V. Nucl. Phys., 18, 638 (1960).
102. Perkins D. H. Proc. Roy. Soc., 203, 399 (1950).

Page 561.

103. Перфилов Н. А., Денисенко Г. Ф. «Ж. эксперим. и теор. физ.», 35, 631 (1958).
104. Перфилов Н. А. и др. «Ж. эксперим. и теор. физ.», 38, 345 (1960).
105. Перфилов Н. А., Ложкин О. В., Шамов В. П. «УФН», 70, 3 (1960).
106. Перфилов Н. А., Шамов В. П., Ложкин О. В. «Докл. АН СССР», 113, 75 (1957).
107. Перфилов Н. А., Ложкин О. В., Остроумов В. И. Ядерные реакции под действием частиц высоких энергий. М.—Л., Изд-во АН СССР, 1962.
108. Пик-Пичак Г. А. «Ж. эксперим. и теор. физ.», 34, 341 (1958).
109. Porile N. T., Tappak S. Phys. Rev., 135B, 122 (1964).
110. Рапопорт Л. П., Крыповецкий А. Г. «Изв. АН СССР. Сер. физ.», 28, 388 (1964).
111. Rayundu G. V. S. Canad. J. Chem., 42, 1149 (1964).
112. Rayundu G. V. S. J. Inorg. and Nucl. Chem., 30, 2311 (1968).
113. Rudstam G., Bruninx E., Pappas A. G. Phys. Rev., 126, 1852 (1962).
114. Rudstam G., Stovenson P. C., Folger R. L. Phys. Rev., 87, 358 (1952).
115. Schopper E. Naturwissenschaften, 25, 557 (1937).
116. Skjeggstad O., Sørensen S. O. Phys. Rev., 113, 1115 (1959).
117. Stein R. J. Phys. (France), 27, 405; 513 (1966).
118. Stein R. Nuovo cimento, 44A, 896 (1966).
119. Stein R. Nucl. Phys., 87, 836; 854 (1967).
120. Tomasini A. Nuovo cimento, 6, 404 (1957).
121. Wolfgang R. et al. Phys. Rev., 103, 394 (1956).
122. Ван Юн-юй и др. «Ж. эксперим. и теор. физ.», 39, 230 (1960).
123. Ван Юн-юй и др. Там же, стр. 527.
124. Векслер В. И. «Докл. АН СССР», 82, 865 (1952).
125. Виноградов А. П. и др. Конференция АН СССР по мирному использованию атомной энергии, 1—5 июля 1955; заседание ОХН, стр. 132, М., Изд-во АН СССР, 1955.

Page 563.

Chapter 10.

NUCLEAR FISSION.

§99. Division of the excited remanent/residual nuclei.

During the discussion of the output/yield of remanent/residual, nuclei in chapter 3 we already noted that in the case of heavy targets the dependence $\sigma(A_{\text{oct}})$ has wide maximum in the region of mass numbers $A_{\text{oct}} \sim A_M/2$ (see Fig. 140). This maximum is connected with the process of the division which we subsequently will characterize as nuclear decomposition to two comparable fragments.

From demonstrative model point of view division it is possible to call/name this phenomenon when nucleus (but further we will examine only the excited nuclei) it experience/tests so powerful oscillation/vibrations that the forces of surface tension prove to be

not in state to retain/hold down it in the form of single system, and nucleus it decomposes (it is divided) to two more or less differing by its value of fragment. ¹.

FOOTNOTE ¹. We will not concern the process of nuclear fission into three fragments. The relative probability of such a process even at an energy of several gigaelectron-volt composes a total of 0.1c/o [12, 27, 51]. Research on nuclear fission into three fragments under the action of high-energy particles makes also only its first spaces. ENDFOOTNOTE.

Apparently, not into one of other fields of physics was invested so many the efforts of the researchers and was accumulated such an abundance of experimental information as in the range of nuclear fission, nevertheless it cannot be said which here continually is understood that all phenomena obtained their explanation. This position reflects the general state of nuclear physics, and the process of division in this sense is concentrated all difficulties of theory, since it is connected with the deepest transformations of nucleus.

In this chapter we will be restricted to the discussion of the

nuclear fission, initiated by high-energy particles; in this case the primary attention let us give to the results of investigations, obtained recently. The reader, who is interested in other aspects of the physics, can turn to survey/coverages and monographs [1, 36, 40, 46, 50, 53, 54, 65, 83, 86, 90, 91, 115].

At present it is experimentally proved that to be divided can not only heavy nuclei of the type of thorium and uranium, but also the nucleus, arranged/located in the middle of the periodic table of elements for example; for this necessary to only transmit to nucleus the excitation energy, which exceeds the threshold of fission reaction. Thus excitations can have the nuclei, which remain after intranuclear cascade. As we saw in chapter 5, these nuclei are characterized by wide distribution both according to their mass and charge numbers and according to the value of excitation energy E^* , up to very high energies. In this case the fission reaction will compete with other possible processes of the transition of the excited nucleus to the ground state, including with the process of evaporation.

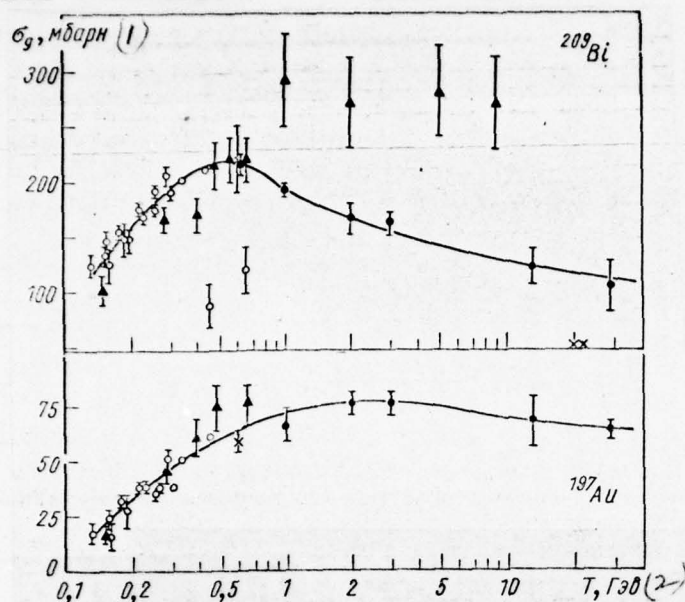


Fig. 427. The fission cross sections of nuclei Au and Bi under the action of protons with a different energy of T : with $T < 0.6$ GeV the curves approximate the average experimental values; with $T > 0.6$ GeV the curves are carried out according to most reliable measurements of Kh'yudis and Katkov [51] (●); ▲, x - the respectively data of the works of Matusevich, etc. [61, 73] and de Karvalo, etc. [24, 25]; ○ - the results of other works, taken from Table 139.

Key: (1) mb. (2) GeV.

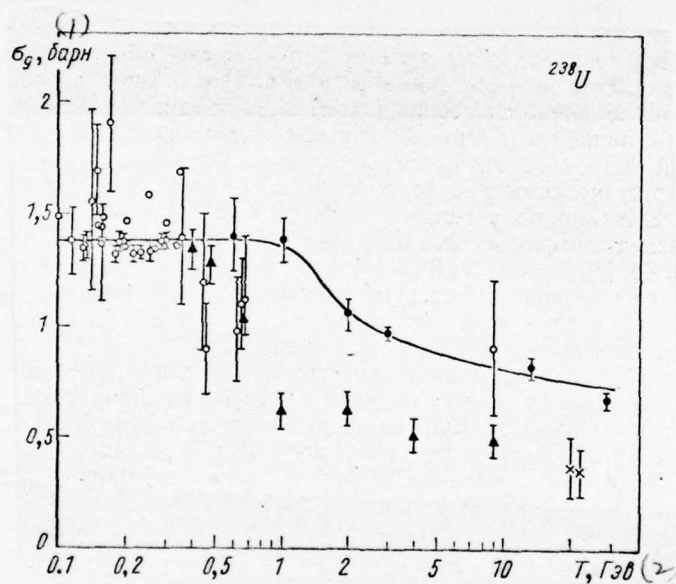


Fig. 428. Fission cross sections of the nuclei of uranium under the action of protons with an energy of T . Designations are the same as in Fig. 427.

Key: (1) barn. (2) . GeV.

Page 565.

Hence, in particular, it follows that the fundamental characteristics of fissionable nucleus, its mass and charge number A_d and Z_d and excitation energy E_d^* , generally speaking, do not coincide with the characteristics of the excited nuclei, which remained after the completion of the cascade stage of interaction.

Excitation energy, the mass and charge numbers of primary fission fragments let us further designate E_i^* , A_i , Z_i ($i = 1, 2$). It is obvious that $E_1^* + E_2^* = E_d^*$; $A_1 + A_2 = A_d$; $Z_1 + Z_2 = Z_d$. However, the fission products, recorded in experiment, usually differ significantly from primary fragments. This is caused by the processes of the evaporation of the primary excited fragments, by the processes of β -transitions in nucleus-products, by delayed neutron emission and by other processes.

Those which are recorded with experiment secondary fragments let us characterize the mass and charge numbers A_i and Z_i , whereupon, as a rule $A_1 + A_2 < A_d < A_M$ and $Z_1 + Z_2 < Z_d < Z_M$, where of the number A_M and Z_M is related to the initial target nucleus.

§100. Fission cross sections, the coefficient of fissionability.

The basic known now experimental values of the fission cross sections of nuclei by rapid protons and neutrons are assembled in Table 139, but for the most in detail studied nuclei ^{238}U , ^{209}Bi and ^{197}Au , are shown also in Fig. 427 and 428. From the preceding information it is evident that the results, obtained by the different authors and with the aid of different procedure, noticeably differ from each other, although the common/general/total laws are visible sufficiently clearly for nuclei of the type of nucleus ^{238}U fission cross section it remains virtually constant in the region of energies $T \lesssim 1$ GeV, and then begins to monotonically decrease, decreasing with $T \simeq 30$ GeV approximately double; the fission cross section of bismuth, mass number of which in all to 130 is less than of uranium, sufficiently rapidly grow/rises with an increase in the energy of primary proton, it passes through the wide maximum in region $T \simeq 0,6$ GeV and then drops to value $\sigma_{\pi} \simeq 100$ mb with $T \simeq 30$ GeV; during passage to even more light nucleus ^{197}Au , the dependence $\sigma_{\pi}(T)$ becomes monotonically increasing in the entire region of energies, large several dozen million electron volts in question.

One should note disagreement in the results of different measurements with energies $T > 0.6$ GeV. Apparently, are most reliable the results of Kh'yudis and Katkov, obtained with the use of contemporary procedure of mica detectors [51]. In experiment were recorded the cases of the divisions into two fragments, each of which has mass number $A_i > 30$. Were thoroughly examined the doubtful cases, which could be division, but due to recording condition one of the fragments it was not observable. The procedure of experiment was checked in gauging experiments on the measurement of the fission cross section of nuclei by thermal neutrons.

A decrease in the fission cross sections of the nuclei of uranium and bismuth with energies of the protons, greater than 1 GeV, was recorded also in experiments de Karvalo, etc. [24, 25]. Obtained with the aid of emulsion procedure data of these experiments will agree with the measurements of Kh'yudis and Katkov with $T \approx 0.6$ GeV, with $T = 20$ GeV they are understated double. It is possible that these disagreements are caused by the different criteria of the selection of dividing events in works [24, 25, 51].

Very considerable and completely incomprehensible disagreement is observed between the data of Kh'yudis and Katkov [51] and the results of the works of Ye. S. Matusevich and of co-authors [61, 73], although in both cases was applied the close procedure (Ye. S.

Matusevich et al. as detector utilized usual glass). If with $T \approx 0.6$ GeV the results of these works are close for the nuclei of gold and bismuth and only to 150/o are distinguished in the case of the nucleus of uranium, then with high energies of the measurement of Ye. S. Matusevich et al. gave almost double smaller section for uranium and substantially large values σ_d for the nucleus of bismuth, whereupon in the latter case completely different and the energy dependency of section $\sigma_d(T)$ ¹.

FOOTNOTE ¹. As it was noted in work [51], it remains unclear, it is how accurate during the use of detectors made of glass in works [61, 73] were recorded the events of high-energy division into two fragments and how reliably we could be separated event with one visible track. ENDFOOTNOTE.

Pages 566-567.

Table 139. Fission cross section of nuclei by high-energy protons.

(1) Ядро	T	(2) σ_d , мбарн	(3) Литература	(1) Ядро	T	(2) σ_d , мбарн	(3) Литература
^{187}Em	156 Mэв	0,015	[99]	^{197}Au	132 Mэв	$17,4 \pm 3,5^{(2)*}$	[105]
	286 »	0,060	[99]		150 »	$16,5 \pm 2,5$	[61]
	340 »	$0,11 \pm 0,06$	[60]		156 »	24 ± 4	[64]
	380 »	0,25	[99]		156 »	24 ± 4	[74]
	300-660 »	$0,32 \pm 0,1$	[102]		158 »	$16,0 \pm 6,4^{2*}$	[105]
	600 »	$(0,1 \pm 0,01)$	[25]		178 »	$32,0 \pm 1,8^{2*}$	[105]
	600 »	$< 0,3^{+0,6}_{-0,3}$	[24]		186 »	$27,4 \pm 7,2^{2*}$	[105]
	600 (5) »	$\leq 0,3$	[51]		216 »	$38,2 \pm 1,9^{2*}$	[105]
	1 Гэв	≤ 2	[51]		230 »	$37,9 \pm 1,2^{2*}$	[105]
	1 »	$7 \pm 2^{(6)}$	[3]		254 »	$35,5 \pm 1,9^{2*}$	[105]
	2 »	≤ 5	[51]		261 »	$38,2 \pm 1,8^{2*}$	[105]
	2 »	$30 \pm 7^{(*)}$	[3]		280 »	46 ± 6	[61]
	3 »	$50 \pm 10^{(*)}$	[3]		288 »	$51,2 \pm 4,2^{2*}$	[105]
	3 »	≤ 5	[51]		303 »	$38,4 \pm 1,6^{2*}$	[105]
	13 »	≤ 5	[51]		336 »	$50,5 \pm 0,8^{2*}$	[105]
	29 »	≤ 5	[51]		390 »	61 ± 8	[61]
					450 »	61	[66]
					480 »	74 ± 10	[61]
					600 »	59 ± 5	[25]
					660 »	75 ± 9	[61]
$^{121,8}\text{Sb}$	660 Mэв	0,25	[68]		1 Гэв (5)	66 ± 7	[51]
					2 »	76 ± 5	[51]
					3 »	76 ± 5	[51]
					13 »	67 ± 11	[51]
					29 »	63 ± 4	[51]
$^{164,9}\text{Ho}$	450 Mэв	$\sim 0,2$	[66]				
^{181}Ta	156 Mэв	$1,6 \pm 0,6$	[74]	$^{207,2}\text{Pb}$	150 Mэв	46 ± 6	[61]
	156 »	$2,0 \pm 0,3$	[18]		280 »	106 ± 11	[61]
	280 »	$2,6 \pm 0,4$	[61]		390 »	130 ± 15	[61]
	390 »	$4,7 \pm 0,7$	[61]		660 »	121 ± 20	[61]
	450 »	5	[66]				
	480 »	$8,3 \pm 1,1$	[61]				
	564 »	$10,1 \pm 1,4$	[61]				
	660 »	$14,0 \pm 1,9$	[61]				
$^{183,9}\text{W}$	460 Mэв	$4,0 \pm 1,6$	[101]				
	600 »	$9,0 \pm 2,2$	[25]				
	660 »	10 ± 3	[101]				
	660 »	21 ± 7	[15]				
$^{186,2}\text{Re}$	150 Mэв	$1,7 \pm 0,3$	[61]	^{209}Bi	132 Mэв	$125 \pm 9^{2*}$	[105]
	280 »	$6,9 \pm 0,6$	[61]		150 »	103 ± 12	[61]
	390 »	$8,1 \pm 1,1$	[61]		154 »	$134 \pm 9^{2*}$	[105]
	450 »	19	[61]		156 »	126 ± 20	[64]
	480 »	$14,7 \pm 2,0$	[61]		156 »	126 ± 16	[74]
	564 »	$13,1 \pm 1,9$	[61]		158 »	$146 \pm 9^{2*}$	[105]
	660 »	$20,5 \pm 2,8$	[61]		178 »	$155 \pm 5^{2*}$	[105]
					186 »	$148 \pm 15^{2*}$	[105]
					194 »	$148 \pm 9^{2*}$	[105]
					216 »	$174 \pm 4^{2*}$	[105]
					230 »	$157 \pm 4^{2*}$	[105]
					254 »	$175 \pm 5^{2*}$	[105]
					261 »	$191 \pm 5^{2*}$	[105]
					280 »	166 ± 11	[61]
					288 »	$205 \pm 9^{2*}$	[105]
					303 »	$190 \pm 5^{2*}$	[105]
					336 »	$200 \pm 2^{2*}$	[105]
					390 »	170 ± 15	[61]
					450 »	210	[66]
					460 »	88 ± 20	[401]
					480 »	214 ± 20	[61]
					564 »	219 ± 20	[61]
					600 »	220 ± 30	[25]
					600 »	216 ± 8	[51]
					660 »	218 ± 20	[61]
					660 »	120 ± 20	[101]
					1 Гэв (5)	290 ± 40	[73]
					1 »	191 ± 5	[51]
					2 »	165 ± 14	[51]
					2 »	270 ± 40	[73]
$^{195,1}\text{Pt}$	150 Mэв	$7,7 \pm 1,2$	[61]				
	280 »	25 ± 3	[61]				
	390 »	32 ± 4	[61]				
	480 »	37 ± 5	[61]				
	660 »	47 ± 6	[61]				

Ядро	T	σ_d , мбарн	Лите- ратура	Ядро	T	σ_d , мбарн	Лите- ратура
^{209}Bi	3 Γ_{36}	161 ± 10	[51]	^{238}U	130 M_{36}	$1345 \pm 56^2*$	[105]
	5 »	280 ± 40	[73]		132 »	$1357 \pm 48^2*$	[105]
	9 »	270 ± 40	[73]		140 »	1560 ± 400	[56]
	13 »	122 ± 15	[51]		140 »	1690 ± 200	[56]
	20 »	~ 50	[24]		150 »	1440	[106]
	21,8 »	~ 50	[24]		154 »	$1435 \pm 48^2*$	[105]
	29 »	105 ± 22	[51]		156 »	1370 ± 250	[64]
^{232}Th	114 M_{36}	$896 \pm 88^2*$	[105]		158 »	$1483 \pm 64^2*$	[105]
	130 »	$889 \pm 28^2*$	[105]		170 »	1900 ± 300	[59]
	132 »	$910 \pm 28^2*$	[105]		178 »	$1320 \pm 36^2*$	[105]
	150 »	950 ± 110	[61]		186 »	$1375 \pm 40^2*$	[105]
	154 »	$970 \pm 32^2*$	[105]		192 »	$1380 \pm 20^2*$	[105]
	158 »	$956 \pm 36^2*$	[105]		194 »	$1363 \pm 40^2*$	[105]
	178 »	$865 \pm 24^2*$	[105]		200 »	1470	[106]
	186 »	$881 \pm 32^2*$	[105]		216 »	$1320 \pm 32^2*$	[105]
	192 »	$856 \pm 24^2*$	[105]		230 »	$1325 \pm 16^2*$	[105]
	216 »	$821 \pm 20^2*$	[105]		250 »	1580	[106]
	230 »	$809 \pm 12^2*$	[105]		254 »	$1335 \pm 40^2*$	[105]
	254 »	$805 \pm 20^2*$	[105]		261 »	$1345 \pm 16^2*$	[105]
	261 »	$821 \pm 24^2*$	[105]		288 »	$1380 \pm 28^2*$	[105]
	280 »	840 ± 70	[61]		300 »	1460	[106]
	288 »	$821 \pm 24^2*$	[105]		303 »	$1385 \pm 36^2*$	[105]
	303 »	$800 \pm 20^2*$	[105]		336 »	$360 \pm 12^2*$	[105]
	336 »	$821 \pm 20^2*$	[105]		340 »	1590	[106]
	390 »	770 ± 15	[61]		350 »	1400 ± 300	[56]
	450 »	670	[66]		390 »	1340 ± 80	[61]
	460 »	740 ± 80	[61]		460 »	1200 ± 300	[56]
	600 »	730 ± 80	[25]		460 »	900 ± 200	[101]
	660 »	670 ± 70	[61]		480 »	1270 ± 80	[61]
	20 Γ_{36}	170 ± 70	[24]		600 »	1405 ± 160	[51]
	21,8 »	200 ± 50	[24]		660 »	1100 ± 200	[101]
^{235}U	114 M_{36}	$1640 \pm 164^2*$	[105]	^{238}U	660 »	1040 ± 75	[61]
	130 »	$1200 \pm 40^2*$	[105]		660 »	1110 ± 300	[56]
	132 »	$1520 \pm 40^2*$	[105]		660 »	970 ± 250	[56]
	150 »	1850 ± 220	[61]		1 Γ_{36}	620 ± 70	[73]
	154 »	$1520 \pm 44^2*$	[105]		1 »	1385 ± 95	[51]
	158 »	$1360 \pm 52^2*$	[105]		2 »	630 ± 70	[73]
	178 »	$1360 \pm 32^2*$	[105]		2 »	1053 ± 69	[51]
	186 »	$1320 \pm 40^2*$	[105]		3 »	969 ± 11	[51]
	192 »	$1382 \pm 16^2*$	[105]		5 »	510 ± 70	[73]
	193 »	$1320 \pm 40^2*$	[105]		9 »	490 ± 70	[73]
	194 »	$1240 \pm 16^2*$	[105]		9 »	900 ± 300	[89]
	216 »	$1280 \pm 24^2*$	[105]		13 »	814 ± 39	[51]
	230 »	$1320 \pm 12^2*$	[105]		20 »	370 ± 130	[24]
	242 »	$1360 \pm 16^2*$	[105]		21,8 »	350 ± 90	[24]
	261 »	$1375 \pm 24^2*$	[105]		29 »	668 ± 34	[51]
	288 »	$1305 \pm 28^2*$	[105]	^{239}Pu	660 M_{36}	1800 ± 150	[62]
	292 »	$1240 \pm 20^2*$	[105]		1 Γ_{36}	1000 ± 120	[73]
	303 »	$1380 \pm 24^2*$	[105]		2 »	810 ± 100	[73]
	336 »	$1300 \pm 20^2*$	[105]		5 »	610 ± 70	[73]
	390 »	1450 ± 150	[61]		9 »	600 ± 70	[73]
^{237}Np	480 »	1340 ± 134	[61]	^{237}Np	280 M_{36}	1580 ± 160	[62]
	660 »	1200 ± 80	[62]		480 »	1520 ± 160	[62]
	1,0 Γ_{36}	670 ± 80	[73]		660 »	1520 ± 160	[62]
	2 »	620 ± 70	[73]		1 Γ_{36}	990 ± 120	[73]
	5 »	520 ± 60	[73]		2 »	820 ± 100	[73]
^{238}U	9 »	530 ± 60	[73]	^{238}U	5 »	710 ± 80	[73]
	70 M_{36}	1470	[106]		9 »	700 ± 80	[73]
	110 »	1490	[106]				
	114 »	$1380 \pm 148^2*$	[105]				

Key: (1). Nucleus. (2) mb. (3). Literature. (4). MeV. (5). GeV.

FOOTNOTE 1. Corrected value is related to the section of formation/education in the emulsion of the pair of heavy tracks. Among such events considerable portion they compose the processes of the simultaneous generation of two fragments (see [51]). ENDFOOTNOTE.

FOOTNOTE 2. Besides the error of measurement indicated there can be even 100/o systematic error.

Page 568.

Friedlander to evaluate fission cross sections by the high-energy protons of the nuclei of lead and uranium utilized data of radiochemical measurements [36]. The upper limit of the fission cross section of the nucleus of uranium with $T = 2.9$ and 28 GeV was thus determined equal respectively 1.28 and 1.23 barn, and lower - 0.83 and 0.48 barn. For lead was obtained the estimation only of the

upper boundary of the section: $\sigma_d \leq 0,27$ barn with $T = 2.9$ GeV and $\sigma_d \leq 0,31$ barn with $T = 28$ GeV. These estimations will agree with the results of Kh'yudis and Katkov [51].

During passage to more light nuclei it decreases both the very value of fission cross section and portion σ_d/σ_{in} , which composes the process of division in the total cross section of inelastic interaction. This portion is conventionally designated as the coefficient of fissionability or simply by the fissionability of nucleus. For nuclei, whose process of division is prevailing as compared with all by others, i.e., for nuclei of the type of thorium and heavier maximum value of fissionability composes more than 0.5; for nuclei in the region of lead and bismuth $\sigma_d/\sigma_{in} = 0.05-0.1$; for even more light nuclei fission probability is so low in comparison with the probability of usual splitting/fission, that experimental information proves to be simply insufficiently to establish the character of energy dependency $\sigma_d(T)$.

N. A. Perfilov [88] focused attention on the fact that the maximum value of fissionability, considered as function of relation Z_M^2/A_M , behaves monotonically

$$(\sigma_d/\sigma_{in})_{max} = \exp\{0,682(Z_M^2/A_M - 36,25)\}. \quad (10.1)$$

As can be seen from Fig. 429, this approximation turns out to be valid for the wide set of nuclei, from uranium and to rare-earth

elements; it is possible to use to evaluate section σ_n when experimental data is insufficient.

§101. Distribution of fission fragments according to their masses.

Figure 430 shows the distribution of the output/yield of nuclear fragments depending on their mass number A_i for the case of interactions with the nuclei of uranium of the protons of different energies. During $T \leq 100$ MeV this distribution has the typical "double-humped" character, well known from experiments on low-energy particles. In high-energy region the mass distribution has only one wide maximum whose center with an increase in energy T slowly is shift/sheared to the side of smaller of mass numbers A_i , a distribution itself in this case it widens itself and it becomes asymmetric. With $T > 1$ GeV the dividing peak, so/such characteristic for low-energy division, is virtually already barely noticeable (this, in particular, impedes value determination of section σ_n by means of the integration of curve $\sigma_n(A_i)$).

It must be noted that the low-energy curves in Fig. 430 show the averaged, smoothed dependence $\sigma_n(A_i)$, real distributions actually never they are strictly symmetrical and single-humped.

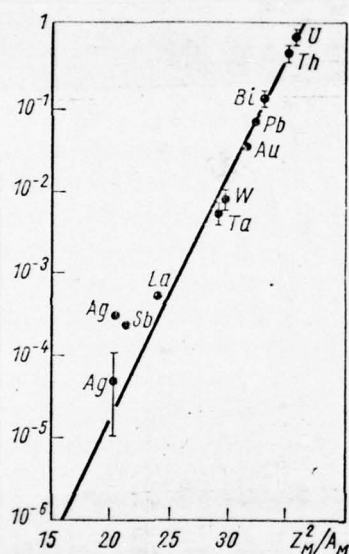


Fig. 429. Dependence of the maximum values of fissionability σ_d/σ_{in} from the value of relation Z_M^2/A_M ($Z^2/A_M \approx Z_d^2/A_M$). Experimental values σ_d correspond in essence of the region of energies $T \approx 0.4-0.7$ GeV. Section σ_{in} is designed by formula $\sigma_{in} = \pi (1.26 A^{1/3} \text{ is } 0.41) \approx 10^{-2}$ barn. Straight line is an approximation of Perfilov (10.1).

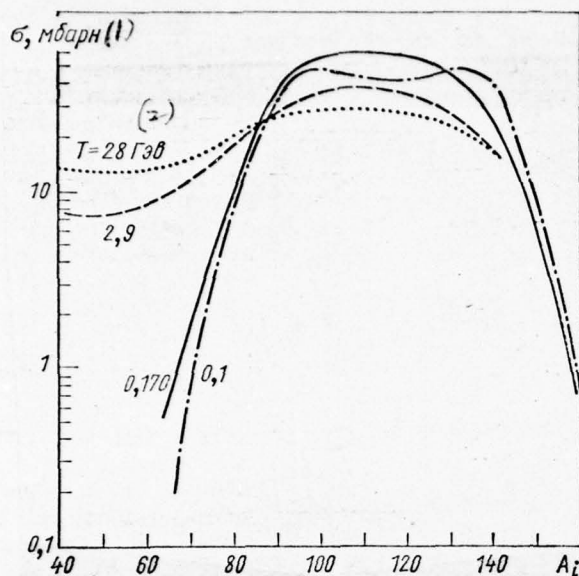


Fig. 430. Mass distribution of the fission fragments of the nuclei ^{238}U , irradiated by protons with an energy of T [36]. Key: (1) mb.

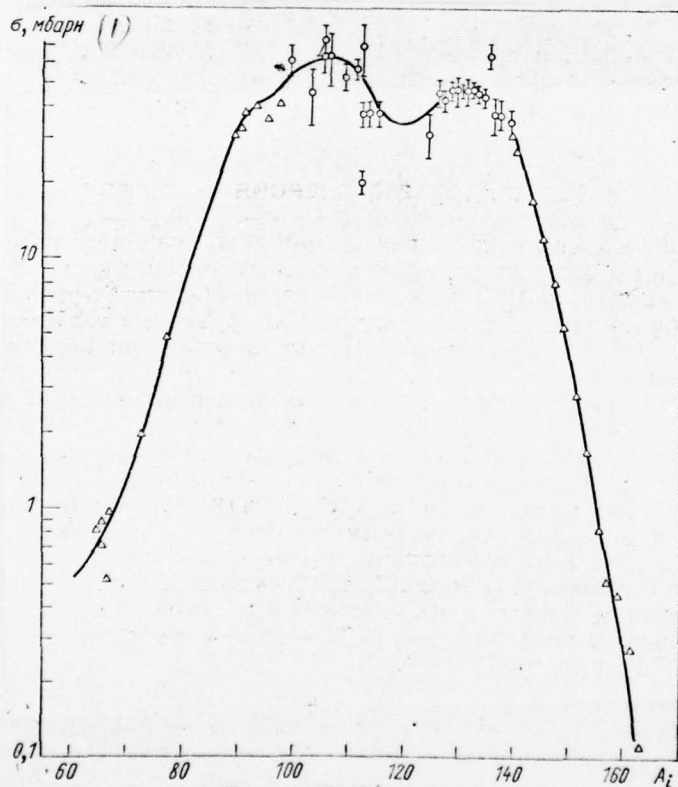


Fig. 4.31.

Fig. 431. Fission yield of nuclear fission U by protons 170 MeV in energy depending on the value of their mass number [85].

Key: (1) mb.

Page 570.

This is evident, for example, from Fig. 431, where is given distribution $\sigma_n(A_i)$ for the nuclear fission of uranium 170-MeV by protons. Unfortunately, now still there are no such detailed measurements of fission yield for other energies.

In the case of more light/lung target nuclei the character of dependence $\sigma_n(A_i)$ remains in general terms the same as for the nucleus of uranium (for example, see Fig. 432); however, maximum is expressed considerably weaker (comp. with Fig. 140). For example, during irradiation of lead by protons with energy $T = 28$ GeV virtually with identical probability are formed fragments in the region of mass numbers $A_i \simeq (30-130)$ [36]. For even more light/lung fragments $A_i < 30$ the section $\sigma_n(A_i)$ sharply will increase during a decrease in the number A_i , that connected with the phenomenon of fragmentation (see Chapter 9).

Figure 433 and 434 in an example of the nucleus of uranium shows

the energy dependency of the sections of the cumulative and independent output/yield of neutron excess and neutron-deficient isotopes. ¹.

FOOTNOTE ¹. The separation of fission yields nucleus- to independent variables and cumulative is connected with possibility to deal only with one isolated fission product (independent output/yield) or actually with the sum of the different fragments, which as a result of the subsequent β -transitions (and thinner - delayed neutron emission) form one and the same end product. The latter, in particular, include all nuclei, which are found at the end of the chain/networks of β -decays. ENDFOOTNOTE.

If in the first case in an entire region of energies $T \geq 100$ MeV of section monotonically they decrease, then the sections of the formation/education of fragments with a neutron deficiency have the clear maximum whose position depends only on the neutron-proton ratio $(A_i - Z_i)/Z_i$.

As can be seen from Fig. 435, than more neutron-deficient nucleus, themes with larger energy appears maximum. In other words, with an increase of energy T the relative yield of neutron-deficient nuclei grow/rises.

§102. Charge dispersion of fragments.

Under the charge dispersion of fragments let us understand the distribution of the fission yield according to isobars during the fixed value of mass number A_i . This term one ought not to confuse with term the charge distribution, which we will further characterize the charge distribution of the target nucleus between two fragments, which were being formed in fission.

Last low energy T the charge dispersion of fragments it is described sufficiently well by the Gaussian curve whose maximum Z_p (i.e. the value of most probable charge) is shifted relative to the line of stability Z_A per three or four units, but the complete width of curve on the half of the maximum value composes a little more than two unity [40, 46, 54, 83]. With an increase in energy T up to several hundreds of million electron volt charge dispersion considerably widens itself (mainly, because of an increase in the output/yield of neutron-deficient fragments), and values Z_p approach line of β -stability. In this case the complete width of curved charge dispersion reaches already three-four unity, and the value of difference $Z_A - Z_p$ lie/rests at range from one to two unit charges [23, 37].

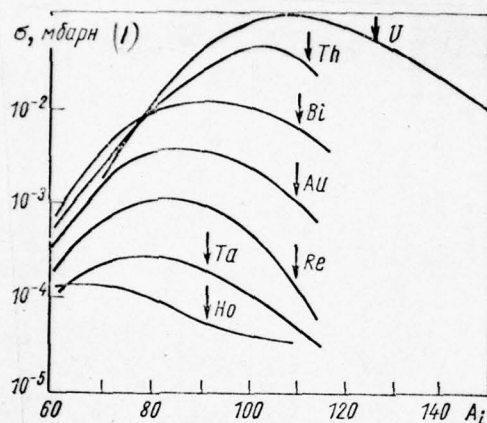


Fig. 432. Mass distribution of the fission fragments of the different nuclei, irradiated by protons 450 MeV in energy [46, 67]. By rifleman/pointers are shown values A_i , equal to the half of the mass number of target nucleus.

Key: (1) mb.

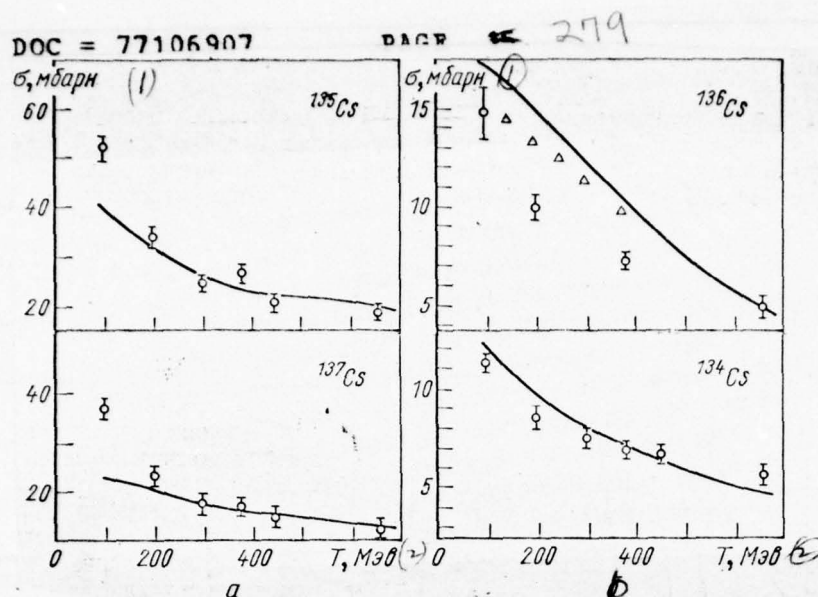


Fig. 433. The cumulative (a) and independent (b) output/yield of the neutron excess fission fragments of nuclei ^{238}U by protons with an energy of T : o, Δ are experimental data respectively from works [37, 105]; curves are a result of the theoretical calculation (see §106). Key: (1) mb. (2). MeV.

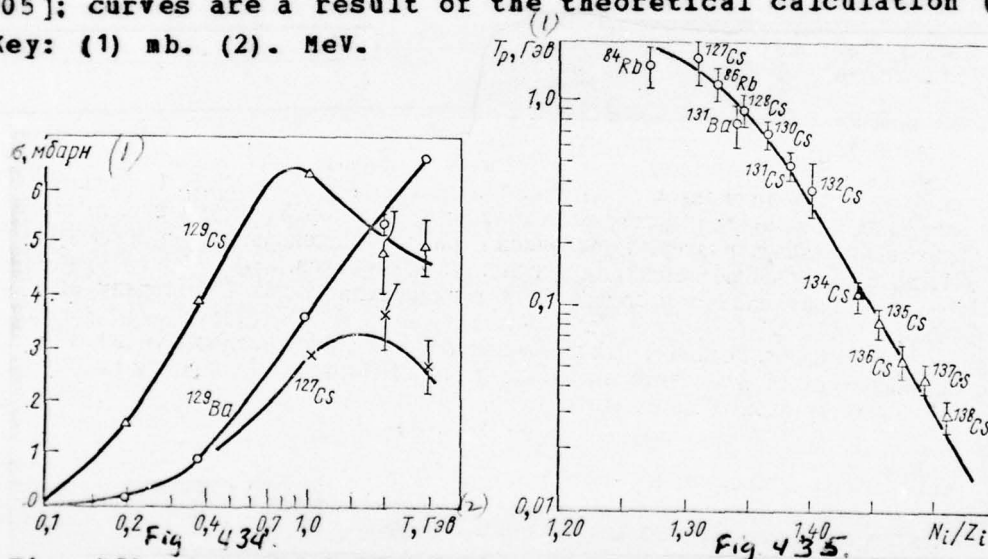


Fig. 434. Output/yield of the neutron-deficient fission fragments of nucleus ^{238}U by protons with an energy of T . Curves approximate experimental data works [37]. These for ^{127}Cs , ^{129}Cs they are related to independent variable, while these for ^{129}Ba - to cumulative fission yield.

Key: (1) mb. (2). GeV.

Fig. 435. The position of the maximum of excitation function for nuclear fission U by the protons: \circ , Δ are experimental data respectively for neutron-deficient and neutron excess fission products from works [23, 37].

Key: (1). GeV.

Page 572.

Increasingly above aforesaid is illustrated by data given in Fig. 436, although follow- to have in form, that the given in this figure curves are not charge dispersion in strict sense of this word, since along the axis of abscissas is deposit/postponed not the charge of fragment Z_i (or difference $Z_i - Z_A$), but relation $N_i/Z_i^{\dagger 1}$.

FOOTNOTE ¹. The selection of this dependence is caused themes that in the region of high energies is a smaller number of convenient for measurement nuclei (in this case experimental curves are shift/sheared to the side of stable nuclei), and the results of

measurements they are related faster to the group of nuclei with close mass numbers, than to one fixed value A_i .

For each mass number A_i necessary would be to select its value Z_A , while the relation N_i/Z_i in practice it does not depend on value Z_A .

ENDFOOTNOTE.

Figure 436 also shows that with $T \gtrsim 1$ GeV in the curves of charge dispersion distinctly they exhibited two maximums. The formation of left, neutron-deficient maximum is connected with high-energy division [2, 37]. The width and the position of the second maximum, which corresponds to neutron excess ($N_i/Z_i \sim 1,5$), are little affected with an increase of T ; the position of this maximum closely to the position of the neutron excess peak in low-energy division. Thus, it may be concluded that the large totality of data (charge dispersion of fragments, their distribution according to masses, the character of excitation functions) indicates that the low-energy division continues to give contribution, also, during nuclear fission by high-energy particles. May let us see below, this is confirmed also by the results of experiments on research on the energy properties of fragments.

The analysis of the results, given in Fig. 437, makes it

possible to establish/install still several other interesting laws governing [36] :1) a difference in the dispersion of the charges of fragments with tenfold being distinguished energies $T = 2.9$ and 28 GeV very insignificantly for uranium and for the more light nuclei of lead; 2) the dispersion of charge strongly depends on the type of the initial fissionable nucleus, during passage to smaller mass numbers sharply descends the fission yield with the large value of relation N_i/Z_i . The latter especially is noticeable for heavy fragments; 3) the double-peaked form of charge dispersion, characteristic for the fragments of uranium with mass numbers about $A_i \simeq 130$, is not observed for more light/lung fragments.

Several words about the charge distribution of the fissionable nucleus between its fragments.

The number of works, dedicated to this question, is small. Analyzing the nuclear fission of bismuth 190-MeV by deuterons, Goyekerman Pearlman [41] send to the conclusion/derivation about the equal "specific charges" of the fragments:

$$Z_1'/A_1' = Z_2'/A_2', \quad (10.2)$$

although it remains unclear, how this conclusion is correct for high-energy nucleon- nuclear interactions with $T > 100$ MeV. Specifically, Peyt considers that to the nuclear fission of uranium and thorium more corresponds the assumption about the equality of the

"lengths" of the chain/networks of the β -decays

$$Z'_{A1} - Z'_{p1} = Z'_{A2} - Z'_{p2}, \quad (10.3)$$

well recommended itself in the range of low-energy division [97].

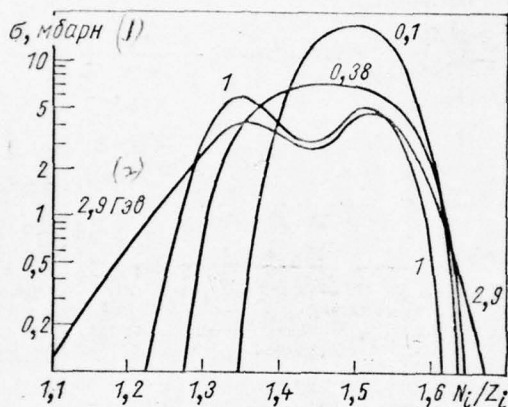


Fig. 436. Charge dispersion of the fission fragments with mass number $A_i = 131$, which were being formed as a result of nuclear fission ^{238}U by the rapid protons of different energy [36].

Key: (1) mb. (2) GeV.

AD-A048 311

FOREIGN TECHNOLOGY DIV WRIGHT-PATTERSON AFB OHIO
INTERACTIONS OF HIGH-ENERGY PARTICLES AND ATOMIC NUCLEI WITH NU--ETC(U)
JUL 77 V S BARASHENKOV, V D TONEYEV
FTD-ID(RS)T-1069-77

F/G 20/8

UNCLASSIFIED

NL

4 OF 6
AD
A048 311



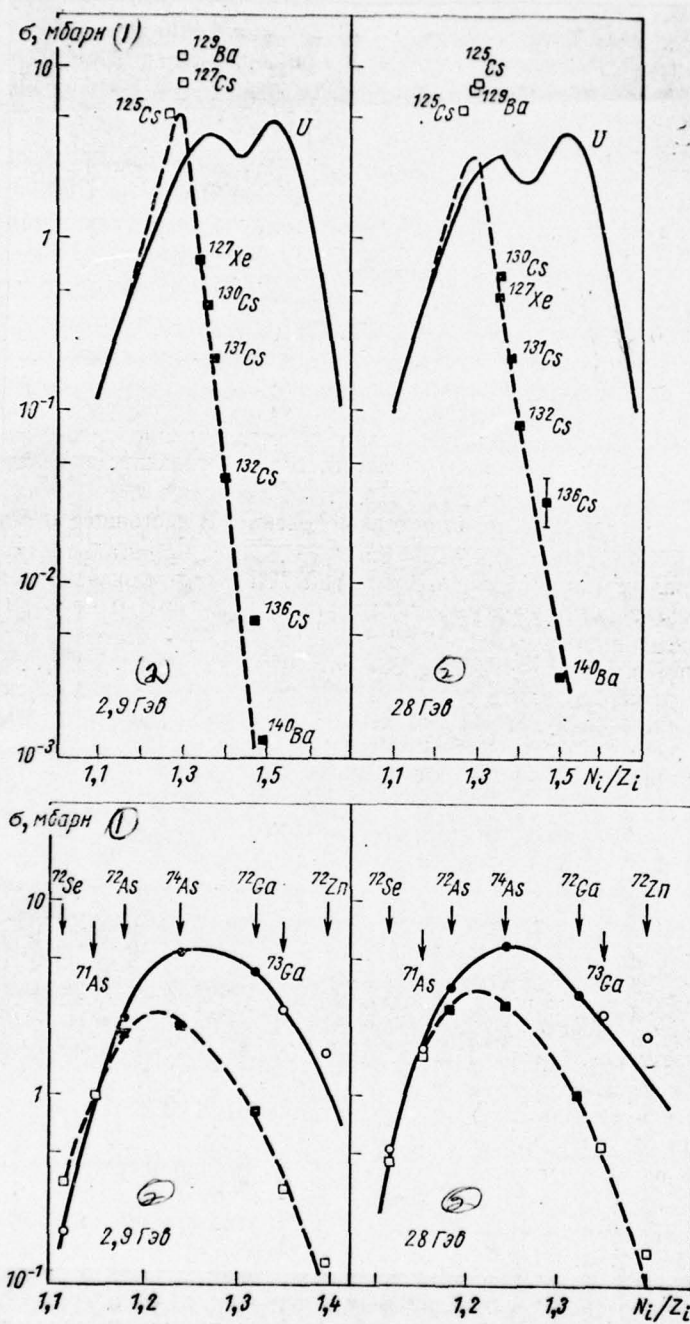


Fig 437.

Fig. 437. Charge dispersion of fission fragments U (unbroken curves) and Pb (dotted line) with different energy of the primary protons T [36].

Key: (1) mb. (2). GeV.

Page 574.

The detailed analysis of the nuclear fission of uranium 170-MeV by protons, carried out in work [85], allowed its author to assert that the experimental data are arranged/located in the range, intermediate between relationship/ratios (10.2) and (10.3). With energies of the primary protons $T > 1$ GeV the assumption of the equality of the lengths of the chain/networks of β -decay is not applicable, at the same time reveal/detected no contradictions with assumption about uniform charge distribution [36]. Unfortunately, a deficiency/lack in the information does not make it possible thus far to make here final conclusions.

§103. Energy characteristics.

The information about kinetic energy of fission fragments \mathcal{E}_i

and the value of excitation energy E_n^* at which occurred nuclear fission, it is possible to obtain by several methods. The widest use received photoemulsion, and recently - the radicchemical methods, using some properties of the recoil nuclei of fission fragments. With these, and also with some other using new methods it is possible to be introduced, for example, in survey/coverages [1, 83, 90]. It is appropriate also to emphasize that on experiment instead of the energy of fissionable nucleus E_n^* , as a rule, actually is recorded excitation energy E^* , which possessed the nucleus immediately after the completion of intranuclear cascade (but for the events, which were being accompanied by the division of remanent/residual nucleus). It is understandable that $\bar{E}_n^* < \bar{E}^*$.

Average total energy of fission fragments. The at present average value of the total energy of fragments $\bar{E} = \bar{E}_1 + \bar{E}_2$ is investigated in detail in the range low and intermediate energies T . In this case it proves to be that this value does not depend on energy and type of initial particle; however, clearly correlate with the value of the parameter $Z_n^2/Z_n^{1/2}$, where A_n and Z_n - the mass and charge numbers of fissionable nucleus [40, 46, 54, 83]. This fact indicates that the kinetic fission energy in essence is determined by energy of coulomb repulsion.

If energy of fragments really/actually is determined only by

coulomb interaction that at high energies it is possible to use empirical relationships, obtained in range small T [83, 111]:

$$\bar{\mathcal{E}} = 0,121 Z_n^2 / A_n^{1/3}; \quad (10.4a)$$

$$\bar{\mathcal{E}} = 12,5 + 0,1092 Z_n^2 / A_n^{1/3}. \quad (10.4b)$$

the experimental analysis of these relationship/ratios at high energies is very difficult, since the experiments are sufficiently complex and, furthermore, remain the unknowns not only of value A_n and Z_n , but also the mass and charge numbers of primary fragments A_i and Z_i . Nevertheless in such cases where such analysis is led to end/lead, the results do not contradict relationship/ratios (10.4). Specifically, Sugarman, etc. [110], studying uranium fission 450-MeV by protons, they showed that the computed value $\bar{\mathcal{E}} = 169$ MeV is in a good agreement with measured on experiment value 163 ± 8 MeV.

It should be noted that despite the fact that the experiment shows the independence of average value $\bar{\mathcal{E}}$ from energy of initial particle, it is possible all the same to expect that this value must somewhat decrease with an increase of T , since in this case decrease the average charge and the mass numbers of fissionable nuclei.

Energy of coulomb repulsion, and, therefore, and value of energy \mathcal{E} , is directly connected with distance between centers of primary fragments at the torque/moment of their separation. If these

fragments were spherically symmetrical, then this distance would be proportional to $\sum (A_i)^{1/3} + (A_j)^{1/3}$ and topmost energy $\bar{\epsilon}$ they would have fragments during the symmetrical division, when $A_1 \simeq A_2$. The experiments with low energies showed that in actuality this not so: fragments, as a rule, strongly deformed result of which is "failure" in distribution $\bar{\epsilon}(A_i)$ near the point of symmetrical division [40, 46, 54, 83].

Page 575.

In Fig. 438 shown analogous distribution for high energies. Is observed certain structure of dependence $\bar{\epsilon}(A_i)$ approximately in the same range that and for nuclear fission ^{235}U by thermal neutrons. Of course, to such parts one should be related with precaution, since the experimental errors $\Delta \bar{\epsilon}$ in Fig. 438 are comparable with the value of these parts; on the other hand, the fact of a weak change of value $\bar{\epsilon}(A_i)$ in range $83 < A^*, < 140$ can be considered completely reliable.

Energy of separate fission fragment. Until now, the discussion concerned the complete medium energy of fission fragments. As concerns kinetic energy of separate fragment \mathcal{T}_i , that the character of its changes it depends substantially on the type of fragment.

From the given Fig. 439 data shows that with energy of primary

proton several hundreds of million electron volt range/paths and, consequently, also kinetic energies of neutron-deficient and neutron excess nuclei are identical. This fact speaks in favor of the single mechanism of the formation/education of fragments in the range of energies T of the order several hundreds of million electron volt. During passage to energies $T > 1$ GeV the range/paths of the impoverished by neutrons nuclei decrease almost double, while the range/paths of neutron excess fragments remain previous, that can be considered as indication of the possibility of another, different from division, the mechanism of the formation/education of fragments with the understated number of neutrons. (Recall that precisely with these products is connected the left peak in curved charge dispersion in Fig. 436 and 437). Into this special feature/peculiarity of the process of nuclear fission at high energies indicated for the first time Aleksander with co-authors [2]. Then this was confirmed the works of other authors [11, 45]. However, all these results were related to fragments with mass number $115 < A_i < 140$. Only in recent work equal to [98] were investigated the fragments of scandium with masses $42 < A_i < 49$.

^ In this case it turned out that, although as in the case of heavier fragments, with passage from $T \sim 0.5$ GeV to energies $T \gg 1$ GeV the dependence of kinetic energy of fragment $\mathcal{E}(A_i)$ from equiprobable becomes "stepped" (Fig. 439), nevertheless the values of this energy for neutron excess nuclei at so/such being distinguished values of T no longer are placed by one straight line and decrease

from value $\mathcal{T} \simeq 80$ MeV at $T = 590$ MeV to $\mathcal{T} \simeq 50$ MeV at $T = 18$ GeV.

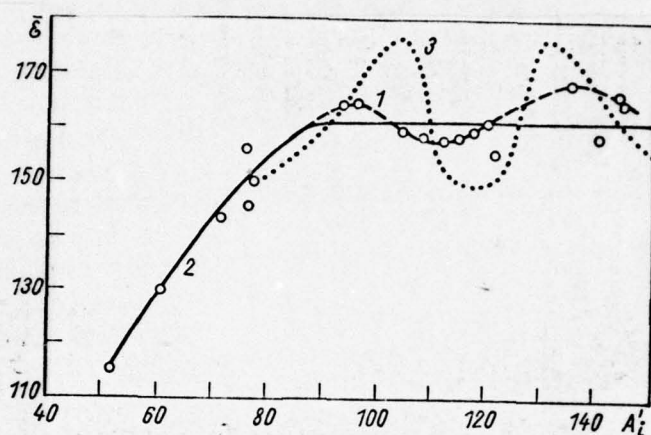


Fig. 438. The dependence of the average value of total energy of the fission fragments of nucleus ^{235}U from mass of one of the two primary fragments at the most probable value of its charge $Z = Z_p$ [110] (division occurs under the action of protons with energy $T = 450$ MeV): 1, 2 - two possible methods of the approximation of the experimental data; 3 - the corresponding results for the case of nuclear fission ^{235}U by thermal neutrons.

Excitation energy of fissionable nuclei. The average excitation energies of the nuclei, which experienced division, \bar{E}^* , are given in Table 140. 1.

FOOTNOTE 1. On a difference in the energies \bar{E}_d^* and \bar{E}^* see page 574.
ENDFOOTNOTE.

Value \bar{E}^* noticeably grow/rises during passage to more light nuclei. In this case increases also the number of low-energy charged particles, which accompany division.

According to the number of particles of the tracking it is possible to judge how changes value \bar{E}^* in range $T > 1$ GeV, where thus far still there are no direct measurements. Specifically, in the work of N. A. Perfilova et al. [89], carried out with $T = 9$ GeV, the average number of protons and α -particles with energies $\mathcal{E} < 40$ MeV, which accompany the nuclear fission of uranium, is obtained equal to 3.84 that considerably greater average values of 1.15 ± 0.06 , that corresponds to energy $T = 660$ MeV [15].

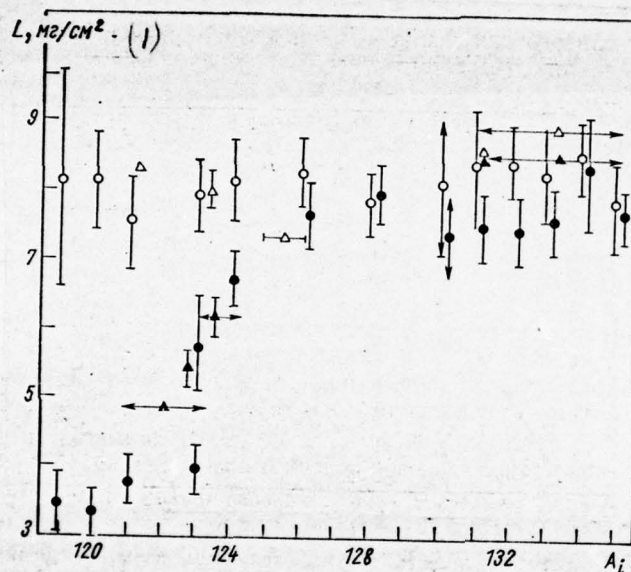


Fig. 439. The dependence of the mean path of the isotopes of iodine, which were being formed during the nuclear fission of uranium ^{238}U by protons with a different energy of T , on their mass number: o, ● - experimental data [11] respectively for $T = 550 \text{ MeV}$ and 18 GeV ; Δ, ▲

are these works [2] for $T = 720$ MeV and 6.2 GeV.

Key: (1) mg/cm².

Table 140. Average excitation energy and the average number of slow charged secondary particles ($\mathcal{T} < 50$ MeV) in the events with division, initiated by rapid protons with an energy of T .

(1) T , Мэв	(2) Уран		(3) Бисмут		(4) Вольфрам	
	\bar{E}^* , Мэв ^①	$\bar{n}_{\alpha p}$	\bar{E}^* , Мэв ^①	$\bar{n}_{\alpha p}$	\bar{E}^* , Мэв ^①	$\bar{n}_{\alpha p}$
140	80±20 [57]	0,76 [101]	190 [101]	1,15 [101]	335 [101]	2 [101]
350	140±40 [57]					
460	130 [101]					
460	(120—150) [110]	1,15±0,06 [15]	196±15 [15]	2,03± ±0,08 [15] 1,77 [101]	240±15 [15]	2,98± ±0,19 [15] 4 [101]
460	165±45 [57]					
660	175±17 [15]					
660	150 [101]	1,16 [101]	230 [101]		440 [101]	
660	185±60 [57]					

Key: (1). MeV. (2). Uranus. (3). Bismuth. (4). Tungsten.

At the same time, as already mentioned above in §57, the analysis of entire totality of known now data on inelastic nucleon- nuclear interactions makes it possible to assert that with $T \gtrsim 5$ GeV of value \bar{E}_n^* they must become approximately constants. Qualitatively this is confirmed also by the weakening of dependences $\sigma_n(A_i)$ and $\sigma_n(N_i/Z_i)$ with $T > 3$ GeV (see above).

Excitation energy of fragments. From the experiments, made by the procedure of recoil nuclei, it is possible to extract value longitudinal the components of the momentum/impulse/pulse of fission fragment [1]. By utilizing further results of cascade calculations, this component can be connected with the average or most probable excitation energy of this fragment [94, 95]. The results of this investigation are given in Fig. 440. As is evident, dependence $E_1^*(A_1)$ turns out to be different for the large and low values A_1 ; the constancy of values E_1^* in range $85 < A_1 < 140$ is the direct/straight reflection of that fact that kinetic energy remains constant/invariable in the range of the same values A_1 (Fig. 438).

It should also be noted that since from the fragments of uranium are emitted in essence the neutrons, Fig. 440 gives the representation simultaneously, also, of the dependence of the output/yield of the average number of neutrons on the mass number of nucleus-fragment [85, 86].

Difference in the mechanisms of the formation/education of neutron-deficient and neutron excess residual-nuclei. Very interesting data were obtained in connection with the study of the double-humped structure of charge dispersion [2, 21, 37, 43-45, 58, 98, 100]. It turned out that the fission energy of neutron-deficient nuclei substantially exceeds the value of the fission energy of neutron excess nuclei. So, during uranium fission by protons with energy $T = 346$ GeV to the output/yield of neutron excess fragments $^{130-135}_{121-124}$ corresponds energy of fissionable nucleus 60-90 MeV, whereas to fragments $^{121-124}_{121-124}$, to those having a neutron deficiency, corresponds energy $\bar{E}^* \approx (210-270)$ MeV [2].

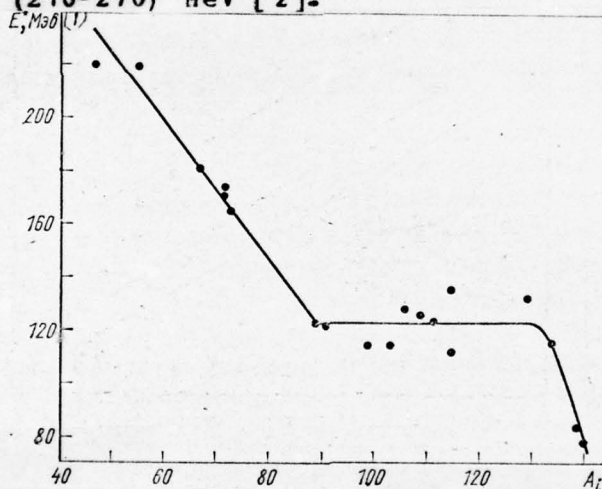


Fig. 440. Dependence of the excitation energy of the remanent/residual fissionable nucleus on the value of the mass number of fragment (at the most probable values of the charge of this fragment $Z = Z_p$) [110] (interaction of protons with the nuclei of uranium with energy $T = 450$ MeV).

Key: (1). MeV.

Page 578.

Very it is remarkable, that the dependence of the excitation energy of fissionable nucleus depending on surplus or neutron deficiency has identical character irrespectively of the value of energy of rapid initial particle and of the value of the mass number of fragment [45] (see Fig. 441, where the slope/inclination of all straight lines is virtually identical); in other words, fragments with a neutron deficiency in all cases are formed as a result of the division of the predominantly highly excited nuclei.

As already mentioned, neutron-deficient fragments in range $T > 1$ GeV simultaneously have also understated value of kinetic energy. ¹.

FOOTNOTE ¹. For example, in the given above example of the nuclear fission of uranium by protons with energy into several gigaelectron-volt value \mathcal{E} for fragments ¹³⁰⁻¹³⁵ are approximately 65 MeV, that under reasonable assumptions about fissionable nucleus comparable with the value of energy of coulomb repulsion; for neutron-deficient fragments energy \mathcal{E} is equal a total of 30-40 MeV. ENDFOOTNOTE.

The totality of all these facts indicates that the supplementary fragment is light nucleus with small mass number and suggests about existence in range $T \gtrsim 1$ GeV of the mechanism of the formation/education of neutron-deficient nuclei, different from division into two fragments [2]. This assumption will agree also with the interpretation of the double-humped structure of charge dispersion as result of two essentially different mechanisms of the formation/education of fragments.

At present still there is no unified opinion about that, by the means of which mechanism are formed neutron-deficient fragments during the interactions of protons with heavy nuclei in range $T > 1$ GeV. The high value of the excitation energy of such fragments indicates that the process of their formation/education must be very rapid and, apparently, nonequilibrium. This consideration at the same time by the fact that the second fragment, as a rule, very light/lung, allowed some authors (for example, see [2, 22]) to assume as one of the possible mechanisms the process of fragmentation. Another group of the authors considers that the neutron-deficient fragments are formed as a result of usual, but very deep nuclear disintegration [11, 44, 100]. In the opinion of these authors, in

favor of this mechanism speaks, in particular, the nearness of the form of neutron-deficient peak in the dispersive charge distribution $\sigma(Z_i)$ and of the charge dispersion of more light nuclei of the type of lanthanum, tantalum and gold. Which of these two mechanisms more corresponds to reality, i.e., this they must first of all solve further experiments.

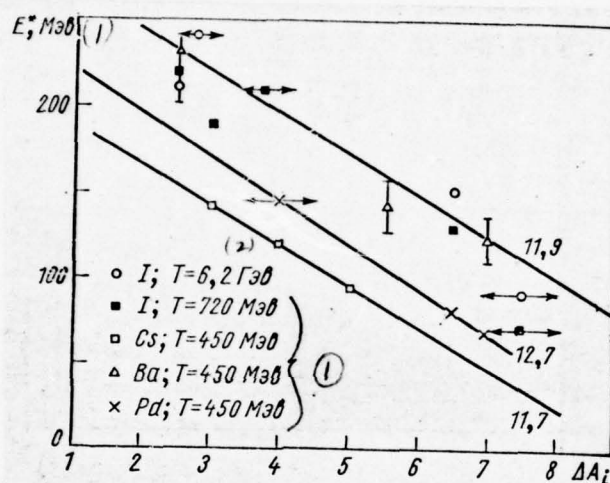


Fig. 441. The correlation of energy of the remanent/residual nucleus E^* and the mass number of fission fragment A_i at the fixed value of the charge of this fragment [98]: x are data for the fragments, which are formed during nuclear fission Pb. All remaining marks are related to nuclear fission U. Energy of the protons, which initiate the division and the type of nucleus-fragment, are shown in figure. For convenience in the comparison experimental points and their

approximating straight lines are shifted along the axis of abscissas so that they would be one above another; in this case along the axis of abscissa is plot/deposited value $\Delta A_i \approx A_i - A_2$, characterizing surplus or a deficiency/lack in the number of neutrons in fragment. Numbers near curves are a tangent of the angle of their slope/inclination.

Key: (1). MeV. (2). GeV.

End section.

Page 579.

§104. Calculation of the probability of nuclear fission.

With the discussion of the methods of the calculation of nuclear fission under the action of high-energy particles it is possible to isolate two independent problems.

First, this - the calculation of probability of fission cross section. Within the framework of cascade-evaporative model the division one should consider as one of possible, that compete with others, channels by means of which remanent/residual nucleus is free/released from excitation energy. For the calculation of this channel it is necessary to know the fission probability of nucleus in each stage of evaporative cascade/stage.

The second task is connected with the calculation of the properties of primary reaction products, if it is known that occurred the division of the determined nucleus (A_n, Z_n) with the assigned excitation energy E_n^* . It is possible to expect that as during the

calculation of evaporative cascade/stage, the solution of this problem does not depend on that, with the aid of which specific mechanism was formed the decomposing excited nucleus.

In the following paragraphs let us examine, to which degree the contemporary state of theory makes it possible to achieve both these purposes. First of all let us discuss methods of the calculation of fission probability W_n .

The dependence of complete fission probability W_n on the of excitation and nature of fissionable nucleus was discussed by many authors (for example, see [10, 38, 39, 117], where is given further bibliography); in this case always was assumed the possibility of the statistical description of phenomenon. Some authors examined the process of division by analogy with evaporation [39]. With the aid of the principle of detailed balance fission probability in this case can be expressed by the section of the reverse reaction of mucous membranes.

Unfortunately, the calculation of this section by itself represents not less complex task, but its experimental values are known only in the range of low energy.

More fruitful/successful turned out to be the approach of Bohr

and Wheeler [10], based on the assumption that processes in the still nondecomposed nucleus - to the left and near crest of the potential barrier (see Fig. 44²) - relatively slow, and the further process of the separation of fragments, to what corresponds range to the right of crest of the potential barrier, is rapid. Fission probability in this case is considered proportional to the ratio of the number of permissible states in vertex to the total number of states of the initial nucleus with excitation energy E_n^* :

$$W_n = \frac{1}{2\pi\hbar\rho(E_n^*)} \int_0^{E_n^* - Q_n} \rho^*(E_n^* - Q_n - \varepsilon) d\varepsilon, \quad (10.5)$$

where ρ^* - the density of the levels of deformed nucleus at vertex;
 Q_n is a barrier height of division (fission threshold). This expression already considers averaging on spins and parities of all states; by the effect of sub-barrier division it is disregarded.

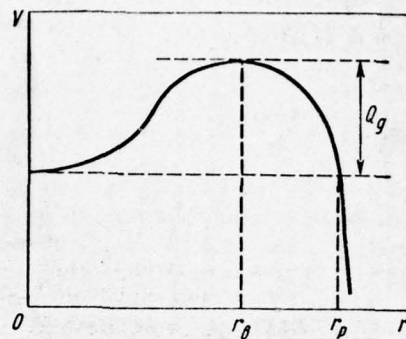


Fig. 442. Effective potential fission barrier: r_a is "apical" point; r_p the point, at which occurs the rupture of nucleus to two fragments and, correspondingly, sharply decreases potential of V ; Q_g is a fission threshold.

Page 580.

If we now to assume that the form of the dependence of the density of levels from excitation energy in deformed nucleus near vertex approximately the same as for the usual excited nucleus, i.e.,

$$\rho^*(E_d^* - Q_d - \varepsilon) \simeq \rho(E_d^* - Q_d - \varepsilon),$$

that, after using discussed in chapter 6 expression (6.56), fission probability (10.5) it is possible to rewrite in the form

$$W_d = \frac{\{(2 \sqrt{a_d(E_d^* - Q_d)} - 1) \exp(2 \sqrt{a_d(E_d^* - Q_d)}) + 1\}}{4\pi a_d \exp(2 \sqrt{a_0 E_d^*})} \simeq \frac{(2 \sqrt{a_d(E_d^* - Q_d)} - 1) \exp(2 \sqrt{a_d(E_d^* - Q_d)})}{4\pi a_d \exp(2 \sqrt{a_0 E_d^*})}, \quad (10.6)$$

where a_0 and a_d are the parameters of the density of the levels respectively initial and deformed nuclei at vertex. In §70 under accurately the same assumptions it was obtained expression (6.89) for the probability of the evaporation of one neutron. Therefore relative fission probability or, in other words, the relation of dividing and evaporative widths, can be written as

$$\frac{W_d}{W_n} = \frac{\Gamma_d}{\Gamma_n} = \frac{k_0 a_n}{a_d(E_d^* - Q_n)} [2 \sqrt{a_d(E_d^* - Q_d)} - 1] \times \exp\{2 \sqrt{a_d(E_d^* - Q_d)} - 2 \sqrt{a_n(E_d^* - Q_n)}\}, \quad (10.7)$$

where a_n is the parameter of the density of the levels of the

nucleus, which remained after neutron emission; $k_0 = h^2/8m_N R^2$; R — nuclear radius; Q_n — threshold for the evaporation of neutron. From this expression it is evident that the competition of the processes of division and evaporation, especially with not very high excitation energies E_n^* , is determined, mainly, by the relationship of the corresponding thresholds of the reactions Q_α and Q_n and of the parameters a_α and a_n .

The fission thresholds of nuclei Q_α are partially measured on experiment; however, for the majority of nuclei they are unknown. The theoretical calculation of these values is independent and quite complex task, connected with the examination of the most energetically favorable form of fissionable nucleus. As a rule, such investigations are based now on the model of drop of liquid [10, 14, 19, 35, 48, 80, 81, 109]. In recent years in this direction were reached considerable successes in connection with the explanation of the role, which play the effects of shell nuclear structure [77, 107, 108]. At the same time during calculations the fission probabilities of the highly excited nuclei fission thresholds are usually determined with the aid of the very rough approximations of the dependence $Q_\alpha(A_n, Z_n)$, obtained in this or another version of liquid-drop model. So, very frequently the threshold is examined as function of two independent parameters: by constant γ , that characterizes surface tension in fissionable nucleus ($\gamma \approx 15-20$ MeV,

see formula (6.41)) and values $(Z_d^2/A_d)_{\text{крит}}$ with the equal to relation coulomb to the doubled surface energy of nucleus $E_R/2E_{\text{пов}} \simeq 46-50$ MeV. In this case

$$Q_d = \gamma A_d^{2/3} f(x), \quad (10.8)$$

where $x = (Z_d^2/A_d)/(Z_d^2/A_d)_{\text{крит}}$, and the form of the function $f(x)$ is determined by the concrete/specific/actual version of liquid-drop model. For example, in the variation examined by Frankel and Metropolis [34],

$$f(x) = 0,728(1-x)^3 - 0,661(1-x)^4 + 3,330(1-x)^5, \quad (10.9)$$

a in Cohen's work and Svyatetskiy [19]

$$f(x) = \begin{cases} 0,83(1-x)^3, & \text{when } 2/3 < x < 1; \\ 0,38(3/4-x), & \text{when } 1/3 < x \leq 2/3. \end{cases} \quad (10.10)$$

True, in the latter case are obtained the strongly high values Q_d and in formula (10.8) it is necessary to introduce the correction, equal to a difference in the experimental value of nuclear mass $M_{\text{эксп}}(A_d, Z_d)$ mass $M_{\text{теор}}(A_d, Z_d)$, designed with the aid of liquid drop model:

$$Q_n = \gamma A_n^{2/3} f(x) - \{M_{\text{SRCB}}(A_n, Z_n) - M_{\text{TCOP}}(A_n, Z_n)\}. \quad (10.11)$$

Page 581.

However, even, after the introduction of correction agreement with experiment succeeds in obtaining only for heavy nuclei, with $Z_n > 90$, whereas in experiments at high energies T in essence occurs the division of the more light/lung remanent/residual nuclei, the probability of formation/education of which after intranuclear cascade is sufficiently great. The same occurs, also, during the use of formula (10.9). As concerns parameter value of the density of levels, during high excitations with sufficiently good degree of accuracy it is possible, apparently, to assume $a_n = a_n$.

In the field of the low and intermediate excitations of the fissionable nuclei of the information about the relative value of widths Γ_n/Γ_n it is possible to obtain from the measured on experiment excitation functions [40, 52, 53, 83, 118]. In this case it proves to be that for heavy nuclei with the charge number $Z \gtrsim 90$ it is possible with good accuracy to consider relation Γ_n/Γ_n not energy-dependent of excitation E_n^* (up to $E_n^* \simeq 40$ Mev) [40, 53, 83] and to approximate it by the expression

$$W_d/W_n = \Gamma_d/\Gamma_n = \exp [0,343 (\alpha_z - A_d)], \quad (10.12)$$

where the constant α_z depends only on charge number Z_d . For nuclei with smaller value Z_d the relation Γ_d/Γ_n becomes already the function of energy E_d^* . If we at the small values of T attempt with the aid of relationship/ratio (10.7) to reproduce the course of the fission cross section of these nuclei, then this turns out to be possible only under condition $a_d > a_n$. The analysis of entire totality of known now data shows that $a_d \simeq 1,2 a_n$.

Above, during the discussion of the experimental data, we saw that the contribution of the processes of nuclear fission with small excitation was essential even when initial particle possesses energy several gigaelectron-volt. This it indicates the necessity of the account of the special feature/peculiarities of the relationship/ratio of the dividing and evaporative widths Γ_d/Γ_n , characteristic for a low-energy range, and with very high energies T .

§105. Performance calculation of fission products.

Adiabatic and statistical approach/approximation. Let us now

move on to the examination of the characteristics strictly of the process of the division of the excited nuclei. Inasmuch as the consecutive theory of division still not there exists at present, for us it is necessary to use different model presentations.

Most widely known and commonly used at present the so-called adiabatic and statistical approaches, based on diametrically opposite assumptions about the relationship of characteristic time of the motion of intranuclear particle $\tau_{\text{част}}$ and of the period of collective motions in nucleus $\tau_{\text{кол}}$: the case $\tau_{\text{част}}/\tau_{\text{кол}} \ll 1$ corresponds to adiabatic approach, in the large (but too great) values of relation $\tau_{\text{част}}/\tau_{\text{кол}}$ correctly statistical approach/approximation ¹.

FOOTNOTE ¹. If relation $\tau_{\text{част}}/\tau_{\text{кол}}$ very greatly, then the internal motion of nucleons can be examined in the approach/approximation in sudden disturbance/perturbation. In more detail about this see in monograph [116]. ENDFOOTNOTE.

A special case of adiabatic approach is the known liquid drop model, with the aid of which was carried out the first thorough theoretical studies of the process of division [10, 35, 48, 116]. The further logical development of this model represents unified model

[8, 9, 96]. However, both these models are intended for the description of spontaneous fission and processes of the division of the excited nuclei with energies on the order of several mega-electronvolt higher than the fission threshold; for the calculation of the division of the highly excited nuclei, which are formed as a result of intranuclear cascade, these models are unsuitable. Furthermore, it is possible to generally doubt the legitimacy of adiabatic approach/approximation for a fissionable nucleus at stage from the torque/moment of the passage of the vertex point to the torque/moment of the separation of fragments [33].

Page 582.

When nonadiabatic processes become so powerful that the energy distribution between different degrees of freedom occurs fast enough as compared with the rate of nuclear distortion, becomes used equilibrium, statistical approach/approximation. It is possible to expect that these conditions are satisfied with very high excitation energies. The latter is confirmed, in particular, by the estimations of Fong [33], which showed that the time, necessary for the separation of fragments, exceeds not only characteristic nuclear time $2R/c$, but also relaxation time τ_{pen} (comp. chapter 6, page 399); therefore, if the state of nucleus at the stage of the separation of fragments is deflected from equilibrium, equilibrium by large

probability it can be restore/reduced again.

As the basis of the theory of Pong is placed the assumption about the fact that the properties of the equilibrium fissionable system are determined by the number of its possible quantum state at the torque/moment of the separation of fragments, and the number of such states is considered equal to the number of possible states of system after division [31, 32]. Then the fission probability of nucleus into two fragments with the mass and charge numbers, equal respectively (A'_1, Z'_1) and (A'_2, Z'_2) , and with excitation energy E^*_1 and E^*_2 can be written as

$$dW_{\alpha}(A'_1, Z'_1, E^*_1, p) = (V/2\pi^2\hbar^3) p^2 \rho_1(E^*_1) \rho_2(E^*_2) dE^*_1 dp, \quad (10.13)$$

where, as before, $\rho_i(E_i)$ - the density of the levels of the i fragment; p is momentum/impulse/pulse of relative motion of fragments in the center-of-gravity system; V - normalizing volume. (Expression (10.13) depends on the parameters only of one fragment, since the parameters of the second are defined as differences: $A_2 = A_{\alpha} - A_1$ and, etc).

Energy distribution of fragments. Let us consider now that total energy E , realized during nuclear fission, is composed of the excitation energy of fissionable nucleus E^*_n and of the energy ΔM , which frees because of a difference in the masses of fissionable nucleus and nucleus-fragments:

$$E = E_n^* + \Delta M = E_n^* + M(A_n, Z_n) - M(A_1', Z_1') - M(A_2', Z_2'). \quad (10.14)$$

This energy transfer/converts to potential energy $U = E_n + \mathcal{D}$, where E_n is Coulomb energy of fragments, a $\mathcal{D} = \mathcal{D}_1 + \mathcal{D}_2$ - energy of their strain, into the excitation energy of fragments $E^* = E_1^* + E_2^*$ and energy of their relative motion $\varepsilon = p^2/2\mu$ (μ - the reduced mass of fragments). Thus,

$$E = U + E^* + \varepsilon. \quad (10.15)$$

The composite probability of fission yield with the determined values A_1' and Z_1' is obtained by the integration of expression (10.13) for all allowed values of energy E_1^* and of momentum/impulse/pulse p (or energy ε):

$$W_n(A_1', Z_1', E - U) = \\ = 4 \sqrt{2} \pi V (\sqrt{\mu}/2\pi\hbar)^3 \int_0^{E-U} V \varepsilon d\varepsilon \int_0^{E-U-\varepsilon} \rho_1(E_1^*) \rho_2(E^* - E_1^*) dE_1^*. \quad (10.16)$$

The concrete/specific/actual form of the function $W_n(A_1', Z_1', E - U)$ depends on the selection of the energy dependency of the density of levels ρ_i . If for this we use expression (6.56), then internal integral easily is calculated by the steepest descent method:

$$\int_0^{E^*} \rho_1(E_1^*) \rho_2(E^* - E_1^*) dE_1^* = 2 \sqrt{\pi} C^2 \frac{V_{a_1 a_2} (E^*)^{3/4}}{(a_1 + a_2)^{5/4}} \exp(2 \sqrt{(a_1 + a_2) E^*}) \quad (10.17)$$

where a_i is the parameter of the density of the levels of the i residual-nucleus; $E^* = E - U - \varepsilon$. It is possible to show that the maximum of integrand in internal integral corresponds to the division of energy E^* precisely such values E_{1}^* and E_{2}^* , at which the fragments have equal temperature [32].

In order to calculate the remaining integral in expression (10.16), let us replace into slowly changing pre-exponential factor value ε most probable, by its "peak" value ε_p , which, as it is easy to be convinced, takes the form ¹

$$\varepsilon_p = \frac{1}{2} \sqrt{\frac{E - U}{a_1 + a_2}} \left(1 - \frac{1}{\sqrt{(a_1 + a_2)(E - U)}} + \dots \right). \quad (10.18)$$

FOOTNOTE 1. In statistical model the energy is distributed proportional to the number of possible states; therefore it is possible to expect that $\varepsilon_p \ll E^*$. As can be seen from relationship/ratios (10.15) and (10.18), this fact really/actually occurs. ENDFOOTNOTE.

Page 583.

Then with an accuracy to unessential constant the probability

$$W_n(A_1, Z_1, E-U) \sim \frac{\sqrt{a_1 a_2} \mu^{3/2}}{(a_1 + a_2)^2} (E-U)^{3/2} \times \\ \times \left[1 - \frac{9}{8} \frac{1}{\sqrt{(a_1 + a_2)(E-U)}} + \dots \right] \exp(2 \sqrt{(a_1 + a_2)(E-U)}). \quad (10.19)$$

Thus, most probable final states with large values of difference $E - U = E_n^* + \Delta M - U$, i.e. other conditions being equal, - state with a minimum potential energy of U .

For the calculation of difference ΔM the Fong was proposed the formula for nuclear masses, which includes shell correction [32]. This correction was found by the empiricism of the comparison of the calculation of the of masses with the masses of stable nuclei in the range of fission fragments and it is 15-25 MeV. shell corrections render/showed especially were great in cases when fission products were close to nuclei with closed shells. This allowed Fong to explain, why the asymmetric nuclear fission is preferred before the symmetrical.

It should be noted that in the calculations of Fong the density

of the levels in the range of magnetic nuclei turned out to be strongly overstated; therefore although for it it was possible to obtain a good agreement of the experimental and theoretical fission yield ^{235}U under the effect of thermal neutrons, subsequent calculations they showed that thus it is not possible to match with experiment the mass distribution of the fragments, which were being formed during division by the thermal neutrons of nuclei ^{239}Pu : in this case instead of that observed in the experiment two-peaked distribution is obtained four-peaked distribution [92]. The overestimate of density levels in near-magic range is connected with the roughness of the mass formula of Fong and used by it shell correction ².

FOOTNOTE ². Most used by Fong name "shell correction" seems very unsuccessful, inasmuch as the non-monotonies, caused really/actually shells, comprise a total of several million electron volts.

ENDFOOTNOTE.

Is more precise - the formula of the masses of nuclei (6.80), proposed by Cameron [16]. Even without taking into account of corrections for intranuclear shells and the effect of pairing this formula gives considerably better/best results, than the formula of

Pong. After preserving in formula (6.80) only those terms which are essential for the process of division, we will obtain (all constants are expressed in million electron volts):

$$M(A, Z) = 31,45(A - 2Z)^2/A + 25,84A^{2/3}(1 - 1,24/A^{2/3}) - 44,24(A - 2Z)^2A^{-4/3}(1 - 1,24/A^{2/3}) + 0,779(Z^2/A^{1/3})[1 - (1,58/A^{2/3}) - 1/Z]. \quad (10.20)$$

Designed with the aid of (10.20) value ΔM are shown in Fig. 443.

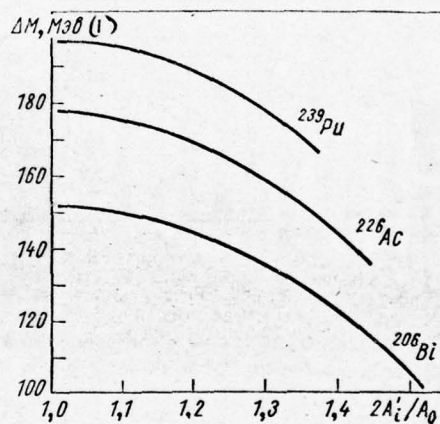


Fig. 443. Energy, which is isolated during division because of a difference in the masses of the initial nucleus and nucleus-fragments during the most probable distribution of their charges. Curves are designed by formula (10.20) for three different nuclei.

Key: (1). MeV.

Page 584.

Surface strain of fragments. Until now, we remained within the framework of purely statistical reasonings. However, the value of potential energy of the fissionable nucleus U depends on nuclear shape at the torque/moment of its separation into two fragments. It is understandable that for determining this form already insufficient only common/general/total statistical considerations and we must draw supplementary model presentations.

In the works of Fong it was assumed that at the torque/moment of separation the nuclear shape coincides with the form of two concerning deformed fragments. If we the form of each of such fragments describe by expression ¹

$$R_i(\theta) = R_{0i} [1 + \alpha_{2i} \mathcal{P}_2(\cos \theta) + \alpha_{3i} \mathcal{P}_3(\cos \theta)], \quad (10.21)$$

where R_{0i} are radii of the undeformed fragments, a \mathcal{P}_i are Legendre's usual polynomials, then, being based on liquid drop model, the strain energy of fragments and their mutual Coulomb energy E_K can be expressed by the parameters of strain α_{Ki} .

FOOTNOTE ¹. In the work of Fong [32] there is no term with α_{2i} , which substantially affects the form of fissionable nucleus (for example,

see [93, 114]). This question becomes especially important in the examination of low-energy division. ENDFOOTNOTE.

Respectively fission probability $W_{\pi}(A', Z', E - U)$ also will depend on these parameters.

It is possible to show that if we are restricted only to linear and quadratic terms, then the strain energy of fragment will take the form

$$\mathcal{E}_i = (0,4E_{i\text{пов}}^0 - 0,2E_{i\text{кул}}^0) \alpha_{2i}^2 + (0,714E_{i\text{пов}}^0 - 0,204E_{i\text{кул}}^0) \alpha_{3i}^2 + 0(\alpha_{3i}^3), \quad (10.22)$$

where $E_{i\text{пов}}^0 = 17,0 (A_i)^{2/3}$ MeV and $E_{i\text{кул}}^0 = 0,71 (Z_i)^2 / (A_i)^{1/3}$ MeV - with respect to surface and coulomb energy of the undeformed nuclei (numerical values of constants are taken for the case $R_{0i} = 1,3 (A_i)^{1/3} 10^{-13}$ cm. [92]).

Coulomb energy and form of fissionable nucleus. Coulomb energy of fragments let us write in the form [32]

$$E_{\kappa} = e^2 Z_1 Z_2 / \sum_{i=1,2} R_{0i} \left\{ 1 - \alpha_{2i} \left[1 - \frac{3}{5} \frac{R_{0i}}{S} \right] + \alpha_{3i} \left[1 - \frac{3}{7} \left(\frac{R_{0i}}{S} \right)^2 \right] \right\}, \quad (10.23)$$

where S - distance between centers of the distributions of the electric charges of the deformed fragments (change in the distance between centers of charge distribution, caused by the divergence of the form of fragments from the spherical, $\Delta R = S - [R_{01} + R_{02}]$) [32].

Relations (R_{0i}/S) weakly depend on the parameters α_{Ki} , and then it is possible to consider constants.

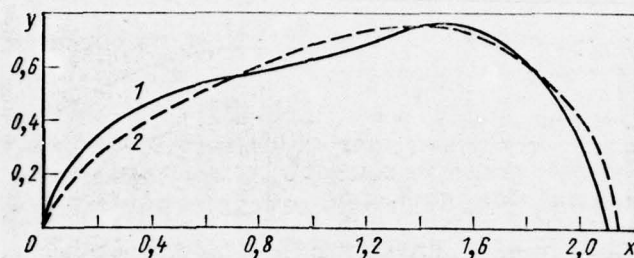


Fig. 444. Designed form of nucleus-fragments in plane (x, y) . Is examined the case, when the ratio of coulomb energy to surface $E_{\text{кул}}^0/E_{\text{пов}}^i = 1.2$: the results of the calculations according to formula (10.21), 2 are the calculation of Pik-Pickak and Strutinskiy taking into account 15 polynomials \mathcal{P}_i in expression (10.21) [93].

Page 585.

The numerical values of these relations are found by the method successive approximation in the vicinity of the most probable values a_{Ki} , which, in turn, are determined from the condition of the minimum of

potential energy $U(\alpha_{ki}) \equiv U(\alpha_{21}, \alpha_{22}, \alpha_{31}, \alpha_{32})$:

$$\frac{\partial U(\alpha_{ki})}{\partial \alpha_{mn}} = \frac{\partial}{\partial \alpha_{mn}} [E_K(\alpha_{ki}) + \mathcal{D}_1(\alpha_{ki}) + \mathcal{D}_2(\alpha_{ki})] = 0, \quad (n=1, 2; m=2, 3). \quad (10.24)$$

This reduces us to the system of four equations with four unknowns whose solution gives the parameters α_{ki} .

With the aid of the obtained thus values α_{ki} and expression (10.21) is determined the corresponding value of distance S . After substituting this value of S and value of the parameters α_{ki} into expression for coulomb energy (10.23), we will obtain a corrected system of equations (10.24) whose solution gives the more precise parameters α_{ki} , and, etc.

Figure 444 shows a typical example of the form of fission fragment, determined by method of successive approach/approximations.

It should be noted that calculated by the method indicated the form of fragments is close to that, which is obtained during more precise calculations taking into account in expansion (10.21) of Legendre's polynomials to 15th order inclusively (see dotted curve in Fig. 444).

Figure 445 and 446 in an example of most probable surface configuration shows, as depends on the mass of fragment energy of its

strain and energy coulomb the interaction of two fragments. We see that the energy of strain $\mathcal{E} = \mathcal{E}_1 + \mathcal{E}_2$ weakly it changes with the change of the mass of fragment, remaining equal approximately ~20 to MeV. Coulomb energy although does not detect "failure" in the range of asymmetric fission (but this, as already mentioned above, it is the solidly established/installed experimental fact for small excitation energies), it has the correct average values, which agree themselves with empirical relationship/ratios (10.4).

Mass distribution and charges of fission fragments. With the aid of equations (10.24) the parameters of strain α_{ni} it is possible to express through any one of them, α , which, according to relationship/ratio (10.23) is located in one-to-one conformity with coulomb energy $E_K = E_K(\alpha)$.

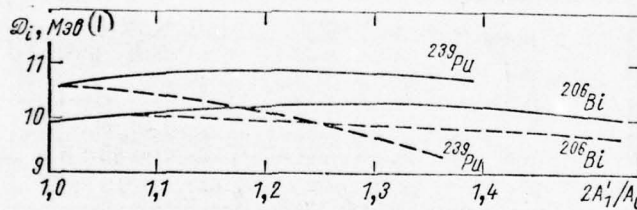


Fig. 445. Dependence of the strain energy of the fragments, which are formed during nuclear fission Bi and Pu from their mass. Curves are designed by formula (10.22).

Key: (1). MeV.

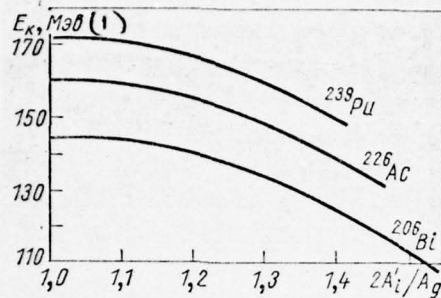


Fig. 446. Dependence of coulomb interaction energy of the fragments, which are formed during nuclear fission Bi, Ac and Pu on their mass. Curves are designed by formula (10.23).

Key: (1) - MeV.

Page 586.

If probability (10.19) is expanded now near the value $(E - U)_p$, which corresponds to the most probable surface configuration of fission fragments, in a series in the degrees of deviation from this

configuration $\delta\alpha$, then, after expressing $\delta\alpha$ by the appropriate change in the coulomb energy $\delta E_K = |E_K - E_{Kp}|$, we will obtain value distribution of Coulomb energy of the fragments:

$$N(A'_1, Z'_1) \sim \exp[-(\delta E_K/F_K)^2], \quad (10.25)$$

where

$$F_K = C_{12} \sqrt{Z'_1 Z'_2} \left(\frac{(E-U)_p}{a_1 + a_2} \right)^{1/4} \left(1 - \frac{3}{4} \frac{1}{\sqrt{(a_1 + a_2)(E-U)_p}} + \dots \right),$$

C_{12} - proportionality factor before term $Z'_1 Z'_2$ in formula (10.23), taken for a most probable configuration.

By integrating distribution (10.25) according to variable δE_K , let us present probability (10.19) in the form ¹

$$W_A(A'_1, Z'_1, (E-U)_p) \sim \sqrt{Z'_1 Z'_2} \mu^{3/2} \frac{\sqrt{a_1 a_2}}{(a_1 + a_2)^{9/4}} (E-U)_p^{7/4} \times \\ \times \left[1 - \frac{15}{8} \frac{1}{\sqrt{(a_1 + a_2)(E-U)_p}} \right] \exp(2 \sqrt{(a_1 + a_2)(E-U)_p}). \quad (10.26)$$

FOOTNOTE 1. The rapid decrease of integrand (10.25) with an increase δE_K makes it possible to expand integration limits to $(-\infty, \infty)$. Since all the calculations we conduct with accuracy to constant factor, as the

estimation of integral it is possible to take the product of the dispersion of integrand by the value of function in maximum.

ENDFOOTNOTE.

This expression actually is the function only of values A'_1 and Z'_1 .

If we now at the fixed value A'_1 expand probability (10.26) in a series in the degrees of deviation of charge Z'_1 from its most probable value $\delta Z'_1 = |Z'_1 - Z'_{1p}|$, then we will obtain the distribution of fission fragments according to magnitude of the charge, after integrating which, let us pass to the mass distribution of fragments.

Most probable charge Z'_{1p} finds from the condition of the maximum of the difference

$$(E-U)_p = E_A^* + M(A_A, Z_A) - M(A'_1, Z'_1) - M(A'_2, Z'_2) - C_{12}Z'_1Z'_2 - \mathcal{D}_p.$$

Strain energy $\mathcal{D}_p = \mathcal{D}_{1p} + \mathcal{D}_{2p}$ weakly depends on charge distribution and this term can be disregarded. Then it is not difficult to ascertain that

$$Z'_{1p} = \frac{(K_1 - K_2) + Z_A(L_2 - C_{12}/2)}{L_1 + L_2 - C_{12}}, \quad Z'_{2p} = Z_A - Z'_{1p},$$

where

$$K_i = \frac{0,779}{(A_i')^{1/3}} - \frac{88,48}{(A_i')^{1/3}} (1 - 1,24/(A_i')^{2/3}),$$

$$L_i = \frac{125,8}{A_i'} + \frac{0,779}{(A_i')^{1/3}} (1 - 1,58/(A_i')^{2/3}) - \frac{176,9}{(A_i')^{4/3}} (1 - 1,24/(A_i')^{2/3})$$

(comp. with expression (10.20)).

The distribution of fragments according to the charge

$$N(A_i', Z_i') \sim \exp[-(\delta Z_i'/F_Z)^2], \quad (10.27)$$

where

$$F_Z = \left(\frac{(E-U)_{pp}}{a_1 + a_2} \right)^{1/4} \left(1 - \frac{7}{8} \frac{1}{\sqrt{(a_1 + a_2)(E-U)_{pp}}} \right) (L_1 + L_2 - C_{12})^{-1},$$

a the second index of difference (E-U) means that this difference is taken with the most probable configuration of fragments and for the most probable value of their electric charge.

After integrating finally distribution (10.27) according to variable $\delta Z'_1$, we will obtain the complete fission probability of nucleus into fragments with mass numbers A'_1 and $A'_2 = A_n - A'_1$:

$$W_{\pi}(A_i, (E-U)_{pp}) = \mu^{3/2} \sqrt{\frac{Z'_{ip} Z'_{2p}}{L_1 + L_2 - C_{12}}} \sqrt{\frac{a_1 a_2}{(a_1 + a_2)^5}} \times \\ \times (E-U)_{pp}^2 \left[1 - \frac{11}{4} \frac{1}{\sqrt{(a_1 + a_2)(E-U)_{pp}}} \right] \exp(2 \sqrt{(a_1 + a_2)(E-U)_{pp}}). \quad (10.28)$$

Page 587.

Relationship/ratios (10.19), (10.25) - (10.28) determine all the fundamental characteristics of primary fission fragments. The further behavior of the excited fragments can be examined within the framework of the model of evaporation (or in explosive model in the case of light/lung fragments and large energy of excitation, see chapter 6). It remains to only add, that within the framework of statistical model the excitation energy E_i^* is distributed proportional to the number of degrees of freedom, i.e., it is proportional to value A_i . Into the complete excitation energy of the i fragment gives load also the strain energy \mathcal{D}_i ; kinetic energy of fissionable nucleus ε , which is distributed between fragments inversely proportional to their masses (i.e. $\sim 1/A_i$), together with coulomb repulsive energy E_R it determines kinetic energy of fission fragments \mathcal{T}_i .

During calculations it is possible with good accuracy to count that in the center-of-gravity system the fragments fly away isotropically.

Other approaches on the calculation of the process of division. Possibility to obtain numerical estimations for all basic values, which characterize division, in conjunction with simplicity of approach was the reason for the popularity of statistical model Pong. In following were undertaken the numerous attempts to improve this model. The majority of these attempts concerns low-energy division and is devoted, mainly, to the explanation of asymmetry in characteristic distributions of fission products.

Newton within the framework of the formal theory of the nuclear reactions of Wigner considered the effect of coulomb barrier on the probability of one method or the other of division [79]. The starting point of its theory is the formula of the width of the channel of division into two fragments

$$\gamma(A'_1, Z'_1, E^*_1, p) = \frac{pR_{\min}}{\mathcal{F}_K^2(R_{\min}) + \mathcal{G}_K^2(R_{\min})} \gamma_0(A'_1, Z'_1, E^*_{11}, p) \quad (10.29)$$

where R_{\min} smallest distance between centers of the inertia nuclear fragments on which these fragments already they can be considered as

separate nuclei; γ_0 - the given width of channel; E_{i1}^* - complete internal energy of fragment, equal to the sum of the excitation energy E^*_{i1} and of strain energy \mathcal{D}_{i1} ; \mathcal{F}_K and \mathcal{G}_K - the known regular and irregular function of coulomb potential [76]. A probability of the defined fission mode now will be written as

$$dW(A'_1, Z'_1, E_{i1}^*, p) = (V/2\pi^2\hbar^3) p^2 \gamma(A'_1, Z'_1, E_{i1}^*, p) \times \\ \times \rho(E_{i1}^*) \rho_2(E - U - E_K - E_{i1}^*) dE_{i1}^* dp, \quad (10.30)$$

that only in terms of factor γ it differs from basic formula (10.13). In this case, just as in the theory of Fong, the number of channels is identified with the number of possible states of nucleus right after its division, the only value E^*_{i1} is replaced by total energy E_{i1} .

after assuming further values R_{AHH} and γ_0 by constants and utilizing for a density somewhat more exact expression, than in the theory of Fong, Newton showed that its theory in state to explain some (but by no means everything) properties of low-energy division.

One must not fail to note that in comparison with the hypothesis of Fong about the statistical equilibrium of the fissionable system the assumption about the constant given width γ_0 is represented by considerably less demonstrative.

Further development Newton's theory received in the work of Cameron [17], where was additionally assumed the dependence of

distance R_{min} from the type of the channel of division. Value R_{min} in this case was selected in the form of $\text{sum } R_{\text{min}} = R_0 + \kappa (E - U - E_R)^{3/2}$, where the first term depends on the mass ratio of fission fragments, and the second considers the expansion of nucleus with an increase of energy of its excitation. The values of parameters R_0 and κ were selected from the condition that the mass distribution of fission fragments, kinetic energy and their other characteristics would agree with those observed in experiment.

In the work of Cameron pump was confirmed Newton's conclusion about the fact that the statistical approach/approximation by itself insufficiently for the complete description of the process of division, and at the same time was again emphasized that this approach/approximation, nevertheless, can serve as a good basis for the understanding of the basic laws governing the process of division.

Page 588.

To the variations in parameter R_0 , which empirically obtained the Cameron pump, was given the physical substantiation in the works of Brunner and Paul [13] with the aid of collective model of nucleus. It turned out to be possible to explain these variations and quantitatively, if one takes into account, that even after their

separation the fragments continue to interact with each other by the means of nuclear forces, by result of which is the change of the value of potential threshold in Newton's model: to the coulomb part of the interaction is added the term, which describes the action of nuclear forces. This term can be interpreted as effect, caused by the formation of the nucleon shells of future fragments.

To the semi-empirical account of the effect of the nuclear shells on of asymmetry of division with small excitation energies within the framework of the simplified statistical approach are dedicated also the works of Newson and Stavinskiy [78, 103]. The first of these authors utilized for the calculation of the density of the levels the proposed to them new method of the account of shell effects in the excited nucleus; as the basis of the calculations of Stavinskiy was placed experimental curve to the dependence of the parameter of the density of levels from mass number A .

One should also note the work of Erba, etc. [29], where within the framework of statistical approach by Ericson's method [30] examined fission of heavy nuclei neutrons, deuterons and by α -particles and for a series of characteristics χ was obtained fair agreement with experiment.

FOOTNOTE 1. Work [55] shows that within the framework of the statistical approach, developed Erikson and with Erb with co-authors [29, 30], it is possible to obtain a good agreement with experiment for mass distributions and according to the average kinetic energy of fragments; however in this case it is impossible to match the theoretical and experimental dependence of the dispersion of kinetic energy of fragment on its mass number. ENDFCOTNCTE.

In summary the statistical theory of division in its contemporary state makes it possible to consider the nonadiabaticity of process, gives the evaluations of its all fundamental characteristics, it can be utilized as basis for a semi-empirical approach to the quantitative description of division finally is at the present time, in essence, the only theory, which makes it possible to calculate the division of highly excited nuclei.

§106. Comparison of the results of the calculation with experiment.

A series of the common/general/total laws governing the process of nuclear fission by high-energy particles can be qualitatively understood already on the basis of those results of the cascade

evaporation calculations, which were given in the preceding/previous chapters. So, a decrease in the fission cross section σ_n with high energies it is possible to explain themes that due to knocking out of the large number of nucleons in the course of intranuclear cascade are formed ever more light/lung remanent/residual nuclei and, therefore, substantially grow/rises the fission threshold. With relatively low energy this T is compensated for by the appropriate increase in the excitation energy of remanent/residual nucleus, but with $T > 1$ GeV the effect of an increase in the fission threshold becomes ever more prevailing and, if we remain within the framework of the usual cascade model, described in chapter 4 and 5, then it should be expected that with $T \gg 1$ GeV the nuclear fission generally becomes extremely rare occurrence ($\sigma_n \rightarrow 0$). In actuality, the observed in experiment number of chase/dislodged from nucleus nucleons and excitation energy E^* with $T \gtrsim 5$ GeV become virtually constants; therefore it is possible to think that the dependence $\sigma_n(T)$ with $T \gg 1$ GeV will be smoother than with smaller energies. By this is explained a weak change in the mass distributions of fragments and their charge dispersion during $T \gtrsim 5$ GeV.

The observed in experiment increase in the output/yield of neutron-deficient fragments also becomes clear, if we recall that the value of fission threshold correlates from value of ratio Z^2/A ; therefore in high-energy range T are more subjected to division those

excited nuclei, which emit the larger number of neutrons.

Page 589.

To quantitative comparison with the experiment of the calculations of the nuclear fission, initiated high-energy particles, is dedicated already is sufficient many works (see, in particular, [4-6, 28, 49, 63, 69, 70, 72, 84, 87, 113, 114, 118]). Unfortunately, in these works were utilized the diverse variants of cascade-evaporative model; therefore their results sufficiently difficult to compare; furthermore, in many works the comparison with experiment is carried out only according to the very small number of characteristics, which were connected mainly from the process of competition of division and corpuscular emission.

In the work of Lindner and Turkevich [72] with experiment they compared the results of the calculations, based on four different assumptions about the properties of the relative probability of the processes of division and evaporation:

1) probability W_d/W_n depends little more than on the mass and charge numbers of fissionable nucleus and does not depend on energy of its excitation;

2) value W_d/W_n does not depend on excitation energy only during small excitations, let us say, with $E^* < 20$ MeV, but for high excitations $W_d/W_n = 0$; in other words, the competition of the processes of division and evaporation occurs only at the last/latter stage of the evaporation, when nucleus sufficiently "it will be cooled";

3) probability W_d/W_n does not depend on excitation energy, if $E^* < 40$ MeV, but with high energies $W_d \gg W_n$ (the so-called "high-energy division" - the case, opposite preceding/previous);

4) the relative probability W_d/W_n is determined by expression (10.7) with the parameter of the density of levels $a_d = a_n$.

The comparison with the results of the measurements of the output/yield of the products of the nuclear disintegration of uranium and thorium 340- MeV by protons showed that a more preferably third of the enumerated above assumptions, although a good quantitative agreement with experiment could not obtain also in this case.

The calculation of the interactions of protons with the nuclei of uranium with $T = 1$ and 2 GeV, carried out by Reytomby Poskantser with the same suppositions as in work [72], it gave the strongly decreased value of the output/yield of the isotopes of uranium and protactinium; true, the dependence of section on excitation energy

furthermore better is transferred by the third of enumerated above assumptions [87].

It should be noted that in both works [72, 87] was utilized the model of intranuclear cascade with the sharp boundary of nucleus and the very simplified examination of the processes of meson formation [75]; in range $T \gtrsim 1$ GeV the latter can lead to very considerable errors. Another reason, on the strength of which to the conclusions of the works [72, 87] one should be related with large precaution, consists in the fact that these conclusions are based on comparison with experiment only the small number of data (specifically, point/item 4 in the work of Lindner and Turkevich it was checked only for two isotopes, ^{232}U and ^{228}U).

The detailed investigation of the fourth of the assumptions indicated about the properties of relative probability W_p/W_n was carried out in our works [4, 5, 113, 114]. In these works with experiment were compared the results of the calculations for the wide energy range $T = 100\text{--}700$ MeV; in this case were examined not only the data on fission probability, but also a series of other characteristics of this process.

The calculated fission cross sections of the nuclei of uranium turned out to be very close to experimental: in the range of energies

$T = 150-400$ MeV section σ_n is approximately 1.4 barn; at a further increase in the energy value σ_n decreases and it reaches 1.2 barn with $T = 660$ MeV (these values are obtained with the parameter of the density of levels $a = A/20$ MeV⁻¹; an increase in this parameter twice leads to 10-15% to an increase in value σ_n).

Good the agreement of experimental and theoretical sections occurs also for the interactions of protons with the nuclei of lead,

FOOTNOTE 1. Cascade calculations in works [4, 5] are executed in approximation of the sharp edge of nucleus. During calculations were not considered also the processes of meson formation; in the range of energies $T < 700$ MeV this justified [by 112]. ENDFOOTNOTE.

Page 590.

Data on the distributions of fission products and the accompanying particles are given in Table 141 and in Fig. 447 and 448. As is evident, the calculated and experimental numbers very close to each other.

In works [4, 5, 113, 114] are designed also the yield cross sections of different isotopes, which are formed during irradiation of the nuclei of uranium ^{238}U by protons with energy $T = 340$ MeV. For the output/yield of the isotopes of neptunium in this case is obtained correct dependence on their mass number; however, the absolute values of sections render/showed approximately double more than observed in experiment.

Correct dependence on mass number detects the calculated output/yield of the isotopes of uranium, although the absolute values in this case almost by an order exceed experimental; exception/elimination are only isotopes with the mass numbers, close to artificial satellite to one mass number $A = 238$, the section of formation/education of which rapidly it decreases and it proves to be even lower experimental values. When evaluating these data it is necessary to keep in mind that the experimental sections, with which are compared the results of the calculations, are substantially understated. This is evident already from the fact that the total cross section of splitting/fission composes 0.28 barns, i.e., is much less than the difference $\sigma_{in} - \sigma_n \simeq (0.4 - 0.45)$ barn. Furthermore, the output/yield of the isotopes of uranium strongly manifests itself the contribution of quasi-free proton scattering, that it was not taken into account in cascade calculations [4, 112, 113].

Table 141. The charged particles, which are formed during the interaction of protons with the nuclei of uranium ^{238}U (\bar{n} is the average number of particles - protons and α -particles; $N(\theta)$ - the number of particles, which escape at an angle θ).

T, Mev	(1) Все заряженные частицы				(2) Заряженные частицы с $\tau < 30 \text{ Mev}$ (3)			
	\bar{n}		$N(0)/N(180^\circ)$		\bar{n}		$N(0)/N(180^\circ)$	
	Теория [113]	Опыт [57]	Теория [113]	Опыт [57]	Теория [113]	Опыт [57]	Теория [113]	Опыт [57]
140	$0,6 \pm 0,06$	$0,40 \pm 0,05$	$7,3 \pm 0,7$	$4,0 \pm 0,5$	$0,36 \pm 0,03$	$0,25 \pm 0,02$	$6,2 \pm 0,6$	$2,6 \pm 0,2$
350	$1,5 \pm 0,1$	$\sim 1,4$	$3,6 \pm 0,3$	$\sim 3,4$	$0,62 \pm 0,06$	$0,56 \pm 0,03$	$1,5 \pm 0,1$	$1,6 \pm 0,1$
460	$1,6 \pm 0,15$	$1,65 \pm 0,24$	$3,3 \pm 0,3$	$3,3 \pm 0,5$	$0,78 \pm 0,07$	$0,86 \pm 0,05$	$1,4 \pm 0,1$	$1,3 \pm 0,1$
660	$2,2 \pm 0,2$	$3,06 \pm 0,41$	$3,2 \pm 0,3$	$3,1 \pm 0,4$	$1,04 \pm 0,01$	$1,05 \pm 0,09$	$1,4 \pm 0,1$	$1,3 \pm 0,1$

Key: (1). All charged particles. (2). Charged particles s. (3). MeV.

(4). Theories. (5). Experiment.

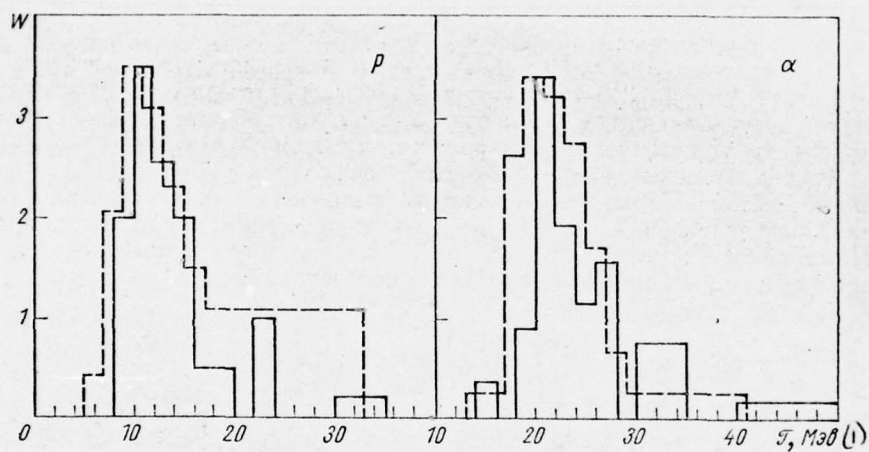


Fig. 447. Energy distribution of protons and α -particles, which accompany nuclear fission ^{238}U under the action of protons 660 MeV in energy. (Dotted line is the experimental data from work [57]).

Key: (1). MeV.

Page 591.

Although in comparison with the total cross section of inelastic interaction the portion of quasi-free scattering is small, its contribution to the output/yield of the isotopes of uranium can be considerable, since after quasi-free scattering nucleus remains with small excitation energy, and therefore within the framework of the assumption in question about the value of relation W_d/W_n the fission probability of this nucleus is small.

Figure 449 shows the yield cross sections of other fission products of nucleus ^{238}U - the isotopes of protactinium, thorium and actinium. These sections better will agree with experiment how this was in calculations [72]. A decrease in the yield cross sections of the isotopes of protactinium in the range of the mass numbers, close to initial $A = 238$, apparently, is also caused by the effect of the peripheral collisions.

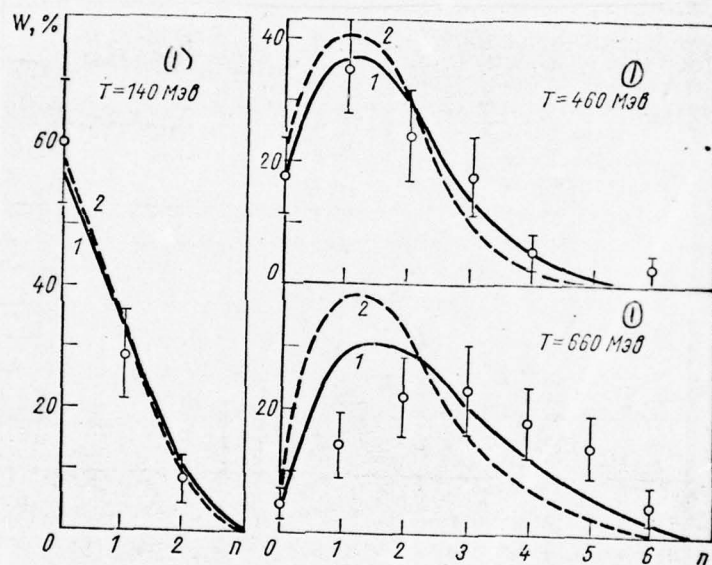


Fig. 448. Distribution of the cases of nuclear fission ^{238}U by protons with an energy of T according to the number of accompanying charged particles n : 1 - the calculation for case of $a = A/20 \text{ MeV}^{-1}$, 2 - the calculation for case of $a = A/10 \text{ MeV}^{-1}$; experimental points - from work [57].

Key: (1) MeV.

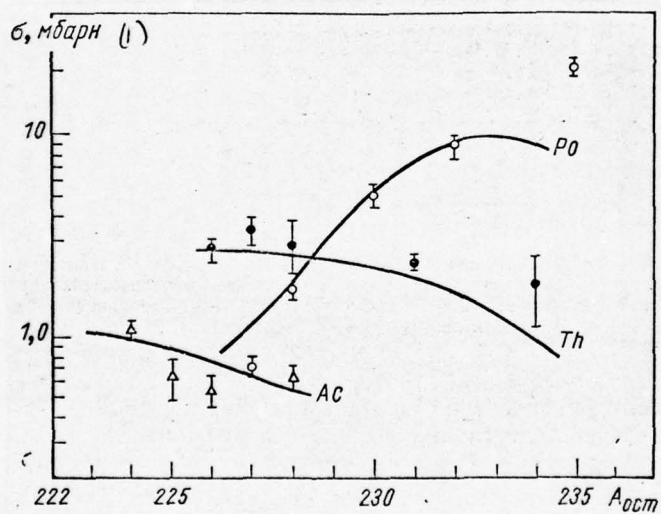


Fig. 449. Sections of the formation/education of various isotopes during nuclear fission ^{238}U by protons with energy $T = 340$ MeV

(experimental points from work [71]).

Key: (1). mb.

Page 592.

Figure 433 gives the results of the calculation of the energy dependency of the output/yield of the isotopes of cesium during nuclear fission ^{238}U . All the curves are calibrated to the value of output/yield ^{135}Cs at $T = 340$ MeV. As is evident, the calculation correctly transfers the common/general/total behavior of excitation functions and relationship/ratio between the yield cross sections of separate isotopes. At the same time the calculated absolute values approximately are twice as lower than experimental.

From the data of Table 142, where the corrected values of the average excitation energy of remanent/residual nuclei, the calculated with consideration of competitions of the processes of division and evaporation, one can see well that to division are subjected the nuclei, which have on the average high excitation energy. This is correct even when division precedes the emission of several evaporative neutrons.

The distribution of dividing events according to the value of energy E_d^* is shown in Fig. 450.

It should be noted that the value of the excitation energy of fissionable nuclei \bar{E}_d^* is sufficiently sensitive to parameter value of the density of levels. For example, if we select $a = A/20$, then the average fission energy of the more light nucleus of lead proves to be considerably larger than for a nucleus ^{238}U , at the same time with $a = A/10$ for both these nuclei are obtained the comparable values E_d^* .

Figure 451 shows that the theoretical fission yield will agree rather well with the results of the measurements: in this case the coincidence with the experiment of the position of the maximum of theoretical histogram indicates that the number of escaping during division nucleons theory also predicts correctly.

Table 142. Excitation energy of the remanent/residual nuclei, which are formed in reactions $p + {}^{238}\text{U}$ with the different energies T (\bar{E}^* - the average excitation energy of the nuclei, which remained after intranuclear cascade. \bar{E}_I^* and \bar{E}_{II}^* are the corresponding medium energies for events without division and for events with division).

(1) $T, \text{ Мэв}$	(2) $\bar{E}^*, \text{ Мэв}$	(3) $\bar{E}_I^*, \text{ Мэв (без деления)}$		(3) $\bar{E}_{II}^*, \text{ Мэв (с делением)}$			(4) $\bar{E}_D, \text{ Мэв}$	
		$a=A/10$	$a=A/20$	$a=A/10$	$a=A/20$	опыт [101]	$a=A/10$	$a=A/20$
140	58	38	27	60	63	80 ± 20	50	47
350	115	32	35	129	137	140 ± 40	58	48
460	122	33	28	137	165	165 ± 45	61	48
660	150	35	53	168	189	185 ± 60	71	58

Key: (1) MeV. (2) ^{MeV} without division. (3) ^{MeV} with division. (4) experiment.

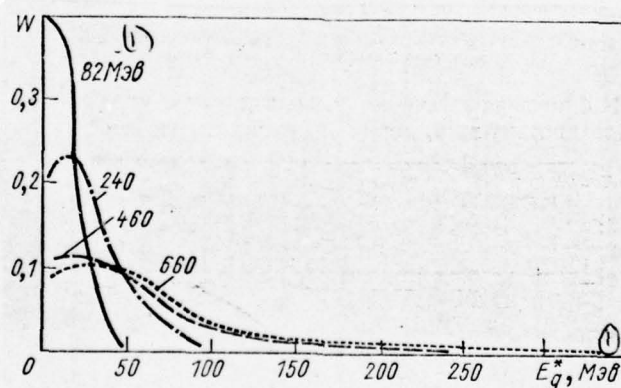


Fig. 450. The energy distribution of excitation of the fissionable

remanent/residual nuclei, formed as a result of the interactions of protons with nuclei ^{238}U with energy T (curves are designed for parameter $A = A/20 \text{ MeV}^{-1}$).

Key: (1). MeV.

Page 593.

A abrupt/steeper decrease in the calculated curve in the range of asymmetric fission in essence is connected with by the utilized during calculations simplifications: the evaporative cascade/stage whose results they served as the initial information, it was calculated for certain medium nucleus with the average excitation spectrum. Reducing of machine count time, this simplification it leads at the same time to certain "compression" of theoretical histogram in Fig. 451. Furthermore, it must be noted that the calculated histogram is calibrated to theoretical section $\sigma_n = 1,4$ barn, well agreeing itself with the average experimental data (see Fig. 428); however in work [106], whence are taken the experimental points, given in Fig. by 451, for a fission cross section obtained overstated value $\sigma_n = 1,59$ barn. The corresponding renormalization of theoretical histogram noticeably improves agreement with experimental curve.

If the comparison of the experimental and theoretical numbers of the emitted charged particles furnishes information on, in essence, about intranuclear cascade and the process of evaporation, which competes with division, then the comparison of data on neutron yield makes it possible to judge the correctness of the calculation of the very process of division.

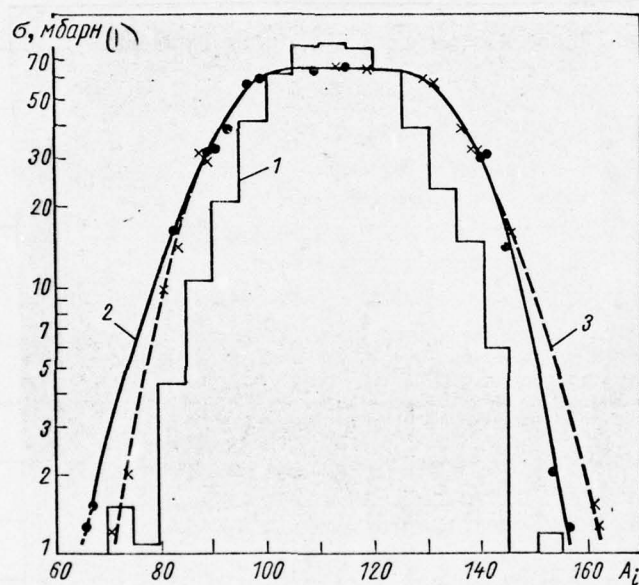


Fig. 451. Fission yield of nucleus ^{238}U by protons 340 MeV in energy; 1 - the calculation by the method of Monte Carlo [4; 5]; 2 - the

approximation of the experimental points from work [106]; 3 - experimental curve, obtained by mirror reflection relative to the "apparent" line of symmetry; \times - the experimental points reflected.

Key: (1). mb.

Table 143. Average number of being born neutrons taking into account one event/report of inelastic interaction.

(1) Взаимодействие	(2) T, Мэв	(3) Теория		(4) Опыт [20]
		$a=A/10$	$a=A/20$	
$p + {}^{207}\text{Pb}$	340	$10,3 \pm 1,0$	$9,0 \pm 0,9$	$12,0 \pm 1,0$
$n + {}^{238}\text{U}$	90	$9,5 \pm 1,0$	$8,0 \pm 1,6$	$11,0 \pm 1,5$
$n + {}^{238}\text{U}$	160	$11,6 \pm 1,2$	$10,5 \pm 1,1$	$14,0 \pm 2,0$
$n + {}^{238}\text{U}$	340	$14,7 \pm 1,5$	$12,5 \pm 1,3$	$17,2 \pm 0,8$

Key: (1). Interaction. (2). MeV. (3). Theories. (4). Experiment.

Page 594.

Such data for nuclei ${}^{238}\text{U}$ and ${}^{207}\text{Pb}$ are given in Fig. 452 and in

Table 143. Agreement of experiment and theory sufficiently good. Certain understating of computed values in Table 143 in comparison with experiment, apparently, is connected, mainly, with inaccuracies in processing the results of measurements in work [20]. (Measurements in this work are carried out for thick targets, and then conducted extrapolation to zero thickness; in this case possibly certain overestimate of results).

The estimation of the number of fission neutrons \bar{n}_n (neutrons, emitted from fission fragments) was obtained by Kharding with $T = 147$ MeV; for the nucleus of uranium obtained value $\bar{n}_n = 13,1 \pm 1,8$, for the nucleus of bismuth $-n_n = 10,0 \pm 2,5$ [47]. The appropriate computed values compose 12.3 ± 1.2 and 12.0 ± 1.2 , if $a = A/10 \text{ MeV}^{-1}$, and 10.9 ± 1.1 and 10.0 ± 1.0 , if $a = A/20 \text{ MeV}^{-1}$ [114].

Thus, comparison with the experiment of the results of the calculation of the different characteristics of fissionable nuclei and fission products shows that when we are speaking about separate values, theory and experiment can be matched under several assumptions about relative probability W_n/W_n . If we for the description of this probability utilize expression (10.7), then it is possible to obtain agreement with experiment simultaneously for a whole series of values;; however, even this does not make it possible to still make a final conclusion about the dependence of relative

probability W_n/W_n on the properties of fissionable nuclei, especially in range $T \lesssim 150\text{--}200$ MeV. Here are required further investigations.

There is large interest also in the propagation of the theory of division into the range of energies $T > 1$ GeV, where it is necessary to already consider the processes of multiple meson formation.

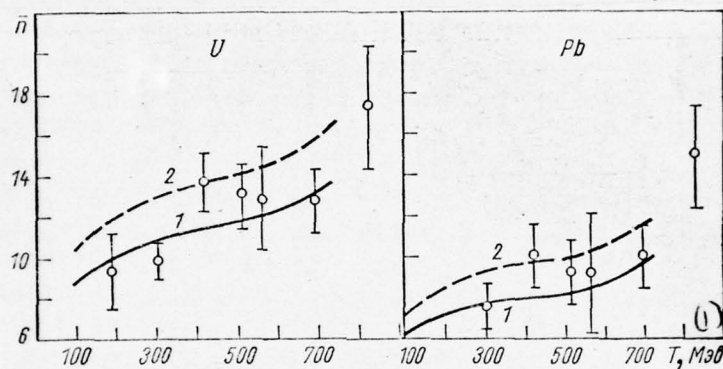


Fig. 452. Average number of neutrons with energy $\mathcal{E} < (25\text{--}30)$ MeV, which escape from the irradiated in proton beam of the different energies T of nuclei Pb and U, taking into account one event/report of the inelastic interaction: 1. , 2. the results of the calculation respectively with $a = A/20$ and $a = A/10$ MeV⁻¹; experimental points are taken from work [7].

Key: (1). MeV.

Pages 595-596.

BIBLIOGRAPHY

1. Alexander J. M. Nuclear Chemistry. Ed. by L. Yaffe. Vol. 1. New York — London, Academic Press, 1968, p. 273.
2. Alexander J. M., Baltzinger C., Gazdik M. Phys. Rev., 129, 1826 (1963).
3. Baker E. W., Katcoff S. Phys. Rev., 126, 729 (1962).
4. Барашенков В. С., Мальцев В. М., Тонеев В. Д. «Изв. АН СССР. Сер. физ.», 30, 322 (1966).
5. Барашенков В. С., Мальцев В. М., Тонеев В. Д. «Изв. АН СССР. Сер. физ.», 30, 337 (1966).
6. Беляев Б. Н., Мурин А. Н. «Атомная энергия», 13, 317 (1962).
7. Berkovitch M. et al. Phys. Rev., 119, 412 (1960).
8. Bohr A. Mat.-fys. medd. Kgl. danske vid. selskab., 26, No. 14 (1952).
9. Bohr A., Mottelson B. R. Mat.-fys. medd. Kgl. Danske vid. selskab., 27, No. 16 (1953).
10. Bohr N., Wheeler J. W. Phys. Rev., 56, 426 (1939).
11. Brandt R. In: Physics and Chemistry of Fission. Vol. II. Vienna, Internat. Atom. Energy Agency Publ., 1965, p. 329.
12. Brandt R. et al. Nucl. Phys., 90A, 177 (1967).
13. Бруннер В., Пауль Г. В сб. «Физика деления ядер». Перев. с англ. и нем. Под ред. В. С. Ставинского. М., Госатомиздат, 1963, стр. 268, 282, 290, 301.
14. Businago V. L., Gallone S. Nuovo cimento, 1, 629; 1277 (1955).
15. Быченко В. С., Перфилов Н. А. «Ядерная физика», 5, 264 (1967).
16. Cameron A. G. W. Canad. J. Phys., 35, 1021 (1957).
17. Камерон А. Дж. В сб. «Физика деления ядер». Перев. с англ. и нем. Под ред. В. С. Ставинского. М., Госатомиздат, 1963, стр. 183.
18. Chu Y. Y., Hahn R. L. Phys. Rev., 164, 1528 (1967).
19. Cohen S., Swiatecki W. J. Ann. Phys., 22, 406 (1963).
20. Crendall W. E., Millburn G. P. J. Appl. Phys., 29, 698 (1958).
21. Crespo V. P., Cumming J. B., Poskanzer A. M. Phys. Rev., 174, 1455 (1968).
22. Cumming J. B. et al. Phys. Rev., 134, B167 (1964).
23. Davies J. H., Yaffe Y. Canad. J. Phys., 41, 762 (1963).
24. De Carvalho H. G. et al. Nuovo cimento, 27, 468 (1963).
25. De Carvalho H. G. et al. Nuovo Cimento, 25, 880 (1962).
26. Deka G. C., Deka K. C. Canad. J. Phys., 46, 2301 (1968).
27. Deleauvais M. et al. Nucl. Phys., 90A, 186 (1967).
28. Dostrovsky I., Fraenkel Z., Rabinovitz. Second Confer. on Peaceful Uses of Atomic Energy. Vol. 15, Geneva, 1958, p. 301.
29. Erba E., Facchini V., Menichella S. Nucl. Phys., 84, 595 (1966).
30. Ericson T. Advances Phys., 9, 425 (1960).
31. Fong P. Phys. Rev., 89, 332 (1953).
32. Fong P. Phys. Rev., 102, 434 (1956).
33. Fong P. Phys. Rev., 135B, 1338 (1964).
34. Frankel S., Metropolis N. Phys. Rev., 72, 914 (1947).
35. Френкель Я. А. «Ж. эксперим. и теор. физ.», 9, 641 (1936).
36. Friedlander G. In: Physics and Chemistry of Fission. Vol. 2, Intern. Atom. Energy Agency Publ., 1965, p. 265.
37. Friedlander G. et al. Phys. Rev., 129, 1809 (1963).
38. Fujimoto Y., Yamaguchi Y. Progr. Theoret. Phys., 5, 76 (1960).
39. Geilikman B. T. In: Proceedings of the International Conference on the Peaceful Uses of Atomic Energy, vol. 2, N.Y., United Nations, 1956, p. 201.
40. Gindler J. E., Huizenga J. R. In: Nuclear Chemistry. Ed. by L. Yaffe. Academic Press, New York — London, 1968, p. 1.
41. Goeckermann R. H., Perlman I. Phys. Rev., 76, 628 (1949).
42. Green A. E. S. Phys. Rev., 95, 1006 (1954).
43. Hagebo E. J. Inorg. and Nucl. Chem., 29, 2515 (1967).
44. Hagebo E., Ravn H. J. Inorg. and Nucl. Chem., 31, 897 (1967).
45. Hagebo E., Ravn H. J. Inorg. and Nucl. Chem., 31, 2649 (1969).
46. Халперн И. Деление ядер. Перев. с англ. Под ред. А. И. Лейпунского. М., Физматгиз, 1962.
47. Harding G. M. Proc. Phys. Soc., A69, 330 (1956).
48. Hill D. L., Wheeler J. A. Phys. Rev., 89, 1102 (1953).

49. Hogan J. J., Sugarman N. Phys. Rev., 182, 1210 (1969).
50. Hudis J. In: Nuclear Chemistry, vol. 1, Ed. by L. Yaffe. New York — London, Academic Press, p. 169.
51. Hudis J., Katcoff S. Phys. Rev., 180, 1122 (1969).
52. Huizenga J. R. Phys. Rev., 109, 484 (1958).
53. Юизенга Дж. Р., Ванденбош Р. В сб. «Ядерные реакции», т. II. Пер. с англ. Под ред. В. С. Попова. М., Атомиздат, 1964, стр. 51.
54. Hyde E. The Nuclear Properties of Heavy Elements. Vol. III. Prentice-Hall, Englewood Cliffs, New Jersey, 1964.
55. Игнатюк А. В., Ставинский В. С., Шубин Ю. Н. Препринт ФЭИ-76, 1967. К статистическому подходу в теории деления.
56. Иванова Н. С. «Ж. эксперим. и теор. физ.», 31, 413 (1956).
57. Иванова Н. С., Пьянов И. И. Там же, стр. 416.
58. Kaufman S. Phys. Rev., 129, 1866 (1963).
59. Kjelberg A., Pappas A. Nucl. Phys., 1, 322 (1956).
60. Kofstad K. Thesis. Univ. of Calif. Report UCRL-2265 (1953). Расщепление и деление ядер серебра.
61. Коньшин В. А., Матусевич Е. С., Регушевский В. И. «Ядерная физика», 2, 682 (1965).
62. Коньшин В. А., Матусевич Е. С., Регушевский В. И. «Ядерная физика», 4, 97 (1966).
63. Kowalski L. Ann. Phys. 9, 211 (1964).
64. Kowalski L., Stephan C. J. Phys. Radiation, 24, 901 (1963).
65. Краут А. В сб. «Физика деления ядер». Перев. с англ. и нем. Под ред. В. С. Ставинского. М., Госатомиздат, 1963, стр. 7.
66. Kruger P., Sugarman N. Phys. Rev., 99, 1459 (1955).
67. Лаврухина А. К., Красавина Л. Д. «Атомная энергия», 2, 27 (1957).
68. Лаврухина А. К. и др. «Ж. эксперим. и теор. физ.», 40, 409 (1961).
69. Le Beyec Y. et al. Nucl. Phys., 88, 215 (1966).
70. Lefort M., Simonoff G., Torrago X. J. Phys. Radiation, 21, 238 (1960).
71. Lindner M., Osborn R. N. Phys. Rev., 103, 378 (1956).
72. Lindner M., Turkevich A., Phys. Rev., 119, 1632 (1960).
73. Матусевич Е. С., Регушевский В. И. «Ядерная физика», 7, 1187 (1968).
74. Maurette M., Stephan C. In: Proceedings the Conference on Physics and Chemistry of Fission, vol. II, Intern. Atomic Energy Agency Publ., 1969, p. 307.
75. Metropolis N. et al. Phys. Rev., 110, 185; 204 (1958).
76. Мотт Н., Мессии Г. Теория атомных столкновений. М., «Мир», 1969.
77. Myers W. D., Swiatecki W. J. Arkiv fys., 36, 343 (1967).
78. Newson H. W. Phys. Rev., 122, 1224 (1961).
79. Ньютон Т. Д. В сб. «Физика деления ядер». Перев. с англ. и нем. Под ред. В. С. Ставинского. М., Госатомиздат, 1963, стр. 169.
80. Nix J. R. Nucl. Phys., 130A, 241 (1969).
81. Nix J. R., Swiatecki W. J. Nucl. Phys., 71, 1 (1965).
82. Nossoff V. G. In: Proceedings of the International Conference on Peaceful Uses of Atomic Energy, vol. 2. N. Y., United Nations, 1956, p. 205.
83. Обухов А. И., Перфилов Н. А. «УФН», 92, 621 (1967).
84. Rapontin J. A., Porile N. T. J. Inorg. and Nucl. Chem., 30, 2891 (1968).
85. Pappas A. C. J. Inorg. and Nucl. Chem., 28, 1769 (1966).
86. Pappas A. C. Z. Naturforsch. a., 21, 995 (1966).
87. Pate B. D., Poskanzer A. M. Phys. Rev., 123, 647 (1961).
88. Перфилов Н. А. «Ж. эксперим. и теор. физ.», 41, 871 (1961).
89. Перфилов Н. А. и др. «Ж. эксперим. и теор. физ.», 38, 716 (1960).
90. Перфилов Н. А., Ложкин О. В., Остроумов В. И. Ядерные реакции под действием частиц высоких энергий. М.—Л., Изд-во АН СССР, 1962.
91. Перфилов Н. А., Ложкин О. В., Шамоу В. П. «УФН», 70, 3 (1960).
92. Pegging J. K., Story J. S. Phys. Rev., 98, 1525 (1955).
93. Пик-Пичак Г. А., Струтинский В. М. В сб. «Физика деления атомных ядер». Под ред. Н. А. Перфилова и В. П. Эйсмонта. М., Госатомиздат, 1962, стр. 12.
94. Porile N. T., Sugarman N. Phys. Rev., 107, 1410 (1957).
95. Porile N. T., Sugarman N. Ibid., p. 1422.
96. Rainwater J. Phys. Rev., 79, 432 (1950).
97. Rate B. D. et al. Canad. J. Chem., 36, 1691; 1707 (1958).
98. Ravn H. J. Inorg. and Nucl. Chem., 31, 1883 (1969).
99. Rind K. W. Thesis. N.Y., Columbia University, 1961. (Цитир. по работе [3].)
100. Rudstam R., Sorenson G. J. Inorg. and Nucl. Chem., 28, 771 (1966).
101. Шамоу В. П. «Докл. АН СССР», 103, 593 (1955).
102. Шамоу В. П. «Ж. эксперим. и теор. физ.», 35, 316 (1958).
103. Stavinsky V. S. Nucl. Phys., 51, 634 (1964).
104. Stephan C. J., Perlaman M. L. J. Inorg. and Nucl. Chem., 30, 2561 (1968).
105. Steiner H., Jungerman J. Phys. Rev., 101, 807 (1956).

106. Stevenson P. S. et al. Phys. Rev., 111, 886 (1958).
107. Струтинский В. М. «Ядерная физика», 3, 614 (1966).
108. Strutinskii V. M. Nucl. Phys., 93A, 420 (1967).
109. Струтинский В. М. «Ж. эксперим. и теор. физ.», 45, 1891; 1900 (1963).
110. Sugarman N. et al. Phys. Rev., 143, 952 (1966).
111. Террелл Дж. В сб. «Физика деления ядер». Перев. с англ. и нем. Под ред. В. С. Ставинского. М., Госатомиздат, 1963, стр. 365.
112. Тонеев В. Д. Сообщение ОИЯИ Б1-2245, Дубна, 1965. Взаимодействие быстрых нуклонов с ядрами. I. Внутриядерный каскад.
113. Тонеев В. Д. Сообщение ОИЯИ Б1-2740, Дубна, 1966. Взаимодействие быстрых нуклонов с ядрами. II. Испарительный каскад.
114. Тонеев В. Д. Сообщение ОИЯИ Б1-2812, Дубна, 1966. Взаимодействие быстрых нуклонов с ядрами. III. Расчет деления ядер.
115. Уилер Дж. А. В сб. «Успехи физики деления ядер». Перев. с англ. и нем. Под ред. Г. Н. Смиреникина. М., Атомиздат, 1965, стр. 7.
116. Wilets L. Phys. Rev., 116, 372 (1959).
117. Ванденбош Р., Хейзенга Дж. Конкуренция деления и испускания нейтронов в зависимости от энергии возбуждения и типа ядер. В кн.: «Труды Второй международной конференции по мирному использованию атомной энергии. Женева, 1958». Избранные доклады иностранных ученых. Т. 2. М., Атомиздат, 1959, стр. 366.

Chapter 11.

INELASTIC COLLISIONS OF NUCLEI.

§107. General characteristic of the experimental data.

Page 597.

The information about the properties of inelastic collision of two nuclei, by which we avail at the present time, is interrupted/fragmentary and very incomplete. The overwhelming majority of these information is related to the range of energies T , which do not exceed several dozen million electron volts by nucleon (see [27, 48, 57], where it is possible to find further bibliography).

With higher energies - if we do not consider interactions with deuterons - all known now experimental data obtained in cosmic radiation. Primary nuclear component in this case is the set of

different nuclei, from the very light/lungs of the type of helium and lithium to nuclei with charges $Z > 30$ (Table 144). Since even by the better/best works the statistics of the recorded interactions does not exceed 200-300, the experimental data, as a rule, are related not to separate primary nuclei, but to some of their groups, which are distinguished by magnitude of the charge Z (Table 145). This, of course, complicates theoretical analysis.

Table 144. Content of separate cell/elements in the flow of cosmic rays with energy $T \gg 1$ GeV/nucleon, c/c.

(1) Авторы	Li	Be	B	C	N	O	F	$Z \geq 10$
(2) Уэддингтон [58]	3,9	1,7	11,6	26,0	12,4	17,9	2,6	23,9
(3) О'Делл и др. [43]	5,3	2,3	7,4	30,0	9,7	19,4	2,4	23,4

Note. Ratio of the number of α -particles to the number of nuclei Li, Be, B $N_\alpha/N_{\text{Li, Be, B}} \approx 47$. Ratio of the number of protons to the number of nuclei Li, Be, B $N_p/N_{\text{Li, Be, B}} \approx 650$.

Key: (1). The authors. (2). Ueddington. (3). O'Dell, etc.

Table 145. Distribution of space nuclei with energy $T \gg 1.5$ GeV/nucleon according to groups depending on the value of their electric charge Z (average according to the data of many authors [35]).

TABLE 145.

$\begin{smallmatrix} L \\ Z = 3 \div 5 \end{smallmatrix}$	$\begin{smallmatrix} M \\ Z = 6 \div 9 \end{smallmatrix}$	$\begin{smallmatrix} H \\ Z \geq 10 \end{smallmatrix}$	$\begin{smallmatrix} MH \\ Z = 10 \div 19 \end{smallmatrix}$	$\begin{smallmatrix} VH \\ Z \geq 20 \end{smallmatrix}$	$\begin{smallmatrix} VVH \\ Z \geq 30 \end{smallmatrix}$
$\begin{smallmatrix} 2.6 \pm 0.8 \\ 0.73 \pm 0.11 \end{smallmatrix}$	$\begin{smallmatrix} 8.75 \pm 2.2 \\ 2.5 \pm 0.25 \end{smallmatrix}$	$\begin{smallmatrix} 3.5 \pm 0.5 \\ .1 \end{smallmatrix}$	$\begin{smallmatrix} 2.5 \pm 0.5 \\ - \end{smallmatrix}$	$\begin{smallmatrix} 1 \\ - \end{smallmatrix}$	$\begin{smallmatrix} (2 \pm 1) \cdot 10^{-4} \\ - \end{smallmatrix}$

Note. The upper row is calibrated to the flow of very heavy nuclei (VH), lower row to the flow of all heavy nuclei (H). All errors are root-mean-square.

Page 598.

Furthermore, the overwhelming majority of the information about the interactions of space nuclei is obtained in experiments on the photoemulsion, where very inaccurately is determined not only the value of the primary energy T , but also the very selection of interactions nucleus + nucleus is made on the basis of the very approximate criteria. Therefore the known now information about the

interactions of high-energy nuclei has a predominantly qualitative, estimated character.

The already simple comparison of the stars, formed in photoemulsion by high-energy space nuclei, shows that then it is possible to distinguish two types: 1) star with the very large number of secondary particles, among which either generally there are no particles with charges $Z > 1$ or - if the impinging nucleus sufficiently heavy - sometimes is contained one-two such particles (Figs. 453 and 454); 2) star with the considerably smaller number of secondary particles, but containing several fragments with charge $Z > 2$ (Figs. 455 and 456).

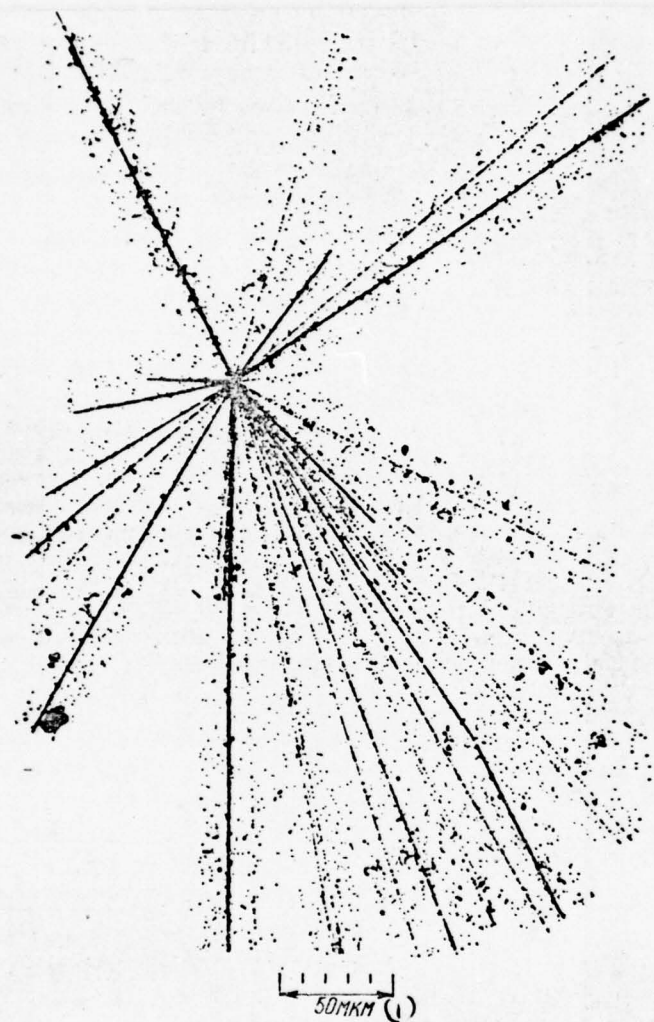


Fig. 453.

Fig. 453. The head-on collision of nucleus Mg with nucleus Br [21, 47]. Nucleus with charge $Z = 12 \pm 2$ as a result of nuclear collision virtually completely decomposes for its component nucleons; in this case is split the target nucleus. Therefore event is related to the same rare cases, when target nucleus can be sufficiently confidently identified. Actually, net charge of all secondary particles, which were being formed as a result of collision, $Z_t \approx 47$, and since energy of the impinging nucleus $T \approx 700$ MeV/nucleon, generation of the large number of mesons is very highly improbable and, therefore, the charge of target nucleus $Z_M \approx Z_t - Z \approx 35$, i.e., nucleus was the nucleus of bromine.

Key: (1). μm .

Page 599.

In this case unlike nucleon- and the pion-nuclear collisions, where the particles with $Z \gg 2$ very rarely are emitted at relativistic rates, during collision with the emulsion of the neutral and heavy nuclei at least the half of particles with $Z \gg 2$ turns out to be relativistic and escape at small angles.

The first type of stars it is possible with to compare with the

central (frontal) collisions, which occur, in small impact parameters, when the impinging nucleus virtually completely is dispersed to separate nucleons, and rare fragments with $Z \geq 2$ are formed mainly during the evaporation of the highly excited residue/remainder of target nucleus.



Fig. 454.

Fig. 454. The star, formed in photoemulsion by nucleus C with an energy of $T \approx 1700$ GeV/nucleon [47] (right figure is continuation of left). As a result of interaction was formed more than 100 charged mesons. About one half of secondary particles it is concentrated in central "shaft". Energy of the impinging nucleus was determined by the angle of the $\theta_{1/2}$, within which was concentrated the half of all secondary particles. As a result of collision the nucleus C decayed into component nucleons.

Page 600.

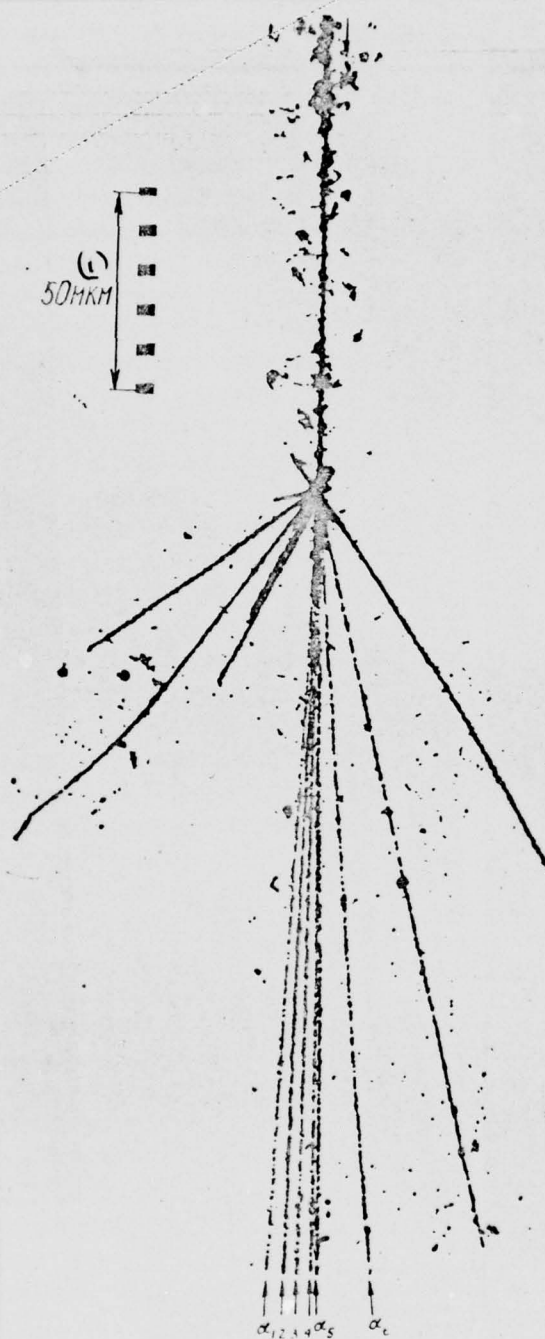


Fig. 455.

Fig. 455.

Nuclear disintegration Mg into α -particles [47]. The type of primary nucleus is established/installed from the analysis of its track. As a result of collision with the nucleus of photoemulsion it was decomposed for six α -particles. As it shows density measurement of grains in the traces of these α -particles, they all flew out at approximately identical rates. The seventh trace with approximately the same density of grains belongs to low-energy deuteron.

Key: (1). μm .

Page 601.

Second type stars it is possible to relate to the peripheral collisions, when the impinging nucleus and target nucleus overlap only partially; in this case is split into nucleons the only part of the impinging nucleus, but its another part it flies further in the form one or of several fragments, which move with the speeds of the same order of value, as the primary impinging nucleus.

Qualitatively this picture makes it possible to understand many parts of the inelastic collision of two nuclei; however, it demands

of course, quantitative confirmation by the calculation.

Unfortunately, substantial changes of the properties of the impinging nucleus and nucleus-target in the process of collision and the need for the simultaneous account of the very large number of particles, which participate in interaction, lead to the fact that we now do not have theory of inelastic collision of high-energy nuclei, if only one of them it is not deuteron or, at the worst, by α -particle.

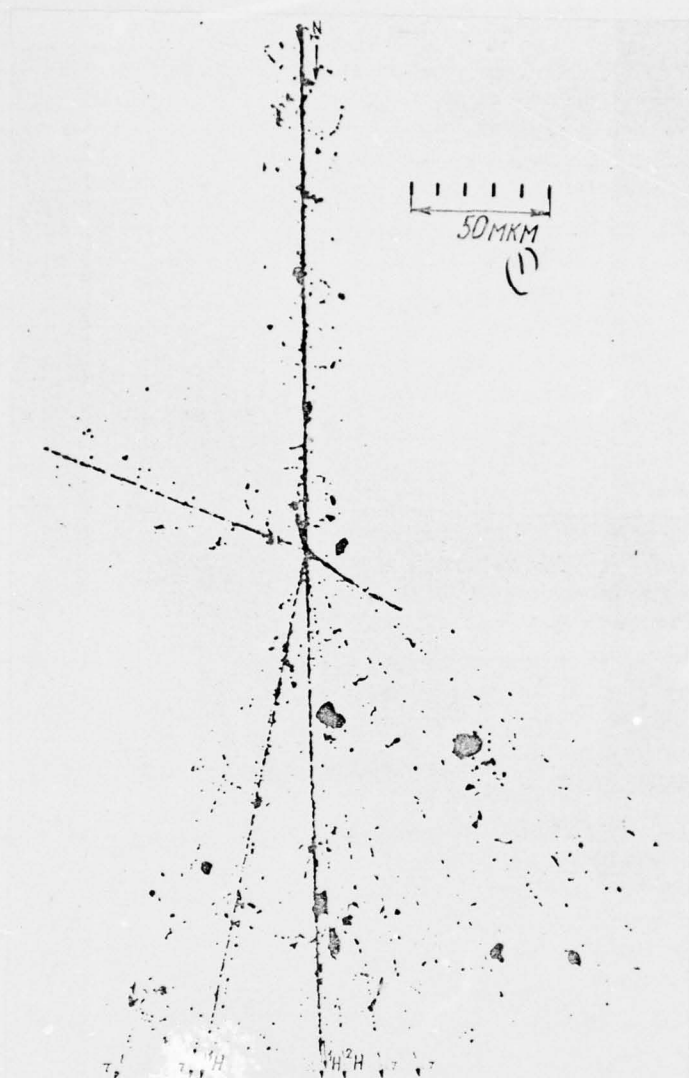


Fig. 456.

Fig. 456. The inelastic collision of the nucleus of nitrogen with an energy of $T \approx 2$ GeV/nucleon with the nuclei of photoemulsion [47]. As a result of collision were formed several π -mesons and nucleus was decomposed on several protons, rapid deuteron and nucleus Li.

Key: (1). μm .

Page 602.

It is necessary also to keep in mind that during the interaction of nucleus with photo emulsion along with interactions of the type "nucleus" + nucleus are possible also the proton-nucleus interactions with hydrogen. For light/lung primary nuclei the contribution of the latter is comparatively small and it is approximately 10o/o; however, for the nuclei of iron this contribution reaches already approximately 20o/o (Table 146) and it one should compulsorily consider during the analysis of the stars, formed by high-energy nuclei.

As a rule, very is with difficulty also to establish/install, with which nucleus of photoemulsion, by light/lung or heavy, occurred collision. The approximate criterion of selection according to the total number of gray and black traces ($n_h \leq 6$ and $n_h > 6$) now turns

cut to be still susceptible/critical, than in the case nucleon and pion- nuclear interactions (see Chapter 3), since the significant part of the stars with the small number of ray/beams n_h is formed as a result of peripheral collisions with the heavy component of photoemulsion.

The probabilities of interactions with the groups of the light/lung and heavy nuclei of photoemulsion depend on the mass number of impinging nucleus sufficiently weakly (see Table 146).

As in the preceding/previous chapters, we first will examine the experimental data, and then let us discuss the theoretical possibilities of the calculation.

Data on integral interaction cross sections of nuclei and their elastic scattering were already examined above, in chapter 1 and 2.

§108. Many secondary particles.

Deuteron-nuclear collisions. Experimental distribution of many particles, which are formed in the inelastic collisions of deuterons with nuclei, are given in Table 147 and Table 165 and 166 in §112.

In its form of the stars, formed in photoemulsion by deuterons, are very similar to the stars, which are formed under the action of nucleons. The basic difference consists in the fact that at just one value of energy T , which is necessary to one nucleon, in deuteron-nuclear collision on the average is born noticeably the larger number of secondary particles, than during collision nucleon + nucleus.

Table 146. Relative probabilities of the inelastic interactions of high-energy nuclei with the different components of photoemulsion Ilford G-5, o/o.

(2) Мишень	(1) Налетающее ядро				
	^4He	^9Be	^{14}N	^{28}Si	^{56}Fe
H	8	11	14	17	20
C, N, O	28	29	30	31	31
Ag, Br	64	60	56	52	49

Note. All these values are calculated by formula (1.12) [47].

Key: (1). Impinging nucleus. (2). Target.

Table 147. Distribution according to the number of ray/beams in the stars, formed by deuterons in photoemulsion, o/c [26].

(1) Число лучей	$T = 45$ Мэв/нуклон	$T = 75$ Мэв/нуклон	$T = 95$ Мэв/нуклон
	(2)	(3)	(4)
2	$28,4 \pm 3$	$26,2 \pm 3$	$28,1 \pm 3,2$
3	51 ± 4	$44,6 \pm 4,1$	$43,2 \pm 3,8$
4	$17,3 \pm 2,3$	$25,1 \pm 3$	$25,2 \pm 2,8$
5	3 ± 1	$3 \pm 1,1$	$3,5 \pm 1,1$
6	$0,3 \pm 0,3$	$1,1 \pm 0,6$	0

Key: (1). Number of ray/beams. (2). MeV/nucleon.

Page 603.

However, this number is less than that would follow to expect if during each inelastic deuteron- nuclear interaction it occurred the "addition" of the independent cascade/stages, initiated by both deuteron nucleons; it is possible to think (and this confirmed in §112) that in many instances the intranuclear cascade gives rise to only one of these nucleons.

Collisions of α -particles with nuclei. Table 148 gives number distribution of secondary charged particles for the inelastic collisions of α -particles with the nuclei of photoemulsion. For a comparison in this same table are shown also the data for interaction $p + Em$ at the very close value of energy $T = 94 \text{ MeV} \approx T_\alpha/4$. The distribution of many shower particles, formed by α -particles with higher energy, it is shown in Fig. 457. We see that during the interactions of α -particles with nuclei is born the considerably larger number of rapid secondary particles, than in inelastic nucleon-nuclear collisions. This follows also from Table 149, where are shown values \bar{n}_s . Even with energies $T \sim 100 \text{ GeV/nucleon}$ the average number of shower particles in collisions $\alpha + Em$ reaches the

same value as in collisions $N + Em$ at $T \sim 10^3$ GeV.

The fact calls attention to itself that in experiment fairly often are observed one or even two rapid secondary protons, in which the rate turns out to be virtually the same as among nucleons, which was a part of primary α -particle. Such cases it is logical to interpret as result of the peripheral collisions, when one or several nucleons, which composed earlier α -particle they fly the initial rate.

Table 148. Distribution according to the number of ray/beams in the stars, formed in photoemulsion by α -particles with energy $T_\alpha = 350$ MeV, % ($T \approx 88$ MeV/nucleon) [49].

(1) Число лучей n	(2) Все звезды	(3) Звезды с одним быстрым прото- ном *1)	(4) Звезды с двумя быстрыми про- тонами *1)	$p + Em$ $T = 94$ Мэв [31] (5)
1	$3,3 \pm 1,1$	$1,3 \pm 0,7$	$2,6 \pm 0,9$	$25,2 \pm 3,5$
2	$26,1 \pm 2,9$	$4,6 \pm 1,2$	$0,6 \pm 0,4$	$43,9 \pm 4,7$
3	$18,9 \pm 2,5$	$3,3 \pm 1$	$0,3 \pm 1$	$12,6 \pm 2,5$
4	$16 \pm 2,3$	$1,6 \pm 0,7$	$0,6 \pm 0,4$	$11,1 \pm 2,3$
5	$17,3 \pm 2,4$	$2,6 \pm 0,9$	—	$6,6 \pm 1,9$
6	$10,1 \pm 1,8$	$1,3 \pm 0,7$	—	$0,5 \pm 0,5$
7	$5,9 \pm 1,4$	—	—	—
8	$1,6 \pm 0,7$	—	—	—
9	$0,6 \pm 0,5$	—	—	—
	100%	14,7%	4,2%	100%

Key: (1). Number of ray/beams. (2). All stars. (3). Stars with one rapid proton 1.

FOOTNOTE 1. Velocity of rapid proton the same as of primary α -particle. ENDFOOTNOTE.

(4). Stars with two rapid protons 1. (5). MeV.

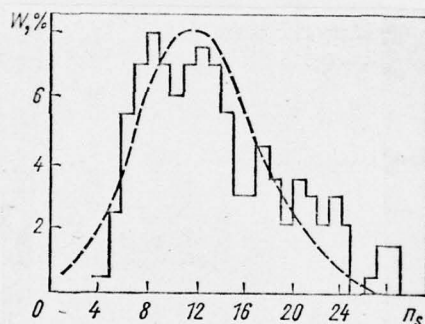


Fig. 457. Distribution $W(n_s)$ in the inelastic collisions of space α -particles with the nuclei of photoemulsion [42]. Dotted curve is a result of the addition of two independent distributions for interaction $N + Em$ during the same value of energy.

Page 604.

Table 149. Average multitude of shower particles, which are formed during the interaction of space nuclei with photoemulsion.

TABLE 149.

(1) Космическое ядро *0	(2) T , Гэв/нуклон	\bar{n}_s	Ядро-мишень 2*; критерий (3) отбора	(4) Литература
α	15 40 40 125 ≥ 250	$28,5 \pm 2,9$ $14,7 \pm 4,2$ 31 ± 10 ~ 28 37 ± 6	$Em; n_s > 4$ $LEm; n_h = 2 \div 5$ $HEm; n_h \geq 6$ $Em; n_s > 4$ $Em; \text{все звезды}$ (5)	[29] [39] [39] [29] [33]
Li	$> 1,5$	$6,5 \pm 1,1$	$Em; \text{ » }$	[3, 19, 23, 50]
Li, Be, B	$2 \div 15$	$7,2 \pm 0,7$	$Em; \text{ » }$	[3]
Be	$> 1,5$	$6,7 \pm 1,1$	$Em; \text{ » }$	[3, 19, 23, 50]
B	$> 1,5$	$9,1 \pm 9,9$	$Em; \text{ » }$	[3, 19, 23, 50]
C	$> 1,5$ $2 \div 15$ 40 40	$11,8 \pm 0,9$ $11,1 \pm 1$ $22,9 \pm 1,1$ $12,5 \pm 0,9$	$Em; \text{ » }$ $Em; \text{ » }$ $Em; \text{ » }$ $LEm; n_h \leq 6$	[3, 19, 23, 50] [3] [56] [56]
C, N, O	$2 \div 15$ 40 40 40	$14,8 \pm 0,6$ $23,7 \pm 0,7$ $9,0 \pm 0,5$ $45,3 \pm 1,5$	$Em; \text{ все звезды}$ (5) $Em; \text{ » }$ $LEm; n_h \leq 6$ $HEm; n_h > 6$	[3] [56] [56] [56]
N	1,5 $2 \div 15$ 40	$9,3 \pm 0,9$ $14,9 \pm 1,4$ $27 \pm 1,4$	$Em; \text{ все звезды}$ (5) $Em; \text{ » }$ $Em; \text{ » }$	[3, 19, 23, 50] [3] [56]
C, N, O, F	3 3 3 3	$5,5 \pm 0,8$ $9,1 \pm 0,9$ $11,9 \pm 1,5$ $19,2 \pm 4,8$	$LEm; n_h = 2 \div 7$ $Em; n_h > 1$ $HEm; n_h \geq 8$ $HEm; n_h \geq 28$	[25] [25] [25] [25]
O	1,5 $2 \div 15$ 40	$11,4 \pm 1,2$ $16,9 \pm 0,9$ $22,2 \pm 1,6$	$Em; \text{ все звезды}$ (5) $Em; \text{ » }$ $Em; \text{ » }$	[3, 19, 23, 50] [3] [56]
Li, Be, C, Mg $Z \geq 3$	≥ 500 $2 \div 15$ $2 \div 15$ $2 \div 15$	131 ± 55 $16,2 \pm 0,4$ $7,2 \pm 0,4$ $26,9 \pm 0,8$	$Em; \text{ » }$ $Em; \text{ » }$ $LEm; n_h \leq 6$ $HEm; n_h > 6$	[33] [3] [3] [3]
$Z \geq 10$	3 3 3 3 $2 \div 15$ ≥ 100	$8,4 \pm 1,1$ $11,7 \pm 1$ $14,3 \pm 1,6$ $28,8 \pm 7,2$ $20,7 \pm 0,8$ ~ 60	$LEm; n_h = 2 \div 7$ $Em; n_h > 1$ $HEm; n_h \geq 8$ $HEm; n_h \geq 28$ $Em; \text{ все звезды}$ (5) $Em; \text{ » }$	[25] [25] [25] [25] [3] [33]

Key: (1). Space nucleus ¹.

FOOTNOTE ¹. Z is a charge of primary space nucleus. ENDFOOTNOTE.

(2). GeV/nucleon. (3). nucleus-target ²; criteria of selection.

FOOTNOTE ². Since in the majority of experimental works are considered also the stars with the number of black and gray ray/beams $n_h \leq 2$, which correspond to interactions with the hydrogen of photoemulsion, the mass and charge numbers of neutral photoemulsion nuclei E_m and LE_m differ from those, that they were shown in introduction. ENDFOOTNOTE.

(4). Literature. (5). all stars.

376
Table 150. Average number of gray and black ray/beams in the stars, formed by nuclei in photoemulsion.

(1) Первичное ядро	$T, \text{ Гэв/нуклон}$ (2)	\bar{n}_g	\bar{n}_b	\bar{n}_h	Ядро-мишень *: критерий отбора (3)	Литература (4)
$p (Z=1)$	6,2 6,2 6,2	$3,58 \pm 0,11$ — $5,24 \pm 0,10$	$5,68 \pm 0,21$ — $9,48 \pm 0,14$	$8,8 \pm 0,2$ $3,9 \pm 0,1$ $14,7 \pm 0,2$	Em ; все звезды LEm ; $n_h = 2 \div 6$ HEm ; $n_h > 6$	[60] [60] [60]
α	15	$6,3 \pm 1,1$	$12,2 \pm 1,3$	$18,5 \pm 2,5$	Em ; $n_s > 4$	[29]
Li, Be, B	$0,1 \div 0,3$ $0,1 \div 0,5$ $2 \div 15$ $2 \div 15$ $2 \div 15$	$3,9 \pm 0,7$ $4,8 \pm 0,7$ $3,0 \pm 0,5$ — — —	$3 \pm 0,6$ $3,7 \pm 0,6$ $4,0 \pm 0,6$ — — —	$6,9 \pm 0,9$ $8,5 \pm 0,9$ $8,3 \pm 0,6$ $4,0 \pm 0,2$ $16,7 \pm 0,8$	Em ; все звезды Em ; » Em ; » LEm ; $n_h = 2 \div 6$ HEm ; $n_h > 6$	[46] [46] [3, 19, 23, 50] ^{2*} [3, 19, 23, 50] ^{2*} [3, 19, 23, 50] ^{2*}
C	$2 \div 15$ 40	$3,2 \pm 0,5$ —	$5,1 \pm 0,7$ —	$8,3 \pm 0,8$ $6,1 \pm 0,7$	Em ; Все звезды Em ; »	[3] [56]
C, N, O	$2 \div 15$ 40 40 40	$3,2 \pm 0,3$ — — —	$4,8 \pm 0,3$ — — —	$8 \pm 0,4$ $7,9 \pm 0,4$ $3,8 \pm 0,4$ $5,6 \pm 0,9$	Em ; » Em ; » LEm ; $n_h = 2 \div 6$ HEm ; $n_h > 6$	[3] [56] [56] [56]
N	$2 \div 15$ 40	$2,8 \pm 0,6$ —	$3,9 \pm 0,7$ —	$6,7 \pm 0,9$ $9,5 \pm 1$	Em ; все звезды Em ; »	[3] [56]
C, N, O, F	$0,1 \div 0,3$ $0,1 \div 0,3$ $0,1 \div 0,3$ $0,3 \div 0,5$ $0,1 \div 0,5$ $0,1 \div 0,5$ $0,1 \div 0,5$ 3 3 3 3 $2 \div 15$ $2 \div 15$ $2 \div 15$	$4 \pm 0,4$ — — $6,8 \pm 0,5$ $5,3 \pm 0,3$ — — $6,1 \pm 0,6$ $1,6 \pm 0,2$ $9,6 \pm 1,1$ $18,7 \pm 4,5$ $3,9 \pm 0,3$ — —	$3,1 \pm 0,3$ — — $5 \pm 0,5$ $4 \pm 0,3$ — — $6,6 \pm 0,7$ $2,5 \pm 0,3$ $9,7 \pm 1,1$ $13,7 \pm 3,5$ $5,1 \pm 0,4$ — —	$7,1 \pm 0,5$ $4 \pm 0,5$ $12,3 \pm 1$ $11,8 \pm 0,7$ $9,3 \pm 0,4$ $4,2 \pm 0,4$ $14,9 \pm 0,4$ $12,7 \pm 1,2$ $4,1 \pm 0,6$ $19,3 \pm 2,2$ $32,4 \pm 8$ $8,0 \pm 0,4$ $4,0 \pm 0,1$ $16,8 \pm 0,5$	Em ; » LEm ; $n_h = 2 \div 6$ HEm ; $n_h > 6$ Em ; все звезды Em ; » LEm ; $n_h = 2 \div 6$ HEm ; $n_h > 6$ Em ; $n_h > 1$ LHE ; $n_h = 2 \div 7$ HEm ; $n_h > 8$ HEm ; $n_h > 28$ Em ; все звезды LEm ; $n_h = 2 \div 6$ HEm ; $n_h > 6$	[46] [46] [46] [46] [46] [46] [46] [25] [25] [25] [25] [25] [3, 19, 23, 50] ^{2*} [3, 19, 23, 50] ^{2*} [3, 19, 23, 50] ^{2*}
O	$2 \div 15$ 40	$3,5 \pm 0,4$ —	$3,0 \pm 0,5$ —	$6,5 \pm 0,6$ $8,6 \pm 0,7$	Em ; все звезды Em ; »	[3] [56]
$Z \geq 3$	$0,1 \div 0,3$ $0,1 \div 0,5$ $2 \div 15$ $2 \div 15$	$4,1 \pm 0,3$ $6,1 \pm 0,3$ $6,0 \pm 0,7$ $10,2 \pm 0,9$	$3,1 \pm 0,2$ $4,6 \pm 0,3$ $5,32 \pm 0,49$ $8,5 \pm 0,5$	$7,2 \pm 0,4$ $10,6 \pm 0,5$ $11,3 \pm 1,2$ $18,7 \pm 1$	Em ; » Em ; » Em ; » HEm ; $n_h > 6$	[46] [46] [3, 44] [44]

TABLE 150. (continuation)

Первичное ядро ①	T , ② Гэв/нуклон	\bar{n}_g	\bar{n}_b	\bar{n}_h	Ядро-мишень*; критерий отбора ③	Литера- тура ④
$Z > 10$	$0,1 \div 0,3$	$4,4 \pm 0,6$	$3,2 \pm 0,5$	$7,6 \pm 0,8$	Em ; все звезды ⑤	[46]
	$0,1 \div 0,5$	$5,8 \pm 0,6$	$4,2 \pm 0,5$	$10 \pm 0,8$	Em ; » »	[46]
	3	$6,7 \pm 0,7$	$6,1 \pm 0,6$	$12,8 \pm 1$	Em ; $n_h > 1$	[25]
	3	$1,8 \pm 0,2$	$2,2 \pm 0,3$	$4 \pm 0,5$	LEM ; $n_h = 2 \div 7$	[25]
	3	$10,7 \pm 1,1$	$9,2 \pm 1$	$20 \pm 2,2$	HEM ; $n_h \geq 8$	[25]
	3	24 ± 6	$11,2 \pm 3$	$35,2 \pm 8$	HEM ; $n_h \geq 28$ ⑤	[25]
	$2 \div 15$	$5,4 \pm 0,4$	$6,5 \pm 0,5$	$8,8 \pm 0,5$	Em ; все звезды	[3, 19, 23, 50] 2*
	$2 \div 15$	—	—	$3,8 \pm 0,1$	LEM ; $n_h = 2 \div 6$	[3, 19, 23, 50] 2*
	$2 \div 15$	—	—	$17,5 \pm 0,7$	HEM ; $n_h > 6$	[3, 19, 23, 50] 2*

Key: (1). Primary nucleus. (2). GeV/nucleon. (3). Target nucleus ¹;
the criterion of selection.

FOOTNOTE 1. See note 2 to Table 149. ENDFOOTNOTE.

(4). Literature. (5). all stars.

FOOTNOTE 2. The average value of the results, obtained in works [3,
19, 23, 50]; values \bar{n}_g and \bar{n}_b are taken their work [3].
ENDFOOTNOTE.

If one considers that α -particle is as much neutrons, as and protons,
then the portion of peripheral collisions with $T = 88$ MeV/nucleon
(see Table 148) it must be knowingly more the third of the number of
all inelastic interactions $\alpha + \text{Em}$. Analysis are rapid particles,
which escape at small angles, it showed that among them many the
deuterons: for 20 recorded in work [49] charged particles relation
 $p:d:t = 7:12:1$.

In the work of the Appa of Roa, etc. [4], carried out with space α -particles with energy $T \gtrsim 6$ GeV/nucleon, the number of secondary protons at velocities, approximately equal to the rate of primary α -particles, was found equal to 1.5 ± 0.5 taking into account one star in photoemulsion, whence it follows that with very high energies with target nucleus, as a rule, interacts the pair of the nucleons of the impinging α -particle. With this conclusion will agree also the results, obtained Nakagawa, etc. [42]: experimental distribution $W(n_s)$ in Fig. 457 very closely to the total distribution, which corresponds to the case, when with the nucleus of photoemulsion on the average it is simultaneous, but independently of each other, they interact two nucleons.

An average multitude of shower particles \bar{n}_s , the forming in inelastic collisions α -particles with nuclei (see Table 149), approximately is twice as more as which is observed in the case of nucleon-nucleus collisions at the equal value of energy T , which is necessary to one nucleon.

The value of an average multitude of gray and black traces in the stars, formed by α -particles, vice versa, is close to the appropriate values for collisions $N + \text{nucleus}$ (Table 150). In this

AD-A048 311

FOREIGN TECHNOLOGY DIV WRIGHT-PATTERSON AFB OHIO
INTERACTIONS OF HIGH-ENERGY PARTICLES AND ATOMIC NUCLEI WITH NU--ETC(U)
JUL 77 V S BARASHENKOV, V D TONEYEV
FTD-ID(RS)T-1069-77

F/G 20/8

UNCLASSIFIED

NL

5 OF 6
AD
A048 311



case in both cases the average number of slow particles in star n_h grow/rises with an increase in many being born shower particles; however, in the case $\alpha + \text{Em}$ this dependence somewhat weaker (Fig. 458).

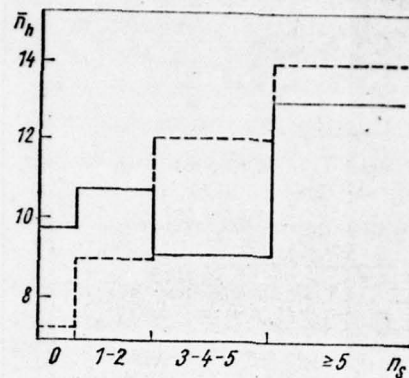


Fig. 458. Dependence of the average number of gray and black traces \bar{n}_h on the number of relativistic traces n_s in stars, formed during irradiation of fotoemulsii by space α -particles with energy $T \gg 1$ GeV/nucleon [18]. Dotted line - the same for interaction $p + Em$ [18].

Page 607.

This, apparently, is connected with the fact that into the group of events with small values \bar{n}_h now enter not only the interactions with

light/lungs, but also the significant part (peripheral) of interactions with the heavy nuclei of photoemulsion.

Many shower particles during the collisions of nuclei with charges $Z \gg 3$. The experimental data on an average multitude of shower particles, which are formed in the photoemulsion, irradiated by nuclei with charge $Z \gg 3$ are given in Table 149 and 151. From these data is distinctly evident a sharp increase in the average number of being born shower particles during transition to the large values of Z . In this case an increase in the charge of primary nucleus leads to a considerably more essential increase in the number of being born particles, than transition to heavier target nuclei in the case nucleon- and pion- nuclear interactions. The latter is connected, in particular, from themes by the fact that the particles, which in the system of the rest of the impinging nucleus slow, during passage to the laboratory system of coordinates considerably increase their energy (Fig. 459).

In stars with the large number of slow particles ($n_h > 6$) on the average is born considerably more shower particles, than in stars with $n_h \leq 6$.

If we disregard the relatively small number of relativistic protons of those escaping from target nucleus, then the difference

between the total number of charged shower particles n_s and the number of relativistic protons n_p can be approximately accepted for the number of charged relativistic π^- mesons, which are formed during the collision: $n_{\pi\pm} = n_s - n_p$ (contribution K^\pm mesons is very small). Specifically, thus obtained values $n_{\pi\pm}$ in Table 151.

Figure 460 shows the distribution of the inelastic interactions of nuclei depending on the value of a change in the charge $\Delta Z = \sum_i |Z_i| - Z$, where Z_i are charges of relativistic secondary particles, and Z - the charge of the impinging nucleus.

Table 151. Average number π^\pm the mesons, which are born during the collision of space nucleus with photoemulsion.

(1) Ядро	(2) $T, \text{ Гэв/нуклон}$	\bar{n}_{π^\pm}			(4) Литература
		все звезды (3)	$1 < n_h \leq 6$	$n_h > 6$	
$p (Z=1)$	6,2	—	$1,9 \pm 0,1$	$2,6 \pm 0,1$	[60]
Li, Be, B	3 $2 \div 15$	— $4,8 \pm 0,6$	4 $3,5 \pm 0,5$	7,6 $6,8 \pm 0,5$	[47] [3, 44]
C	$2 \div 15$ 40	$6,3 \pm 0,7$ $19,2 \pm 1$	— —	— —	[3] [56]
C, N, O	3 $2 \div 15$ 40	— $9,8 \pm 0,5$ 21,4	4 $5,6 \pm 0,6$ $10,0 \pm 0,6$	10 — $40 \pm 1,4$	[47] [3] [56]
N	$2 \div 15$ 40	$9,8 \pm 1,1$ $22,9 \pm 1,3$	— —	— —	[3] [56]
C, N, O, F	$2 \div 15$ 40	$10,5 \pm 0,5$ $22,7 \pm 1,3$	$4,4 \pm 0,4$ —	$9,9 \pm 0,8$ —	[3, 44] [56]
O	$2 \div 15$ 40	$11,8 \pm 0,8$ $22,7 \pm 1,6$	— —	— —	[3] [56]
$Z \geq 3$	$2 \div 15$	$12,1 \pm 1,1$	$5,5 \pm 0,4$	$18,8 \pm 3,6$	[3, 44]
$9 \leq Z \leq 19$	3	—	3,4	10,5	[47]
$Z \geq 10$	$2 \div 15$	$13,1 \pm 0,7$	$4,7 \pm 0,5$	$14,4 \pm 0,9$	[3, 44]

Key: (1). Nucleus. (2). GeV/nucleon. (3). All stars. (4). Literature.

Page 608.

Most frequently - especially with $n_h = 0, 1$ occur interactions with $\Delta Z = 0$, when are not formed relativistic mesons. The formation/education of mesons is more probably during the central collisions, which are characterized by the large number of slow particles n_h (see Fig. 460b and c). Specifically, with this is connected more rapid increase in the set $\bar{n}_{\pi\pm}$ during passage to the large values of Z in stars with the number of ray/beams $n_h > 6$ in Table 151; with $n_h \leq 6$ (and the fixed/recorded energy T taking into account one nucleon) the values $\bar{n}_{\pi\pm}$ change considerably slower.

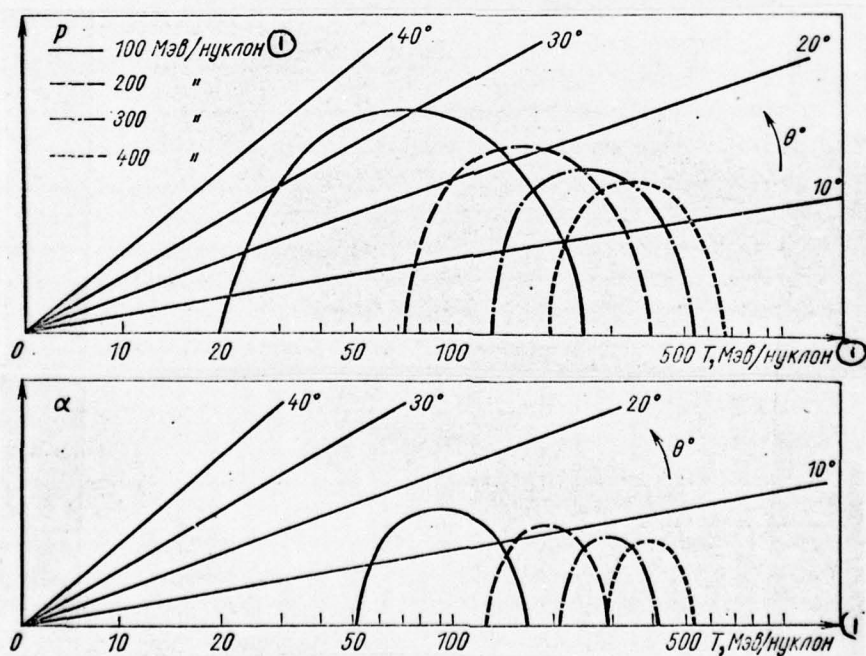


Fig. 459.

Fig. 459. The range of the solved energies in the laboratory coordinate system for α -particles and the protons, emitted by the impinging nucleus during its collision with the medium nucleus of photoelement [46]; θ is an angle with respect to the direction of the motion of the impinging nucleus in the laboratory coordinate system. Is shown energy of the primary nucleus T .

Key: (1). MeV/nucleon.

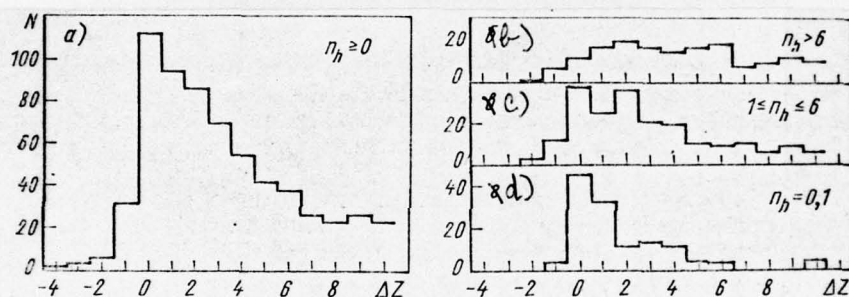


Fig. 460. Number of the inelastic collisions of space nuclei with the nuclei of photoemulsion during $T \gg 1.5$ GeV/nucleon, which are accompanied by different changes in the charge ΔZ [47]: a) - the distribution of all stars, formed by space nuclei with charge $Z \gg 3$; b), c), d) - the distribution of stars with the different number of

gray and black traces, formed by nuclei with charge $3 \leq Z \leq 8$.

Page 609.

In distributions in Fig. 460 are encountered negative values ΔZ up to $\Delta Z = -4$. Values $\Delta Z = -4, -3$ can be ascribed to errors in determination ΔZ , especially when the charge of initial particle is great. However, the frequency, which meet the values $\Delta Z = -1$, testifies, apparently, to completely real effect. This effect can be connected with the processes of charge exchange, during which the colliding proton converts into neutron without the formation/education of charged mesons [47]. Some cases, which correspond to small positive values ΔZ , also can be ascribed to the similar processes, during which the neutrons are converted into protons. However, large positive values ΔZ are definitely connected with the formation/education of mesons.

It is interesting to note that the peripheral collisions, when from primary nucleus "are separated" only small fragments, they occur by such form, as if each nucleon of fragment interacted with target nucleus virtually independent of other nucleons. The mean value of relation $n/\Delta A$, where ΔA - the number of the "separated" nucleons, only by a little is less than which is observed for nucleon-nuclear

collisions with equal energy of $T/\text{nucleon}$ ¹.

FOOTNOTE ¹. ΔA it is equal to a difference in the mass number of primary impinging nucleus and the mass number of corresponding nucleus-remainder or sum of the mass numbers of the fragments, for which decomposes this remaining nucleus: $\Delta A = A_{\text{непр}} - \sum_i A_{i \text{ непр. осат.}}$
ENDFOOTNOTE.

For example, with $T \approx (1 - 20) \cdot 10^3 \text{ GeV/nucleon}$ in the work of Abraham, etc. [1] for stars with $n_h < 6$ and $n_h \geq 6$ are obtained respectively values $\overline{n_s/\Delta A} \geq 8.6 \pm 1.7$ and $\overline{n_s/\Delta A} \geq 17.1 \pm 1.6$; value $\overline{n_s}$ nucleon- nuclear interactions with $T \approx (0.7 - 1.4) \cdot 10^3 \text{ GeV}$, obtained in this same work, is 11.5 ± 3.3 for $n_h < 6$ and 17.3 ± 5.2 for $n_h \geq 6$.

Some authors (for example, see [1] and monograph [41], pages 303) they consider that a specific multitude is close to many shower particles from nucleon-nuclear collision not only for peripheral, but also in the general case of the inelastic collision of two nuclei.

Figure 461 shows that an average multitude of shower particles increases approximately proportional to the value of the mass number of primary impinging nucleus $A_{\text{непр}}$. This indicates that each nucleon

of the impinging nucleus on the average bears approximately the identical number of shower particles.

Many heavily ionizing particles. As concerns the slow particles, which leave in photoemulsion gray and black traces, with energies $T \gtrsim 1$ GeV/nucleon the suppressing number of these particles it escapes from target nucleus and therefore their property they characterize the processes, which develop precisely in this nucleus (particles, connected with the impinging nucleus, in the laboratory system of coordinates, as a rule, relativistic; comp. with Fig. 459).

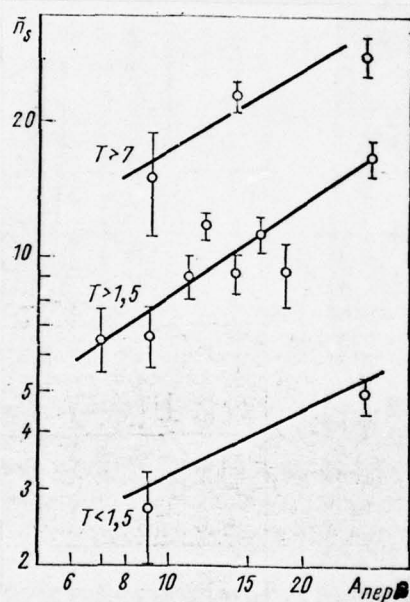


Fig. 461. Dependence of the average number of shower particles on the mass number of primary impinging nucleus [2, 38] (interaction with photoemulsion with energies T , GeV/nucleon).

As we will see below, the properties of b-particles are explained well evaporative model; therefore these particles characterize, in essence, remanent/residual nucleus; hence also it follows that as in the case nucleon- nuclear interactions, particles with gray traces they are formed at the stage, which precedes the formation of an excited nucleus-remnant and their multiplicity can be considered as a measure of the intensity of the cascade which developed inside the nucleus-target.

It is reasonable to consider that each gray trace signifies the loss of one charge by the nucleus-target (the contribution of π^\pm -mesons is insignificant). Then the charge of the excited nucleus-remainder at the moment preceding the evaporation process, $Z_{\text{oct}} \simeq Z_M - n_g$, where Z_M - the charge of the nucleus-target. In other words, the value n_g characterizes the dimensions of the excited residual nucleus.

The particles connected with the bombarding nucleus provide a substantial contribution to the low-energy component of secondary particles only with energies $T < 1$ GeV/nucleon. In particular, in this case the composition of the g-particles includes a considerable portion of the particles emitted in the process of evaporation of big and the decay of small heavily excited fragments of the bombarding nucleus which were formed as a result of collisions (see Fig. 459).

Thus, a comparison of the properties of g-particles in high-energy collisions of N+nucleus and nucleus+nucleus permits studying the difference in the cascade stage, and a comparison of the properties of b-particles - the difference in the evaporative stage of these two types of interactions.

Fig. 462 shows typical total distributions of traces of g- and b-particles formed during inelastic collisions high-energy nuclei with photoemulsion. The first, which turns on itself attention in these distributions, this large number of multiple-pronged stars, considerably larger than in the ~~made~~ nucleon- or pion-nuclear interaction (even if energies primary nucleon and π -meson reach several thousand GeV. It is evident also that the interactions with $n_h = 0; 1$ most probable.

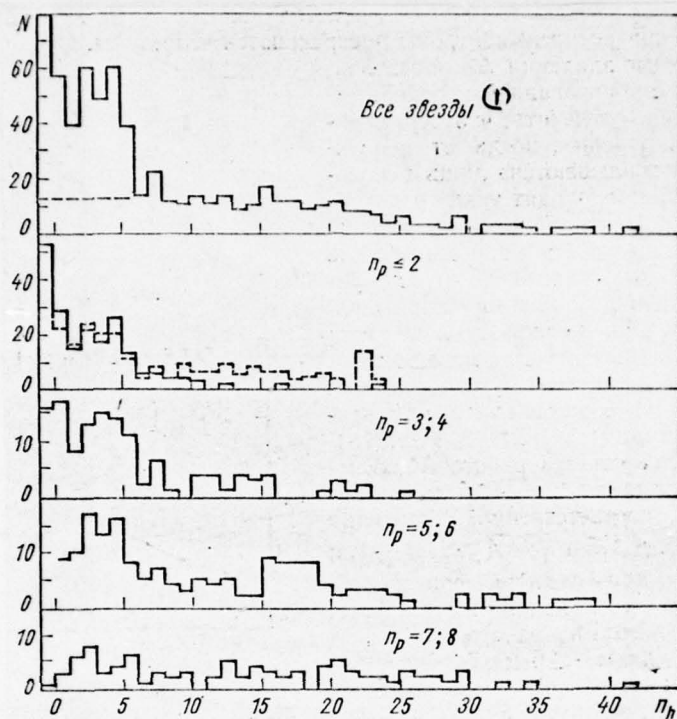


Fig 462.

Fig. 462. Number distribution of heavily ionizing particles in the stars, formed in photoemulsion by space nuclei with charge $Z \gg 6$ during $T \approx 40$ GeV/nucleon [56]: n_p is a number of shower protons in star. In the case $n_p \leq 2$ by dotted line is shown distribution $W(n_h)$ for interactions $\alpha + \text{Em}$ [56], calibrated to the number of stars with $n_h = 0$. By dotted line with $n_h \leq 6$ in the upper figure is estimated shown the contribution of peripheral interactions nucleus + HEm.

Key: (1). All stars.

Page 611.

Furthermore there is a second very clearly expressed peak with $n_h \approx 5$, after which begins sharp decrease and then values $W(n_h)$ are almost constant up to $n_h \approx 20$.

A change in the character of distribution $W(n_h)$ during $n_h = 6-7$ can be explained by the presence of two strongly being distinguished groups of nuclei in photoemulsion. Interactions of space nuclei with the light/lung component of the photoemulsions, which are frequently accompanied by the complete disintegration of target nucleus, give contribution with maximum with $\bar{n}_h \approx \bar{Z}_{\text{ser}} \approx 5$. From that fact that this maximum distinctly exhibited in experimental

distributions ¹, it may be concluded that in stars with the number of ray/beams $n_h = 2 \div 6$ the contribution of peripheral interactions with the heavy nuclei of photoemulsion is comparatively small.

FOOTNOTE ¹. It is interesting to note that in the case nucleon- and pion- nuclear interactions this anomaly is expressed very weakly (see Chapter 3) despite the fact that the relative numbers of splitting/fissions, caused by collisions with the light/lung component of photoemulsion, in this case approximately the same as during interactions nucleus + Em. The formation/education of maximum is an effect of the complete disintegration of the light/lung photoemulsion nuclei in collisions nucleus + Em. ENDFOOTNOTE.

The value of this contribution can be rate/estimated approximately into 20-25o/o, if one assumes that the interactions a nucleus + HEM with $n_h < 6$ have, speaking in general terms, the same distribution of traces as during $n_h = 6 \div 20$ (dotted line in upper Fig. 462) ².

FOOTNOTE ². The composite probability of interactions with the heavy component of photoemulsion is obtained in this case equal to $51 \pm 60/o$ in a good agreement with theoretical data by Table 146 [56].

ENDFOOTNOTE.

When the number of shower protons $n_p \leq 2$, distribution $W(n_h)$ for the case nucleus + Em is sufficiently close to the distribution of particle tracks h- during interaction $\alpha + \text{Em}$; considerable disagreements are observed only with $n_h > 10$. With passage to large values n_p quickly is reduced the contribution of events with $n_h = 0, 1$ and is smoothed peak with $n_h \simeq 5$; during very large values n_p distribution $W(n_h)$ becomes almost constant up to $n_h \simeq 30$. The average number of slow particles n_h grow/rises proportional to the number of relativistic protons (Fig. 463).

From Table 150, where for a comparison are given also data for interactions p + Em and p + HEm with $T = 6.2$ GeV it is apparent that an average multitude of gray and black traces in the stars, which were being formed during the inelastic collisions of nuclei, independent of the nature of the impinging nucleus very close to the appropriate values for nucleon- nuclear collisions and in range $T \gtrsim 5$ GeV/nucleon within the limits of experimental errors remains actually constant/invariable.

Since, however, the effectiveness of the detection of stars with $n_h = 0, 1$ in the case of the interactions of two nuclei and in the case of

nucleon-nuclear collisions can considerably be distinguished, is more reliable comparison of the properties of these two interaction modes in the stars $n_h > 1$, the recording efficiency of which in both cases is approximately identical. Table 150 shows that in the stars, where $n_h = 2 \div 6$, average multitudes of low-energy particles \bar{n}_h for interactions nucleon + nucleus + nucleus are really/actually identical. In large stars with track population $n_h > 6$ on the average is born somewhat larger quantity of h-particles, than in the case of nucleon-nuclear collision; however, a difference in the values \bar{n}_h seems surprisingly small, if we consider the large difference in the number of nucleons, which participate in these two interaction modes, and the considerable difference in the number of being born shower mesons.

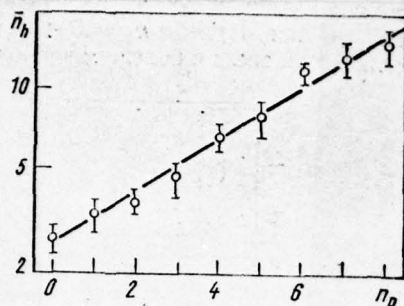


Fig. 463. Dependence of an average multitude of the heavily ionizing particles \bar{n}_h on the number of relativistic protons, emitted during inelastic interactions with the nuclei of the photoemulsion of space nuclei with charges $Z \geq 3$ and energy $T \approx 40$ GeV/nucleon [56].

Page 612.

From data given Table 150, then shows that the difference in the number of slow secondary particles in cases when with the nucleus of photoemulsion collide high-energy nucleon or nucleus, it is caused by the difference in the number of being born g-particles. Even more

vividly this is exhibited during the comparison of the distributions of the gray ray/beams $W(n_g)$. While in proton-nucleus interactions distribution $W(n_g)$ remains actually constant/invariable almost with a triple increase of energy T from 6.2 to 22.5 GeV (Fig. 464), passage to nuclear collisions in photoemulsion leads to a considerable decrease in the number of events in interval $n_g = 0 \div 5$ on the contrary, to an essential increase in the quantity of stars with the large number of gray ray/beams $n_g > 10$.

If we consider that the g- particles are the nucleons of loss in the same way as this occurs in the case of nucleon- nuclear collisions, then it may be concluded that during the collision of two nuclei into the process of interaction is involved the considerably larger number of intranuclear nucleons, than in the case of the nucleon or of pion-nuclear collision. At the same time from the data of Table 150 and from Fig. 464 it follows that the number of particles with black traces - both with small $n_h < 6$, and at large values n_h - remains almost constant/invariable during the replacement of the impinging nucleon by nucleus. Differences are noticeable only for the very large stars with $n_b > 15$, which actually were not observed in the case of collision nucleus + Em [44]; however the statistical accuracy of measurements is still insufficiently great in order that it would be possible to insist on this difference.

Hence it is possible to draw the conclusion that at high energies the process of the disintegration of target nucleus - especially the stage, connected with the evaporation of remanent/residual nucleus, very weakly depends on the nature of incident particle.

Somewhat large values \bar{n}_b , observed in the case of the collisions of nuclei with $n_h > 6$, indicate that the central collisions of nuclei are accompanied by the more spallation of target nucleus, than nucleon-nuclear collisions.

Number of secondary particles and the value of the excitation energy, transferred to target nucleus. The number of particles, emitted in the process of evaporation, is the function of a radius of the remanent/residual nucleus, which was being formed after of nucleus-target flew out cascade s- and g-particles. Therefore in order to compare the value of the excitation energy, transmitted to target nucleus during the inelastic collision of two nuclei, with the excitation energy of the remanent/residual nucleus, which is formed in the case nucleon- of nuclear interaction, convenient to select the events, in which the excited remanent/residual nuclei in the beginning of the process of evaporation would have identical size/dimensions.

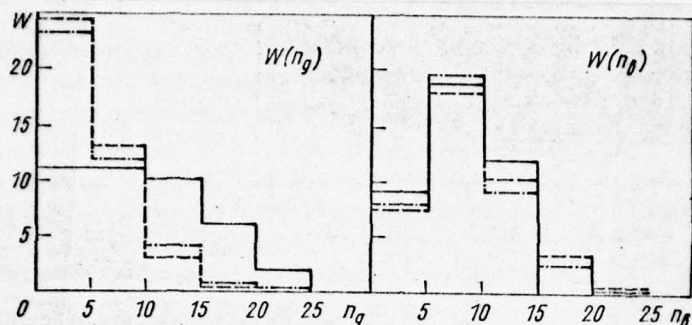


Fig. 464. Distribution of gray and black ray/beams in the stars, formed in photoemulsion by protons with energy $T = 6.2$ and 22.5 GeV (respectively broken and dot-dash histogram [60]) and by space nuclei with an energy of $T \approx 2-15$ GeV/nucleon (continuous histogram [44]). Are selected only events with $n_h > 6$. In each figure everything three histograms are calibrated to one and the same collision frequency.

Page 613.

It has already been stated above that the number of gray tracks in a

star may serve as a measure of the value of the residual nucleus while the mean plurality of of black ray/beams \bar{n}_b is the measure of the value of the excitation energy of this nucleus. Consequently, in order to obtain the representation of a difference in the excitations of remanent/residual nuclei, formed during the collisions of high-energy nucleons and nuclei with photoemulsion, one should compare an average multitude of black ray/beams in stars with the equal number of gray ray/beams. This comparison is carried out in Fig. 465. From this figure it is evident that with the fixed/recorded number of gray traces an average multitude \bar{n}_b in the case of nucleon-nuclear collisions is noticeably more. This means that the cascade recoil nucleons (g-particle) in nucleon- nuclear interaction on the average betray nucleus-target larger energy content how this it occurs with the interaction of two nuclei.

As in the case of nucleon- nuclear collisions, the average number of black ray/beams in stars with $n_h < 16$, formed by high-energy nuclei, approximately is proportional to the number of gray ray/beams. In other words, if the number of g-particles is small, then each such particle gives on the average the identical contribution to the excitation energy of nucleus-target. On the contrary, in very large stars an average multitude \bar{n}_b becomes, apparently, almost being independent of the number of gray ray/beams (see Fig. 465).

It is possible to indicate a whole series of the reasons, on the strength of which is disrupted the proportionality \bar{n}_b and n_g in large stars. This, first of all, is connected with the fact that with an increase in the excitation energy, i.e., during passage to large stars sharply grow/rises the probability of the emission of fragments with $Z \geq 3$, thanks to which substantially decreases the total number of particles, emitted by remanent/residual nucleus. Furthermore, in cases when the excitation energy of remanent/residual nucleus is very great, some evaporative particles can obtain this high energy, that their photographic tracks are identified as gray; this leads to a decrease in the set \bar{n}_b and simultaneously raises the number of gray ray/beams. The form of distribution in Fig. 465 is very sensitive to this effect. There are other reasons for the disturbance of proportionality \bar{n}_b and n_g [44].

In conclusion let us note that the value of the energy, transferred to target nucleus, is very weakly correlated with the number of mesons, which are formed during interaction.

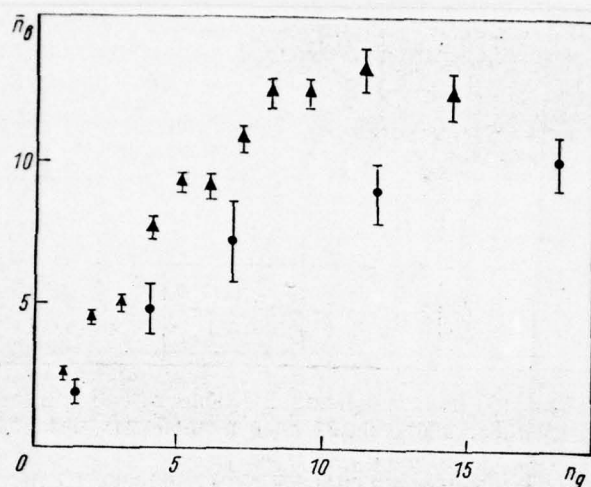


Fig. 465. Average multitude of black traces \bar{n}_b in photoemulsion stars with the different number of gray traces $\bar{n}_b = f(n_g)$ [44]: ● - for interactions nucleus + nucleus with $T \approx 2-5$ GeV/nucleon; ▲ - for proton-nucleus interaction with $T \approx 6.2$ GeV.

Page 614.

§109. Formation/education of α -particles and heavy fragments.

The characteristic feature of the inelastic collisions of nuclei is the formation/education of the considerable number of rapid α -particles and the heavier fragments, which take away the noticeable part of the energy of primary nucleus. In nucleon- and pion-nuclear collisions the formation/education of such high-energy α -particles, but the themes of heavier fragments, is incomparably more rare event (see Chapter 8 and 9).

Table 152 shows that 60-70o/o of the inelastic collisions of neutral space nuclei in photoemulsion is accompanied by the formation/education of α -particles and fragments. For the interactions of heavy nuclei this percentage is still above.

Because of large ionizing power the traces of high-energy fragments differ from the fine/thin traces of shower mesons and nucleons, at the same time of which it is possible to differ from the gray and black traces of evaporative particles, since they significantly are more powerfully collimated in the direction of the

motion of primary nucleus (see Fig. 153 and 154). Difficulties in the identification of these fragments appear only v during the collisions of the nonrelativistic nuclei, when the angles of emission of rapid fragments are very considerable and overlap with the angles of emission of evaporative particles from target nucleus. In this case it is required more detailed analysis, and satisfactory measurements can be conducted hardly ever [41, 47].

During the interaction of α -particles with nuclei the fragments with charge $Z = 2$ escape, in essence, from target nucleus and in the same way as this occurs in nucleon-nuclear collisions, their large part has low energy; with $T \gtrsim 1$ GeV/nucleon the escape probability of rapid nuclei ${}^3_2\text{He}$ composes a total of about 50/o [4]. In the collisions of more heavy nuclei the probability of the formation/education of relativistic α -particles considerably above and rapidly grow/rises with an increase in the charge of the impinging nucleus. In the photoemulsion stars, formed by space nuclei with $Z \gtrsim 10$, this probability comprises already about 70o/o (see Table 153). With an increase in charge Z rapidly grow/rises the number of cases, when simultaneously are born two, three and larger number of α -particles.

Table 152. The probability of the inelastic collision of space nucleus with an energy of $T \geq 1$ GeV/nucleon in photoemulsion, with which this nucleus decomposes to single-charged particles and N of fragments with charges $Z \geq 2$ [19, 38, 41, 50], c/o.

(1) Налетающее ядро	$N = 0$	$N > 0$	$N > 1$	$N > 2$
C, N, O $Z \geq 10$	36 ± 3 19 ± 3	64 ± 4 81 ± 6	26 ± 2 49 ± 5	6 ± 1 26 ± 3

Key: (1). Impinging nucleus.

Table 153. Relative probabilities of the appearance of relativistic α -particles during the splitting/fissions of different nuclei as a result of their interaction with photoemulsion.

(1) Первичное ядро	(2) Число α -частиц							$W_{\alpha}, \%$
	0	1	2	3	4	5	6	
Li, Be, B	96	60	16	0	0	0	0	44
C, N, O	193	100	57	26	0	0	0	49
$9 \leq Z \leq 19$	67	58	29	14	6	3	0	62
$Z \geq 20$	11	11	9	5	2	3	0	72

Note. W_{α} is a portion of the collisions, as a result of which appear such α -particles. The data of tables are based on the analysis of 770 stars, formed relativistic primary with medium energy $T \sim 3$ GeV/nucleon [47].

Key: (1). Primary nucleus. (2). Number of α -particles.

Page 615.

Table 154. Average number of α -particles, which are formed during the inelastic interaction of space nucleus with photoemulsion.

(1) Космическое ядро	(2) $T, \text{ Гэв/нуклон}$	\bar{n}_α	Ядро-мишень*; критерий отбора (3)	Литература (4)
α	88	$> 0,23^{2*}$	Em; все звезды (5)	[49]
Li, Be, B	$0,1 \div 0,5$ $\geq 1,5$ $2 \div 15$	$0,60 \pm 0,3$ $> 0,5^{3*}$ $0,85 \pm 0,25$	Em; » » Em; » » Em; » »	[49] [47] [3]
C	$2 \div 15$ 40	$0,5 \pm 0,2$ $1,0 \pm 0,2$	Em; » » Em; » »	[3] [56]
C, N, O	$\geq 1,5$ $2 \div 15$ $2 \div 15$ $2 \div 15$ $> 7,5$ 40 40 40	$0,78^{3*}$ $0,73 \pm 0,13$ $0,87 \pm 0,15$ $0,53 \pm 0,18$ $0,93 \pm 0,06$ $0,83 \pm 0,13$ $1,1 \pm 0,2$ $0,38 \pm 0,14$	Em; » » Em; » » LEm; $n_h \leq 6$ HEm; $n_h > 6$ Em; все звезды (5) Em; » » LEm; $n_h \leq 6$ HEm; $n_h > 6$	[47] [3] [3] [3] [6, 43] [56] [56] [56]
N	$2 \div 15$ 40	$0,6 \pm 0,3$ $0,7 \pm 0,2$	Em; все звезды (5) Em; » »	[3] [56]
C, N, O, F	$0,1 \div 0,3$ $0,3 \div 0,5$ $0,1 \div 0,5$ 3 3 3 3 $2 \div 15$	$0,67 \pm 0,15$ $0,88 \pm 0,20$ $0,65 \pm 0,16$ $1,25 \pm 0,1$ $1,45 \pm 0,2$ $1,1 \pm 0,15$ $0,15 \pm 0,04$ $0,69 \pm 0,12$	Em; » » Em; » » Em; » » Em; $n_h > 1$ LEm; $n_h = 2 \div 7$ HEm; $n_h \geq 8$ HEm; $n_h \geq 28$ Em; все звезды (5)	[46] [46] [46] [25] [25] [25] [25] [3]
O	$2 \div 15$ 40	$0,9 \pm 0,2$ $0,74 \pm 0,2$	Em; » » Em; » »	[3] [56]
$Z \geq 3$	$0,1 \div 0,3$ $0,1 \div 0,5$ $2 \div 15$ $2 \div 15$ $2 \div 15$	$0,9 \pm 0,1$ $0,9 \pm 0,1$ $0,9 \pm 0,1$ $1,0 \pm 0,14$ $0,80 \pm 0,14$	Em; » » Em; » » Em; » » LEm; $n_h \leq 6$ HEm; $n_h > 6$	[46] [46] [3] [3] [3]
$9 \leq Z \leq 19$	1,5	$1,11^{3*}$	Em; все звезды (5)	[47]
$Z \geq 10$	$0,1 \div 0,3$ $0,1 \div 0,5$ 3 3 3 3 $2 \div 15$ $2 \div 15$ $2 \div 15$ $> 7,5$	$1,6 \pm 0,4$ $1,5 \pm 0,3$ $1,4 \pm 0,1$ $1,6 \pm 0,2$ $1,3 \pm 0,1$ $0,6 \pm 0,15$ $1,2 \pm 0,2$ $1,1 \pm 0,3$ $1,3 \pm 0,3$ $1,30 \pm 0,09$	Em; » » Em; » » Em; $n_h > 1$ LEm; $n_h = 2 \div 7$ HEm; $n_h \geq 8$ HEm; $n_h \leq 28$ Em; все звезды (5) LEm; $n_h \leq 6$ HEm; $n_h > 6$ Em; все звезды (5)	[46] [46] [25] [25] [25] [25] [3] [3] [3] [43]
$Z \geq 20$	$\geq 1,5$	$1,65^{3*}$	Em; » »	[47]

Key: (1). Space nucleus. (2). GeV/nucleon. (3). Target nucleus ¹; the criterion of selection.

FOOTNOTE ¹. See note ² to Table 149. ENDFOOTNOTE.

(4). Literature. (5). All stars.

the -----

FOOTNOTE ². The corrected value relates only to those α -particles, whose rate is almost such as of initial particle. ³. The only relativistic α -particles. ENDFOOTNOTE.

End Section.

Page 616.

The experimental values of an average/mean multitude of α -particles for different energies and the different nuclei, which interact with photoemulsion, are assembled in Table 154. This multitude sufficiently weakly depends on energy of the impinging nucleus T , and with fixed values of T and Z decreases with passage to stars with the large number of gray and black ray/beams. The latter can be explained by the more spallation of the impinging nucleus during central collisions.

The representation of of the average/mean characteristics of photoemulsion stars, which contain α -particles, can be obtained from Table 155.

Table 156 for several most frequently being encountered in practice substances are assembled the experimental values of the parameters of fragmentation P_{ij} , defined as the average number of fragments of the type "j", which are formed during the splitting/fission of the impinging nucleus of the type i . (More detailed data can be found in monographs [41, 47] and in the article [32]; there it is possible to find further bibliography). As is

evident, the number of fragments with charge $Z \geq 3$ composes the very significant magnitude, the large, the greater the charge of the impinging nucleus. At the same time the parameters of fragmentation sufficiently weakly change with an increase in the mass of target nucleus and energy of the impinging nucleus T.

Table 155. Average characteristics of photoemulsion stars with the α -particles and of the stars, which contain fragments with charge $Z > 3$. Stars are formed by space nuclei with energy $T > 1.7$ GeV/nucleon [45].

(1) Первичное ядро	(2) Звезды с α -частицами		(3) Звезды с осколками $Z \geq 3$		
	\bar{n}_p	\bar{n}_h	\bar{n}_p	\bar{n}_h	$\bar{Z}_{\text{оск}}$
$3 \leq Z \leq 9$	1,9	3,0	2,1	4,0	4,6
$Z \geq 10$	5,6	8,7	6,0	8,6	7,8

$\bar{Z}_{\text{оск}}$ is the average charge of the being born fragments.

Key: (1). Primary nucleus. (2) Stars with α -particles. (3). Stars with fragments.

Table 156. Parameters of fragmentation P_{ij} for the interaction of space nuclei with different substance with energy $T > 7.5$ GeV/nucleon.

(1) Мишень	(2) Первичное ядро i	(3) Фрагменты j				(4) Литература
		α	L	M	H	
Углерод (5)	L	$0,48 \pm 0,11$	$0,13 \pm 0,06$	—	—	[34]
	M	$1,05 \pm 0,11$	$0,29 \pm 0,04$	$0,09 \pm 0,03$	—	[34]
	H	$1,31 \pm 0,15$	$0,23 \pm 0,05$	$0,30 \pm 0,05$	$0,27 \pm 0,05$	[34]
Воздух (6)	L	$0,51 \pm 0,08$	$0,15 \pm 0,05$	—	—	[22]
	M	$1,00 \pm 0,08$	$0,24 \pm 0,03$	$0,11 \pm 0,02$	—	[22]
	H	$1,34 \pm 0,12$	$0,26 \pm 0,04$	$0,29 \pm 0,04$	$0,17 \pm 0,03$	[22]
Полиэтилен (7)	L	$0,87 \pm 0,15$	$0,17 \pm 0,07$	—	—	[22]
	M	$0,90 \pm 0,08$	$0,30 \pm 0,04$	$0,09 \pm 0,02$	—	[22]
	H	$1,41 \pm 0,19$	$0,36 \pm 0,07$	$0,16 \pm 0,05$	$0,27 \pm 0,06$	[22]
Эмульсия (8)	M	$0,93 \pm 0,06$	$0,21 \pm 0,02$	$0,19 \pm 0,02$	—	[6, 43]
	H	$1,30 \pm 0,09$	$0,14 \pm 0,03$	$0,33 \pm 0,04$	$0,31 \pm 0,04$	[43]

Key: (1). Target. (2). Primary nucleus. (3). Fragments. (4). Literature. (5). Carbon. (6). Air. (7). Polyethylene. (8). Emulsions.

Table 157 in an example of interactions with the photoemulsion of the neutral group of space nuclei shows the composition of the fragments, which associate the formation of different remanent/residual nuclei. The multiple production of fragments, as a rule, is accompanied by the escape of one or several α -particles.

In order to compare the probabilities of the formation of different remanent/residual nuclei during the splitting/fission of target nucleus in the collision of two nuclei and in collision nucleon + nucleus, let us examine the ratio of the number of stars with a quantity of the gray and black ray/beams $a < n_h \leq b$, which appear during inelastic interactions two nuclei, to the appropriate number of stars from nucleon- the nuclear interaction:

$$\mathcal{R} = n(a < n_h \leq b)_{\text{нн}} / n(a < n_h \leq b)_{\text{НЯ}}.$$

It is not difficult to consider, that this value is equal to the relation of the yield cross sections of remanent/residual nuclei with charges $(Z_M - b) \leq Z < (Z_M - (a + 1))$ in inelastic collisions nucleus + nucleus and nucleon + the nucleus:

$$\mathcal{R} = \sum_Z \sigma(Z)_{\text{нн}} / \sum_Z \sigma(Z)_{\text{НЯ}}.$$

Addition here is fulfilled through all charges from $(Z_M - b)$ to $(Z_M - (a + 1))$, Z_M the initial charge of target nucleus. (Recall that each gray or black trace is connected with the loss of one charge nucleus target; the

contribution of low-energy mesons and the small number of slow multiply-charged particles can be disregarded).

The values of relation \mathcal{R} for the case of the interactions of space nuclei with photoemulsion with $T \simeq (2 \div 15)$ GeV/nucleon [3, 19, 23, 50] and the proton-nucleus interactions with $T = 6,2$ GeV [60] are shown in Fig. 466. The fact that these values differ significantly from unity, attests to the fact that the formation of remanent/residual nuclei in two interaction modes in question occurs differently.

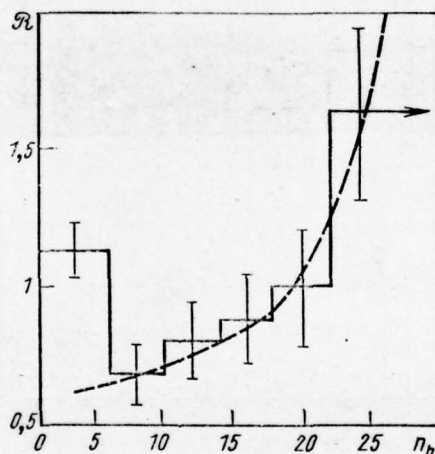


Fig. 466. Value of relation $\mathcal{R} = n(a < n_h \leq b)_{\text{MPT}} / n(a < n_h \leq b)_{\text{NPT}}$ in the different intervals a-b [44]. Events with $n_h = 0, 1$ are reject/thrown. Dotted line is an approximation of the average values \mathcal{R} for the case of interactions with heavy nuclei.

Table 157. Fragments, which are formed during nuclear disintegration C, N, O with an energy of $T \approx 40$ GeV/nucleon as a result of their interactions with photoemulsion [56].

(1) Остаточ- ное ядро	(2) Осколки	(3) Число осколков	%	(1) Остаточ- ное ядро	(2) Осколки	(3) Число осколков	%
He	α	122	100	C	3α 2Li	41 0	52,6 0
Li	Li	20	100	N	N $B + \alpha$ $\text{Li} + 2\alpha$ $\text{Li} + \text{Be}$	18 9 0 0	66,7 33,3 0 0
Be	Be 2α	14 91	13,3 86,7	O	O $C + \alpha$ $\text{Be} + 2\alpha$ 4α 2Be $\text{Li} + \text{B}$	3 6 1 2 0 0	25,0 50,0 8,3 16,7 0 0
B	B $\text{Li} + \alpha$	23 15	60,6 39,4				
C	C $\text{Be} + \alpha$	26 11	33,3 14,1				

Key: (1). Remanent/residual nucleus. (2). Fragments. (3). Number of fragments.

Page 618.

In interval $1 < n_h \leq 6$ value \mathcal{R} is close to unity. This it is possible to explain themes that into this interval fall the stars, caused by interactions both with light/lung and with heavy by the components of photoemulsion. In the first case frequently occurs the virtually complete the disintegration of target nucleus regardless of the fact, is the incident particle nucleus or nucleon. During interaction with heavy component, the nature of incident particle also is not very important, since stars with $n_h \leq 6$ are formed, in essence, during peripheral collisions with target nucleus.

A decrease in the values \mathcal{R} with $n_h \simeq 6$ occurs because of the fact that interactions with light nuclei give contribution only with $n_h \leq 6$.

Large stars with the number of ray/beams $n_h > 6$ are most convenient for the comparison of the probabilities of the formation of remanent/residual nuclei, since in this case we deal only with one group of heavy target nuclei. The value of relation \mathcal{R} here considerably differs from unity: if the formation of remanent/residual nuclei with charge $Z \leq (Z_M = 20)$ more probably in

nucleon-nuclear collisions, then light nuclei with an even smaller charge are formed predominantly in collisions nucleus + nucleus.

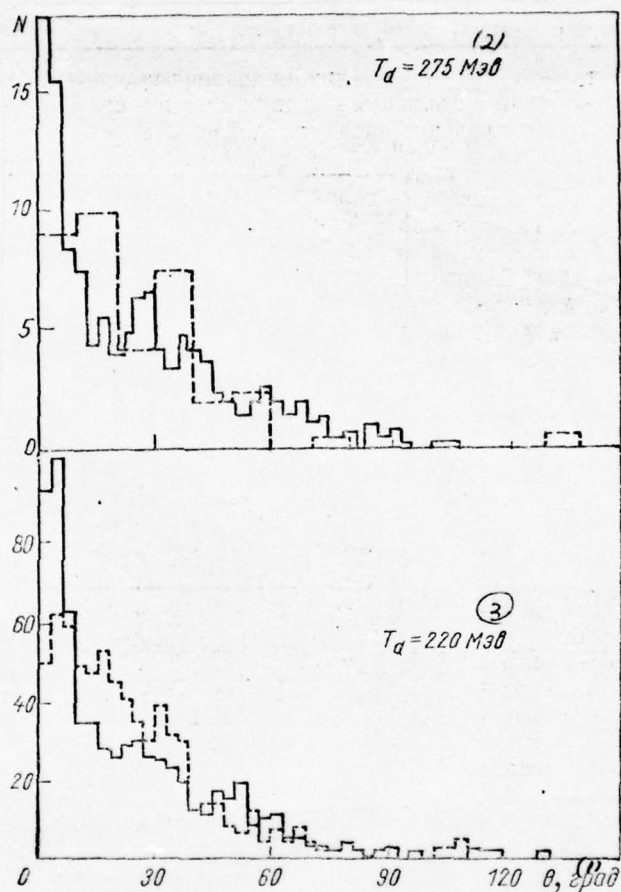


FIG. 467.

Fig. 467. The angular distributions of rapid protons ($T_p > 50$ MeV), that are formed during the bombardment of photoemulsion with deuterons with energy T_d . Continuous histograms are the calculation for the medium nucleus of photoemulsion ^{70}Ga according to cascade model without taking into account of the diffusivity of nuclear boundary (see §112); dotted line - the experimental data from works [5, 53].

Key: (1). deg. (2). MeV.

Page 619.

§110. Angular distributions of secondary particles.

deuteron- nuclear interactions. The distributions of the angles of emission of particles, which are born in the inelastic collisions of deuterons with nuclei, are similar to those observed in the case nucleon- of nuclear interactions with energy $T \simeq T_d/2$, if we do not consider the sharp peak in the region of very small angles, caused by the processes of the disintegration of deuteron as a result of the peripheral processes of stripping, coulomb and diffraction

splitting/fissions (Figs. 467 and 468).

With an increase of energy of deuteron secondary particles ever more are concentrated in the region of small angles. At the fixed value of primary energy T_d the passage to heavier targets is accompanied by the broadening of the angular distribution, which, however, it is very small. For example, with $T_d = 190$ MeV in work [30] for the average half angle $\bar{\theta}_{1/2}$ is obtained the dependence

$$\bar{\theta}_{1/2} = \frac{180}{\pi} (0,155 + 0,0006Z). \quad (11.1)$$

A sevenfold increase of the charge from $Z = 13$ (aluminum) up to $Z = 92$ (uranium) is accompanied only by a 300/o increase in the angle $\bar{\theta}_{1/2}$.

Angular particle distributions in collisions $\alpha + \text{nucleus}$. The typical angular distributions of the charged shower particles for this case are shown in Fig. 469 and 470. Peak in the region of small angles is almost wholly caused by the contribution of the very rapid protons whose energy is close to the initial energy of the nucleons, which was a part of the impinging α -particle: $\mathcal{E} \simeq T_\alpha/4$. One should also expect that certain impurity/admixture in the region of small angles give the protons, which were being formed in the course of intranuclear cascade within target nucleus. The secondary mesons are distributed in considerably wider angular interval.

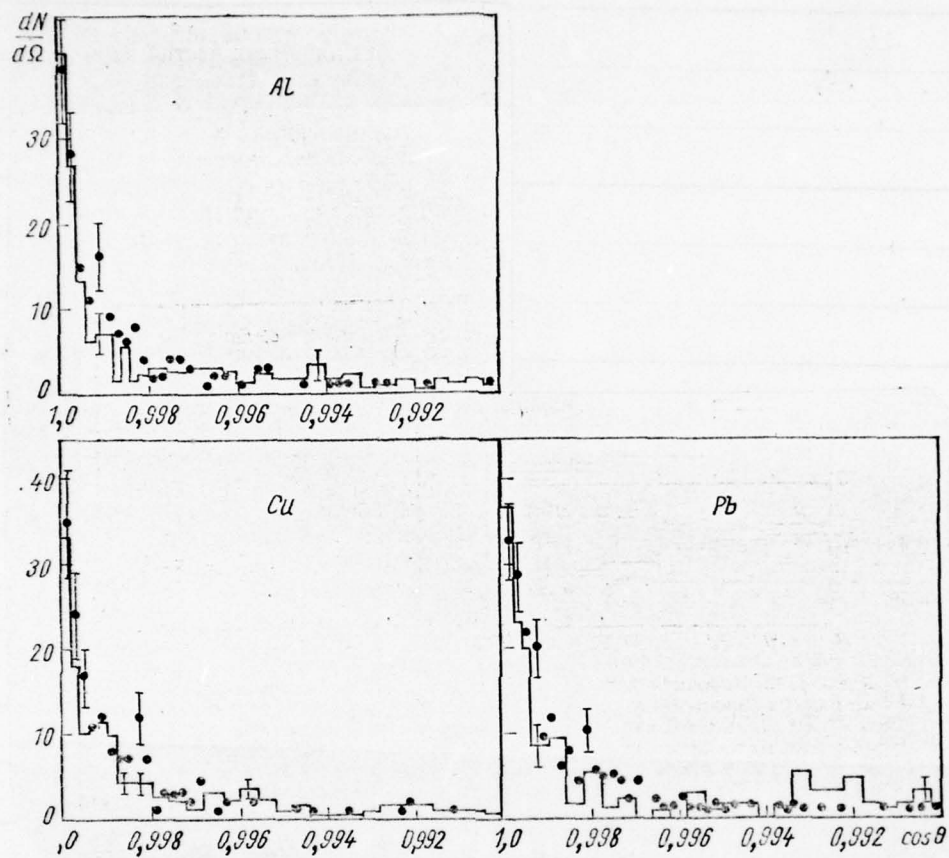


FIG. 468.

Fig. 468. The angular distributions of the protons (in arbitrary unity), formed during nuclear bombardment Al, Cu and Pb by deuterons with energy $T = 2.1$ GeV. Histograms are the calculation according to cascade theory taking into account the diffusivity of nuclear boundary (see §112); point - the experimental data from work [36].

Page 620.

The special role of protons with energy $\mathcal{E} \simeq T_\alpha/4$ is exhibited with smaller energies of α -particles (order several hundreds of million electron volt). This is distinctly evident, for example, in angular distribution of singly charged secondary particles in Fig. 470. Secondary particles at velocities, close to the speed of primary α -particle, always have very small angle of emission. All this indicates that secondary particles with energies $\mathcal{E} \simeq T_\alpha/4$ are the nucleons, which was earlier part of the impinging α -particle and noninteracted with target nucleus.

In comparison with the angular distribution of shower particles from inelastic nucleon-nuclear interactions the shower particles, which are formed in collisions $\alpha + \text{nucleus}$, have distribution, more concentrated in the region of small angles. This is observed both with small and during high energies (see Fig. 468-471 and Table 158)

The typical angular distributions of gray and black ray/beams in the stars, which are formed during the inelastic collisions of α -particles with the nuclei of photoemulsion, are shown in Fig. 469. In the margins of error in the measurements these distributions do not differ from the appropriate angular particle distributions from nucleon-nuclear collisions.

Figure 471 shows the distributions of secondary doubly charged particles. The differences for interactions $p + Em$ and $\alpha + Em$ in this case also in practice are not observed. In both cases of distribution $W(\theta)$ sufficiently insignificantly they differ from isotropy with the small advantage of the escape of particles into forward half sphere. All this makes it possible to assert that the doubly charged particles in inelastic collisions $\alpha + Em$ (in essence this α -particle) are formed, mainly, in the process of evaporation.

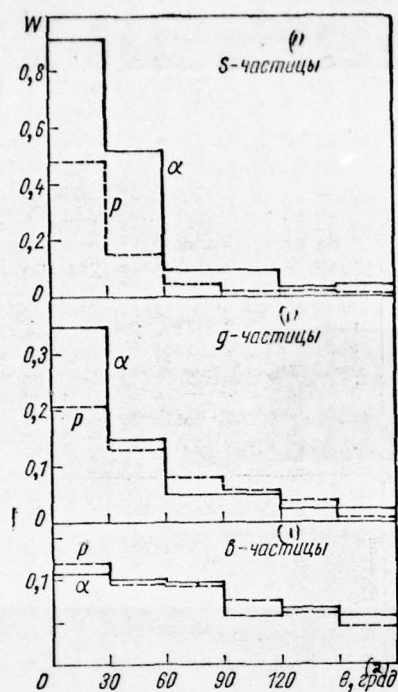


FIG 469.

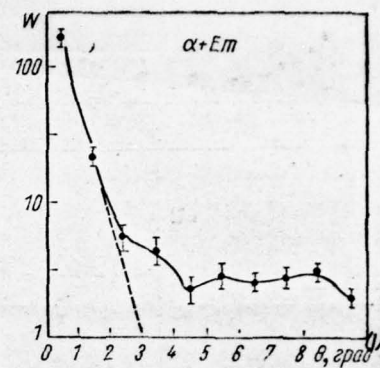


FIG. 470.

Fig. 469. The angular distributions of the secondary charged particles in the photoemulsion stars, formed by space protons and α -particles with an energy of T , greater than 1 GeV/nucleon [18].

Key: (1). particle. (2). deg.

Fig. 470. The angular distribution of shower particles in the photoemulsion stars, formed by space α -particles with an energy of T , greater than 6 GeV/nucleon [4] (by dotted line is noted the distribution of the secondary very rapid protons).

Key: (1). deg.

Table 158. The average half angle of emission of shower particles in inelastic collisions $\alpha + \text{Em}$ with very high energies (according to the data [29]; were take/selected only events with $n_s > 4$)

$T, (M)$ Гзе/нуклон	$\theta_{1/2}, (A)$ град
~ 15	$22,0 \pm 6,5$
~ 125	$5,3 \pm 0,9$

Key: (1). GeV/nucleon. (2). deg.

Page 621.

Shower particles, which are born during the collisions of more heavy nuclei. The angular distributions of the shower particles, which are born in the inelastic interactions of nuclei with charge $Z > 2$, in general terms the same as for collisions $\alpha + \text{nucleus}$. Particles are strongly collimated in the region of small angles; with a decrease in the angle θ sharply grow/rises the contribution of protons with the energies, close to energy of the nucleons, which was a part of the impinging nucleus. This one can see well, in particular, in Fig. 472, where are given the angular distributions of the shower particles, formed in photoemulsion by the neutral group of space nuclei with an energy of $T \approx 40 \text{ GeV/nucleon}$. In the stars, where the number of relativistic protons n_p close to the total number of shower particles n_s , the average angle of emission of particles is considerably less than in the stars, where is great the number of mesons n_π .

Figure 473 gives the angular distributions of shower particles from the interactions, generated by space nuclei with charge $Z \geq 3$ and energy $T \approx (2-15) \text{ GeV/nucleon}$. As in Fig. 472, is distinctly

observable sharp peak in the region of very small angles (at $\theta \lesssim 3^\circ$). From the fact that was said in the preceding/previous sections, it is possible to expect that this peak was formed by the protons, which did not experience direct collisions with intranuclear nucleons; the protons, which participated in intranuclear collisions, and the newly born in this case particles were distributed in wider angular cone around the central cone of the protons.

In order to explain, is how justified this picture, Fig. 473 shows the angular distributions of the pions, which were being formed in N - N-collisions with the energies, close to the medium energy of the nucleons of the impinging nucleus $T = 5-10$ GeV. Distributions are calibrated to the total number of shower mesons $n_\pi = \sum (n_s - n_p)$, where the addition it is fulfilled through all that which was recorded stars ¹.

FOOTNOTE ¹. The distributions of mesons are calculated under the assumption of isotropic dispersion/divergence and constant momentum/impulse/pulse in the center-of-gravity system N + N [3]. However, because of the effect of the relativistic compression of angles with passage to the laboratory coordinate system these simplifications are unessential, and distribution in Fig. 473 can be considered the sufficiently good approximation of the true angular distribution of pions. ENDFOOTNOTE.

In region $\theta > 25^\circ$, i.e., during $\cos \theta < 0.9$, the experimental distribution of shower particles will agree well with calculated which together with Fig. 472 confirms assumption about the fact that the overwhelming majority of the s-particles, which escape at wide angles, are pi-mesons. As concerns disagreements at small angles, they they are represented by too considerable in order that them it would be possible to ascribe to inaccuracies in the calculation of the distribution of mesons, to explain by statistical errors in the experimental histogram or to interpret only as contribution of several noninteracted protons of primary nucleus. Apparently, it is more reasonable to assume that for peak in the region of very small angles are significantly critical the protons, which are formed during the processes, connected with splitting/fission and the subsequent evaporation of the impinging nucleus (comp. with Fig. 459).

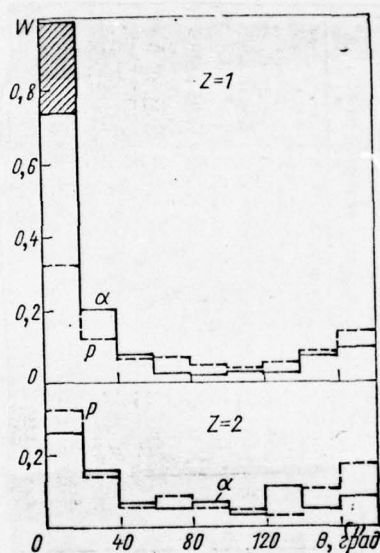


Fig. 471. Angular distributions of secondary one- and doubly charged particles in the photoemulsion, irradiated by protons with energy $T = 94$ MeV [31] and α -particles with energy $T = 88$ MeV/nucleon [49] (by

shading is noted the contribution of particles at velocities, approximately equal to the speed of primary α -particle).

Key: (1). deg.

Page 622.

Along with the total angular particle distribution s - of all stars in left Fig. 473 is shown also the distribution of shower particles only for stars with the number of gray and black traces $n_h > 8$ and containing not one rapid fragment. Such stars can be considered as result of the central collisions of the impinging nuclei with the heavy nuclei of photoemulsion. Between two distributions occurs excellent agreement in interval $\theta = 3.9-12^\circ$ (in this interval both distributions are calibrated to the identical number of particles), at the same time peak at $\theta < 2.2^\circ$ completely is absent from the group of the events, which correspond to central collisions, as this it was to be expected, on the basis of our assumption about the origin of particles, forming this peak.

In three right figures 473 (a, b and c) the total angular distribution for central collisions are represented depending on the number of h-ray/beams in star. Distributions are again calibrated to

the identical number of particles in interval $\theta = 3.9-12^\circ$. In Fig. a, which corresponds to interactions with the light nuclei of photoemulsions and to peripheral collisions with its heavy component, is distinctly observable narrow peak at $\theta < 2.2^\circ$. The particles, which give the contribution to this peak, can be the noninteracted with target protons of the impinging nucleus and the protons, which arose as a result of evaporation or in the process of more rapid decomposition/decay of the highly excited fragments of the impinging nucleus. Such fragments, as a rule, are formed during peripheral collisions, when with target nucleus intensely interact a total of several nucleons of the impinging nucleus; energy and angle of emission of fragment are close to the appropriate values for a parent nucleus.

Distributions in Fig. b can be compared to collisions with the heavy nuclei of photoemulsion. Peak in the region of small angles in this case appears considerably smaller. This is caused themes that the probability to the nucleon of the impinging nucleus to fly through target nucleus or past it without interaction considerably decreases as a result of an essential increase in the size/dimensions of this nucleus. It is possible therefore to consider that the basic contribution to the shaded region in Fig. b give, apparently, the protons, which arose in the processes of evaporation and decomposition/decay of the excited fragments, which chipped off

during peripheral collisions.

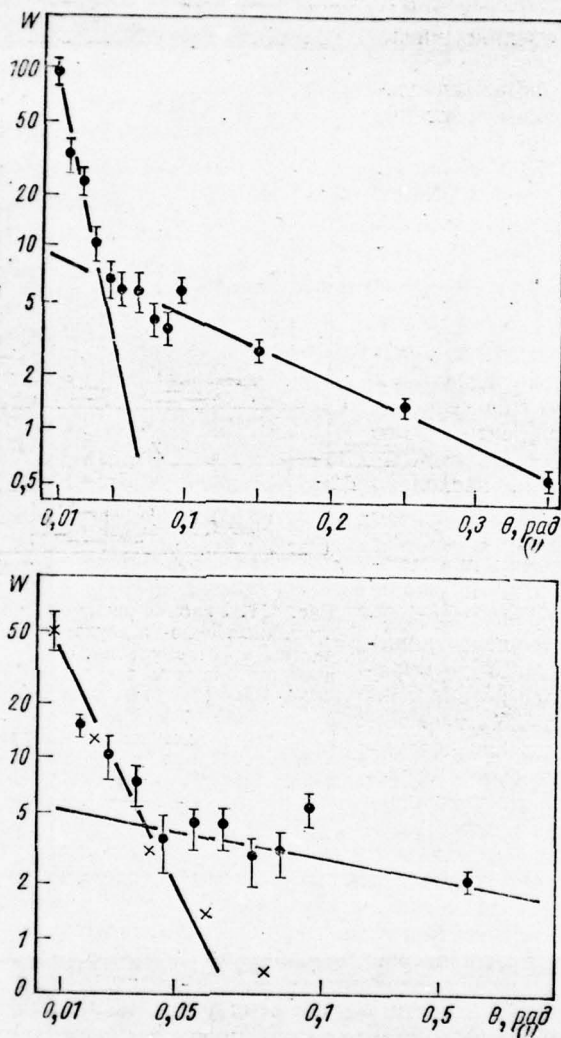


Fig. 472. The angular distribution of α -particles from the stars, formed in photoemulsion by nuclei C, N, O with an energy of $T \approx 40$ GeV/nucleon [56]: in lower figure \times, \bullet — distribution for stars with the small and large number of being born mesons $n_\pi = n_s - n_p$ (respectively $n_\pi < n_p \approx n_s$ and $n_\pi > 0.8 n_s$).

key: (1). deg.

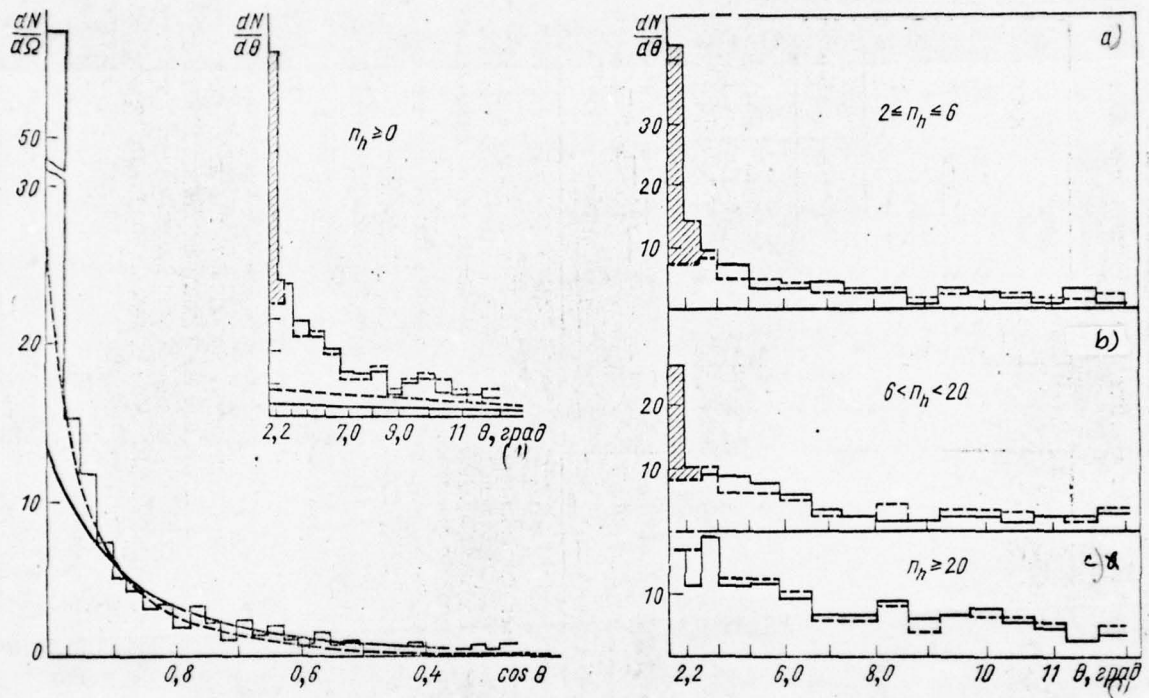


FIG. 473.

Fig. 473. Angular distribution of the frequency of the escape of shower particles in stars with the different number of h-ray/beams, formed by space nuclei during $T \approx (2-15)$ GeV/nucleon [3]: continuous histograms is a result of measurements for all stars with the indicated in figure value n_h ; broken histograms - the result of measurements for "central" collisions with the heavy nuclei of emulsion. By shading is noted the contribution of the protons whose part was a part of the impinging nucleus, and another part was formed upon decay of the highly excited fragments of this nucleus. In the left figure is separately represented the distribution for the interval of angles $\theta \leq 12^\circ$; by continuous and dotted curves are shown the distributions of the pions, which were being born in N - N-collisions respectively with energy $T = 5$ and 10 GeV.

Key: (1) - deg.

Page 624.

In distributions in Fig. c, which correspond to central collisions with heavy nuclei and which are accompanied by the almost complete splitting/fission of the impinging nucleus on separate nucleons, the peak in the region of small angles entirely disappears.

Thus, the observed in experiment structure of the angular distributions of shower particles will be in complete agreement with our picture of the inelastic collision of two nuclei.

The supplementary confirmation of the considerable role of evaporative particles in narrow cone at $\theta < 2.2^\circ$ can be obtained, if we among the stars, which give the contribution to distributions in Fig. a, select those, that correspond to the collisions of approximately identical nuclei. In this case on the strength of symmetry number, energy and angles of emission of s-particles in the systems of the coordinates, where either the impinging nucleus or target nucleus are found in rest, on the average must be identical. Therefore, converting into the system of the rest of the impinging nucleus the angles, which black ray/beams have in the laboratory coordinate system, it is possible to obtain the distribution, which approximately coincides with the angular distribution, which in the laboratory coordinate system they have particles, which were being formed as a result of the evaporation of the fragments of the impinging nucleus.

As showed the calculations, made in work [3], the obtained in this way distribution is really/actually concentrated in region $\theta \lesssim 2-3^\circ$.

Distribution of gray ray/beams in the collisions of nuclei with $Z \geq 3$. In Fig. 474 angular distributions of gray ray/beams from the stars, formed by the space nuclei of different energies, are compared with angular to particle distributions g^- from proton-nucleus interactions. During $T \geq 1$ GeV these distributions, in spite of a difference in the kinetic energies of bombarding protons and nuclei and different targets, are close to each other.

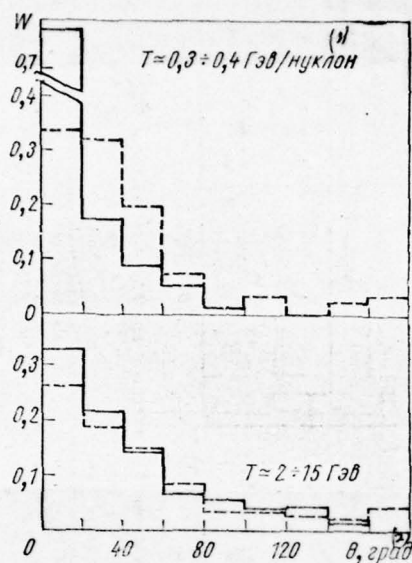


FIG. 474.

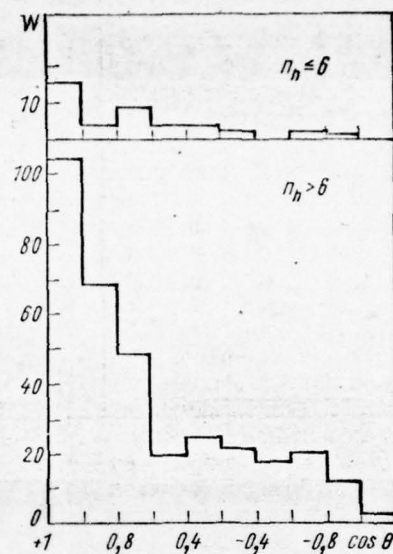


FIG. 475.

Fig. 474. The angular distributions of the gray ray/beams $dN/d\Omega$ in the stars, which were being formed during interactions with the photoemulsion of protons and space nuclei with an energy of T ,

GeV/nucleon. Continuous and broken line of histogram in the upper figure - respectively the interaction of nuclei and protons [14, 46]. Energy of g-particles $T > 100$ MeV. Continuous histogram in lower figure is distribution for interactions nucleus + Em [46], dotted line is experimental data Loka, etc. [37] for interactions p + NEm with $T = 950$ MeV. Energy of g- particles in lower figure $T > 25$ MeV.

Key: (1). GeV/nucleon. (2). deg.

Fig. 475. The angular distribution of gray ray/beams in the stars, formed during the interactions of space nuclei with light/lungs ($n_h \leq 6$) and with the heavy ($n_h > 6$) nuclei of photoemulsion. Energy of the impinging nuclei $T \approx 2-15$ GeV/nucleon [3].

Page 625.

The angles, hearth by which outgoing particles with gray traces, are sufficiently weakly sensitive to the number of h-ray/beams in star (Fig. 475). All this indicates that in the case of the collision of two nuclei of g-particle also, apparently, they are the recoil nucleons, which were being formed in target nucleus in the course of the rapid (cascade) stage of process.

Somewhat different situation in the region of energies T , which do not exceed several hundreds of million electron volt by nucleon; in distributions $W(\theta)$ during the collisions of two nuclei in this case is observed the considerable surplus of gray traces at small angles $\theta < 10-20^\circ$. This is caused by the fact that with low energy T g -particles are still many protons, emitted in the processes of evaporation and rapid decomposition/decay of the excited fragments of the impinging nucleus (see Fig. 459). To these protons there is no conformity in nucleon-nuclear collisions; therefore the latter one should compare only with the distributions of g -ray/beams from the central nuclear collisions, when the impinging nucleus almost completely disintegrates to nucleons and is not formed into its excited fragments. Figure 476 shows that the contribution in the interval of small angles really/actually originates from peripheral collisions. The histogram, which relates to central collisions, is sufficiently close to the distribution of g -ray/beams in proton-nucleus collisions. ("Central" collisions in Fig. 476 are approximately determined from the condition that in the star would be not more than one α -particle and not at all would be heavier fragments; all the remaining collisions were considered "peripheral".)

During $\theta > 20^\circ$ distributions of g -ray/beams from central and peripheral collisions coincide; this is connected with the fact that as a result of purely kinematic relationship/ratios (see Fig. 459)

virtually all protons, emitted by the excited fragments of the impinging nucleus, escape into interval $\theta < 20^\circ$. For this same reason, independent of the nature of incident particle, turn out to be identical angular particle distributions g^- to energies $\mathcal{E} = 30 - 100$ MeV in Fig. 477.

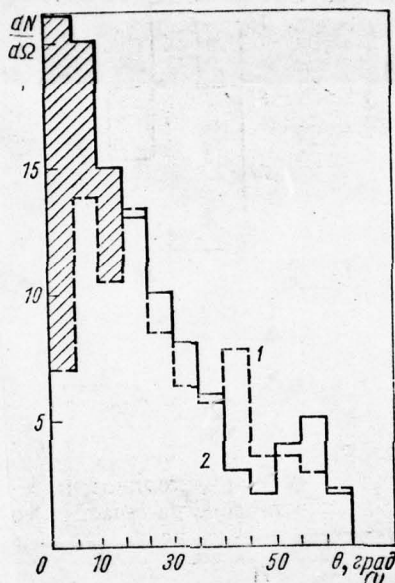


Fig. 476. The angular distribution of gray traces in the photoemulsion stars, which were being formed during the central (1)

and peripheral (2) collisions of space nuclei with an energy of $T \approx 0.3-0.4$ GeV/nucleon. The shaded region is the contribution of the protons, emitted by the excited fragments of impinging nucleus [46]. Distributions are calibrated to the identical number of particles in interval $\theta > 20^\circ$. Energy of g^- particles $T > 100$ MeV.

Key: (1). deg.

Table 159. The mean angle, into which escapes the half of particles with black traces, the forming during interaction space nuclei with charge $Z \geq 3$ with nuclei photo-emulsin [2].

$T, (g)$ Гэв/нуклон	Критерий отбора (2)	$\theta_{1/2}, \text{ град}$
$> 1,5$	Все звезды (4)	80
$> 1,5^{(1)}$	$n_h > 7$	80
$< 1,5^*$	Все звезды (4)	75
$< 1,5^*$	$n_h \leq 7$	69
$< 1,5^*$	$n_h > 7$	77

* Средняя энергия $\bar{T}=0,6$ Гэв/нуклон.

Key: (1). GeV/nucleon. (2). Criterion of selection. (3). deg. (4). All stars.

FOOTNOTE 1. Medium energy $\bar{T} = 0.6$ GeV/nucleon. ENDFOOTNOTE.

Page 626.

Black ray/beams. The typical angular distributions of black ray/beams in the stars, which are formed during the interactions of two nuclei, are shown in Fig. 478. Although in comparison with g-, but themes more with s-particles, these distributions are considerably more close to isotropic, is distinctly observable the preferred escape of particles into forward half sphere (Table 159). With $T \simeq 2-15$ GeV/nucleon the relation of the numbers of particles, which escape respectively into front/leading and rear hemispheres, composes 1.5 ± 0.1 and it remains virtually themes during a decrease in the energy of the impinging nucleus T almost by two orders. Very weakly depends on energy T the form of distribution $W(\theta)$.

The distributions of black ray/beams in the stars, formed during the collisions of two nuclei and during collisicns $p + Em$, virtually are not distinguished.

All these properties of b-particles can be understood, if we

assume that they are formed in the process of the evaporation of the excited nucleus, which remains after the escape of cascade particles from target nucleus. Since this nucleus has sufficiently noticeable speed in the direction of the motion of the impinging nucleus (see below, page 631), angular particle distribution $b-$ in the laboratory coordinate system is anisotropic.

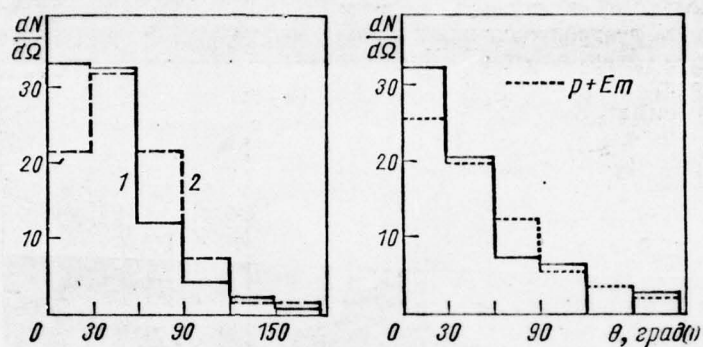


Fig. 477. Angular distribution of g-particles with energy $\mathcal{E} = 30 - 100$ MeV: in the left figure are compared the distributions from the stars, formed by space nuclei in two different energy bites; during $T = 0.1-0.3$ GeV/nucleon (1) and during $T = 0.3-0.4$ GeV/nucleon (2). In the right figure are compared the angular distributions from interactions nucleus + Em and p + Em during $T = 0.3-0.5$ GeV/nucleon [14].

Key: (1) - deg.

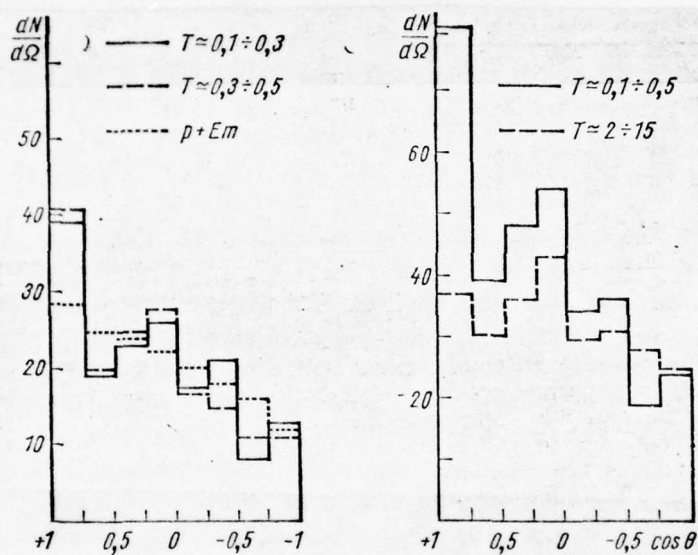


Fig. 478. Distribution of the angles of emission of the b^- particles, which are formed during the interactions of space nuclei with photoemulsion with the different energies T , GeV/nucleon [46]. By points in the left figure is shown the distribution of black ray/beams in proton-nucleus collisions during $t \approx 0.3-0.4$ GeV [14].

Page 627.

Some different in distributions during small and during the high energies T in right Fig. 478 can be explained by the supplementary contribution in the range of the small angles of the low-energy protons, emitted by the excited fragments of the impinging nucleus (see the solved kinematic region for protons with $T \approx 100$ MeV/nucleon in Fig. 459).

The angular distributions of α -particles and heavy fragments. The distribution of doubly charged particles from inelastic collisions $\alpha + \text{Em}$ was already given in Fig. 471. One should think that besides evaporative particles and this distribution certain contribution give also the rapid α -particles, driven out into the region of small angles by cascade nucleons and mesons. However, as in the case nucleon- of nuclear interactions, the contribution of such particles is insignificant.

Figure 479 and 480 shows the typical angular distributions of the low-energy and rapid α -particles, which are formed during interactions in the photoemulsion of space nuclei with charges $Z \gg 3$. Rapid α -particles escape, in essence, at small angles and then it is

possible to examine as arisen as a result of the evaporation (or rapid decomposition/decay) of the fragments of the impinging nucleus. Corresponding calculation, made on the assumption that in the system of the rest of each of these fragments the dispersion/divergence of α -particles occurs isotropically with medium energy $T \approx 2-3$ MeV/nucleon, gives distribution well agreeing themselves with experimental (for example, see broken histogram in average/mean Fig. 480). Divergences occur only at wide angles, where there are α -particles, which it is difficult to explain by evaporative process; most likely these particles are formed by means of their direct knocking out from target nucleus by rapid cascade nucleons and mesons.

With an increase in the energy of the impinging nucleus T the angular distribution of α -particles is moved into region ever smaller angles (Table 160).

The experimental data on the dependence of the angular distribution of α -particles on the charge of the impinging nucleus are contradictory. In works [19, 23] their average angle of emission $\bar{\theta}$ noticeably increases during passage to more heavy nuclei. On the contrary, in work [45] this angle remains virtually being independent of the charge of space nucleus (see Table 160). The same can be said about the average/mean angle of emission of fragments with charge $Z \gg$

3.

An example of the angular distribution of such fragments is given in Fig. 480. Characteristic feature here - the concentration of fragments in the region of small angles.

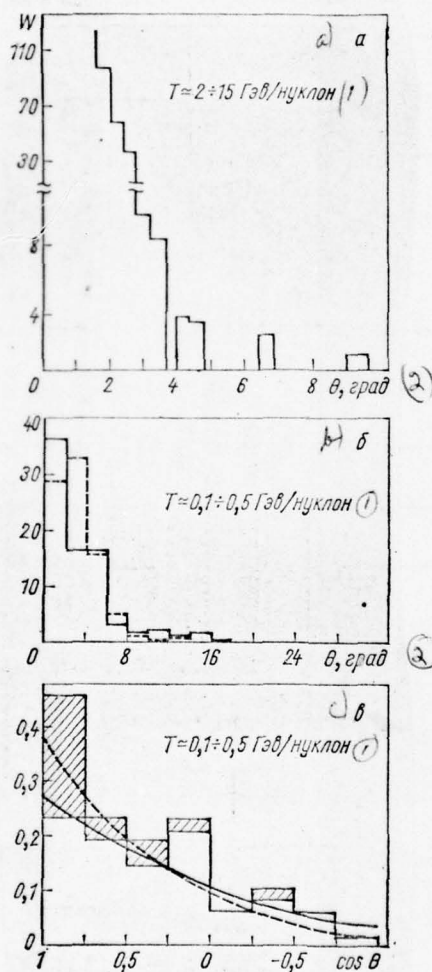


Fig. 479.

Fig. 479. The angular distributions of α -particles in the stars, formed by space nuclei with a different energy of T:

a) the distribution of shower α -particles [45]; continuous histograms in Fig. b) and c) - for α -particles with energy \mathcal{E} with respect $>$ 50 MeV/nucleon and 14-100 MeV/nucleon [46]; broken histogram in Fig. b) - the distribution of the α -particles, which are formed during the evaporation of the fragments of colliding nucleus (calculation [46]); shaded area in Fig. c) - the contribution of slow α -particles with $\mathcal{E} = 400 \div 100$ MeV/nucleon; continuous and dotted curves in Fig. c) are designed according to the theory of evaporation in assumption that the excited remanent/residual target nucleus has a velocity $\beta = v/c$ in the direction of the motion of the impinging nucleus, equal to with respect 0.015 and 0.024.

Key: (1). GeV/nucleon. (2) degree.

Page 628.

Average characteristics of the stars, which contain fragments with $Z \geq 3$, perecisleny in Tabl. 155. These characteristics comparatively differ little from the characteristics of stars with α -particles; partly this is explained themes that the α -particles and

heavier fragments are observed in one and the same stars.

§111. Energy of particles.

The information about energy particle distributions during the inelastic collisions of two nuclei, by which we avail at the present time, is very scanty. Except one experiment on deuterons (Fig. 481) we actually nothing know about the energy properties of shower particles and have only several partial data on energy distribution among strongly ionized particles.

The general idea of the character of the energy distribution of the gray ray/beams, which are formed during the collision of two nuclei, can be obtained from Fig. 482. During $T \gtrsim 1$ GeV this distribution is very close to the energy distribution of g-particles from nucleon-nuclear collisions. Being based, however, on the given above data on angular distributions, it is possible to expect noticeable differences with energies T of the order several hundreds of million electron volt to nucleon.

Table 160. Root-mean-square angle $\bar{\theta} = \sqrt{\bar{\theta}^2}$ to the direction of the motion of the space nucleus, hearth by which in the laboratory coordinate system escape the formed in photoemulsion α -particles and heavier fragments.

(1) Ядро	(2) T, Гэв/нуклон	(3) $\bar{\theta}$, град	
		(4) α -Частицы	(5) Осколки с $Z \geq 3$
Li, Be, B	$\geq 1,5$	$1,1 \pm 0,14$ [19, 23]	—
$3 \leq Z \leq 9$	$\geq 1,7$	$0,99 \pm 0,14$ [45]	$0,47 \pm 0,14$ [45]
C, N, O	$\geq 1,5$	$1,47 \pm 0,11$ [19, 23]	$0,48 \pm 0,06$ [19, 23]
	≥ 9	$0,62 \pm 0,07$ [19, 23]	—
$Z \geq 9$	$\geq 1,5$	$1,83 \pm 0,18$ [19, 23]	$1,2 \pm 0,13$ [19, 23]
	≥ 9	$0,69 \pm 0,07$ [19, 23]	—
$Z \geq 10$	$\geq 1,7$	$1,14 \pm 0,13$ [45]	$0,52 \pm 0,10$ [45]
$Z \geq 20$	$\geq 1,5$	$2,52 \pm 0,26$ [19, 23]	—

Key: (1). Nucleus. (2). T, GeV/nucleon. (3). deg. (4). α -particles.
(5). Fragments with $Z \geq 3$.

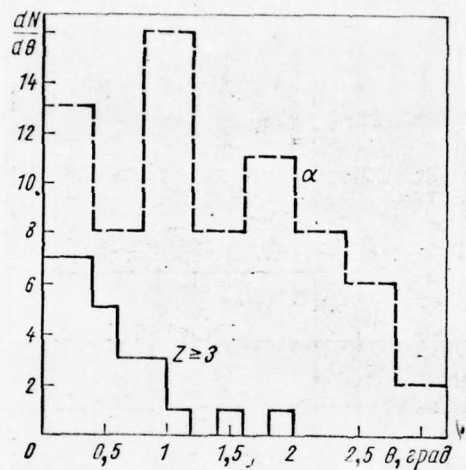


Fig. 480. The angular distributions of α -particles and fragments with charge $Z \geq 3$, which were being formed during the bombardment of photoemulsion with space nuclei with charges $Z \geq 3$ and energy $T \approx 2-15$ GeV/nucleon [45].

Key (1). in, deg.

Table 161. Mean kinetic energy of particles with gray and black traces.

(1) Взаимодействие	(2) $T, \text{ ГэВ/нуклон}$	(3) $\bar{T}_g, \text{ Мэв}$	(3) $\bar{T}_b, \text{ Мэв}$
$p + Em$ [8]	9	120 ± 12	11 ± 10
(4) Ядро + Em [44] ($Z \geq 3$)	$2 \div 15$	134 ± 5	$10,9 \pm 0,5$

Key: (1). Interaction. (2). T , GeV/nucleon. (3). g , MeV. (4). Nucleus + Em.

Page 629.

The average kinetic energies of the b-particles, which are formed in inelastic collisions nucleus + Em and $p + Em$, are also close to each other (see Table 161).

Figure 483 shows dual differential distributions for range low energy T . These distributions are explained well by the theory of evaporation (as it is shown in work [15], in this way it is possible to explain about 95o/o of all emitted protons).

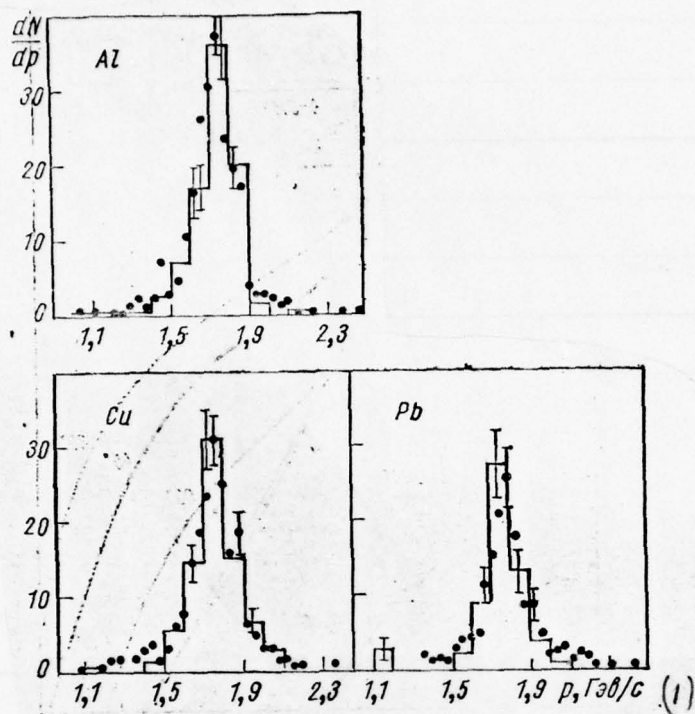


Fig. 481. The momentum distribution of the protons (in arbitrary units), formed during inelastic interaction with nuclei Al, Cu and Pb of deuterons with energy $T_d = 2.1$ GeV. Histograms are the calculation according to cascade theory taking into account the diffusivity of nuclear boundary (see §112); point - the experimental data from work [36].

(1). GeV/s.

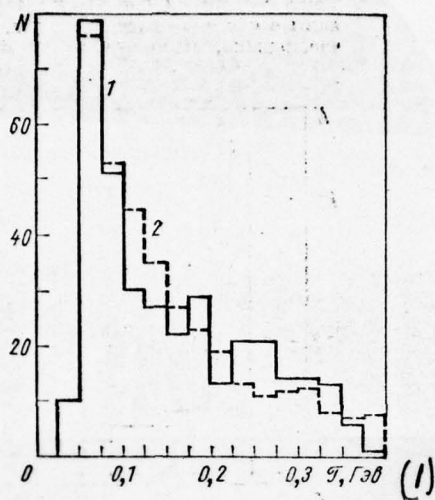


Fig. 482. Number distribution of gray ray/beams according to the value of their energy [3]:

1 - for the photoemulsion stars, formed by space nuclei with an energy of $T \approx 2-15$ GeV/nucleon; 2 - energy distribution for interactions $p + {}^{100}\text{Ru}$ during $T = 940$ MeV, designed according to cascade model.

Key: (1) . GeV.

Page 630.

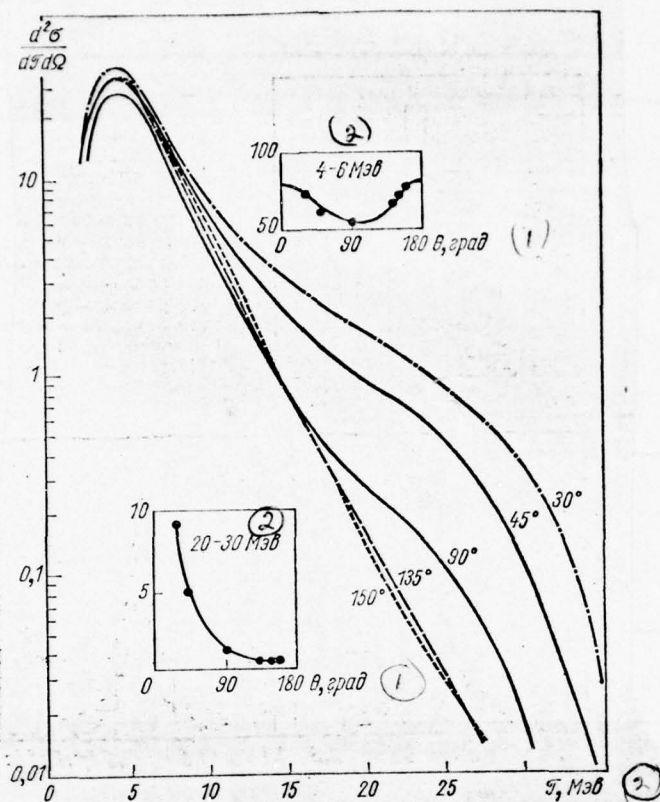


Fig. 483. Dual differential distributions of the protons, which were being formed during irradiation of nucleus ^{58}Ni by α -particles with energy $T = 42$ MeV [15]. (Angle θ and energy T are given in the center-of-gravity system, which in this case, however, differs little from the laboratory coordinate system.)

Key: (1). V, deg. (2). MeV.

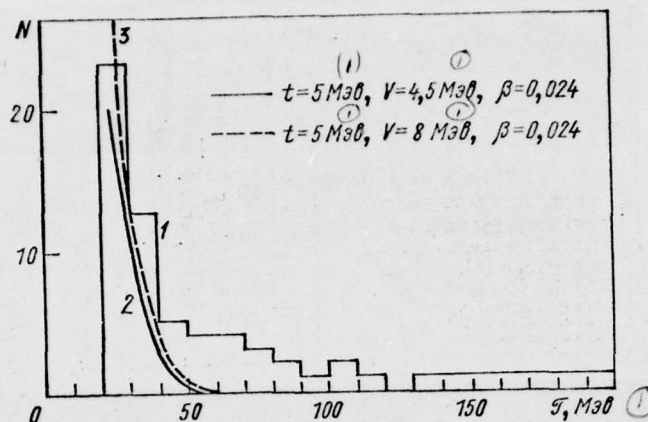


Fig. 484. The energy distribution of α -particles from interaction nucleus + Em during $T \approx 2-15$ GeV/nucleon [46]:

1 - experiment for interval of $20 < \mathcal{T} < 200$ MeV; 2, 3 - the calculation according to vaporization theory with the indicated in figure values of the parameters (β is the velocity of target nucleus, which it had during the process of evaporation).

Key: (1). MeV.

Page 631.

In the distribution of α -particles of the high-energy interactions of space nuclei with photoemulsion attention is drawn to the rather large number of particles with energy $T > 50$ MeV (i.e. larger than 10-15 MeV/nucleon) whose emission it is not possible to ascribe to the process of evaporation (Fig. 484 and 485). It is necessary to think that these are the particles, which arose as a result of their direct knocking out from target nucleus in the course of the rapid stage of interaction. The latter is confirmed also themes that almost all these particles escape into forward half sphere.

Table 162 gives the experimental values of the velocity of the recoil of nucleus-target. This recoil of nucleus occurs, in essence, because of the absorption of cascade g-particles. In comparison with the unklon-nuclear interactions during collision of two nuclei, speed of β is noticeably more.

Tables 162. Velocity of the recoil of target nucleus $\beta = v/c$.

(1) Взаимо- действие	(2) T, Гэв/нуклон	β	(3) Литера- тура
$p + Em$	9	0,014	[16, 24]
	14	0,010	
	19	0,015	
	24	0,015	
	25	0,010	
(4) Ядро + Em (Z \geq 3)	< 1,5 ($\bar{T} = 0,6$)	0,043	[2]
	< 1,5	0,060 ($n_h \leq 7$)	
	< 1,5	0,036 ($n_h > 7$)	
	> 1,5	0,029	
	> 1,5	0,029 ($n_h > 7$)	
	2-15	0,022	[3, 44]

Key: (1). Interaction. (2). T, GeV/nucleon. (3). Literature. (4).
Nucleus + Em (Z \geq 3).

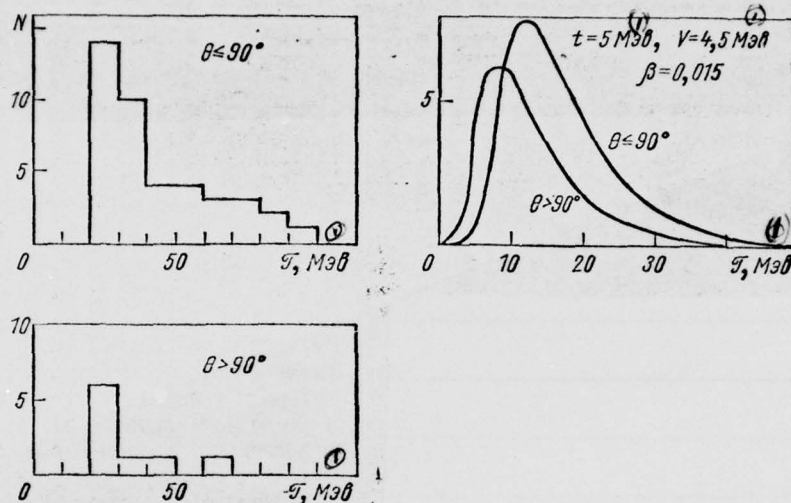


Fig. 485. Energy distribution of α -particles in the stars, formed by space nuclei with an energy of $T \approx 2-15$ GeV/nucleon [46]. Is examined interval $20 \leq \mathcal{E} \leq 100$ MeV, θ - the angle of emission of α - particle in the laboratory coordinate system. Curved on right figure are designed with the aid of vaporization theory.

Key: (1) MeV

Page 632.

§112. Theory-deuteron of nuclear interactions.

The calculation of inelastic deuteron- nuclear interactions is of now special interest, in the first place, in connection with the applied questions of the construction of the high-current generators of neutrons (see, in particular, report [55]), in the second place, as example, available to a comparatively simple and precise calculation and at the same time making it possible to study a series of the important parts, characteristic for the interactions of nuclei (interference of intranuclear cascades, the excitation energy of nuclei, the effect of the diffusivity of nuclear boundary and, etc).

The first attempt at the calculation of the inelastic collisions of high-energy deuterons with nuclei was undertaken by A. P. Zhdanovs and F. G. Lepekhn, who by the Monte-Carlo method investigated

interactions 280-MeV of deuterons with carbon [62]. The results of the calculations of these authors did not contradict assumption about the mechanism of intranuclear cascade; however, inaccuracies in the calculation (it was examined a total of 60 drawings within the framework of the extremely simplified model) and the poverty/scarcity of known at that time experimental material excluded the possibility of the more determined conclusions.

The use of the high-speed electronic computers makes it possible to fulfill at present the calculations of cascade/stages with the minimum theoretical limitations, is accumulated also considerable experimental information for different targets. All this makes it possible to obtain completely single-valued conclusions about the character of inelastic deuteron- nuclear interactions [10, 11, 28].

Model and the method of the calculation. Let us consider deuteron as weakly body-fixed system, "dumbbell" from proton and neutron, the distance between which is fix/recorded and equal the average "to diameter" of deuteron $D = 4.3 \cdot 10^{-13}$ cm. The direction of the axis of such by dumb-bells is isotropically distributed in space, and since the orbital angular moment of deuteron is equal to zero, its orientation it does not change during motion. The attached nucleons have relative momentum p ; to evaluate the distribution of this momentum/impulse/pulse we utilize the function

$$W(p) d^3p = \frac{\hbar}{\pi D} \cdot \frac{d^3p}{(p^2 + \hbar^2/D^2)^2}$$

being square the Fourier-components of the approximate wave function of the deuteron

$$\psi(r) = \frac{1}{\sqrt{2\pi D}} \cdot \frac{\exp(-r/D)}{r}$$

As showed the calculations, the parts of distribution $W(p)$ weakly manifest themselves the given below results of the calculations.

For a target nucleus let us utilize a model of the degenerate Fermi gas with diffuse boundary.

The cases, when with the nucleon of target nucleus interacts only one of the nucleons of the nucleus of deuterium, and by the second it continues motion virtually without a change in its momentum/impulse/pulse, are related to the reaction of stripping; this reaction let us consider as special case of inelastic deuteron-nuclear interaction and is include/connected its contribution to all

the given below results of calculations ¹.

FOOTNOTE ¹. In our work [11] were made also the calculations for a nucleus with sharp edge. In this case one should count that with nucleus interact only the those deuterons, the center of gravity of which passes from the center of target nucleus at a distance, which does not exceed $R + D/2$, where R , a "rigid" radius of this nucleus,.

It is necessary to keep in mind that in model with sharp edge the section of stripping is obtained that which was by somewhat understated, since the consequence of low binding energy of the deuteron of its splitting/fission they can occur, also, on the distant diffuse periphery of nucleus. Nevertheless in comparison with serber's known model [52] such a calculation is all the same is more complete, since in this case automatically is considered the possibility of stripping within nucleus (when one of the deuteron nucleons passes the nucleus without interaction) and unlike [52] is not utilized approach/approximation $D/2R \ll 1$. ENDFOOTNOTE.

Sometimes it proves to be that the caught into nucleus nucleons of the deuterium (both nucleons or one, as it takes place in the reaction of stripping) passes this nucleus without interaction; in

such cases it is considered that the deuteron not interact with nucleus.

During calculations, generally speaking, one should consider the cases of elastic scattering the impinging deuteron on intranuclear nucleons.

Page 633.

For the calculation of such collisions it is possible to utilize known experimental sections N - d-reactions. However, since section elastic N - d-reaction rapidly decreases with an increase of energy, elastic N - d-scattering within nucleus very weakly affects the results of calculations [11].

Let us consider that with inelastic N - d-reaction the intranuclear collision (in the region of energies of the order several hundreds of million electron volt this, as a rule, elastic collision) experience/tests only one of the deuteron nucleons, another nucleon retains its momentum/impulse/pulse. The further behavior of these nucleons and the behavior of the nucleon, caught into nucleus in the reaction of stripping, is examined in the framework of the usual model of intranuclear cascade.

Thus, problem is reduced on the calculation of the intranuclear cascade, initiated immediately by two nucleons deuteron dumb-bells or one of them - in the case, when occurs stripping. For the calculations it is possible to use the circuit, in detail described in chapter 4. Deexcitation of the residual-nucleus, which was being formed after escape from the target nucleus of rapid cascade particles, let us examine with the aid of usual evaporative model (see Chapter 6).

Sections deuteron- of nuclear interactions. The theoretical and experimental values of the sections of the interaction of deuterons with nuclei are given in Table 163 and 164. We see that the account of the diffusivity of nuclear boundary considerably changes the value of sections; the agreement of the calculated and experimental sections in this case is improved.

Theoretical sections σ_{in} in Table 163 and 164 include the section of stripping processes σ_{st} , when one of the nucleons, entering the nuclear composition of deuterium, the proton or the neutron, flies without interaction, and another interacts with target nucleus. Such processes automatically are considered with the Monte-Carlo playing off of nuclear interactions and are included in all given below calculation data.

Table 163. Sections of inelastic deuteron- nuclear interactions σ_{in} with $T = T_d/2 = 80$ MeV/nucleon, barn.

(1) Данные	²⁷ Al	⁶⁴ Cu	¹⁸¹ Ta	²⁰⁷ Pb	²³⁸ U
A a	0,96±0,02	1,53±0,03	2,70±0,05	2,85±0,06	3,13±0,07
B b	1,11±0,06	1,96±0,07	3,66±0,20	3,70±0,18	4,03±0,14
B c	1,16±0,06	1,99±0,07	3,68±0,20	3,72±0,18	4,05±0,14
F d	0,966±0,05	1,76±0,17	3,13±0,30	3,44±0,17	3,81±0,15

Note. A - the calculation for a nucleus with sharp edge; b - the calculation taking into account the diffusivity of the boundary of target nucleus; c - is the calculation taking into account the diffusivity of the boundary of target nucleus and contribution of the diffraction splitting/fission of deuteron; d are experimental data [40].

Key: (1). Data.

Table 164. Sections of the inelastic interactions of deuterons with nuclei with $T=T_d/2=1.05$ GeV/nucleon, barn.

(1) Мишень	(2) Теория				(3) Опыт [36] $\sigma_{p\ st}$
	σ_{in}	σ_{Serb}	σ_{st}	$\sigma'_{p\ st}$	
^{27}Al	$1,24 \pm 0,04$	0,26	$0,84 \pm 0,06$	$0,41 \pm 0,03$	$0,29 \pm 0,07$
^{64}Cu	$2,08 \pm 0,04$	0,34	$1,12 \pm 0,08$	$0,60 \pm 0,04$	$0,55 \pm 0,14$
^{207}Pb	$4,05 \pm 0,18$	0,52	$1,62 \pm 0,16$	$1,12 \pm 0,12$	$0,95 \pm 0,24$

Key: (1). Target. (2). Theories. (3). Experiment [36].

Page 634.

Table 164 shows that the calculated by us sections of stripping σ_{st} several times exceed the appropriate values, designed in serber's approximation semi-classical formula [50]

$$\sigma_{Serb} = \sigma_{p\ Serb} + \sigma_{n\ Serb} = \frac{\pi}{2} RD = \frac{\pi}{2} r_0 DA^{1/3}.$$

by Table 164 sections σ_{Serb} indicated are related to $r_0 = 1.3 \cdot 10^{-13}$

cm.; it is easy to see that by a change of value r_0 within reasonable limits it is not possible to remove disagreements with experiment.

In work [36] was measured only the part of the section σ_{st} , namely - the section of the processes, in which after interaction with nucleus remains high-energy proton. This section (in Table 164 it markedly σ'_{pst}) is the sum of the section of proton stripping σ_{pst} and the sections of the process, during which the neutron of the nucleus of deuterium flies without interaction, and proton after collision with target nucleus escapes in the direction, close to the initial direction of the motion of deuteron. Theoretical and experimental sections σ'_{pst} will agree well with each other.

To the calculated sections σ_{in} one should still add the section of the diffraction and coulomb splitting/fissions of deuteron σ_d and σ_K . Section σ_d for diffuse rdra-target can be designed by the method of Yu. A. Berezhny and Ye. V. Inopin [13]. The corrected thus sections σ_{in} are shown in Table 164. Corrections for diffraction splitting/fission are small (for copper $\sigma_d/\sigma_{in} \simeq 1,5\%$, for the nucleus of uranium $\sigma_d/\sigma_{in} \simeq 0,5\%$).

As concerns coulomb corrections, their calculation for a diffuse nucleus it is fairly complicated problem, especially if one considers that some of the free nucleons, which were being formed as the result of the splitting/fission of deuteron in the region of the diffuse boundary of nucleus, can, in turn, experience nuclear interactions.

Although the question concerning allowance for diffraction and coulomb splitting/fissions requires also further study, the comparison of the calculated and experimental data (see also lower) it indicates that in that which is examine/considered by us the models with diffuse nuclear boundary these corrections, apparently, are not essential.

In all given below theoretical data of correction for diffraction and coulomb splitting/fissions they are not considered, agreement with experiment succeeds in obtaining, also, without these corrections ¹.

FOOTNOTE ¹. In experiments on the photcemulsion of the process of diffraction and coulomb splitting/fissions virtually not at all they are record/fixed. ENDFOOTNOTE.

Many secondary particles. Table 165 and 166 gives the distributions of inelastic interactions according to the number of being born charged particles, and in Fig. 486 - the dependence of the average number of emitted neutrons on the mass number of target

nucleus. The data Table 165 characterize the rapid, cascade stage deuteron- of nuclear interaction; Table 166 and Fig. 486 also take into account evaporative stage. In all cases is observed the fair agreement of experimental and calculated values for both values of the parameter of the density of the levels of excited residual-nucleus, $a = A/10$ and $a = A/20 \text{ MeV}^{-1}$.

It should be noted that calculation data in Table 165 and 166 are obtained in model with the sharp edge of target nucleus; the correct account of the diffusivity of nuclear boundary comparatively little changes these calculations. This is connected with the fact that the photoemulsion method, which was being applied in works [5, 53] for the investigation of charged particles, substantially understates the contribution of the distant peripheral interactions, which are accompanied by the stripping of the deuteron, when nucleus remains in the weakly excited state, and the formed in the reaction of stripping free proton escapes at very small angle to the direction of the initial motion of deuteron.

Table 165. Distribution according to the number of rapid protons (with energy $\mathcal{E} > 50$ MeV) in the stars, formed in photoemulsion 275-MeV by deuterons, o/o.

(1) Число протонов	(2) Опыт [5]	(3) Теория
0	$47,9 \pm 3,5$	$45,8 \pm 3,4$
1	$46,8 \pm 3,5$	$50,3 \pm 3,6$
2	$5,3 \pm 1,1$	$3,9 \pm 1,0$

Key: (1). Number of protons. (2). Experiment [5]. (3). Theories.

Page 635.

Such events in photoemulsion it is very difficult to record, and the experimental data better will agree with the cascade model, which does not consider the diffusivity of nuclear boundary. If we introduce the appropriate discrimination, also, into the calculations, which consider the diffusivity of nuclear boundary, then their results will be in a good agreement with photoemulsion data and within the limits of statistical errors they will coincide with the results, obtained in the approach/approximation of the sharp

boundary of nucleus. However, for obtaining the agreement of the calculated and experimental values on Fig. 486 it is completely necessary to consider the diffusivity of target nucleus.

Energy and angular distributions. The given in Fig. 467 and 487 spectra of the secondary protons, measured in photoemulsion, will agree well with the calculation, if we again reject/throw the contribution of the stripping particles, which appear during peripheral interactions on boundary. (Especially is significant in this respect the distribution in Fig. 487b, which relates to the rapid particles, emitted at small angles $\theta \leq 10^\circ$, and nevertheless well agreeing itself with theoretical).

By very sensitive to the portion of stripping processes characteristic are the energy spectra of particles, measured at small angles.

Table 166. Distribution according to the number of ray/beams in the stars, formed by deuterons in photoemulsion, o/o. The cases A and B are designed respectively for the parameters of the density of levels $a = A/10$ and $a = A/20 \text{ MeV}^{-1}$.

(1) Число лучей n	$T = T_d/2 = 110 \text{ Мэв/нуклон}$ (2)			$T = T_d/2 = 137,5 \text{ Мэв/нуклон}$ (2)		
	(3) Опыт [53] (*)	Теория (4)		(3) Опыт [5]	Теория (4)	
		А	Б		А	Б
0	—	$6,0 \pm 0,5$	$5,0 \pm 0,5$	$23,5 \pm 5,3$	$10,4 \pm 0,7$	$7,4 \pm 0,6$
1	$12,8 \pm 0,9$	$22,4 \pm 1,0$	$21,0 \pm 1,1$	$21,2 \pm 5,0$	$15,8 \pm 0,9$	$17,0 \pm 1,0$
2	$33,2 \pm 1,5$	$29,9 \pm 1,9$	$26,5 \pm 1,8$	$22,4 \pm 5,1$	$17,5 \pm 1,0$	$23,4 \pm 1,1$
3	$22,0 \pm 1,2$	$23,8 \pm 1,5$	$22,2 \pm 1,1$	$16,5 \pm 4,4$	$22,5 \pm 1,1$	$18,0 \pm 1,0$
4	$16,5 \pm 1,0$	$14,2 \pm 1,0$	$15,9 \pm 1,0$	$9,4 \pm 3,3$	$17,5 \pm 1,0$	$15,5 \pm 0,9$
5	$10,5 \pm 0,8$	$6,7 \pm 0,5$	$8,5 \pm 0,6$	$4,7 \pm 2,3$	$10,0 \pm 0,7$	$11,0 \pm 0,7$
6	$3,0 \pm 0,5$	$2,1 \pm 0,3$	$3,7 \pm 0,4$	$2,3 \pm 1,6$	$4,5 \pm 0,4$	$5,2 \pm 0,4$
7	$2,0 \pm 0,4$	$0,6 \pm 0,1$	$1,5 \pm 0,2$	0	$1,3 \pm 0,2$	$1,6 \pm 0,2$
8	0	$0,3 \pm 0,1$	$0,7 \pm 0,1$	0	$0,5 \pm 0,1$	$0,6 \pm 0,1$
9	—	—	—	0	—	$0,3 \pm 0,1$

Key: (1). Number of ray/beams n. (2). MeV/nucleon. (3). Experiment [53] 1. (4) Theories

FOOTNOTE 1. In work [53] were not examined the events, in which are

formed the only neutral particles ($n = 0$; therefore theoretical distributions are calibrated to the total number of stars with $n > 0$.

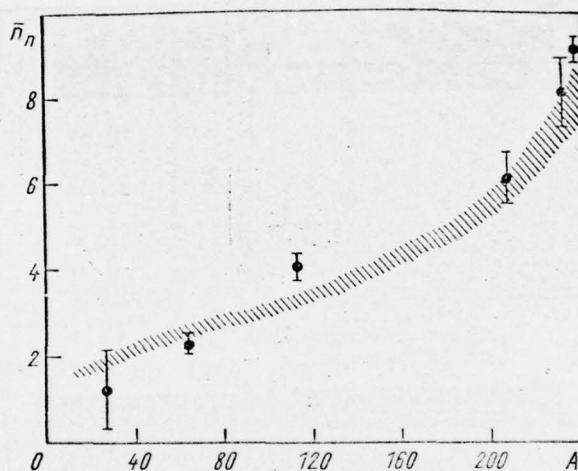


Fig. 486. Average [number] the neutrons, which are formed in inelastic deuteron- nuclear interaction with $T_d \approx 160$ MeV:

A , the mass number of target nucleus. The shaded region corresponds to the values \bar{n}_n calculated for the parameters of the density of

levels $a = (A/10) - (A/20) \text{ MeV}^{-1}$; experimental points are related to primary beam of deuterons with energy $T_d = 190 \text{ MeV}$; however, as a result of ionizing losses in the thick targets, which were being utilized during measurements [20], effective energy deuteron- of nuclear interactions $T_d \approx 160 \text{ MeV}$.

Page 636.

Such spectra are depicted on Fig. 488 and 489 for interactions with the nuclei of uranium and carbon. In both cases the agreement of theory with experiment sufficiently good - considerably better than for the calculations, executed in approximation of the sharp boundary of nucleus.

It focuses on itself attention on the sensitivity of the results of calculations to a change in the parameters of the distribution of Vuds - Sakson

$$\rho(r) = \rho_0 \{1 + \exp[(r-c)/a]\}^{-1},$$

used by us for the description of the density of intranuclear nucleons. As can be seen from Fig. 489, even a comparatively small

AD-A048 311

FOREIGN TECHNOLOGY DIV WRIGHT-PATTERSON AFB OHIO
INTERACTIONS OF HIGH-ENERGY PARTICLES AND ATOMIC NUCLEI WITH NU--ETC(U)
JUL 77 V S BARASHENKOV, V D TONEYEV
FTD-ID(RS)T-1069-77

F/G 20/8

UNCLASSIFIED

NL

6 OF 6

AD
A048 311



END

DATE
FILMED

2-78

DDC

change in parameters a and c noticeably makes agreement worse with experiment.

Table 167 and 168 with experiment compares the results of the calculation of the angular characteristics of neutrons and protons, which appear in inelastic deuteron-nuclear collisions with low energy $T = 17-95$ MeV/nucleon, but in Fig. 468 and 481 - the angular and energy distributions of the secondary protons during $T = 1.05$ GeV/nucleon - only known at present high-energy data. Agreement with experiment in all cases, even with $T = 17$ and 45 MeV/nucleon completely satisfactory.

Conclusions. Thus, the described in chapter 4 cascade model makes it possible to obtain satisfactory agreement with all known now experimental data on inelastic deuteron- nuclear interactions with energies, large several dozen to megaelectronvolts per nucleon. This it proves, that such interactions occur by the imposition of the cascade/stages, initiated by the nucleons of the nucleus of deuterium. The interference of the cascade/stages, when with one and the same by intranuclear nucleon occurs the interaction of the rapid particles, which belong to the cascade/stages, initiated both proton and the neutron of the impinging nucleus of deuterium, is negligible. The latter, however, to a considerable degree is caused by the relatively greater average distance between nucleons in the nucleus

of deuterium; during the interaction of more heavy nuclei this can render/show not thus.

The decomposition/decay of the excited residual-nucleus is described well by the usual theory of evaporation.

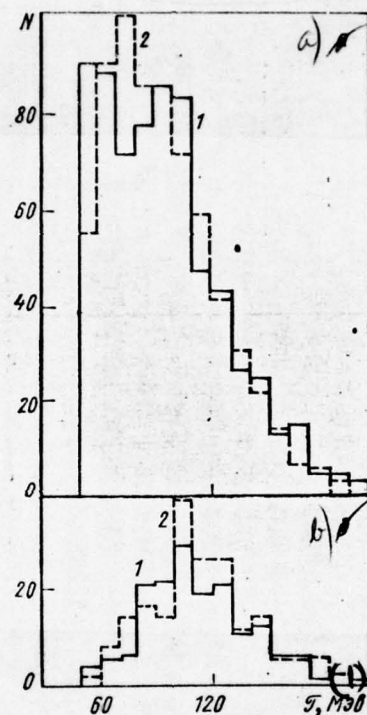


Fig. 487. The energy spectrum of the rapid protons, which are formed during interaction with the photoemulsion of deuterons with energy $T = 110$ MeV/nucleon:

a) all protons with energy $E > 50$ MeV; b) the protons, which escape at angles $\theta < 10^\circ$; 1 - the calculation for the medium nucleus of photoemulsion ^{70}Ga , 2 are experimental data from work [53].

KEY: (1). MeV.

Tables 167. Width of the angular distribution of the neutrons, which are formed during the interaction of deuterons with different nuclei during energy $T = T_d/2 = 95$ MeV.

(1) Ядро	(2) $\theta_{1/2}$, град	
	(3) Теория	(4) Опыт
$^{27}_{13}\text{Al}$	$9,0 \pm 1,5$	$9,3 \pm 0,5$
$^{181}_{73}\text{Ta}$	$11,5 \pm 1,5$	$11,4 \pm 0,5$
$^{207}_{82}\text{Pb}$	$11,6 \pm 1,5$	$11,7 \pm 0,5$
$^{238}_{92}\text{U}$	$12,6 \pm 1,5$	$12,0 \pm 0,5$

Key: (1). Nucleus. (2). deg. (3). Theories. (4). Experiment ¹.

FOOTNOTE ¹. The corrected values calculated by formula (11.1), which approximates the experimental data in work [30]. ENOFOOTNOTE!

Page 637.

For the energy distributions of the being born nucleons is characteristic the peak in region $T = T_d/2$.

Table 168. The energy dependency of the angular distributions of the charged particles, which are formed during irradiation of photoemulsion by deuterons with an energy of T , o/o

$$W(\theta_1; \theta_2) = \int_{\theta_1}^{\theta_2} N(\theta) \sin \theta d\theta / \int_0^{\pi} N(\theta) \sin \theta d\theta$$

(1) $\theta_1 - \theta_2$, град	(2) $T = 17,5 \text{ Мэв/нуклон}$		(2) $T = 45 \text{ Мэв/нуклон}$		(2) $T = 65 \text{ Мэв/нуклон}$		(2) $T = 95 \text{ Мэв/нуклон}$	
	Опыт [26] (3)	Теория (4)	Опыт [26] (3)	Теория (4)	Опыт [26] (3)	Теория (4)	Опыт [26] (3)	Теория (4)
0 ÷ 30	37,0 ± 2,0	57,7 ± 2,9	36,2 ± 2,0	42,7 ± 2,1	33,7 ± 1,9	35,2 ± 1,7	29,4 ± 1,8	30,8 ± 1,5
30 ÷ 90	43,7 ± 2,2	28,4 ± 1,4	39,7 ± 2,1	36,4 ± 1,8	38,5 ± 2,1	42,4 ± 2,1	42,7 ± 2,2	45,0 ± 2,2
90 ÷ 150	14,5 ± 1,3	11,9 ± 0,6	18,0 ± 1,4	15,2 ± 0,7	21,0 ± 1,5	16,3 ± 0,8	20,6 ± 1,5	17,7 ± 0,9
150 ÷ 180	4,8 ± 0,7	2,0 ± 0,1	6,1 ± 0,8	5,7 ± 0,3	6,8 ± 0,9	6,1 ± 0,3	7,3 ± 0,9	6,5 ± 0,3

Note. The given theoretical data are related to the parameter of the density of levels $a = A/10 \text{ MeV}^{-1}$; within the limits of statistical errors they coincide with the appropriate values,

[Key on following page]

designed for $a = A/20 \text{ MeV}^{-1}$. With $T = 17.5 \text{ MeV/nucleon}$ the calculation, it is understandable, it has only tentative value. Since comparison conducts with photoemulsion data, is reject/thrown the contribution of particles, which are formed as a result of interactions at the distances, greater than nuclear radius R .

Key: (1). deg. (2). MeV/nucleon. (3). Experiment [26]. . (4). Theories.

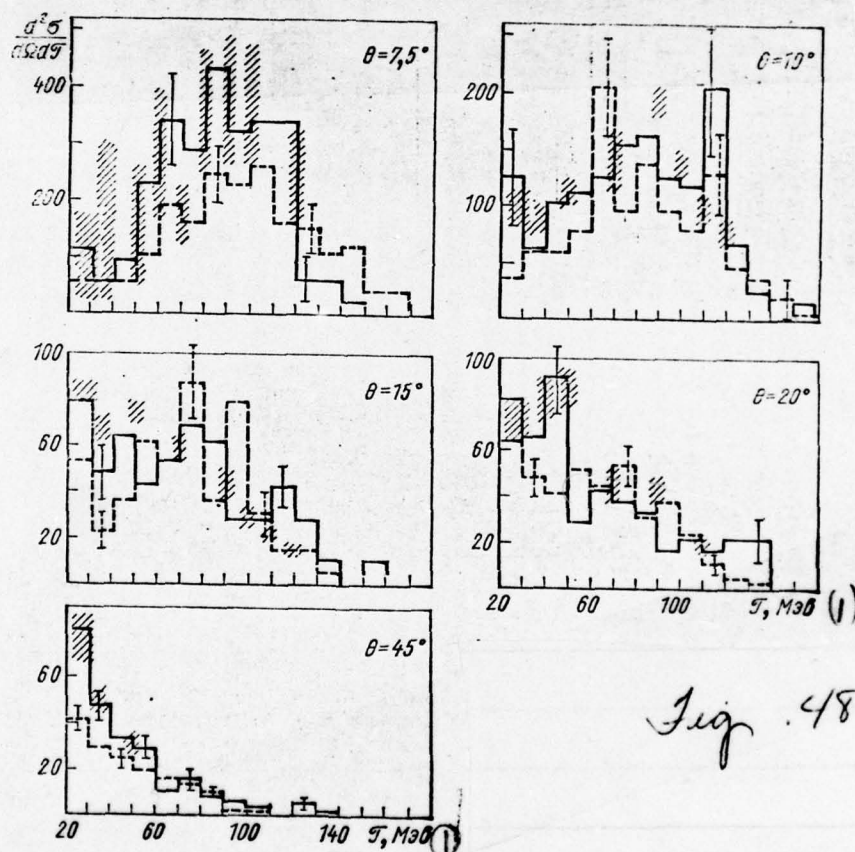


Fig. 488.

Fig. 488. The energy spectrum of the protons, which are formed in the inelastic interaction $d + {}^{238}\text{U}$ with $T_d = 190$ MeV:

θ is an angle of emission of proton in the laboratory coordinate system; continuous histograms - the results of the calculation taking into account the diffusivity of the boundary of nucleus; dotted line is the calculation in the approach/approximation of the sharp edge of nucleus without taking into account of diffraction and coulomb splitting/fissions; by shading are shown to an error in the experimental data from work [51].

Key: (1). MeV.

Page 638.

The particles, driven out from nucleus by rapid deuteron, are strongly collimated in the direction of the motion of this deuteron. During passage to heavier target nuclei the angular distribution of rapid nucleons widens itself, which is connected with the large number of intranuclear interactions. In comparison with nucleon and pion nuclear interactions in the case of interactions $d + \text{nucleus}$ considerably more essential turns out to be the diffusivity of nuclear boundary. If this diffusivity is does not considered, then

with theory it is possible to match only average characteristics, or rough measurements in photoemulsion; all values, which relate to the region of small angles, they are obtained by substantially understated. Corrections for diffraction and coulomb splitting/fissions turn out to be not important; however this question requires even more careful study.

One should also expect that in the same way as this occurs in the case of pion- and nucleon-nuclear collisions, the examined mechanism of the inelastic interactions of deuterons with nuclei must undergo change with energies $T = T_d/2 \gtrsim 5$ GeV/nucleon.

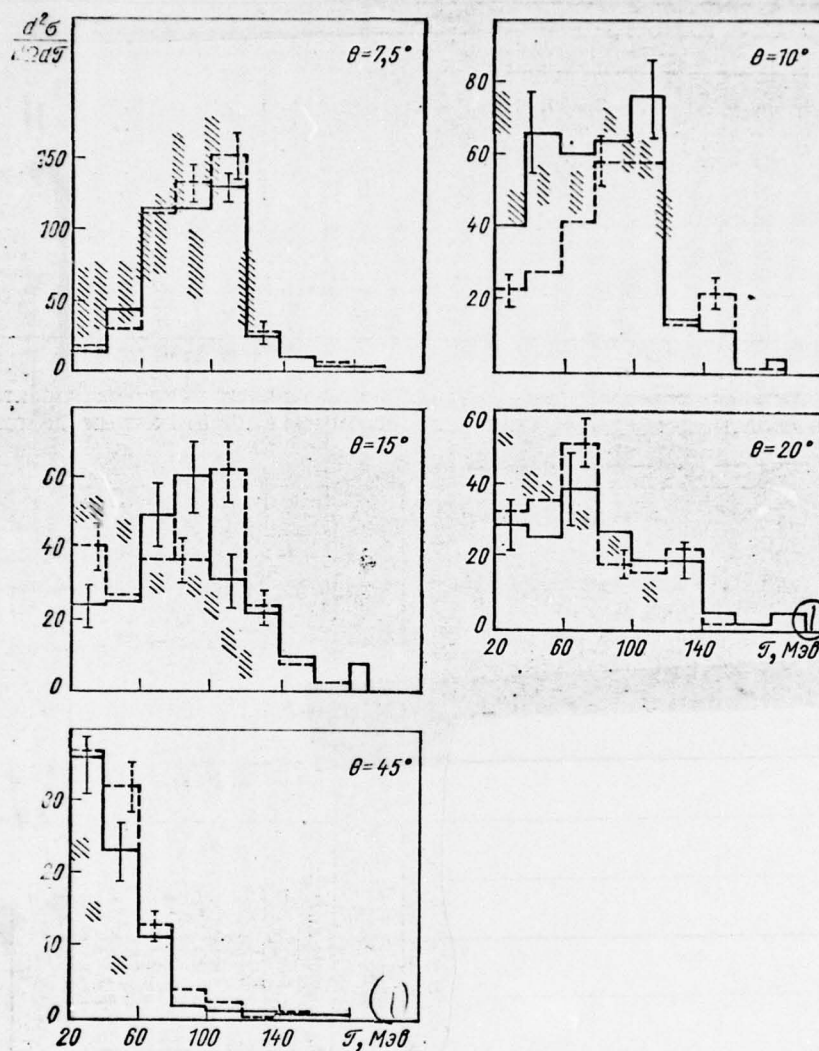


Fig. 489.

Fig. 489. The energy spectrum of the protons, which are formed in the inelastic interaction $d + {}^{12}\text{C}$ with $T_d = 190$ MeV:

θ - the angle of emission of proton in the laboratory coordinate system; continuous histograms are the calculation for the values of the parameters $a = 0.50 \cdot 10^{-13}$ cm. and $c = 0.98 A^{1/3} \cdot 10^{-13}$ cm., obtained for a nucleus ${}^{12}\text{C}$ in the experiments of Khofshtadter; dotted line is the calculation with parameters $a = 0.545 \cdot 10^{-13}$ cm. and $c = 1.05 A^{1/3} \cdot 10^{-13}$ cm. With dotted line are noted errors in the experimental data from work [51].

Page 639.

§113. Calculation of the inelastic collisions of α -particles with nuclei.

From theoretical point of view such a calculation is of paramount interest as example of interaction with the nucleus of very compact multinucleon system; this is very important also in practical relation, since about 60/o of cosmic radiation compose high-energy α -particles. At the same time, is known at present altogether only

one work of A. I. Vikhrova et al. [61], in which is undertaken an attempt at the calculation of inelastic collisions $\alpha + \text{nucleus}$. The examined in work [61] cascade model is very simplified, during calculations used a series insufficient justified assumptions, nevertheless the results of this work make it possible to determine those point/items of the cascade theory, which turn out to be most essential in its propagation in the case of the inelastic collisions of two nuclei.

Model of the intranuclear cascade, initiated by α -particle. For the calculations in work [61] is applied cascade- evaporative model in the approach/approximation of the sharp edge of target nucleus. A radius of this nucleus is set/assumed by equal to $1.3 \times A^{1/3} \cdot 10^{-13}$ cm. The potential, which acts on α -particle within nucleus, is approximated by square well 40 MeV deep. By the interference of the cascade/stages, caused by the separate nucleons of the impinging α -particle, it is disregarded.

The essential simplification, used in work [61], will be that that during all interactions with nucleus the impinging α -particle is considered as unit, in difference, for example, from the examined above model of the deuteron collisions, where in certain cases with the nucleus-target-target, having the sharply designating boundary, can interact only one of the nucleons, forming part of deuteron. As

we will see below, the neglect of the structure of α -particle is reason, why some values, designed in work [61], strongly differ from the experimental. The processes of the coulomb and diffraction splitting/fissions of α -particles in work [61] also are not examined. During calculations were accepted into consideration both the elastic and inelastic collisions of α -particles with the nucleons of target nucleus. The type of collision is determined by the value of the relation of sections $\sigma_{in}(\alpha N)$ and $\sigma_{el}(\alpha N)$, the determined from analysis known experimental data at different energies ¹; in this case the properties of the interactions of α -particles with protons and neutrons are considered identical.

FOOTNOTE ¹. Sections $\sigma(\alpha N)$ and $\sigma(N\alpha)$ differ only in terms of the selection of the system. ENDFOOTNOTE.

The angular distributions of the scattered α -particles from elastic α - N-collisions also are determined on the basis of the approximate approximation of known now experimental points. In the calculation inelastic α - N-collisions are included the channels

$$\alpha + N \rightarrow \begin{cases} p + N + t; & \text{(I)} \\ n + N + {}^3\text{He}; & \text{(II)} \\ 2p + 2n + N & \text{(III)} \end{cases}$$

Collisions with the formation/education of deuterons in view of the loose coupling of nucleons in deuteron separately are not examined; in all cases deuteron is represented as totality of two separate nucleons, but the section of such reactions is related to corresponding channels (I) - (III).

The relationship/ratio of the probabilities of channels (I) - (III) was estimated on the basis of the experimental data [54], the relating to energy nucleons $T = 90$ MeV, that corresponds to energy of α -particles outside nucleus $T_\alpha \approx 360$ MeV. Since such data with other energies now it is unknown, the authors [61] were forced to make a rough assumption about the fact that the relationship/ratio between channels (I) - (III) does not depend on energy.

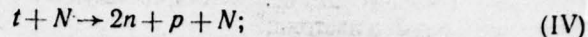
The subsequent behavior of the formed as a result of intranuclear collisions nuclei t , ${}^3\text{He}$ and ${}^4\text{He}$ also is examined within the framework of cascade mechanism. The calculations here substantially are impeded by the extreme meagerness of the experimental data on interactions $t + N$ and ${}^3\text{He} + N$.

Page 640.

A deficiency/lack in the experimental information it was necessary to complete to some assumptions whose validity can be checked only by the comparison of the results of the calculation with experiment. Specifically, it is assumed that the relation of sections σ_{in}/σ_{el} and the angular distribution of the elastic scattered particles in collisions $t + N$ and ${}^3\text{He} + N$ the same as for collisions $\alpha + N$ ¹.

FOOTNOTE ¹. Certain justification to this assumption is that observed in experiment during $T = 660$ MeV the angular distributions of protons in the reactions of elastic scattering on nuclei ${}^3\text{He}$ and ${}^4\text{He}$ in the margins of error in the measurements coincide with each other; with other energies the experimental data, unfortunately when they are absent. ENDFOOTNOTE.

During the calculation of the inelastic collisions of nuclei t and ${}^3\text{He}$ are considered the reactions



and it was considered that secondary particles in the center-of-gravity system have isotropic angular distribution and identical momentum/impulse/pulse.

The calculation of the evaporative stage of process in work [56] is made for the parameter of the density of levels $a = 0.15 \text{ MeV}^{-1}$.

Results of the calculation. Table 169 gives the sections of the inelastic interactions of α -particles with several light/lung and heavy nuclei. These sections are considerably less than the values, determined with the aid of semi-rational formula (1.12), and the experimental values, measured for close nuclei (see §4) with $T \approx 50\text{--}100 \text{ MeV/nucleon}$. Differences are wholly caused themes that during calculations were taken into account the size/dimensions of the impinging α -particle, as a result of which will turn out to be those which were lost all the interactions with impact parameters $R < \rho < R + R_\alpha$, where R_α is the mean radius of α -particle (see note on page 632).

In Fig. 490 for different angular intervals are compared the

calculated and experimental spectra of protons $d^2\sigma/d^2\mathcal{T}d\Omega$. Although the calculation is very rough, theoretical histograms on the whole badly/poorly do not transfer the course of experimental curves; considerable differences are observed only in the left lower figure - in the case of interaction $\alpha + {}^{108}\text{Ag}$ at $\theta = 0-65^\circ$.

Table 169. Sections of the inelastic interactions of α -particles with nuclei, designed in the work of A. I. Vikhrova et al. [61], mb.

(1) T, Мэв/нуклон	^{14}N	^{27}Al	^{93}Nb	^{108}Ag
51,3	—	452	—	1190
95	297	455	1080	—

Key: (1). T, MeV/nucleon.

Table 170. Output/yield of particles of the different types in inelastic collisions $\alpha + ^{27}\text{Al}$ and $\alpha + ^{108}\text{Ag}$ with T = 51.3 MeV/nucleon, mbarn/ster.

(1) Сечение	$\theta = 0 \div 65^\circ$		$\theta = 100 \div 180^\circ$	
	^{27}Al	^{108}Ag	^{27}Al	^{108}Ag
$\sigma(p)$	180 (277)	342 (304)	77,3 (94,5)	108 (104)
$\sigma(t)$	12,5 (11,5)	20,4 (10,1)	3,9 (3,66)	2,4 (4,1)
$\sigma(^3\text{He})$	14,5 (10,6)	21,6 (8,37)	2,1 (1,63)	0,394 (0,835)
$\sigma(^4\text{He})$	58,0 (138)	81,6 (104)	16,9 (34,5)	7,5 (43)

Note. In brackets are shown the experimental data from work [7].

Key: (1). Section.

Page 641.

In Table 170 for the same angular intervals, as Fig. 490, gives the sections of the formation/education of protons, α -particles and the heavier fragments

$$\sigma = 2\pi \int_{\theta_1}^{\theta_2} \sin \theta d\theta \int_0^{\mathcal{T}_{\text{max}}} \frac{d^2\sigma}{d\mathcal{T} d\Omega} d\mathcal{T}.$$

From this table it is evident that for angles $\theta = 100-180^\circ$, where

escape in essence the evaporative particles, the agreement of calculation data with experiment sufficiently good, with the exception of the output/yield of α -particles, which proves to be considerably lower than measured on experiment. For particles, which escape at angles $\theta = 0-65^\circ$ and connected, mainly, with the cascade stage of process, the agreement is considerably worse, especially for α -particles and fragments t and ^3He .

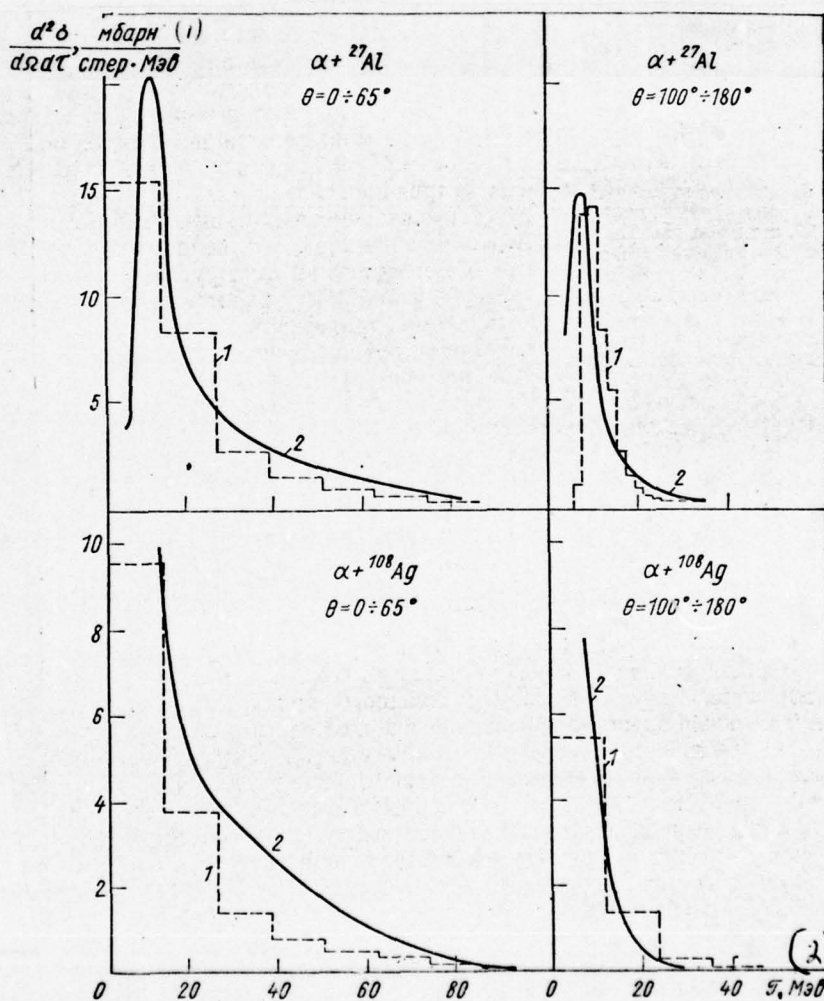


Fig. 490.

Fig. 490. Energy distribution of the protons, which are formed during the interactions of α -particles with the nuclei of aluminum and silver during $T = 51.3$ MeV/nucleon and escaping into the determined interval of angles θ :

1 - calculation [61]; 2 - the experimental data [7].

Key: (1). mbarn/ster \cdot MeV. (2). MeV.

Page 642.

Disagreements with experiment are caused both inaccuracy in the sections, used in work [61], and by deficiency/lacks in the used version of cascade model, especially by neglect of the contribution of peripheral interactions in region $R < \rho < R + R_\alpha$. The latter understates also the output/yield of protons. Figure 491 shows total angular distribution of all charged particles, which are formed in the photoemulsion, irradiated by α -particles. Is distinctly evident the noticeable excess of the experimental output/yield of particles in the region of small angles. This also to a considerable degree occurs due to neglect of the contribution of peripheral interactions, as a result of which are lost all the collisions, during which with target nucleus interacts only the part of the nucleons, entering the

composition of α -particle, but other, in free or in bound state, flies by virtually in the same direction, as primary α -particle.

Rough estimates, made in the work of A. I. Vikhrova et al. [61], show that the fundamental characteristics of the inelastic interactions of α -part with poisons can be explained within the framework of cascade- evaporative model, if one takes into account the diffusivity of nuclear boundary (but in model with sharp edge - the size/dimensions of the most impinging α -particle). For a more detailed agreement with experiment is required also the refinement of the properties of the elastic and inelastic interactions of nuclei t, ^3He and ^4He with intranuclear nucleons.

As in the case nucleon- and pion-nuclear collisions, for agreement with the experiment of the output/yield of α -particles and heavier fragments it is necessary to consider to the cluster structure of target nucleus.

§114. Calculation of the collisions of heavy nuclei.

The analysis of the experimental data shows that in the collision of two high-energy nuclei it is possible to isolate the

rapid stage of process, which is accompanied by the formation/education of a large quantity of shower particles and particles of lower energy, which are characterized by gray photographic tracks, and the slower stage, connected with the decomposition/decay of the excited residue/remainers of the impinging nucleus and target nucleus. Upon decay of the residue/remainder of target nucleus escape low-energy particles with black photographic tracks; the particles, connected with the decomposition/decay of the residue/remainder of the impinging nucleus as a result of purely kinematic effect turn out to be in the laboratory coordinate system rapid and are a part of shower particles. The rapid stage of the interaction of two nuclei in its properties differs significantly from nucleon- nuclear interaction; the property of slow stage in both these interaction modes are sufficiently similar.

The most essential feature of the inelastic interactions of nuclei is that in process takes part the large number of nucleons of the impinging nucleus, each of which gives rise to within target nucleus the cascade/stage of secondary particles.

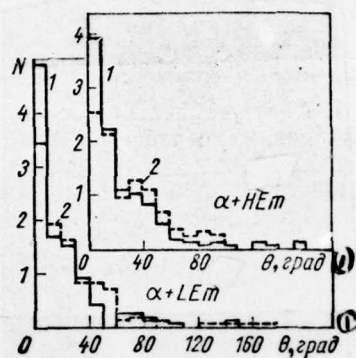


Fig. 491. The angular distribution of the number of the charged particles (into relative units), which are formed during the interaction of and- particles with energy $T = 95$ MeV/nucleon with the light/lung and heavy nuclei of the photoemulsion:

1 - the experimental data [59]; 2 - calculation [61] respectively for nuclei ^{14}N and ^{94}Nb .

Key: (1) θ , degree.

Page 643.

If the collision of nuclei occurs with impact parameter ρ , then the average number of nucleons of the impinging nucleus, which participate in interaction,

$$N_H(\rho) = \int \int \int_{-\infty}^{+\infty} d_H(x-\rho, y, z) \{1 - \exp[-n_M(x, d)]\} dx dy dz, \quad (11.2)$$

where $n_M(x, y) = \sigma \int_{-\infty}^{+\infty} d_M(x, y, z) dz$ - the average number of collisions, which it experience/tests nucleon, moving along the direction of the motion of primary nucleus (this direction is selected as z axis); σ is section N - N-interaction; d_H and d_M - nucleon distribution in the impinging nucleus and in target nucleus.

Figure 492 shows the estimation of function $N_H(\rho)$ for the collisions of different nuclei, obtained by Alexander, etc. [2]. In actuality the number of collisions $N_H(\rho)$ even is somewhat more, since the impinging nucleons can experience/test both inelastic and elastic collisions within target nucleus. (In work [2] it is considered that $\sigma = 30$ mb, i.e., $\sigma \simeq \sigma_{in}$ (NN).).

On the average during inelastic collision with the nucleus of

photoemulsion it participates

$$\bar{N}_H = 2\pi \sum_i \sigma_{Hi} N_{Mi} \int_0^\infty N_H(\rho) \rho d\rho / \sum_i N_{Mi} \quad (11.3)$$

the nucleons of the impinging nucleus. Here σ_{Hi} is a section of the inelastic interaction of the impinging nucleus with the nucleus of the i type, which forms part of photoemulsion; N_{Mi} - the number of nuclei of the i type in 1 cm^3 .

Values \bar{N}_H for different space nuclei are given in Table 171. As is evident, in collision participates the considerable number of nucleons. In connection with this now it is possible to indicate in any case three basic questions, on solution of which depends substantially the further development of the theory of the inelastic interactions of two nuclei [9].

1. As to consider a change in the properties of nucleus-target with its filling with the nucleons of the impinging nucleus and how substantially this change will pronounce on cascade calculations?

2. Which contribution does give the interference of the cascade/stages, generated by the different nucleons of the impinging nucleus?

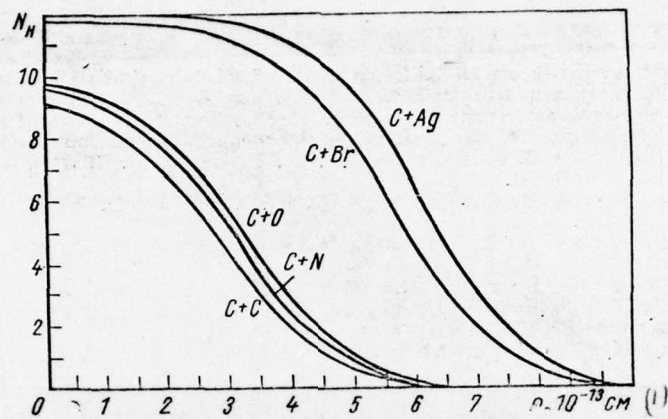


Fig. 492. Average number of nucleons the colliding nucleus C , which experience/test inelastic collision within different target nuclei [2].

Key: (1). cm.

Table 171. Number of nucleons of the impinging nucleus, which experience/test inelastic interaction with the nucleus of

photoemulsion with energy $T \geq 1$ GeV/nucleon ¹.

(1) Налетающее ядро	Li	Be	B	C	N	O
N_H	3,5	4,3	5,0	5,3	5,7	6,3

FOOTNOTE ¹. According to the data [2]; elastic intranuclear interactions are not included in this number. ENDFOOTNOTE.

Key: (1) Impinging nucleus

Page 644.

3. Is such the relative probability of the different splitting/fissions of the impinging nucleus during peripheral collisions (especially in model with the sharp edge, where part of the impinging nucleus in general does fly by, without experiencing interaction)?

It is possible to hope that the methods of the calculation of the inelastic collisions of deuterons and α -particles with nuclei be managed comparatively simple to propagate on somewhat more heavy nuclei. Nevertheless to the present time it is made still not of one cascade calculation of the inelastic collisions of nuclei with charge $Z \geq 3$.

BEST AVAILABLE COPY

Bibliography

1. Abraham F. et al. Phys. Rev., 159, 1110 (1967).
2. Alexander G. et al. Nuovo cimento, 20, 648 (1961).
3. Andersson B., Otterlund I., Kristiansson K. Arkiv. fys., 31, 527 (1966).
4. Appa Rao M. V. K., Daniel R. R., Neelakanthan K. A. Proc. Indian Acad. Sci., A43, 181 (1956).
5. Appa Rao M. V. K., Lavakare P. J. Nuovo cimento, 29, 321 (1963).
6. Badhwara G., Durgaprasad N., Vijavalakshmi B. Proc. Ind an Acad. Sci., 61, 374 (1965).
7. Bailey L. E. Report of California Univ. UCRL-3334 (1956). Угловые и энергетические распределения заряженных частиц, излученных при высокоэнергетической бомбардировке различных элементов.
8. Barashenkov V. S. et al. Nucl. Phys., 14, 522 (1959/60).
9. Барашенков В. С., Гудима К. К., Тонеев В. Д. «Изв. АН СССР. Сер. физ.», 32, 352 (1968).
10. Барашенков В. С., Гудима К. К., Тонеев В. Д. «Ядерная физика», 10, 760 (1969).
11. Барашенков В. С., Гудима К. К., Тонеев В. Д. «Ядерная физика», 9, 528 (1969).
12. Baumann G., Braun H., Güer P. In: Conference International sur les Interactions de Particles on Haute Energie avec les Noyaux Complexes. Leysin, 1963.
13. Бережной Ю. А., Инопин Е. В. «Ядерная физика», 6, 1197 (1967).
14. Bernardini G., Booth E. T., Lindenbaum S. J. Phys. Rev., 85, 826 (1952); 88, 1017 (1952).
15. Боданский Д. В. сб. «Прямые процессы в ядерных реакциях». Перев. с англ. Под ред. А. А. Оглоблина. М., Атомиздат, 1965, стр. 77.
16. Богачев Н. П. и др. «Ж. эксперим. и теор. физ.», 44, 493 (1963).
17. Богачев Н. П. и др. «Ж. эксперим. и теор. физ.», 44, 1869 (1963).
18. Ceccarelli M., Quarenì G., Zorn G. T. Nuovo cimento, 1, 669 (1955).
19. Cester R. et al. Nuovo cimento, 7, 371 (1958).
20. Crandall W. E., Millburn G. P. M. J. Appl. Phys., 29, 698 (1958).
21. Dainton A. D., Kent D. W. Philos. Mag., 41, 963 (1950).
22. Fridlander M. W. et al. Philos. Mag., 8, 1691 (1963).
23. Fowler P. H., Hilier R. R., Waddington C. J. Philos. Mag., 2, 293 (1957).
24. Gajewski W. et al. Nucl. Phys., 58, 17 (1964).
25. Гагарин Ю. Ф., Иванова Н. С., Куликов В. Н. Препринт Физико-технического института им. А. Ф. Иоффе, № 235, Ленинград, 1969. Взаимодействие релятивистских тяжелых ядер космических лучей с ядрами фотоэмульсии.
26. Gardner F., Peterson V. Phys. Rev., 75, 264 (1959).
27. Greider K. R. Annual Rev. Nucl. Sci., 15, 291 (1966).
28. Гудима К. К. Диссертация, ОИЯИ, Дубна, 1969. Механизм неупругих взаимодействий частиц с ядрами в области ускорительных энергий.
29. Гуревич И. И. и др. «Ж. эксперим. и теор. физ.», 34, 265 (1958).
30. Helmholtz A. C., McMillan E. M., Sewell D. C. Phys. Rev., 72, 1003 (1947).
31. Hodgson P. E. Philos. Mag., 45, 190 (1954).
32. Judek B., Van Heerden I. J. Canad. J. Phys., 44, 1121 (1966).
33. ICEF Collaboration. Nuovo cimento, Suppl., 1, 1039 (1963).
34. Koshiha M. et al. Nuovo cimento, Suppl., 1, 1091 (1963).
35. Кужевский Б. М. Диссертация, МГУ, М., 1969. Проблема зарядового спектра галактических космических лучей и ядерные реакции.
36. Lander R. L. et al. Phys. Rev., 137B, 1228 (1965).
37. Lock W. O. et al. Proc. Roy. Soc., A231, 368 (1955).
38. Lohrmann E., Teucher M. Phys. Rev., 115, 636; 642 (1959).
39. Lohrmann E. et al. Phys. Rev., 122, 672 (1961).
40. Millburn G. P. M. et al. Phys. Rev., 95, 1268 (1954).
41. Мурзин В. С., Сарычева Л. И. Космические лучи и их взаимодействие. М., Атомиздат, 1968.

Bibliography (cont'd)

Page 645.

42. Nakagawa S., Tanaka S., Ito K. Preprint, 1961. (Цитир. по монографии [41].)
43. O'Dell M., Shapiro M., Stiller B. J. Phys. Soc. Japan, 17, Suppl., A III, 23 (1962).
44. Otterlund I. Arkiv fys., 38, 467 (1968).
45. Otterlund I., Andersson B. Arkiv fys., 35, 133 (1967).
46. Otterlund I., Resman R. Arkiv fys., 39, 265 (1969).
47. Пауэлл С., Фаулер П., Перкинс Д. Исследование элементарных частиц фотографическим методом. Перев. с англ. М., Изд-во иностр. лит., 1962.
48. Proceedings of the Third Conference on Reactions between Complex Nuclei. Berkeley and Los Angeles, Univ. of California Press, 1963.
49. Quarenzi G., Zorn G. T. Nuovo cimento, 1, 1282 (1955).
50. Rajopadhye V. Y., Waddington C. J. Philos. Mag., 3, 19 (1958).
51. Schechter L. et al. Phys. Rev., 90, 633 (1933).
52. Serber R. Phys. Rev., 72, 1008 (1947).
53. Соловьева Л. П. «Ж. эксперим. и теор. физ.», 31, 1086 (1956).
54. Tannenwald P. E. Phys. Rev., 89, 508 (1953).
55. The AECL Study for an Intense Neutron Generator Report AECL-2600. Chalk River, Ontario, 1966.
56. Tsuzuki Y. J. Phys. Soc. Japan, 16, 2131 (1961).
57. Труды международной конференции по физике тяжелых ионов. Дубна. Издание ОИЯИ Д7-3202, Д7-3548, 1966.
58. Waddington C. J. J. Phys. Soc. Japan, 17, Suppl. A111, 63 (1962).
59. Willoughby D. S. Phys. Rev., 101, 324 (1956).
60. Winzeler H. Nucl. Phys., 69, 661 (1965).
61. Вихров А. И. и др. «Ядерная физика», 11, 36 (1970).
62. Жданов А. П., Лепехин Ф. Г. Труды ИАН, 9, 41 (1959).

BEST AVAILABLE COPY

UNCLASSIFIED

SECURITY CLASSIFICATION OF THIS PAGE (When Data Entered)

REPORT DOCUMENTATION PAGE		READ INSTRUCTIONS BEFORE COMPLETING FORM
1. REPORT NUMBER FTD-ID(RS)T-1069-77	2. GOVT ACCESSION NO.	3. RECIPIENT'S CATALOG NUMBER
4. TITLE (and Subtitle) INTERACTIONS OF HIGH-ENERGY PARTICLES AND ATOMIC NUCLEI WITH NUCLEI (CHAPTER 7 thru 11)		5. TYPE OF REPORT & PERIOD COVERED Translation
		6. PERFORMING ORG. REPORT NUMBER
7. AUTHOR(s) V. S. Barashenkov, V. D. Toneyev		8. CONTRACT OR GRANT NUMBER(s)
9. PERFORMING ORGANIZATION NAME AND ADDRESS Foreign Technology Division Air Force Systems Command U.S. Air Force		10. PROGRAM ELEMENT, PROJECT, TASK AREA & WORK UNIT NUMBERS
11. CONTROLLING OFFICE NAME AND ADDRESS		12. REPORT DATE 1972
		13. NUMBER OF PAGES 504
14. MONITORING AGENCY NAME & ADDRESS (if different from Controlling Office)		15. SECURITY CLASS. (of this report) UNCLASSIFIED
		15a. DECLASSIFICATION/DOWNGRADING SCHEDULE
16. DISTRIBUTION STATEMENT (of this Report) Approved for public release; distribution unlimited		
17. DISTRIBUTION STATEMENT (of the abstract entered in Block 20, if different from Report)		
18. SUPPLEMENTARY NOTES		
19. KEY WORDS (Continue on reverse side if necessary and identify by block number)		
20. ABSTRACT (Continue on reverse side if necessary and identify by block number) 20		

DD FORM 1473

1 JAN 73

EDITION OF 1 NOV 65 IS OBSOLETE

UNCLASSIFIED

SECURITY CLASSIFICATION OF THIS PAGE (When Data Entered)

UNCLASSIFIED

SECURITY CLASSIFICATION OF THIS PAGE (When Data Entered)

REPORT DOCUMENTATION PAGE		READ INSTRUCTIONS BEFORE COMPLETING FORM
1. REPORT NUMBER FTD-ID(RS)T-1069-77	2. GOVT ACCESSION NO.	3. RECIPIENT'S CATALOG NUMBER
4. TITLE (and Subtitle) INTERACTIONS OF HIGH-ENERGY PARTICLES AND ATOMIC NUCLEI WITH NUCLEI (CHAPTER 7 thru 11)		5. TYPE OF REPORT & PERIOD COVERED Translation
		6. PERFORMING ORG. REPORT NUMBER
7. AUTHOR(s) V. S. Barashenkov, V. D. Toneyev		8. CONTRACT OR GRANT NUMBER(s)
9. PERFORMING ORGANIZATION NAME AND ADDRESS Foreign Technology Division Air Force Systems Command U.S. Air Force		10. PROGRAM ELEMENT, PROJECT, TASK AREA & WORK UNIT NUMBERS
11. CONTROLLING OFFICE NAME AND ADDRESS		12. REPORT DATE 1972
		13. NUMBER OF PAGES 504
14. MONITORING AGENCY NAME & ADDRESS (if different from Controlling Office)		15. SECURITY CLASS. (of this report) UNCLASSIFIED
		15a. DECLASSIFICATION/DOWNGRADING SCHEDULE
16. DISTRIBUTION STATEMENT (of this Report) Approved for public release; distribution unlimited		
17. DISTRIBUTION STATEMENT (of the abstract entered in Block 20, if different from Report)		
18. SUPPLEMENTARY NOTES		
19. KEY WORDS (Continue on reverse side if necessary and identify by block number)		
20. ABSTRACT (Continue on reverse side if necessary and identify by block number) 20		

DD FORM 1 JAN 73 1473 EDITION OF 1 NOV 65 IS OBSOLETE

UNCLASSIFIED

SECURITY CLASSIFICATION OF THIS PAGE (When Data Entered)

REPORT DOCUMENTATION PAGE	
1. REPORT NUMBER	2. GOVT ACCESSION NO.
3. REPORT DATE	4. TITLE (and Subtitle)
5. AUTHOR(s)	6. PERFORMING ORG. REPORT NUMBER
7. AUTHORING AGENCY NAME (if different from Controlling Office)	8. CONTRACT OR GRANT NUMBER(s)
9. CONTROLLING OFFICE NAME AND ADDRESS	10. PROGRAM ELEMENT PROJECT, TASK AREA & WORK UNIT NUMBERS
11. REPORT DATE	12. NUMBER OF PAGES
13. SECURITY CLASS. (of this report)	14. DISTRIBUTION STATEMENT (of this report)
15. DECLASSIFICATION/DOWNGRADING SCHEDULE	16. DISTRIBUTION STATEMENT (of the abstract entered in Block 20, if different from Report)
17. SUPPLEMENTARY NOTES	
18. KEY WORDS (Continue on reverse side if necessary; and identify by block number)	
19. ABSTRACT (Continue on reverse side if necessary; and identify by block number)	
20	

DISTRIBUTION LIST

DISTRIBUTION DIRECT TO RECIPIENT

ORGANIZATION	MICROFICHE	ORGANIZATION	MICROFICHE
A205 DMATC	1	E053 AF/INAKA	1
A210 DMAAC	2	E017 AF/ RDXTR-W	1
B344 DIA/RDS-3C	8	E404 AEDC	1
C043 USAMIA	1	E408 AFWL	1
C509 BALLISTIC RES LABS	1	E410 ADTC	1
C510 AIR MOBILITY R&D	1	E413 ESD	2
LAB/FIO		FTD	
C513 PICATINNY ARSENAL	1	CCN	1
C535 AVIATION SYS COMD	1	ETID	3
C557 USAIC	1	NIA/PHS	1
C591 FSTC	5	NICD	5
C619 MIA REDSTONE	1		
D008 NISC	1		
H300 USAICE (USAREUR)	1		
P005 ERDA	1		
P055 CIA/CRS/ADD/SD	1		
NAVORDSTA (50L)	1		
NAWPNSCEN (Code 121)	1		
NASA/KSI	1		
AFIT/LD	1		